

## ECALS MILESTONE REPORT

**Title:** A Probabilistic Analysis of Environmental DNA Monitoring Results in the Chicago Area Waterway System

**ACRCC Framework Item:** 2.6.3: Probabilistic Model, 2013 Framework

**Milestone Date:** November 26, 2014

**ECALS Project Management Plan Tasks:** Milestone 3.5.4: Draft Final Report on the Probabilistic Model.

**Contributors:** Martin T. Schultz, Carl F. Cerco, Brian E. Skahill, Richard F. Lance, Mark R. Noel, Patricia K. DiJoseph, David L. Smith, Michael P. Guilfoyle.

Engineer Research and Development Center, US Army Corps of Engineers, Vicksburg, MS.

Please direct questions or comments about this report to Dr. Martin T. Schultz, ([Martin.T.Schultz@usace.army.mil](mailto:Martin.T.Schultz@usace.army.mil), (601) 634-4313).

### Executive Summary

This milestone report summarizes progress to develop a model that can be used to help understand and interpret results of the environmental deoxyribonucleic acid (eDNA) monitoring program in the Chicago Area Waterway System (CAWS). The monitoring program has been in place since 2009 and its purpose is to indicate whether or not bighead carp or silver carp are present in the CAWS. This is accomplished by analyzing water samples to determine whether or not eDNA specific to these species is present. Although some water samples have tested positive for the presence of the target genetic markers associated with these species, there is ambiguity over the interpretation of these results. One bighead carp was removed from Lake Calumet in 2010, but conventional sampling programs have not otherwise been able to confirm the presence of the target species despite extensive fishing effort. In addition, a set of secondary sources of Asian carp eDNA have been documented. Secondary sources are alternate means by which Asian carp eDNA might be released into the CAWS.

The overall objective of Framework Item 2.6.3 is to resolve some of the ambiguity around interpretation of eDNA monitoring results. This has been accomplished by developing a model that provides natural resource managers with the ability to use eDNA monitoring results as a basis for making probabilistic statements about the source(s) of eDNA detected in monitoring samples and the presence of live bighead carp and silver carp upstream of the electric fish barrier, which is located at Romeoville, Illinois. In the course of developing this model, several other methods have been developed and demonstrated. For example, these include methods to characterize uncertainty in target marker concentrations using eDNA monitoring

results and methods to infer the amount of the target species needed to support observed eDNA concentrations in the absence of secondary sources.

This milestone report is the third and final report in a series. The first milestone report, submitted in August, 2013, presented a conceptual model. Since submitting the first milestone report, ECALS has worked to develop the ideas described in those conceptual models and to express them quantitatively so that probabilistic statements can be made. A second milestone report, which was not publicly released, was submitted in June, 2014. That report described several separate models and methods of making inferences from eDNA monitoring data. Much of the material in the second milestone report has been carried forward to support this final milestone report. This final report completes modeling and inference tasks that were in progress at the time of the second milestone report. A flowchart describing the analytical approach used in this study is provided in Figure 1.1 of the main report.

Key accomplishments and results described in this report include:

- Developed a model to simulate the probability of detecting bighead carp and silver carp target markers using methods approved in the Quality Assurance Product Plan (QAPP) and carried out an extensive set of laboratory experiments to parameterize that model. Results are described in Section 2 of this report. These results show that, at low concentrations, Asian carp target markers are difficult to detect and the polymerase chain reaction (PCR) assay has a high false negative rate. This appears to be the result of processing and division of water samples prior to the assay. In addition, bighead carp target markers are much more difficult to detect than silver carp markers because of differences in the target marker primers.
- Developed and implemented a method to estimate target marker concentrations in the CAWS using the results of the eDNA monitoring program, which indicate only presence or absence of the target marker in a sample. The methods are described in Section 3. Results show that Asian carp target marker concentrations vary over time and space in the CAWS. Probability distributions characterizing uncertainty in target marker concentrations are summarized in Appendix 4.
- Estimated target marker degradation rates using the results of laboratory experiments. Results show that Asian carp DNA released from a primary source can be described as consisting of two fractions, fast and slow. Approximately 80 percent of the eDNA is in the fast fraction and has a mean decay rate of  $0.456 \text{ d}^{-1}$ , which is equivalent to a half life of about 1.5 days. The remaining 20 percent is in the slow fraction and has a mean decay rate of  $0.089 \text{ d}^{-1}$ , which corresponds to a half life of approximately 7.8 days. At these rates, approximately ten percent of a target marker concentration would remain after ten days, and approximately 1.4 percent would remain after 30 days. These results are discussed in Section 4.
- Described the spatial and temporal distribution of potential secondary sources of eDNA in the CAWS and estimated loading factors to characterize activities that may generate

secondary source loads. Results of these analyses are described in Section 4 of this report and are used in simulating eDNA fate and transport in the CAWS.

- Developed a three-dimensional grid to represent the hydrography of the CAWS between Lake Michigan and Dresden Lock and Dam, and simulated flows in the CAWS between Lake Michigan and Lockport Lock and Dam for the period 2009-2012 using the Computational Hydrodynamics in Three Dimensions (CH3D) model. The results of this simulation are incorporated into a water quality fate and transport model, which is described in Section 4.
- Parameterized and validated a high fidelity water quality fate and transport model (HFFTM), developed using CE-QUAL-ICM, to simulate selected water quality constituents in the CAWS and model the fate and transport of eDNA. A seasonally averaged steady-state water quality box model is derived and parameterized from the HFFTM to support a Bayesian Markov chain Monte Carlo (MCMC) simulation. Both models are described in Section 5.
- Calibrated parameters of secondary source loading rate functions to seasonal target marker concentrations in nineteen CAWS reaches using Bayesian MCMC simulation. Results are used to rank secondary sources in terms of the number of copies of the eDNA target marker that they contribute to the system. These results are summarized for the entire CAWS in Table ES.1, which reports the probability that each potential secondary source is the largest contributor. Results show that either combined sewer overflows (CSOs) or navigation (NAV) is probably the largest single contributors of eDNA to the CAWS. Section 6 discusses results specific to CAWS reach and season.

Probabilistic Rank	Secondary Source of eDNA in the CAWS					
	BRD	CSO	LMI	FDS	FIN	NAV
Largest	0	0.623	0	0	0	0.377
2nd largest	0.003	0.377	0.015	0.02	0.008	0.577
3rd largest	0.128	0	0.282	0.296	0.272	0.023
4th largest	0.204	0	0.287	0.246	0.252	0.01
5th largest	0.292	0	0.232	0.232	0.236	0.007
6th largest	0.373	0	0.185	0.206	0.231	0.005

Table ES.1: Probabilistic ranking of secondary sources in terms of total contribution of eDNA to the CAWS. Column headings are: BRD = Piscivorous birds, CSO = Combined sewer overflows, LMI = Lake Michigan inflows, FDB = Recreational fishing derbies, FIN = Fishing nets, and NAV = Commercial navigation.

- Post-processed the results of the Bayesian MCMC to estimate the fraction of eDNA detected in monitoring samples that originated from each potential secondary source. These results are summarized for the entire CAWS in Tables ES.2. For example, for the CAWS as a whole, an expected 42 percent of Asian carp target markers detected in monitoring samples originated from CSOs and an expected 29 percent originated from navigation. Only about three percent of the silver carp target markers are attributed to piscivorous bird feces. These results are summarized by reach and season in Section 6.

	Secondary Source of eDNA in the CAWS					
	BRD	CSO	FDB	FIN	LMI	NAV
Expected fraction	0.03	0.42	0.06	0.06	0.15	0.29

Table ES.2: Expected fraction of eDNA originating from one of six potential secondary sources over the course of one year for the entire CAWS. See Table ES.1 for definitions of abbreviations.

- Estimated how much silver carp would be required to generate the target marker concentrations that have been observed in the CAWS using Bayesian MCMC simulation. These results show that, if live fish were the only source of Asian carp eDNA, between 4 and 6 metric tons of silver carp would have to be resident in and distributed throughout the CAWS upstream of the electric barrier to sustain the target marker concentrations observed in the waterway. These results are discussed in more detail in Section 6.
- Simulated target marker concentrations from secondary sources using the high fidelity fate and transport model. These results show that the fraction of eDNA originating from any one secondary source tends to vary greatly depending on where and when a water sample was collected. These results also show that hydrologic forces in the CAWS vary over space and time. Under certain conditions, eDNA may be transported long distances from its point of release. Numerical results of the simulations are discussed in detail in Section 7.
- Demonstrated how the probability that a target species is present at a search site can be estimated using data on the level of fishing effort when the target species was not captured in the course of fishing. This is accomplished using a Bayesian updating approach and requires an estimate of the single sample detection probability appropriate for the search site. Since estimates of this probability were not readily available for use in this project, a density dependent probability is employed for heuristic purposes. Results are summarized in Table ES.3 for selected CAWS reaches. Results show that conventional fishing effort by the Monitoring and Response Work Group (MRWG) has greatly increased confidence in the absence of larger quantities of the target species. For smaller quantities of the target species fishing effort has not been sufficient to reduce the probability of target species presence. Results of this analysis are discussed in Section 8. These probabilities are used as inputs to a Bayesian network model that has been devised for statistical inference from eDNA monitoring data.

Target species mass (t)	Selected CAWS Reach (see Figure 3.1)					
	NSC	CRM	CR2	CR5	LKC	CRD
0.001 – 0.005	0.500	0.500	0.500	0.500	0.500	0.500
1.5-1.75	0.428	0.500	0.446	0.500	0.343	0.457
5 – 6	0.273	0.500	0.323	0.500	0.099	0.357
10 – 11	0.133	0.500	0.196	0.499	0.015	0.246

Table ES.3: Prior probability of target species presence given conventional fishing effort (2009-2012, all gear types) by target species mass (metric tons, t) and reach.



- Developed and parameterized a Bayesian network model to make inferences about the presence of live bighead carp and silver carp in the CAWS using the results of the eDNA monitoring program. The Bayesian network, which integrates all of the preceding analysis into a single coherent framework for inference, uses eDNA monitoring results to update the prior probabilities of target species presence listed in Table ES.3 to posterior probabilities. These probabilities are conditioned on the target species mass in the target reach or in one of the reaches upstream. Posterior probabilities updated using the frequency of are listed for the gates open season (approx June 1 to October 15) in Table ES.4 and for the gates closed season in Table ES.5. Section 9 describes the Bayesian network and presents specific numerical results for six CAWS reaches where eDNA samples were frequently collected between 2009 and 2012.

<b>SEASON: Gates Open</b>						
<b>Target species mass (t)</b>	<b>Selected CAWS Reach (see Figure 3.1)</b>					
	<b>NSC</b>	<b>CRM</b>	<b>CR2</b>	<b>CR5</b>	<b>LKC</b>	<b>CRD</b>
0.001 – 0.005	0.479	<b>0.512</b>	<b>0.566</b>	0.500	0.481	<b>0.507</b>
1.5-1.75	0.407	<b>0.512</b>	0.481	0.473	0.444	0.456
5 – 6	0.256	<b>0.512</b>	0.324	0.418	0.384	0.360
10 – 11	0.123	<b>0.512</b>	0.236	0.369	0.349	0.289

Table ES.4: Posterior probability of target species presence for gates open season given the fraction of eDNA monitoring samples testing positive for the silver carp target marker during the period 2009 – 2012 by target species mass (metric tons, t) and reach.

<b>SEASON: Gates Closed</b>						
<b>Target species mass (t)</b>	<b>Selected CAWS Reach (see Figure 3.1)</b>					
	<b>NSC</b>	<b>CRM</b>	<b>CR2</b>	<b>CR5</b>	<b>LKC</b>	<b>CRD</b>
0.001 – 0.005	0.450	<b>0.514</b>	<b>0.537</b>	0.500	<b>0.573</b>	<b>0.610</b>
1.5-1.75	0.380	<b>0.514</b>	0.457	0.473	<b>0.536</b>	<b>0.564</b>
5 – 6	0.235	<b>0.514</b>	0.315	0.418	0.474	0.474
10 – 11	0.111	<b>0.514</b>	0.236	0.369	0.437	0.404

Table ES.5: Posterior probability of target species presence for gates closed season given the fraction of eDNA monitoring samples testing positive for the silver carp target marker during the period 2009 – 2012 by target species mass (metric tons, t) and reach.

Tables ES.4 and ES.5 show the posterior probability that some quantity of target species (silver carp) is present in or upstream of a CAWS reach. Bold text indicates that the target species is more likely to be present than not. This is true in CRM and for smaller quantities of the target species in CR2, LKC, and CRD. Each cell is shaded a different color to indicate the effect of eDNA evidence on the probability of target species presence. The cell is shaded blue if the effect of eDNA evidence is to decrease the probability (posterior is less than the prior), and red if the effect of eDNA evidence is to increase the probability (posterior is greater than the prior). For example, all of the cells in NSC are coded blue because the posterior probability is less than the prior after observing the evidence from eDNA monitoring. Conclusions about the

presence of live silver carp in the CAWS vary by reach and season. In general, the eDNA monitoring program in the CAWS does not seem to provide strong evidence in favor of the hypothesis that Asian carp are present. For larger quantities of fish, this is a strong conclusion. However, this conclusion tends to be weaker for smaller quantities of fish because inference is more difficult.

The analytical results and insights developed over the course of this project are directly applicable to the hydrodynamic simulation period for which they were developed, 2009 – 2012. However, they also provide a reasonably good basis for making generalizations outside of the simulation period as long as the hydrology and other factors likely to influence the distribution of eDNA in the CAWS remain similar from year to year. For example CSOs and navigation have been identified as most likely being the largest secondary sources of eDNA in the CAWS. Barring significant changes in the system over time, there is no reason why that would not also be true in 2013 and in future years. Similarly, the Bayesian network models described in this report have been parameterized for the period 2009-2012. These models update a prior probability of target species presence to a posterior probability, indicating whether or not evidence from eDNA monitoring has increased or decreased the probability of target species presence and whether target species presence is more likely than not. Natural resource managers can continue to use these models in the CAWS as long as the prior probabilities of target species presence are updated to reflect conventional fishing effort during the period of analysis.

The probability of target species presence in the CAWS can be calculated using the models described in this report. Specific numerical results have been developed in this report for silver carp. These probabilities vary from reach to reach and from season to season. Viewed collectively, and considering that secondary sources are likely to be contributing Asian carp eDNA to the system, these results strongly suggest that larger quantities of silver carp are not present in the CAWS. However, the strength of this conclusion diminishes as smaller quantities of silver carp are considered. For smaller quantities of silver carp, eDNA evidence may tilt in favor or against the presence of the species, but the posterior probabilities themselves are not strongly for or against target species presence. Regardless of how the eDNA evidence and posterior probabilities point, results of these analyses should not be used to justify complacency in the fight to prevent Asian carp from gaining access to the Great Lakes. On the contrary, this report suggests that continued vigilance and efforts to deter Asian carp are needed.

# **A Probabilistic Analysis of Environmental DNA Monitoring Results in the Chicago Area Waterway System**

Draft Final Report

ACRCC Framework Item 2.6.3

November 26, 2014

Martin T. Schultz, Carl F. Cerco, Brian E. Skahill, Richard F. Lance, Mark R. Noel,  
Patricia K. DiJoseph, David L. Smith, Michael P. Guilfoyle

Engineer Research and Development Center  
United States Army Corps of Engineers  
3909 Halls Ferry Road  
Vicksburg, MS.

Questions and comments about this report should be directed to Dr. Martin T. Schultz,  
[Martin.T.Schultz@usace.army.mil](mailto:Martin.T.Schultz@usace.army.mil), (601) 634-4313.

## Table of Contents

<b>1. Introduction .....</b>	<b>1</b>
Purpose and Organization of this Report.....	4
<b>2. Detection of eDNA in Monitoring Samples .....</b>	<b>4</b>
Collection of a Filtered Water Sample from the Source .....	6
Extraction of eDNA from a Filtered Sample to an Elution .....	7
Removal of a Replicate from the Elution .....	8
Conventional Polymerase Chain Reaction (cPCR).....	8
<b>3. eDNA Monitoring Data and Bayesian Inference of Source Water Concentrations.....</b>	<b>11</b>
Summary of eDNA Monitoring Data .....	12
Bayesian Inference of Target Marker Concentrations.....	13
Target Marker Concentrations in the North Shore Channel (NSC).....	14
<b>4. Precursors to Modeling the Fate and Transport of eDNA .....</b>	<b>17</b>
Primary Source Loading Rates .....	17
Target Marker Degradation Rate.....	17
Loading Factors for Secondary Sources .....	19
<b>5. A Model to Simulate eDNA Fate and Transport.....</b>	<b>26</b>
The Hydrodynamic Model.....	26
High-Fidelity eDNA Fate and Transport Model (HFFTM).....	27
Steady-State Fate and Transport Model (SSFTM).....	29
Data Sources used in Developing the Fate and Transport Models.....	30
Results of TDS Calculations.....	32
Insights from the Age Computations .....	33
A Demonstration of eDNA Fate and Transport Simulation Capabilities .....	34
<b>6. Loading Rates for Potential Sources of eDNA .....</b>	<b>35</b>
Loading Rate Functions.....	36
Bayesian Markov Chain Monte Carlo (MCMC) .....	36
Implementation of Bayesian MCMC to Estimate SSFTM Input Parameters.....	37
Implementation of Bayesian MCMC to Estimate eDNA Source Loading Rates.....	38
<b>7. High-Fidelity Simulation of eDNA Fate and Transport .....</b>	<b>43</b>
Loads and Boundary Conditions .....	43

Secondary Source Simulation Results .....	45
Primary Source Simulation Results .....	47
Summary of Conclusion based on HFFTM Simulation Results.....	49
<b>8. Prior Probabilities of Target Species Presence.....</b>	<b>50</b>
Conventional Fisheries Surveillance in the CAWS .....	50
Single Sample Gear Detection Probabilities .....	51
Calculating the Prior Probability of Target Species Presence .....	52
Challenges to Implementation and Approach .....	53
<b>9. A Bayesian Network for Inference about the Presence of Live Asian Carp .....</b>	<b>54</b>
The Bayesian Network .....	55
Statistical Inference about the Presence of Silver Carp from eDNA Monitoring Data .....	62
Statistical Inference for Silver Carp in Lake Calumet .....	64
Sensitivity of Posterior Probabilities to Parameterization of the ALL_ACTIVE Node .....	67
Sensitivity of Bayes Factor to Parameterization of the ALL_ACTIVE Node.....	68
Results of the Probabilistic Model for Silver Carp .....	70
<b>10. Conclusion .....</b>	<b>75</b>
<b>11. Literature Cited .....</b>	<b>77</b>
<b>Figures.....</b>	<b>85</b>
<b>Tables .....</b>	<b>189</b>
<b>Appendices.....</b>	<b>245</b>

## 1. Introduction

Asian carp were imported into the United States in the 1970's to control phytoplankton and macrophytes in fish ponds and wastewater treatment lagoons (Kolar *et al.* 2007). Over the past thirty years, these fish have expanded their range within the Mississippi River Basin. Two planktivorous species of Asian carp are of particular concern. Bighead carp (*Hypophthalmichthys noblis*) and silver carp (*H. molitrix*) are highly efficient filter feeders that have caused significant ecological damage in the Mississippi River Basin by undermining food webs and outcompeting native fish populations in the habitats where they become established (Chick and Pegg 2001, Kolar *et al.* 2007). Were these fish to become established in Lake Michigan, they could harm native fish populations.

Efforts to prevent Asian carp from colonizing Lake Michigan have focused on the Chicago Area Waterway System (CAWS) because it is the principal hydrologic connection between the Mississippi River Basin and Lake Michigan. The Illinois River, a tributary of the Mississippi River, is connected to Lake Michigan via the Chicago Sanitary and Ship Canal (CSSC), which was constructed in the late 1890's to transport sewage from Chicago away from Lake Michigan, the source of the city's drinking water (Changnon *et al.* 1996, MWRD 2008). The leading edge of the Asian carp invasion is presently considered to be at river mile 278 of the Illinois River, at the Dresden Island pool, about 55 miles downstream from Lake Michigan. However, on rare occasions, individual adult fish have been captured and removed from the pool below Lockport Lock and Dam.

Since 2002, the US Army Corps of Engineers (USACE) has operated an electric fish barrier at Romeoville, Illinois, about 35 miles downstream from Lake Michigan. The fish barrier is designed to prevent the Asian carp invasion front from reaching Lake Michigan via the CAWS. Fish that challenge the barrier are stunned by a non-lethal electrical charge. Although the fish barrier greatly reduces the probability that the Asian carp invasion front will advance toward Lake Michigan via the CAWS, several scenarios under which fish might penetrate or circumvent the barrier may exist (Rasmussen *et al.* 2011) and studies of the barrier's effectiveness are ongoing (ACRCC 2012). There are also other pathways by which the fish might reach waters upstream of the barrier (ACRCC 2012). For example, adult Asian carp are occasionally found in land locked lakes and ponds in the Chicago area. These appear to have been released as fry or fingerlings when lakes and ponds were stocked (ILDNR 2011, USGS 2013).

Over the past several years, a conventional fisheries surveillance program has been implemented in the CAWS to detect the possible presence of bighead and silver carp. This program deploys electrofishing boats and nets at fixed and randomly selected sites to determine the numbers and types of species present. Between 2010 and 2012, monitoring crews logged over 9,600 hours sampling at fixed and randomly selected sites throughout the CAWS upstream of the barrier (MRWG 2013a). On June 22, 2010, commercial fishermen working in Lake Calumet in the course of fixed site monitoring captured a bighead carp weighing 8.9 kg. The

ACRCC's Monitoring and Rapid Response Work Group<sup>1</sup> (MRRWG) conducted a rapid response action during the period June 23 – July 7, 2010. No additional bighead or silver carp were captured during that rapid response action (MRRWG 2012). No bighead or silver carp have been captured or otherwise observed in the CAWS upstream of the electric fish barrier since June 22, 2010. MRWG continued implementing its conventional fisheries surveillance programs through 2013.

Between 2009 and 2012, USACE and partner agencies have been collecting water samples from the CAWS and testing those samples for the presence of deoxyribonucleic acid (DNA) specific to bighead and silver carp. Aquatic organisms release DNA into the environment through bodily excretions such as feces, urine, sperm, eggs, and rotting carcasses. This environmental DNA (eDNA) is assumed to degrade quickly. Until recently, it has been assumed that the presence of bighead and silver carp DNA in water samples indicate that a fish has recently been present near the location where the sample was collected. Water samples were collected over the course of 68 sampling events. Of the samples collected within and upstream of the electric fish barrier, bighead carp DNA was detected in 43 of 5,522 water samples tested for bighead carp and silver carp DNA was detected in 236 of 5,503 water samples tested for silver carp (MRWG 2013c). Responsibility for the eDNA monitoring program was transferred to the US Fish and Wildlife Service (USFWS) in 2013. During 2013, the USFWS detected silver carp eDNA in 21 of the 396 water samples tested for silver carp eDNA and detected no bighead carp eDNA in the 417 water samples it tested for bighead carp eDNA (USFWS 2014).

Positive detections of bighead and silver carp eDNA at a monitoring location during two or more consecutive eDNA monitoring events may, at the discretion of fisheries managers, trigger rapid response actions to remove the fish using fishing gear or poison. Between 2010 and 2012, eleven rapid response actions were undertaken employing an estimated 11,330 man hours. No bighead or silver carp have ever been captured during these rapid response actions or during the course of any other MRRWG sampling activity undertaken above the electric barrier. The use of eDNA evidence as a trigger for rapid response actions was discontinued in 2013 because of the lack of success in capturing the target species and uncertainty about how to interpret eDNA monitoring results (MRWG 2013b).

It is possible that bighead and silver carp are present in the CAWS in very low numbers, and therefore difficult to capture or detect using conventional surveillance methods (Jerde *et al.* 2011, Jerde *et al.* 2013). While a very low number of individuals might explain the detection of eDNA and the inability to capture or detect the fish, recent studies have also suggested that eDNA evidence should be interpreted carefully (ECALS 2013, Wilcox *et al.* 2013). The detection of eDNA belonging to a particular species in a water body should not, by itself, be taken as proof that a live member of that species is present in that water body because too little is known about factors influencing the distribution of eDNA. For example, it has been shown that eDNA can be transported to the CAWS and released by fish-eating birds, boats, barges, fishing gear and storm sewers (ECALS 2013, MRWG 2013b). Any one or a combination of these sources could provide an alternate explanation for the presence of bighead and silver carp eDNA in the CAWS upstream of the electric fish barrier. Similarly, because eDNA can be difficult to

---

<sup>1</sup> In 2013, the Monitoring and Rapid Response Workgroup (MRRWG) was renamed the Monitoring and Response Workgroup (MRWG).

detect at low concentrations, the failure to detect eDNA in a system should not be interpreted as proof that the fish are absent.

Difficulty of interpreting results of the eDNA monitoring program can be attributed to the lack of secondary evidence that would help corroborate conclusions about the source of eDNA detected in monitoring samples or the presence of live bighead carp or silver carp in the CAWS. Darling and Blum (2007) outlined several ways that DNA-based methods *might* be used to monitor invasive species distributions. DNA-based methods are most commonly used to confirm the identity of a previously identified specimen, or to identify specimens that cannot be otherwise classified because of, for example, a lack of trained personnel or a lack of unique morphological characteristics at a given life stage. eDNA-based methods are a subset of DNA-based methods. DNA is extracted from an environmental sample such as water or soil and isolated in an elution. A sample of the elution is then subjected to polymerase chain reaction (PCR) to determine whether or not a particular genetic marker, the target marker, is present. This target marker is a section of DNA with a nucleotide sequence that is believed to be unique to the target species. Unlike DNA-based methods, the DNA is not associated with a carcass or other corporeal evidence that might help corroborate the identity or presence of the target organism that shed the DNA. Thus, conclusions from eDNA studies are based entirely on the results of the PCR test.

Studies that have attempted to validate eDNA-based methods to determine invasive species distributions have also collected secondary evidence to confirm the presence of the organisms by other means, such as sound. Ficetola *et al.* (2008) screened water samples collected from ponds in France to detect the American bullfrog (*Rana catesbeiana* = *Lithobates catesbeianus*), an invasive species. Detections were validated using pre-existing census data of “high-quality.” Goldberg *et al.* (2011) collected water samples from five streams on the Payette National Forest to test for DNA belonging to the Rocky Mountain tailed frog (*Ascaphus montanus*) and the Idaho giant salamander (*Dicamptodon aterrimus*). These streams were known to be habitats for these species before the environmental samples were collected. Foote *et al.* (2012) investigated the feasibility of using eDNA methods to detect harbor porpoise (*Phocena phocena*) in the Baltic Sea. Acoustic detection at the time of sample collection was used to confirm the presence of the porpoise at monitoring sites. These and other studies (Thomsen *et al.* 2012a, DeJean *et al.* 2012, Olson *et al.* 2012, Wilcox *et al.* 2013) demonstrate the potential value of eDNA as a means of determining species ranges.

In contrast to the studies that attempt to validate eDNA-based methods, evidence that could help to corroborate conclusions based on eDNA monitoring in the CAWS are absent. Although one bighead carp was captured in Lake Calumet in 2010, no bighead carp or silver carp have been captured since despite thousands of man-hours of fishing effort. There are countless ways that eDNA might be distributed in the environment and, no ways to easily deduce how eDNA detected in a monitoring sample may have arrived at the location where the monitoring sample was collected. This is particularly true in aquatic environments where water may transport substances that are suspended in the water column to places that are a long way from where the substances were released into the water column (Foote *et al.* 2012, Goldberg *et al.* 2011). The lack of certainty about where the DNA found in an environmental sample originated and how it arrived at the monitoring location is one of the main challenges of using eDNA based



methods. This explains why so much emphasis in this project is placed on modeling the fate and transport of eDNA in the CAWS.

### *Purpose and Organization of this Report*

This report summarizes ECALS efforts to develop a probabilistic model that will assist in understanding and interpreting the Asian carp eDNA monitoring results in the CAWS. Specific modeling objectives are to 1) estimate the probability that a potential secondary source is in fact the source of eDNA detected in monitoring samples from the CAWS; and 2) estimate the probability that the target species (silver carp and bighead carp) are presented in the CAWS given eDNA monitoring results and other available information. Figure 1.1 provides a flow chart of outlining how the probabilistic model was developed to respond to these questions, which are highlighted in text boxes O and N, at the bottom of the flow chart.

The organization of this report follows the process outlined in Figure 1.1. Section 2 describes a model to simulate the probability of detecting bighead carp and silver carp target markers as a function of target marker concentration in a monitored water body. An extensive set of laboratory experiments were carried out in support of this effort to parameterize selected variables. The methods used in these studies are summarized in appendices. Section 3 describes a process for making statistical inferences about target marker concentrations in a monitored water body using the results of the eDNA monitoring program. Section 4 of this report describes how selected parameters used in the fate and transport models were estimated, including the degradation rate, the shedding rate from live fish, and secondary source loading factors. Section 5 describes a high-fidelity water quality simulation model that models the fate and transport of eDNA in the CAWS. That model incorporates hydrography and hydrodynamics that were developed specifically to support probabilistic modeling objectives. A seasonally averaged steady state water quality box model has been derived from the high-fidelity water quality simulation model to support estimation of loading rates from secondary sources. Section 6 describes a Bayesian Markov chain Monte Carlo (MCMC) simulation method to derive eDNA loading rates for secondary sources. Section 7 describes results of simulations using the high fidelity fate and transport model (HFFTM). Section 8 describes how the probability of target species presence can be calculated using information from conventional fisheries surveillance level of effort. These probabilities serve as prior probabilities to be updated using results from the eDNA monitoring program. Section 9 describes development and parameterization of a Bayesian network model for drawing inferences from eDNA monitoring data. The model is parameterized for six CAWS reaches where eDNA monitoring samples were consistently collected during the period 2009-2012. Statistical inference is demonstrated using the model. Section 9 concludes the report by describing potential improvements in the probabilistic model and a set of general findings based on the efforts to support its development.

## **2. Detection of eDNA in Monitoring Samples**

Asian carp eDNA is detected in monitoring samples from the CAWS using PCR. PCR tests for the presence of a genetic marker, which is a strand of DNA that is unique to the species of interest. This strand of DNA is called the “target marker.” PCR is capable of detecting very small quantities of the target marker in an environmental sample. Sample collection and analysis

procedures used in the CAWS were originally developed at the University of Notre Dame with funding from USACE (USACE 2012). An independent peer review of the eDNA methodology by Environmental Protection Agency's (EPA's) Great Lakes National Program Office in 2009 assessed the reliability of analytical procedures at the University of Notre Dame. The review expressed confidence in the methodology and procedures. The EPA review did not address interpretation of eDNA monitoring results in regards to the presence or absence, proximity, or abundance of carp in the study area (Blume *et al.* 2010). USACE subsequently contracted with Battelle Memorial Institute for a second independent peer review of the eDNA methodology. The review found that the eDNA methodology was sound in principle and presented several advantages over conventional surveillance methods. However, it also identified some key limitations of the approach. In particular, the review concluded that detection of eDNA does not provide conclusive proof of species presence and does not provide information on the size or age of individuals or the size of a population, if present (BMI 2012).

Sample collection and analysis procedures are described in the Quality Assurance Product Plan (QAPP) and, with a few exceptions, follow those developed by the University of Notre Dame (USACE 2012). Samples of water (usually two liters) are collected from the CAWS and filtered through one or more 1.5 micron glass fiber filters. Filters are then shipped on dry ice to a laboratory where the eDNA is extracted from the filter paper using a MoBio Power Water DNA Isolation Kit ® and separated from non-DNA extracts by centrifugation. A 100 µl elution containing the sample is then stored at -20 deg. C for PCR. PCR is an iterative process of heating and cooling the sample to denature the eDNA and amplify a genetic marker that is specific to the target species. Theoretically, the concentration of a target species marker will double each time the sample is heated and cooled. Samples can be analyzed using two types of PCR: conventional PCR (cPCR) and quantitative PCR (qPCR). The cPCR assay is strictly a test for the presence or absence of the marker. Samples testing positive for the genetic marker using the cPCR assay are sequenced to confirm that they come from the target species. The qPCR assay detects the presence of the marker and estimates the target marker count. Samples that test positive using qPCR are assumed to be specific to the target species and are typically not sequence confirmed. Currently, only the cPCR assay is included in the QAPP as an approved technique for Asian carp eDNA monitoring studies in the CAWS.

This section of the report describes a model to estimate the probability of detecting a target marker in a water body and the laboratory studies undertaken to estimate parameter values for that model. The probability that a polymerase chain reaction (PCR) replicate will test positive is a function of the target marker concentration from the sampled water body (i.e., *source water*). The model describes four processes related to sample collection and analysis: 1) collection of a filtered water sample from the source; 2) extraction of eDNA from a filtered sample to an elution; 3) removal of a replicate from the elution; and 4) conventional polymerase chain reaction (cPCR), which is an analytical test for the presence or absence of a target genetic marker. The abbreviation cPCR is used to distinguish between cPCR and quantitative PCR (qPCR), which is an assay to estimate of the quantity of a target marker in solution. This model of the sample collection and analysis process incorporates six sources of uncertainty. These include: 1) the number of target markers captured in a two liter water sample; 2) extraction efficiency; 3) the number of target markers extracted in a PCR replicate; 4) PCR efficiency or inhibition; 5) the probability of detection; and 6) the ability to confirm that the genetic sequence

of PCR products matches that of the target marker. Interim results are presented to demonstrate how the model can be used. In Section 3, outputs of this model are used to derive the ambient concentration of eDNA in source water, which is necessary for understanding how eDNA is distributed in the CAWS.

### *Collection of a Filtered Water Sample from the Source*

If the source water concentration of eDNA is known, the mean number of target markers captured in a water sample can be estimated:

$$N_S = C_M V_S$$

$N_S$	Number of eDNA target markers in the monitoring sample
$C_M$	Target eDNA marker concentration at the site (copies/L)
$V_S$	Volume of the monitoring sample (L)

Each water sample is filtered soon after its collection. Although some eDNA may be lost in the process of filtration, it is believed that filtration is an efficient means of capturing eDNA. This model assumes there are no losses in the filtration process. The number of particles in repeated samples of the same size taken from a common source will vary as a result of random sampling error. This error can be modeled using a Poisson distribution if it is assumed that the particles are randomly distributed, the source is homogenous, the concentration is constant, and the samples are independent (Gosset 1907, in Emelko *et al.* 2010). The Poisson distribution describes variability in the number of objects contained in replicate samples taken from a homogenous solution, provided the samples are small in relation to the volume. The variable  $N_S$  is now a discrete random variable with probability mass function:

$$p[N_S | \mu_{N_S}] = \frac{(\mu_{N_S})^{N_S} \cdot \exp(-\mu_{N_S})}{N_S!}$$

Where  $p[N_S | \mu_{N_S}]$  is the probability of observing  $N_S$  copies of the target marker in a random sample from a well-mixed water body with target marker concentration  $C_M$ . The variable  $\mu_{N_S}$  is the mean number of target markers in the monitored water body and is the parameter of the distribution. For the purpose of this analysis, our assumption is that particles are well-mixed in the water body.

If eDNA particles are bound up in cells or groups of cells, eDNA particles may have a clumped distribution in the water column. If so, fewer water samples will contain at least one target marker, but those water samples that do contain at least one marker will tend to contain a larger number of markers. Emelko *et al.* (2010) note that the Poisson distribution underestimates variability if the particles are clumped (the concentration is patchy) and, in such cases, the negative binomial distribution may provide a better characterization of random sampling error. ERDC adapted this model to simulate a clumpy distribution of particles in the water column and determined that the effect of clumping was to greatly increase the variability in target marker counts and detection rates, but otherwise there was no effect on the outcome of the simulation over many realizations of the model. This suggests that, if the distribution of eDNA in the water

column is clumped, a larger number of samples will be needed to detect the presence of the target marker in the water body.

The higher the mean concentration in source water, the greater the probability of capturing any given number of target markers in the water sample. Figure 2.1 illustrates this effect by showing the probability of capturing less than or equal to  $N_S$  markers in a two liter sample of source water. For example, this figure shows that, if the target marker concentration in source water is one copy/L, the probability of having no more than one copy of the target marker in a two-liter monitoring sample is 0.406. If the target marker concentration in source water is 10 copies/L, the probability of having at most 20 copies of the target marker in the two-liter monitoring sample is 0.56. At low source water concentrations, the number of target marker copies contained in the sample will be low. Figure 2.2 shows Poisson probability mass functions for a two liter sample from a site with  $C_M = 1$  and 10 copies per liter to illustrate variability in the target marker counts of water samples. For  $C_M = 1$  copies per liter, the target marker count in a two liter water sample ranges from 0 to 10 copies. For  $C_M = 10$  copies per liter, the target marker count in a two liter water sample will range from about 4 to 40 copies.

#### *Extraction of eDNA from a Filtered Sample to an Elution*

The filter is shipped to the laboratory on ice. It is assumed that there is no degradation of the eDNA in the sample. The glass fiber filter is ground up and the eDNA is extracted from the filter into a 100  $\mu$ l elution using bead extraction. Extraction efficiency is the fraction of target marker on the filter that remains in the elution after the extraction process is complete. After extraction, the number of target markers in the elution can be estimated:

$$N_E = N_S E_{EXT}$$

$N_E$  Number of target markers in the elution

$E_{EXT}$  Efficiency of the extraction process

In general, manufacturers of DNA extraction kits are far more interested in the purity of the substance extracted from a filter than extraction efficiency, so extraction efficiencies tend to be low (Monroe, p.c., 2014). Although ERDC conducted a set of experiments to quantify extraction efficiency, these were unsuccessful. Uncertainty in extraction efficiency is represented here as a triangular distribution with a lower bound of 0, a median of 0.15, and an upper bound of 0.3 (Figure 2.3). This represents a general consensus of individuals responsible for carrying out the analysis of CAWS water samples at the Engineer Research and Development Center (ERDC).

The concentration of the target marker in the elution is expressed in copies/ $\mu$ l, and is calculated assuming a 100  $\mu$ l elution:

$$C_E = N_E V_E^{-1}$$

$C_E$  Concentration of target marker in the elution (copies/ $\mu$ l)

$V_E$  Initial elution volume ( $\mu$ l)

### *Removal of a Replicate from the Elution*

One or more replicates are extracted from each elution for the PCR assay. As PCR replicates are extracted from the elution, the number of particles captured in each replicate will vary as a result of random sampling error. Thus, eight aliquots extracted sequentially for a PCR assay will each contain a different number of target markers,  $N_A$ . Provided the aliquot is small relative to the elution volume, this variability can be described using a Poisson distribution with the parameter equal to the mean or expected concentration of the elution,  $\mu_{N_A}$ , calculated for a specific target marker concentration in source water:

$$p[N_A|\mu_{N_A}] = \frac{(\mu_{N_A})^{N_A} \cdot \exp(-\mu_{N_A})}{N_A!}$$

Poisson probability mass functions for selected values of  $C_M$  are illustrated in Figure 2.4 to demonstrate that replicates extracted for PCR may contain few markers as a result of processing and division of water samples. For example, at  $C_M = 10$  copies/L, more than 97 percent of replicates will contain no target markers. At  $C_M = 100$  copies/L, about 74 percent of replicates will contain no target markers, and at  $C_M = 1,000$  copies/L, more than 99 percent of replicates will have fewer than 10 target markers.

### *Conventional Polymerase Chain Reaction (cPCR)*

A cPCR assay is used to determine whether or not a replicate contains the eDNA target marker. In the absence of PCR inhibition, the ability to detect the presence of the target marker can be described as a function of the number copies of the markers in the replicate. When target marker counts are low, there is less chance that the primer will successfully locate and bind with the marker. Replication of DNA during PCR requires molecular interaction (hydrogen bonding) between a primer (short DNA polymers) and a target DNA segment (or template DNA). The template DNA is almost always a very small fraction of the total DNA in a sample. For example, in a single cell containing  $2.5 \times 10^9$  base pairs, a template marker consisting of 191 base pairs represents  $8.0 \times 10^{-6}$  percent of total DNA. The interaction between primers and template is a random process. During PCR, heat drives primers and templates around in the PCR solution. In the course of this mixing, primers and templates collide at which point replication can occur. If the template DNA is too rare, the template and primers may not interact or interact so infrequently that the desired PCR product, or amplicon, is not produced or is produced in such low quantity that it is undetectable.

Experiments were conducted at ERDC to estimate parameters of a probability distribution characterizing the probability of detection. Details of these experiments are summarized in Appendix 1. A summary of experimental results is provided in Table 2.1. Between 30 and 60 replicates of each concentration (660 cPCR replicates total) were analyzed to determine the fraction of replicates testing positive for the target marker and parameters of a gamma distributions were estimated from the experimental results using the method of moments:

$$p[DETECT = TRUE | N_A] = \int_0^{N_A} \frac{\lambda_D^{k_D} N_A^{k_D-1} \exp(-\lambda_D N_A)}{\Gamma(k_D)} dN_A$$

Estimates of the parameter values are listed in Table 2.2. Probability of detection curves and experimental data are illustrated in Figure 2.5. Results show that the bighead carp target marker is somewhat easier to detect than the silver carp target marker.

A cPCR assay may produce a false positive result if the PCR reaction amplifies eDNA from a non-target species (Darling and Mahon 2011). Therefore, if a cPCR assay tests positive for eDNA, the amplicons emitting the signal are isolated and sequenced to confirm that their nucleotide sequence matches that of the target species. The QAPP does not prescribe what tolerance (e.g., percent deviation) should be used in accepting or rejecting the nucleotide sequence of amplicons. PCR products were accepted as matching the target marker if a BLAST search executed in GenBank (Benson et al. 2011) indicated that the best available match was the target species. Otherwise, the cPCR replicate was regarded as testing negative for the target marker.

ERDC conducted a series of experiments to estimate the probability of successfully sequencing bighead carp and silver carp markers when the cPCR assay indicated positive detection of the marker (Appendix 2). Experimental results are summarized in Table 2.3. Gamma distributions were fit to the results of the experiment using the method of moments to create functions representing the probability of successful sequencing.

$$p[SEQUENCE = TRUE | N_A] = \int_0^{N_A} \frac{\lambda_S^{k_S} N_A^{k_S-1} \exp(-\lambda_S N_A)}{\Gamma(k_S)} dN_A$$

Estimates of the parameters are listed in Table 2.4. The probability of successful sequencing is illustrated in Figure 2.6, which plots the experimental results and the cumulative probability functions. Results show that silver carp detections were much easier to confirm than bighead carp detections and this appears to be a function of target marker counts in the replicate. Differences in the ability to detect and sequence genetic markers are not uncommon and can be attributed to characteristics of the primer. Relative to the silver carp marker, the bighead carp marker has a low melting temperature in the forward primer and a relatively high self-complementarity in both the forward and reverse primers, which reduces primer effectiveness (Primer3Plus; Untergasser et al. 2007). The silver carp reverse primer also exhibits a relatively high likelihood for self-annealing, but otherwise the forward and reverse primers for this species meet conventional metrics for “good” primers.

The probabilities of detection and successful sequencing can be multiplied to estimate the probability that a PCR replicate tests positive (*POS*) as a function of the number of target markers in the replicate,  $N_A$ :

$$p(REPLICATE = POS | N_A) = p(DETECT = TRUE | N_A) \cdot p(SEQUENCE = TRUE | N_A)$$

The equation assumes that probability of detection and the probability of successful sequencing are independent given the number of target markers in the replicate. This function is illustrated in Figure 2.7, which shows that the joint probability of detection and successful sequencing of bighead carp is considerably lower than that for silver carp. This may help explain why bighead carp detections are rarer in the CAWS than silver carp detections.

The probability of detecting and successfully sequencing the target marker in a cPCR replicate given the source water concentration,  $p(\text{REPLICATE} = \text{POS} | C_M)$ , is:

$$p(\text{REPLICATE} = \text{POS} | C_M) = \sum_{N_A} p[N_A | \mu_{N_A}] \cdot p(\text{REPLICATE} = \text{POS} | N_A)$$

Where,  $N_A$  is a function of  $C_M$  and is estimated by Monte Carlo simulation. Figure 2.8 plots illustrative results of the simulation. The probability of detecting and successfully sequencing bighead carp and silver carp target markers increases as source water concentration increases. For example, results show that, given a source water concentration of 1000 copies/L, the probability of detecting and successfully sequencing the bighead carp target marker is about 0.08, while the probability of detecting and successfully sequencing the silver carp marker is about 0.66. This difference is attributed to the relative difficulty of confirming bighead carp detections by genetic sequencing, as previously discussed.

A cPCR assay typically consists of multiple replicates. The QAPP prescribes eight replicates of a water sample be analyzed to determine whether or not that water sample contains the target marker. Following cPCR, each replicate is examined to determine whether or not a fluorescent signal indicating presence of the target marker is visible. If fluorescence is visible in one or more replicates, the one emitting the strongest signal is selected for genetic sequencing to confirm that the amplicons match the target species. If the sequence matches that of the target species marker, the water sample is positive. If the sequence does not match, or if no replicates produce a fluorescent signal, the water sample is negative.

The greater the number of replicates run, the greater the probability of observing at least one positive replicate and, therefore, observing a positive assay. The probability that at least one replicate in a set of  $k$  replicates will test positive can be calculated:

$$p[\text{ASSAY} = \text{POS} | C_M] = 1 - (1 - p[\text{REPLICATE} = \text{POS} | C_M])^k$$

Figure 2.9 plots the probability of a positive assay for eight replicates. Figure 2.10 shows how the probability of a positive assay varies with source water target marker concentration and the number of replicates used in the assay. For example, if eight replicates are used in the PCR assay and the source water concentration of the target marker is 100 copies/L, the probability of detecting a bighead carp marker is 0.013 and the probability of detecting a silver carp marker is about 0.211. The figure shows that the probability of detecting the target marker increases with both the number of replicates used in the assay and the source water target marker concentration.

The number of replicates or water samples needed to achieve a desired level confidence in the results of the assay can be estimated from the probability of detection model. Table 2.5

shows the number of replicates that would be needed to achieve a detection probability equal to at least 0.50, and 0.95 at selected source water concentrations. At lower target marker concentrations, the number of replicates needed may exceed 100, which is the maximum number of replicates available from a two-liter water sample that is processed and reduced to a 100  $\mu$ l elution. When target marker concentrations are low, multiple water samples may be collected to compensate for low confidence in determining whether the target marker is present in a monitored water body. This model can also assist in evaluating whether or not it is more advantageous to increase the number of water samples or increase the number of cPCR replicates.

This probability of detection model helps explain why different laboratories that analyze the same water sample seem to have so many conflicting results. For example, suppose three laboratories will conduct the assay on portions of the same water sample. This may lead to two laboratories classifying a sample as negative while the third laboratory classifies the same water sample as positive. Discrepancies in classifying water samples as positive or negative can be attributed to a high false negative rate. A false negative occurs when an assay fails to detect the target marker in a sample (or a replicate) that contains the target marker (Darling and Mahon 2011). At low source water concentrations, processing and division of the water sample lead to low copy numbers in PCR replicates, which tends to increase the false negative rate.

This probability of detection model can be used in a variety of different ways to help inform eDNA monitoring programs and to help interpret eDNA monitoring results. For example, the parameters of a sampling program can be established given a reliability objective. Suppose that a reliability objective is expressed in terms of achieving at least a 95 percent probability of detecting a target marker at an ambient concentration of 50 copies per liter. This probability of detection model can be used to calculate the number and volume of water samples and the number of cPCR replicates that would be needed to achieve that objective. The reliability objective specifies the sensitivity of the assay because source water concentrations will not be known a priori.

The volume of source water sampled is an important sampling program parameter because the larger the volume, the greater the probability of capturing one or more target markers, if present. Figure 2.11 shows the effect of sample volume on the probability that a cPCR assay consisting of eight replicates is positive. If source water concentration is 100 copies/L, a cPCR assay consisting of eight replicates has a probability of detection equal to 0.0112 if one 0.4 liter sample is collected, a 0.2090 probability of detection if one 2 liter sample is collected, and a 0.5424 probability of detection if one 4 liter sample is collected.

### **3. eDNA Monitoring Data and Bayesian Inference of Source Water Concentrations**

This section of the report summarizes results of the eDNA monitoring program in the CAWS. These data are used in conjunction with results from a Monte Carlo simulation of the probability of detection model to estimate source water concentrations using Bayesian updating. An understanding of source water concentrations is essential for interpreting the results of an eDNA monitoring program. Concentration estimates provide insights into the distribution of eDNA in the CAWS, which in turn provides a basis for making inferences about the strength and



location of eDNA sources relative to monitoring locations. An example is presented for the North Shore Channel (NSC) to illustrate the method for the purpose of this milestone report. ERDC has completed this analysis for all CAWS reaches and monitoring events.

### *Summary of eDNA Monitoring Data*

Between 2009 and 2013, USACE and its partner agencies, Illinois Department of Natural Resources (ILDNR), US Fish and Wildlife Service (USFWS), and US Geological Survey (USGS) collected and analyzed 7,256 water samples from the CAWS during 78 monitoring events. Data were provided by USACE Chicago District (LRD). Table 3.1 lists the date of each monitoring event. The column labeled “Season” refers to whether or not lock gates were open or closed at the time samples were taken. During winter months, between approximately October 15 and May 31, lock gates are kept closed to limit the volume of water diversions from Lake Michigan. During summer months, between approximately June 1 and October 14, lock gates are kept in the open position to increase flow in the CAWS.

A summary of the eDNA monitoring results is provided in Tables 3.2 and 3.3. These tables show when and in which reaches sampling crews collected water samples and what fraction of the monitoring samples tested positive for bighead carp or silver carp, respectively. For example, during monitoring event #1, on June 29, 2009, sampling crews collected samples in a reach designated CR8 (see next paragraph). Samples stored in coolers that contained control blanks testing positive for either the bighead carp or silver carp target marker were excluded from this analysis. This affected 41 water samples. A blank cell in one of these tables indicates that no samples were collected in that reach on that date. In several cases, no results are listed for a monitoring event. On these dates, sampling crews worked in reaches outside the boundaries of the CAWS. These areas have been excluded from this summary because they are non-contiguous to the study area. Appendix 4 includes similar tables showing the number of samples tested for each species and the number of positive eDNA monitoring samples.

ERDC segmented the CAWS between Lake Michigan and Dresden Lock and Dam into 25 main stem reaches, including four tributaries that represent boundaries of the study area: Lake Michigan (LMI), North Branch of the Chicago River (NBC), Little Calumet River (LCR), and Grand Calumet River (GCR). The location of each main stem reach is described in Table 3.4 and illustrated in Figure 3.1. Since creation of Figure 3.1, CRC has been divided into two reaches. CRU is the upstream portion of CRC that runs from CRB to O’Brien Lock and Dam. CRV is the downstream portion of CRC that runs from O’Brien Lock and Dam to the confluence of the Little Calumet River with the Grand Calumet River at the head of CRD. The principal CAWS tributaries - NBC, LCR, and GCR are shown in Figure 3.1 and listed in Table 3.1 because water samples were occasionally obtained from the downstream portions of these reaches and these reaches are referenced in the table to account for all of the CAWS samples. Samples taken in Lake Michigan near the mouth of the Calumet River during the 2009 and 2010 monitoring season have been assigned to CRA.

Each main stem reach may contain one or more backwaters, or barge slips that are designated by a four-character code: CRAA, CRAB, CRAC, etc. The first three characters identify the main stem reach to which the backwater or barge slip belongs. The fourth character

is assigned sequentially beginning at the upstream boundary of the reach. For example, CRAA is at the first backwater or barge slip encountered as one moves down stream and CRAB is the second backwater or barge slip encountered, etc. Backwaters and barge slips are sub-regions of the main stem reaches. Therefore, when aggregating eDNA monitoring data to make inferences about target marker concentrations, data from each main stem reach – including backwaters and barge slips - is pooled to estimate the frequency of positive detections. When estimating target marker concentrations, estimates of the concentration apply equally to the main stem and to backwaters and barge slips within that reach. In general, there was an insufficient quantity of monitoring data available to support treating the backwaters and barge slips separately from the main stem reaches of which they are a part.

### *Bayesian Inference of Target Marker Concentrations*

The concentration of the target marker in source water can be estimated using Bayesian inference in conjunction with the probability of detection simulation results. This procedure for inference yields an estimate of the target marker concentration in the form of a posterior probability distribution. This characterization of the uncertainty in the concentration becomes refined as observations accumulate over the course of the eDNA monitoring program.

A probability distribution for the target marker concentration in each reach is derived from information on the frequency of positive detections by applying Bayes rule to update a prior distribution on the concentration to a posterior distribution. Bayes rule computes a posterior probability from a prior probability of the hypothesis,  $p[C_M = c]$ , and the likelihood of observing the evidence given the hypothesis,  $p[e|C_M = c]$ :

$$p[C_M = c|e] = \frac{p[e|C_M = c]p[C_M = c]}{\sum_{j=1}^J p[e|C_M = c]p[C_M = c]}$$

The index  $j$  is an index of concentrations and  $C_M$  is the concentration. This posterior probability is the probability of the hypothesis,  $C_M = c$ , given the evidence from eDNA monitoring,  $e$ . As new evidence is obtained in the course of a subsequent monitoring event, this posterior will serve as the new prior distribution on the concentration and the Bayesian updating procedure will be repeated to obtain a revised posterior probability distribution.

The prior probability of the hypothesis is calculated from a prior distribution characterizing uncertainty in the target marker concentration. Before monitoring data are available, a uniform prior distribution is used to represent that there is no prior information about the target marker concentration. A uniform prior distribution has no influence on the outcome of the analysis, although it creates an upper bound on the posterior. The concentration variable is discretized to 601 intervals and the probability of each concentration interval is calculated from the uniform prior distribution:

$$p[C_M = c] = \left( \frac{(c + 2.5) - b}{b - a} \right) - \left( \frac{(c - 2.5) - b}{b - a} \right)$$

The uniform distribution used in this analysis ranges from a lower bound,  $a = 0$ , to an upper bound,  $b = 3000$  copies/L. An upper bound of 3000 was chosen because that concentration is well above the concentrations associated with observed frequencies of positive detections in the CAWS.

The evidence available from the eDNA monitoring program is the fraction of water samples testing positive for target markers of bighead carp and silver carp. The likelihood of observing the evidence given each possible concentration interval is computed from Monte Carlo simulation results taking 50,000 realizations of the model at each concentration interval. The procedure for generating likelihoods is as follows. For each realization of the simulation, generate  $k = 8$  independent realizations of  $N_A$  to represent eight replicates being drawn from the same elution. The probability of detection and successful sequencing is calculated for each replicate and the probability that the cPCR assay is positive is calculated:

$$p[ASSAY = POS | C_M] = 1 - \prod_{k=1}^K (1 - p[REPLICATE_k = POS | C_M])$$

Realizations of the simulation are then binned by  $p[ASSAY = POS | C_M]$  into 100 intervals representing potential frequencies of positive detection. The likelihood,  $p[e | C_M = c]$ , is the fraction of realizations in a concentration interval that fall into a frequency bin. Bayes rule is applied using the calculated likelihood and the prior distribution to derive a probability mass function on the target marker concentration.

Lognormal and gamma distributions were fit to the posterior probability mass functions and mean squared errors for these two distributions were compared. Results of this comparison are summarized in Figure 3.2. Lognormal distributions tended to provide a better fit for silver carp, while gamma distributions tended to provide a better fit for bighead carp. However, gamma distributions tended to fit much better overall. Lognormal distributions resulted in very large errors in reaches where concentrations tended to be very low. Therefore, the gamma distribution was chosen to represent the posterior. A summary of gamma distribution parameters is provided in Appendix 4, as are the 5<sup>th</sup>, 95<sup>th</sup>, and 50<sup>th</sup> percentiles derived from those distributions.

Each time a reach is monitored and a frequency of positive detections is calculated, the Bayes rule can be applied to derive a probability distribution on the target marker concentration. After the initial monitoring event, the posterior probability distribution becomes the prior distribution for the subsequent monitoring event. In this way, information from the monitoring program accumulates over time. An example is presented to illustrate the value of this approach.

#### *Target Marker Concentrations in the North Shore Channel (NSC)*

The Bayesian updating approach to interpreting evidence from eDNA monitoring is demonstrated for the North Shore Channel (NSC). The NSC was sampled sixteen times between 2009 and 2013 (see Table 3.3). Prior to the first monitoring event, a uniform prior distribution characterizes beliefs about the concentration, the median concentration is 1500 copies/L and the 90 percent confidence interval ranges from 145 to 2855 copies/L. This prior represents the best

available information about the concentration until the first monitoring samples are collected during monitoring event #13, on October 22, 2009 (see Table 3.2). During monitoring event #13, no bighead carp target markers were detected in the NSC, but the frequency of positive detections for silver carp was 0.1111. Bayes rule is applied to update the prior distributions representing uncertainty in the concentrations. As shown in Table 3.5, uncertainty in the bighead carp target marker concentration is updated to a median of 103 copies/L with a 90 percent confidence interval of 0 – 1076 copies/L. Uncertainty in the silver carp marker is updated to a median of 214 copies/L with a 90 percent confidence interval of 5 – 1315 copies/L.

The prior distribution is updated each time the reach is monitored. The next time water samples were collected in the NSC was on April 20, 2010, during event #21. No samples tested positive for the bighead carp target marker, but the frequency of positive detections for silver carp was 0.0149. These results reinforce belief that bighead carp target marker concentrations in the reach are low, and the median concentration is updated to 42 copies/L and a 90 percent confidence interval from 1 to 277 copies/L. Similarly, new information on the frequency of positive detections for the silver carp target marker is used to update the estimate of the median concentration to 110 copies/L with a 90 percent confidence interval from 13 to 394 copies/L (Table 3.5). This process of updating the characterization of uncertainty in the concentration continues each time the reach is monitored. Figures 3.3 and 3.4 plot the evolution of population distribution functions (PDFs) characterizing uncertainty in the concentrations.

Median target marker concentrations and confidence bounds for each monitoring event are illustrated in Figure 3.5. The estimated median of the target marker concentration decreases through the third monitoring event. During event #38, one out of 110 water samples tested positive for the bighead carp target marker. This caused the estimate of the median concentration to nearly double, from 29 copies/L to 52 copies/L. Following that monitoring event, the NSC was sampled another twelve times, but the bighead carp target marker was not detected again, so estimates of the median concentration decrease from 52 copies/L to 13 copies/L. However, the rate of decrease after event #38 is greatly reduced because of that single positive water sample.

In the preceding example, the last posterior probability distribution is carried forward as the prior distribution for the next iteration of Bayesian updating because it represents the best available information about the concentration. The implication is that there is a single concentration to be characterized in the reach and that concentration remains the same over the period that posterior probability distributions are carried forward. This approach will not reveal seasonal differences in the concentration and cannot be used to identify trends in the concentration over time. An alternate approach might be to recognize that there are two distinct hydrologic seasons in the CAWS (seasons) and, because hydrology exerts a strong influence on concentrations, there may be two distinct concentrations to be estimated. Taking this approach, one would divide each year into two averaging periods, or seasons. At the end of each season, the last posterior in each reach would be carried forward as the prior distribution at the beginning of that season in the following year.

The alternate Bayesian updating procedure described has been implemented to characterize target marker concentrations in each reach during two seasons of interest: “Gates

Open” and “Gates Closed.” Sluice gates in the NSC are opened about June 1 to divert water from Lake Michigan and increase flow in the system. Sluice gates are closed about October 15<sup>th</sup> to limit diversions from Lake Michigan. This creates a substantially different environment because flows in the upper NSC will tend to be much higher during the gates open season, creating a dilution effect that reduces concentrations. If the eDNA source were local to the NSC, one might expect that concentrations would tend to be lower during the gates open season than the gates closed season because water diversions into the reach tend to dilute the system. Alternatively, if eDNA loads are associated with inflows to the reach, one might expect that concentrations would tend to be higher during the gates open season.

An example is provided for the NSC. Figure 3.6 shows the PDFs for seasonal target marker concentrations in the NSC after the final monitoring event of each season. The last monitoring event during the gates open season was #75, on June 19<sup>th</sup>, 2013. The last monitoring event during the gates closed season was #78, on November 7, 2013. For bighead carp, the concentration during the gates closed season appears to be slightly higher than it was during the gates open season. The lower concentration during the gates open season might be an indication of dilution caused by increased flow; however, this conclusion is not reinforced by a similar result for silver carp. Results for silver carp show that the gates open and gates closed concentrations are similar. A closer look at the data shows that the effect can be attributed to a single bighead carp target marker detection during the gates closed season, which shifted the distribution. Another interpretation, which is based on a frequentist interpretation of the posterior distributions, is that there is no statistically significant difference in the two seasonal concentrations.

The alternate Bayesian updating procedure described here is motivated by an interest in characterizing target marker concentrations on a seasonal basis to reveal how target marker concentrations might be influenced by differences in the hydrologic regime. However, this example also serves to underscore the difficulty of making inferences using the Bayesian approach when sampling frequency and intensity are low (*e.g.*, the single detection of bighead carp eDNA). A second concern with implementing the Bayesian approach on a seasonal basis is that monitoring efforts during the gates closed season tend to be less frequent and to occur either at the very beginning of the gates closed season, in the late fall, or toward the very end of the gates closed season, in the early spring. Although the hydrologic regime is similar in both cases, non-hydrologic environmental forces influencing the system may be very dissimilar. For example, there may be temporal differences in temperature or secondary source loads that do not coincide with gates open and gates closed conditions.

Other issues arise when applying the Bayesian inference procedure to eDNA monitoring results in general. A prior distribution must be chosen. This study adopts a uniform prior distribution between 0 and 3000 copies/L, which implies a strong a priori belief that the target marker concentration is non-zero ( $> 0.998$ ). This choice could be justified by prior knowledge that a target marker had previously been detected in a monitored water body. Another issue is choice of the upper bound of the prior distribution on the concentration. In this study, the upper bound represents a point that is well above the ambient concentrations suggested by the frequencies of positive detection. The reason for this is that, as the frequency of positive detections approaches one, the ability to make meaningful inferences diminishes and the choice

of the upper bound on the prior begins to exert a strong influence on the concentration estimate. The question remains, when beginning a study in a location where the target species eDNA has not previously been detected, what prior distribution should be used?

#### 4. Precursors to Modeling the Fate and Transport of eDNA

This section of the report describes the characterization of several variables that are pertinent to modeling the fate and transport of eDNA in the CAWS. These variables include primary eDNA loading rates, secondary eDNA loading factors, and the eDNA degradation rate. The purpose of an eDNA fate and transport model is to facilitate inferences about the location and strength of eDNA sources in the CAWS.

##### *Primary Source Loading Rates*

A primary source of eDNA is a live bighead carp or silver carp. Live bighead carp and silver carp release DNA into the environment through bodily excretions such as feces, urine, sperm, eggs, and shed cells. Data from Klymus *et al.* (2013), who measured eDNA loads from juvenile (60-100 mm) and sub-adult (100 -300 mm) fish in the laboratory, are used here to estimate a primary source loading rate. Data were transformed using natural logarithms and linear regression was applied to estimate the shedding rate (copies/hr) as a function of fish weight (grams):

$$\hat{s} = 0.9432 \ln(w) + 9.1789$$

(0.0435)                      (0.2059)

The adjusted  $R^2$  is 0.9086. Standard errors are given in parentheses. Figure 4.1 plots the data, the estimate, and the 95 percent confidence bounds. This function can be used to estimate the target marker load from a unit weight of fish. For example, the mean shedding rate from one kilogram of sub-adult fish would be  $13.99 \times 10^6$  copies/hr and the standard error is  $10.37 \times 10^6$  copies/hr. The 90 percent confidence bound on the estimate ranges from 2.5 – 52 million copies/hr. A probability distribution characterizing the shedding rate distribution is shown in Figure 4.2.

##### *Target Marker Degradation Rate*

Most investigators tend to agree that eDNA degrades rapidly in the environment, and this has provided one of the primary justifications for inferring target species presence at the study site where eDNA is detected (Ficetola *et al.* 2008, Jerde *et al.* 2011). Degradation of eDNA occurs by hydrolysis and may be influenced by environmental conditions, such as temperature, pH, microbial activity, and light or ultra-violet radiation. Matsui *et al.* (2001) reported that extracellular DNA fragments up to 400 base pairs (bp) in length can persist for up to one week in lake water at 18 deg. C (Ficetola *et al.* 2008). Thomsen *et al.* (2012a) found that even small eDNA fragments, up to 100 bp in length, degrade beyond detectability within days. Dejean *et al.* (2011) quantified extracellular DNA degradation rates using American bullfrog tadpoles and Siberian sturgeon (*Acipenser baerii*) sub-adults (20 cm); these authors found that DNA could be detected in more than five percent of samples for up to 25 and 17 days, respectively. However,

DNA fragments may persist in the environment for very long periods of time. Adsorption to mineral and humic substances protects the DNA from extracellular microbes that would otherwise degrade unbound DNA in solution (Levy-Booth *et al.* 2007). Very cold conditions can also retard degradation. Willerslev *et al.* (2004) report that eDNA may persist for several hundreds of thousands of years in very cold environments (Dejean *et al.* 2011, Thomsen *et al.* 2012).

ERDC conducted a series of laboratory experiments to evaluate how quickly the bighead carp and silver carp target markers degrade in the environment. These studies are described in (Lance *et al.*, 2013). Degradation rate trials that were carried out under conditions simulating those that might actually be encountered in the CAWS were used to estimate degradation rates for the water quality model. Patterns in the data suggested the existence of two eDNA fractions: a larger fraction that degrades relatively quickly and a smaller fraction that degrades relatively slowly. Each fraction was assumed to follow a first-order decay pattern:

$$C(t) = C_0 \cdot e^{-k \cdot t}$$

in which:

$C(t)$  = copies at time  $t$

$C_0$  = initial copies at  $t = 0$

$k$  = decay rate ( $d^{-1}$ )

The relationship was linearized to facilitate determination of  $C_0$  and  $k$  through linear regression:

$$\ln(C) = \ln(C_0) - k \cdot t$$

The duration of the trials was 14 to 28 days with sampling more frequent during the initial portion of each trial (e.g. 0, 1, 2, 3, 5, 7 days). Inspection of the data indicated the initial rapid decay phase lasted three to five days (see Figure 4.3a). The “fast” decay rate was determined through consideration of the data from the first three days of each trial. The “slow” decay rate was determined through consideration of the data commencing on day five. The regressions provided estimates of the initial concentration of each fraction (as the intercept of the linearized equation). The “fast” fraction of the total eDNA,  $F(\text{fast})$ , was determined from the estimated initial concentrations:

$$F(\text{fast}) = \frac{C_0(\text{fast})}{C_0(\text{fast}) + C_0(\text{slow})}$$

The “slow” fraction was determined as  $1 - F(\text{fast})$ .

Table 4.1 reports estimates of the slope parameter for the fast and slow eDNA fractions, and an  $R^2$  for each regression. Parameter estimates for the fast eDNA fraction are listed in Table 4.3 and were highly significant ( $p < 0.01$ ). These results indicated that roughly 80 percent of the initial eDNA was in the “fast” fraction. The fast fraction has a mean decay rate of  $0.456 d^{-1}$ . Estimates of the slow decay rate parameter were highly significant ( $p < 0.01$ ) for some trials, but insignificant for others. The mean of significant decay rates for the slow fraction was  $0.089 d^{-1}$ .

Uniform distributions were fit to the estimated decay rates to characterize uncertainty in these values. The mean and standard deviation of these distributions are summarized in Table 4.2. The mean of the fast decay rate calculated from the distribution was  $0.463 \text{ d}^{-1}$  and the mean of the slow decay rate calculated from the distribution was  $0.079 \text{ d}^{-1}$ . The decay rate can also be interpreted as a half life, which is the length of time required for one half of the substance to decay. The mean half-life is 1.5 days for the fast fraction and 8.8 days for the slow fraction.

### *Loading Factors for Secondary Sources*

A source of eDNA is an object, event or activity that could release bighead carp and silver carp eDNA into the CAWS. Live fish are classified as primary sources of eDNA. All other sources are classified as secondary sources. Potential secondary sources in the CAWS include: 1) piscivorous bird feces, 2) combined sewer overflows (CSOs), 3) Lake Michigan inflows, 4) Mud-to-Parks Program sediment, 5) commercial navigation, 6) commercial fishing nets, and 7) recreational fishing derbies. In previous reports, ECALS has documented the potential for each of these sources to transport bighead carp and silver carp eDNA (ECALS 2013, Merkes et al. 2014). Any one or a combination of these secondary sources could explain the presence of eDNA in the CAWS.

This section of the report documents estimation of loading factors for each of the potential secondary sources in the CAWS. A loading factor is a measure of the occurrence or intensity of each secondary source in each reach. In subsequent analysis, ECALS will implement an inverse modeling procedure, Bayesian Markov Chain Monte Carlo (MCMC), to estimate loading rates for each secondary source. A loading rate is the amount of target marker released per unit loading factor (copies/loading factor). Table 4.1 lists the loading factors that are described in this section and the loading rates that will be estimated.

#### *a. Piscivorous bird feces*

Fish-eating birds are common in the CAWS. Species include double-crested cormorant (*Phalacrocorax auritus*), American white pelican (*Pelecanus erythrorhynchos*), great blue heron (*Ardea herodias*), great egret (*Ardea alba*), bald eagle (*Haliaeetus leucocephalus*), and osprey (*Pandion haliaetus*) (ECALS 2013). The double-crested cormorant is believed to be the most common of the piscivorous bird species. There are at least three large colonies of cormorants located in and around the CAWS: Baker's Lake, Lake Renwick, and ArcelorMittal Steel Mill (Figure 4.4). ECALS obtained throat and cloacal swabs from fifteen cormorants at Baker's Lake rookery during the 2012 field season and found that eight (47 percent) tested positive for either bighead carp or silver carp eDNA (Guilfoyle et al. 2013, ECALS 2013). Other ECALS studies, conducted by USGS, showed that bighead carp and silver carp eDNA could be detected in the fresh feces of captive cormorants up to seven days after their last meal of carp and in dried feces that were left outside, exposed to the elements, for up to 30 days after defecation (ECALS 2013).

Birds are often implicated as a source of water quality problems. A number of authors have developed models to estimate the portion of nutrient loads that can be attributed to avian fecal deposits (Scherer et al., 1995, Hahn et al., 2007). These models require reliable estimates



of bird populations, diet, fecal composition, and spatial and temporal patterns of fecal deposition. These data were not available for the study area. Because data on bird populations in the study area are limited, the approach used here is to assume that bird feces will be distributed to CAWS reaches in proportion to the surface area of those reaches. The implicit assumption in this approach is that birds are distributed randomly throughout the CAWS and do not prefer some locations of the CAWS over others.

The loading factor for birds is defined as the surface area available to receive fecal deposits that may contain bighead carp and silver carp eDNA. Loading rates from birds will be estimated from Bayesian MCMC as eDNA copies/m<sup>2</sup>. Reach surface areas are provided in Table 4.4. There are 19 main stem reaches. If backwater or barge slips are present in the reach, the reach is sub-divided into a main stem portion and a set of backwater and barge slips, indexed from A to L.

*b. Combined sewer overflows (CSOs)*

The City of Chicago wastewater system is a combined sewer system in which sanitary and storm flows are conveyed in the same pipes. When the capacity of the system is exceeded during major storm events, untreated wastewater may be discharged directly into the CAWS. Figure 4.5 shows the locations of CSO discharge points in the CAWS. Studies by ECALS in 2011 and 2012 documented the presence of both bighead carp and silver carp DNA in combined sewer discharge to the CAWS (ECALS 2012). The origin of this DNA is uncertain; however, Asian carp is a feature in the diet of ethnic communities and is sold in Asian fish markets in the Chicago area. Bighead carp and silver carp DNA may have entered the combined sewer system through storm drains near fish markets that sell Asian carp. Fish markets often display and store fish on ice that must be periodically changed during the day as the ice melts. Melted “slushy” ice that is dumped onto streets and parking lots may eventually enter the storm sewer system that leads to the CAWS. Bighead carp and silver carp DNA may also enter the combined sewer system in household kitchen waste.

The loading factor for CSOs is CSO discharge volume. ECALS obtained data on the volume of combined sewer discharges from Metropolitan Water Reclamation District (MRWD), Chicago. Table 4.5 lists seasonal CSO discharge volumes to the CAWS for calendar years 2009 through 2012. Overflow volumes were calculated by MWRD at individual CSO outfalls based on rainfall and drainage area. ECALS aggregated the CSO discharge volumes by reach and season.

*c. Inflows to the CAWS from Lake Michigan*

The CAWS is the principal hydrologic connection between the Mississippi River Basin and Lake Michigan. The Illinois River, a tributary of the Mississippi River, is connected to Lake Michigan via the CAWS. The CAWS was constructed in the late 1890’s to transport sewage from the City of Chicago away from Lake Michigan, the source of the city’s drinking water (Changnon et al. 1996, MWRD 2008). Water is diverted from Lake Michigan to help maintain flow and flush the system, particularly in summer months. Because flows in the CAWS are from Lake Michigan towards the Illinois River, any substances that are suspended or dissolved in Lake Michigan water may enter the CAWS.

Water from Lake Michigan is diverted into the CAWS at three locations in the Chicago area. A sluice gate at the Wilmette Pump Station near Evanston, IL, allows water to flow from Lake Michigan into the NSC. The Chicago River Controlling Works (CRCW) controls the diversions of water from Lake Michigan into CRM. Diversions of water into the Calumet River at the head of CRA are controlled by lock gates at TJ O'Brien Lock and Dam.

The presence of silver carp eDNA in Lake Michigan has been documented through a single positive eDNA sample collected on December 8, 2009. The University of Notre Dame, working under contract to the US Army Corps of Engineers Chicago District, collected three water samples near the north slip, between Park #566 and Park #523, about 850 m north of the Calumet River entrance. One of these three samples tested positive for silver carp eDNA. Samplers returned to this site on March 30, 2010, to collect five more samples. No bighead carp or silver carp eDNA was detected in these samples. Samplers returned again on July 20, 2010, and took another 17 samples from the area in Lake Michigan between the Calumet River entrance and the breakwater. No bighead carp or silver carp eDNA was detected in these samples.

The loading factor for inflows to the CAWS is diversion volume ( $\text{m}^3/\text{day}$ ). Data on diversions of water from Lake Michigan were obtained from MRWD. These data are listed in Table 4.6. Inflows from other tributaries to the CAWS, such as the North Branch of the Chicago River and the Grand Calumet River, were not considered to be a potential source of bighead carp or silver carp eDNA in the CAWS.

*d. Mud-to-Parks Program sediment*

The Mud-to-Parks Program transports dredged material from the Illinois River near Peoria, IL to brownfield sites near Chicago, where the goal is to reclaim former industrial lands by improving soil conditions. Dredged material is loaded into barges and transported from Peoria to the deposition site, where it is offloaded (Marlin 2004). Since 2001, deposition has occurred at three locations: the Paxton 1 Landfill, Park 523, and Park 566. The Paxton 1 Landfill, a former Superfund site, is located near the shores of Lake Calumet (Marlin 2003). Parks 523 and 566 are located at the former US Steel South Works manufacturing site on the banks of Lake Michigan, just north of the Calumet River entrance. In 2013, ECALS tested samples of dredged material from one of the barges that was waiting to be offloaded in the North Slip, which separates Parks #523 and #566. Bighead carp and silver carp eDNA was detected in the Mud-to-Parks sediment. It should also be noted that the positive detection of silver carp eDNA in Lake Michigan (described in the preceding section) occurred in the North Slip. This detection occurred in 2009, one to two years after deposition to Park #566 in 2007.

It is not clear how eDNA attached to sediment would make its way into the CAWS. Mud-to-Parks program managers report that berms to prevent surface erosion from the park sites have been constructed, but occasional strong rains can cause runoff from these sites. It is also possible that eDNA attached to sediment might leach through the porous soil layer into groundwater and then mingle with water from Lake Michigan or the CAWS. While these are conceivable routes of entry into the CAWS, representation of these processes in water quality

models developed to support the probabilistic modeling effort is difficult. Those models contain no representation of the boundaries with deposition sites because they are not contiguous with the hydrodynamic grid. In addition, the bulk of any eDNA load would be to Lake Michigan rather than the CAWS. Once eDNA has become mixed in the Lake Michigan water column, it is impossible to distinguish it from eDNA that was released from other sources that may also be contributing to Lake Michigan.

No loading factors are calculated for Mud-to-Parks program sediment because it appears that any eDNA attached to sediment would move from the parks into Lake Michigan, where it could not be distinguished or tracked in the water quality models before entering into the CAWS. Therefore, loads associated with the Mud-to-Parks program are confounded with any other sources that may be contributing load to Lake Michigan inflows these sources could not be identified or distinguished in this analysis. If Mud-to-Parks Program sediment is contributing eDNA load to the CAWS, it will be classified as part of the Lake Michigan eDNA load.

*e. Commercial navigation*

Commercial navigation is likely to be a secondary source of eDNA in the CAWS. In the past, commercial vessels have been sighted travelling north through Lockport Lock and Dam and the electric fish barrier with silver carp carcasses on their decks (ECALS 2013). If carcasses are disposed of in the waterway above the fish barrier, rotting carcasses may become a source of eDNA that is detectable in monitoring samples. Regulations are now in place that require crews to clear all fish carcasses from their decks prior to passing through the electric fish barrier. There is evidence that eDNA can also adhere to barge hulls. ECALS conducted a study to investigate the hypothesis that eDNA could be transported on commercial boat and barge hulls by obtaining DNA swabs from 20-foot commercial fishing boats and agency fishing boats. The swabs tested positive for both bighead carp and silver carp DNA (ECALS 2014, Merkes et al. 2014). Commercial vessels may become a source of eDNA if slime residue washes off of the hulls as the vessels move through the water.

ERDC created a loading factor for commercial navigation that represents the residence time of commercial vessels in each CAWS reach. Loading factors are estimated from National Automatic Information System (NAIS) data collected by the US Coast Guard between 2009 and 2013. The NAIS collects information about commercial vessel movements in real time to identify each vessel and determine its location at six second intervals. This information is stored by NAIS so that vessel position can be tracked. Data are collected as follows. Commercial vessels are required to have an Automatic Identification System (AIS) transponder on board and to transmit information about their identity and location. Transceivers are located along waterways (*e.g.*, on the shore or on top of lock and dam structures) to receive data from each vessel as it passes within range. Data are compiled and stored by US Coast Guard in real time.

ERDC analyzed historic records of AIS transmissions from commercial vessels operating in the CAWS and created a database summarizing commercial navigation traffic in each reach. The database includes information on:

- Entrance time into reach,
- Exit time out of reach,

- Residence time in reach,
- Whether or not the vessel went below Dresden Lock and Dam,
- Stop order of vessel since being downstream of Dresden Lock and Dam,
- Time since vessel had been downstream of Dresden Lock and Dam,
- Whether or not the vessel went below the electric fish barrier,
- Stop order of vessel since being downstream of the fish barrier,
- Time since vessel had been downstream of the fish barrier,
- Vessel path through reach.

The stop order keeps track of how many times a vessel enters a reach after having been downstream of a reference point. Records for individual vessels are then aggregated by year, season, and transit history (whether the vessel had been below Dresden within the past three months) to create a composite residence time for all vessels in the reach. The composite residence time is an indicator of the intensity of navigation traffic in each reach and is used in this study as a loading factor. Table 4.8 reports the composite residence time in each reach for 2012 and 2013. Prior to 2012, AIS data from the CAWS are incomplete, so composite residence times could not be calculated for the period 2009 – 2011. Composite residence times from 2012 were applied to these years.

Navigation records are incomplete for calendar years prior to 2012 because NAIS was still in the process of being implemented and coverage was incomplete. During the phase-in period, not all commercial vessels were equipped with transponders or were required to transmit AIS signals, and some vessels equipped with transponders may not have operated those transponders while in the CAWS. Records may also be incomplete because of failures on the receiving end, as well. During the phase-in period, transceiver coverage in the CAWS may have been sparse and it is possible that some transceivers may not have been functioning properly. These factors affect the quality of the data used in this study. Table 4.8 does not report results for years prior to 2012 because NAIS was being phased-in during that period.

The accuracy of the navigation records can be evaluated by determining the vessel sampling rate, the ratio of the number of vessel trips that NAIS records to the sample size, which is the number of vessel trips that a second qualified sensor records during the same time period. If the probe sample size is less than one, NAIS is missing vessel trip counts. The sample size used in this study to evaluate the accuracy of NAIS records includes commercial vessels only. Recreational vessels and vessels with non-staff passengers are excluded from the sample. The identified source of the “ground truth” number of vessels for years 2009, 2010, and 2011 is The Great Lakes and Mississippi River Basin Study (GLMRIS) Report (USACE 2014). The identified source of this data for years 2012 and 2013 is the U. S. Army Corps of Engineers Lock Performance Monitoring System’s (LPMS) lockage reports. Vessel counts were compiled from lock-master reports at Dresden Lock and Dam, Lockport Lock and Dam, and T. J. O’Brien Lock and Dam. Reports were not compiled for Chicago Lock and Dam because commercial navigation traffic accounts for a small fraction of the lockage at that location.

The commercial vessel sampling rate at each location is reported by month for calendar years 2012 and 2013 in Table 4.9. The sample size used in calculating these sampling rates were obtained from monthly LPMS reports for 2012 and 2013. Monthly LPMS data were not available for prior years. Table 4.9 shows that the completeness of the navigation data tends to

be greater at some locations than at others, and tends to improve at all locations over time. Table 4.10 reports the commercial vessel sampling rate on an annual basis, from 2009 through 2013. The sample size used in calculating these sampling rates were reported on an annual basis in USACE (2014). USACE (2014) did not report sample size at Dresden Lock and Dam. The table shows that no commercial vessels were tracked by AIS during 2009 and 2010, and that fewer than half of vessels were tracked by AIS in 2011.

*f. Commercial fishing nets*

Following detection of eDNA in the CAWS in 2009, the Monitoring and Response Work Group (MRWG) was established to carry out a conventional fisheries surveillance program in the CAWS. The goal of this program is to document the presence of Asian carp, determine their relative abundance and distribution, and develop information on non-target fish species in the CAWS. The MRWG is a collaborative effort of the ILDNR and USFWS Columbia, Carterville, and La Crosse Fish and Wildlife Conservation Offices (MRWG 2013). Since 2010, MRWG has implemented three distinct sampling programs upstream of the electric fish barrier. The Fixed and Random Site (FRS) monitoring program deploys standardized fishing gear on a scheduled basis at a set of regularly sampled (e.g., fixed) sites, where bighead carp and silver carp are likely to be found, and at randomly selected sites throughout the CAWS. Between 2010 and 2012, MRWG also implemented a Rapid Response (RR) program. The purpose of the RR program was to apply intense fishing effort at locations where the eDNA monitoring program had detected bighead carp or silver carp eDNA with the goal of capturing the source, which seemed likely to be a live fish. Although not preceded by detection of bighead carp eDNA upstream of O'Brien Lock and Dam, one bighead carp was captured in Lake Calumet in July, 2010. No bighead carp or silver carp have been captured in the CAWS since then. In 2013, the RR program was changed to a Planned Intensive Sampling (PIS) program. The PIS program puts less emphasis on responding quickly to eDNA detections and more emphasis on planning and agency coordination to maximize the effectiveness of the fishing effort.

The most common gear types used in MRWG's conventional surveillance programs are electrofishing boats and commercial gill nets and trammel nets. When fish are captured, blood, slime, feces, and epithelial tissue accumulate on the monofilament nets over time and some of this material will wash off the net when it is rinsed. Prior to May 4, 2013, commercial nets and fishing boats that had previously been used to capture bighead carp and silver carp in carp infested waters were also being used to implement the FRS, RR, and PIS programs upstream of the electric fish barrier. Thus, it is possible that eDNA detected in monitoring samples could have been introduced into the CAWS through these conventional surveillance programs.

ERDC conducted a study to determine whether or not bighead carp and silver carp DNA could be detected in water used to rinse gill nets and trammel nets (ECALS 2014). Bighead carp and silver carp DNA were detected in rinse water and the number of copies in net swatches of known size was estimated using qPCR. Results showed that a single fishing net, 300 ft by 13 ft in length, can hold tens to hundreds of billions ( $4.0 \times 10^{10}$  to  $3.56 \times 10^{11}$ ) of copies of a target marker. Fishing nets that had been kept in storage for five months prior to testing also tested positive for bighead carp and silver carp target markers. These nets had target marker counts in the millions ( $1.5 \times 10^6$  -  $13.4 \times 10^6$ ). The hulls of five commercial fishing boats were also tested

for bighead carp and silver carp eDNA. DNA swabs from 25 cm<sup>2</sup> sections of boat hull immediately following fishing activity contained thousands to tens of thousands ( $3.5 \times 10^3$  -  $54.7 \times 10^3$ ) of target marker copies. After the boat hulls were washed, target marker counts ranged from 10 to ten thousand copies ( $9 \times 10^0$  -  $1.2 \times 10^3$ ), depending upon what cleaning procedures had been applied. ERDC estimates that the hull of a single 24 ft aluminum boat could contain tens to hundreds of millions ( $3.3 \times 10^7$  -  $51.2 \times 10^8$ ) of target markers immediately after fishing and from several thousand to hundreds of millions of copies ( $8.6 \times 10^4$  -  $1.08 \times 10^8$ ) after cleaning and DNA removal procedures.

The loading factor that best characterizes commercial fishing boat and net use in the CAWS is the length of gill or trammel net deployed during the monitoring period. The loading factors used in this analysis are calculated from information provided by ILDNR in a database describing the date, time, location, and level of fishing effort in the CAWS. Table 4.11 shows the length of commercial gill and trammel net deployed by reach, as reported by ILDNR. The database contained no information on the distribution of FRS sampling in 2010 and no information on RR sampling effort during the period 2010 through 2012. ERDC used 2011 fishing effort to estimate the level of effort in 2010 as follows. MRWG (2012) reports 23.8 miles (383.02 100-meters) of commercial fishing nets were set in the course of FRS monitoring between June and September, 2010. The corresponding FRS effort between June and September 2011 is 474.12 100-meters. ERDC took the gear set records from June through September 2011 at their reported locations and weighting the effort by 0.80785, which is the ratio of 383.02 and 474.12. In calculating the loading factors for this source, ERDC excluded all commercial gill net and trammel nets used after the use of potentially contaminated gear was discontinued on May 4, 2013. Although other types of gear have also been deployed, this loading factor emphasizes gill and trammel nets because they are, with the exception of electrofishing boats, the most commonly deployed gear type used in these programs. Rapid response fishing effort and the distribution of fishing effort over time and space was based on annual summary reports provided in MRWG reports (MRWG 2012, MRWG 2013a).

*g. Recreational fishing derbies*

Recreational boats are widely used throughout the CAWS and may be a secondary source of bighead carp and silver carp eDNA. Types of recreational boats used in the CAWS include fishing boats, sailboats, yachts, and crew boats for sculling or rowing. As with boats used in commercial navigation and in conventional fisheries surveillance programs, recreational boats may become contaminated with eDNA through contact with carp-infested water. The boat may transport this eDNA to carp-free waters where it washes off the hull and becomes available for transport in the water column. No generally applicable loading factor capable of characterizing the spatial and temporal variability of all recreational boating activity in the CAWS was identified.

This study focuses on recreational fishing boats as a potential secondary source of eDNA in the CAWS. Lake Calumet and the Calumet-Saganashkee (Cal-Sag) Channel are popular fishing destinations. The loading factor for recreational fishing boat activity in the CAWS is based on fishing tournaments. ILDNR compiled data from fishing tournament permit applications for the period 2012 – 2014. Data are summarized in Table 4.11. Permit

applications state the date and location of the event, the number boats expected to participate in the event, and the launch site. If the number of entrants is given as a range, the upper bound is assumed and if the number of entrants is not listed, ten entrants is assumed. A recreational boat day occurs in a reach if a fishing tournament entrant would need to transit through any portion of that reach in order to access the fishing site from the official launch site. Table 4.12 summarizes loading factors for 2012 – 2014 by season and the three-year mean loading factor for each reach. Loading factors for 2012 were used to represent the intensity of recreational fishing activity for 2009-2011 because no records of fishing derby permits were available for those years.

## **5. A Model to Simulate eDNA Fate and Transport**

This section of the report describes progress in modeling the transport and fate of eDNA in the Chicago Area Waterways System (CAWS). Three individual models are in use for these purposes. The first is a three-dimensional hydrodynamic model that computes transport processes with a high degree of spatial and temporal resolution. Transport processes from the hydrodynamic model are provided to a fate and transport model which computes the concentration of eDNA as a function of loading, decay, and other influences. The hydrodynamic and fate and transport models have subsequently been abstracted into a simplified steady-state model, which is used in the following section of this report to make inferences about loading rates from potential eDNA sources in the CAWS.

### *The Hydrodynamic Model*

Transport processes in the CAWS are computed with the CH3D-WES hydrodynamic model. CH3D-WES is a general-purpose hydrodynamic model for use in lakes, rivers, estuaries, and coastal waters. The model provides computations of surface level, velocity, vertical diffusion, temperature, and salinity. The model operates by computing numerical solutions to the basic equations of continuity, motion, and mass conservation (Johnson et al., 1991).

Numerical solutions to the governing equations are determined by the finite-difference method on a computational grid which represents the CAWS as a network of discrete volumes or cells. A curvilinear non-orthogonal coordinate system is used in the horizontal plane. In practical terms, this feature optimizes the fit of the grid to complicated geometries. A Z-plane coordinate system, in which the number of layers varies according to local depth, is used in the vertical direction. Thickness of all layers is constant except for the surface layer which varies according to surface level at the system boundaries, wind stress, and other factors.

The system is represented on two independent grids. The first grid (Figure 5.1) extends from Wilmette through the Chicago Sanitary and Ship Canal (CSSC) down to Lockport. A branch extends through the Cal-Sag Channel to the O'Brien Lock and Dam. Properties of this grid include:

- 4,428 surface cells
- 22,678 total cells
- 3 to 8 layers in vertical
- average grid cell is 30 x 60 m in extent

- surface layer = 2 m thick at mean surface level
- sub-surface layers = 1 m thick

Forcing functions for the computed hydrodynamics include flows at Wilmette, the Chicago River Control Works (CRCW), O'Brien Lock and Dam as well as major water reclamation plants (WRP's), pumping stations, and combined sewer overflows (CSO's). The time step for the numerical solution is on the order of seconds.

The second grid (Figure 5.2) extends from Lake Michigan to O'Brien and includes Lake Calumet. The two independent grids are necessitated by the configuration and operation of the O'Brien Lock and Dam. The geometry, lock operations, and gate operations cannot be represented in a spatially-continuous hydrodynamic model. Characteristics of the second grid include:

- 1,236 surface cells
- 4,579 total cells
- 1 to 8 layers in vertical
- average grid cell is 40 x 80 m in extent
- surface layer = 2 m thick at mean surface level
- sub-surface layers = 1 m thick

Hydrodynamics in this section are forced primarily by surface level in Lake Michigan and by operations at O'Brien. Care was taken to match flows at O'Brien to records and to flows specified as boundary conditions on the first grid. As with the first grid, the time step for numerical solution is on the order of seconds.

Hydrodynamic simulations were completed on two grids for the individual years 2009 – 2012. A series of quality control checks were conducted to ensure the forcing functions and boundary conditions were correctly implemented and the results were satisfactory. The checks included:

- Compare computed flows to records at major control structures
- Compare implemented inflows to records at major WRP's
- Compare computed flow to United States Geological Survey gauge at Lemont

The results satisfied these and other quality control checks. Transport information was stored for subsequent use by the fate and transport model.

#### *High-Fidelity eDNA Fate and Transport Model (HFFTM)*

The transport and fate of eDNA are computed using the CE-QUAL-ICM (or simply ICM) water quality model. ICM is a flexible, widely-applicable water quality model which finds its most frequent use in the examination of eutrophication problems (e.g. Cerco et al., 2010). The foundation of CE-QUAL-ICM is the solution to the three-dimensional mass-conservation equation for a control volume. Control volumes correspond to cells on the model computational grid. Solution to the mass-conservation equation is via a finite-difference method. The time step



for numerical integration is determined by stability requirements but is usually on the order of seconds to minutes. Transport information is provided by the hydrodynamic model at hourly intervals.

ICM incorporates a suite of more than thirty state variables that can be implemented individually or in combination. Substances that are not represented in the standard suite can often be substituted for one of the standard variables or else included via minor code modifications. The following state variables are included in the simulation of eDNA fate and transport.

*a. eDNA*

eDNA is quantified as copies per m<sup>3</sup> (or copies m<sup>-3</sup>). Decay is represented as a first-order process:

$$\frac{\delta}{\delta t} eDNA = -k \cdot eDNA$$

in which:

eDNA = extracellular DNA (copies m<sup>-3</sup>)  
k = first order decay rate (d<sup>-1</sup>)

Eight eDNA variables are included in the model. The multiple eDNA variables allow for isolation of eDNA from multiple sources and/or for the specification of eDNA fractions with different decay rates.

*b. Total dissolved solids (TDS)*

TDS are a conservative (non-reactive) tracer. The TDS concentration is used to validate and illustrate the transport processes as represented in the fate and transport model.

*c. Age of water*

Age is a model variable which represents the time a water volume at a specific location has resided within the CAWS. Age can be used to examine and compare residence time in various portions of the system.

ICM has been applied for four years, 2009 – 2012, on two grids. The model is run at the Department of Defense High-Performance Computing Center in Vicksburg. A one-year simulation on the larger grid, with one or two eDNA variables activated, consumes one hour cpu while running in parallel on 74 processors. A one-year simulation on the smaller grid, with one or two eDNA variables activated, consumes five hours cpu running in serial mode on one processor. The application process involves a substantial effort including data assembly, preparation of model input files, and processing of model outputs. The data sources are described in a separate section of this report. In brief, boundary conditions at the edges of the

computational grid and at each inflow must be determined for each model state variable. These are assembled into multiple model input files and the model is executed in a series of runs. Results from these runs are compared to observations and adjustments may be made to model parameters to improve agreement between computations and observations. Model results are examined in multiple formats. These include time series at specific locations, spatial distributions along axes at specified time intervals, and summaries over seasons and spatial reaches. Spatial distributions are examined along three axes: Lockport to Wilmette, Lockport to O'Brien, and O'Brien to Lake Michigan.

### *Steady-State Fate and Transport Model (SSFTM)*

The HFFTM provides computations of target marker concentration with a high degree of spatial and temporal resolution. However, the time and resources required to assemble, execute, and analyze each model run preclude the completion of the large number of model runs which may be necessary to make statistical inferences about eDNA loading rates from multiple potential sources. For this purpose, a steady-state model with reduced resolution has been developed. The steady-state model allows for rapid execution and analysis of large numbers of model runs based on alternate sets of loads and parameters. Significant computations on the steady-state model are subject to subsequent repetition and analysis on the highly-resolved grids.

The steady-state approach is justified by noting that the system has two basic states. During the interval from roughly June 1 to October 15, the structures at Wilmette, CRCW, and O'Brien Lock and Dam are managed to flush the CAWS with Lake Michigan water, flowing towards Lockport. This period is denoted as "gates open." For the remainder of the year, flow from Lake Michigan through the structures is restricted. The gates are closed. Steady-state models are constructed for the "gates open" and "gates closed" intervals of each of the years 2009 – 2012.

For the steady-state approach, the system is divided into 56 well-mixed reaches (Figures 5.3, 5.4). (For the steady-state approach, there is no need to divide the CAWS into two at the O'Brien Lock and Dam.) Solution is via the finite-section approach (Thomann, 1972). At steady state, the concentration of a dissolved substance in each reach, denoted by  $k$ , is given by:

$$\sum_j -Q_{k,j} \cdot (\alpha_{k,j} \cdot s_k + \beta_{k,j} \cdot s_j) + E_{k,j} \cdot (s_j - s_k) - V_k \cdot K_k \cdot s_k + W_k = 0$$

in which:

- $Q_{k,j}$  = flow from reach  $k$  to adjacent reach  $j$
- $s_k$  = concentration of dissolved substance in reach  $k$
- $\alpha_{k,j}, \beta_{k,j}$  = weighting coefficients that determine concentration at interface of reach  $k$  and  $j$
- $E_{k,j}$  = exchange coefficient between reach  $k$  and adjacent reach  $j$
- $V_k$  = volume of reach  $k$
- $K_k$  = decay coefficient in reach  $k$
- $W_k$  = loading to reach  $k$

Combining the equations for each reach produces a matrix which is solved for unknown concentrations in each reach.

The geometrical characteristics of the reaches are obtained by consolidating cells in the high-fidelity grids. Flows are obtained by averaging flows in the hydrodynamic model over the gates open and gates closed periods. Weighting and exchange coefficients are obtained through a process in which the model is first applied to TDS. The coefficients are determined empirically by adjusting values to optimize agreement between computed and observed TDS. These values are retained in subsequent model application to eDNA.

Steady-state models were set up for the gates open and gates closed periods of each year 2009 – 2012. The initial set-ups were completed in Excel spreadsheets. Quality assurance checks were conducted and initial parameter values were assigned using the spreadsheets and , which were then coded in the C programming language for high-speed, repetitive execution. Next, optimum values of exchange and weighting coefficients were determined. During the conversion process, the formulations were subject to additional quality assurance checks and results from the C version were compared to results from the spreadsheets for consistency between the two versions.

#### *Data Sources used in Developing the Fate and Transport Models*

Multiple data bases were accessed to provide the information needed to set up, execute, and validate the multiple models. Data bases accessed include the following.

##### *a. Flow and surface level*

Flow and surface level records for the model period were retrieved for the following stations maintained by the United States Geological Survey:

- 05536105 NB Chicago River at Albany Avenue at Chicago, IL
- 05536290 Little Calumet River at South Holland, IL
- 05536890 Chicago and Sanitary Ship Canal nr Lemont, IL
- 05536140 Chicago and Sanitary Chip Canal at Stickney, IL

Flows at Albany Avenue and at South Holland were used as tributary inputs in the hydrodynamic model. Observations at Lemont and Stickney were used to validate computations from the hydrodynamic model.

##### *b. Water reclamation plants (WRPs)*

Monthly records of flow, effluent temperature, and effluent concentrations of BOD and DO were obtained for the Calumet, Stickney, and Northside WRP's from an on-line data base maintained by the Metropolitan Water Reclamation District of Greater Chicago (MWRD). Flows were input to the hydrodynamic model. Effluent TDS loads, based on a characteristic concentration of  $500 \text{ g m}^{-3}$ , were used in the fate and transport model TDS calculations.

c. *Flows at Major Control Structures*

Daily flow records were obtained for major control structures including:

- Wilmette Pumping Station
- Chicago River Controlling Works
- O'Brien Lock and Dam
- Lockport Powerhouse and Lock

Flows at the first three listed were used to provide boundary conditions for the hydrodynamic model. Flow records at Lockport Lock and Dam were used to validate flows computed by the hydrodynamic model at that location.

d. *Combined Sewer Overflows (CSOs)*

As with many cities, Chicago is served by a combined sewer system in which sanitary and storm flows are conveyed in the same pipes. During major storm events, the sewer system and WRP's are overwhelmed and water overflows into the CAWS. The Tunnel and Reservoir Plan (TARP) aims to eliminate the occurrence of these CSO's. Under the plan, stormwater is captured in a series of tunnels and reservoirs, pumped to WRP's, and treated before discharge to the CAWS. The TARP has been partially implemented. Overflows still occur, however. The overflows have two origins. One type of overflow occurs when the volume of stormwater exceeds the pumping station capacity and stormwater is released into the CAWS. These releases occur at a limited number of pump station locations. The second type of overflow occurs at locations where stormwater from local collection sewers is concentrated and routed into the TARP. When the volume of water is greater than the capacity of the "drop shafts" the excess overflows into the CAWS. There are hundreds of locations distributed widely in the CAWS where overflows of this type potentially occur. The occurrence and duration of overflow incidents are monitored. The overflow volumes are calculated based on rainfall and drainage area.

Data on CSO's discharges was provided by MWRD. Information was reported for overflow incidents for individual collection sites as well as major and minor pump stations. Information included overflow volume and BOD load. The MWRD groups CSO's into three regions: Stickney, North Shore, and Calumet. We followed this pattern and summed volumes into daily values by region. Flows at the Racine Avenue Pumping Station (RAPS), located at the head of Bubbly Creek, were kept separate since this flow source is removed from the location of the other CSO's. Flows at a total of four locations, Stickney, North Shore, Calumet, and RAPS, were input to the hydrodynamic model on a daily basis. Daily TDS loads, based on a characteristic concentration of  $500 \text{ g m}^{-3}$ , were input to the fate and transport model for the TDS calculations.

e. *Ambient Water Quality Monitoring Program (AWQMP)*

The MWRD operates the AWQMP within the CAWS. Surface water quality samples are collected at monthly intervals at nearly 70 stations. Station coordinates were located on the

model grids and data (DO, temperature, TDS) for the years 2009 – 2012 was retrieved from the MWRD web site. The AWQMP data was supplemented with DO, temperature, and conductivity observations collected concurrent with the 2012 eDNA sampling. Conductivity was converted to TDS via the relationship  $\text{TDS (g m}^{-3}\text{)} = 0.67 * \text{conductivity (}\mu\text{S cm}^{-1}\text{)}$ . The TDS observations were processed for use as boundary conditions and for use in comparison with fate and transport model computations.

### *Results of TDS Calculations*

TDS were included in the fate and transport model to aid in validation of the transport processes calculated by ICM, based on cell geometry, volumetric flows, and vertical diffusion transferred from the hydrodynamic model. Summaries of computed and observed TDS for the year 2012 are presented in Figures 5.5 and 5.6. The summaries are average values, over reaches, for the gates open (June 1 to October 15) and gates closed (January 1 to May 30 and October 16 to December 31) seasons.

Computed and observed values tend to be lowest in the reaches which interface with Lake Michigan e.g. NSC, CRM, CRA. TDS increases with distance downstream and the highest concentrations occur in the segments near Lockport. The increase reflects TDS loads which enter the system from tributaries, WRPs, and CSOs. In the case of observations, the TDS concentrations may also reflect distributed sources, such as road salt, which are not represented in the model. While discrepancies occur, the model provides good representation of the TDS concentrations and trends in reaches in the CSSC computational grid. The comparisons support the conclusion that volumetric inflows to the system are accurate and that mass transport is well-represented.

The computed TDS concentrations fall short of the observations in the interior reaches of the Lake Calumet computational grid. The shortfall may be attributed to one or more of three distinct origins: observations, loads, or transport. The observations in LKC, CLK, and CRB (Figure 5.4) are exclusively from the eDNA monitoring program and the observations in CRU are a mixture of AWQMP and eDNA programs. The measures collected in connection with eDNA monitoring may be biased or the factor used to convert conductivity to TDS may be inappropriate for this region. A second possibility is the existence of an unknown TDS load. No significant tributary, CSO, or WRP discharges to the interior of the region represent by the Lake Calumet grid, but a lesser inflow or distributed source (e.g. rainfall/runoff) may exist. The predominant direction of transport through the Lake Calumet grid is from Lake Michigan, a region of low TDS concentration, towards the Cal-Sag Channel, a region of higher TDS concentration. Significant transport in the opposite direction is prevented by the structure and operation of the O'Brien Lock and Dam. However, some water will be moved upstream through lock operations and leakage. This water is characterized by high TDS concentration due to loading from the Little Calumet River and the Calumet WRP. Once upstream of the structure, TDS from below O'Brien can be propagated further upstream via meteorological tides in Lake Michigan. The oscillating meteorological tides are represented in the model but the volume of water moved upstream through the structure is difficult to quantify. Nor is it known if the TDS in this volume are sufficient to increase concentration throughout the Lake Calumet region.

Inconsistent observations and/or unknown loads are the most likely reason for the excess of observed TDS over calculated TDS in the region of Lake Calumet.

### *Insights from the Age Computations*

The “age” variable indicates the time a water volume at a specific location has resided within the CAWS. New water introduced from Lake Michigan, a tributary, a WRP, or a CSO has zero age. Age at a specific location can increase or decrease depending on the passage of time and also on the ages of water volumes from various origins that make up the mixture at the location. The age of water extending along the CSSC from Lockport to Wilmette is shown during gates closed (February 2012, Figure 5.7) and gates open (July 2012, Figure 5.8) intervals. When the gates are closed, the water in the upper reaches of the NSC has age in excess of 20 days. The only source of new water is a small volume of leakage through the structure. The age plummets at the location of the Northside WRP (roughly km 73) due to the introduction of new water from the WRP as well as intermittent CSO volumes. Age increases with distance downstream, then plummets a second time due to new water introduced from the Stickney WRP, at the juncture of reaches CR3 and CR4. Age increases as water moves downstream and shows a step increase at the junctures of reaches CR4 and CR5 due to mixing with older water flowing down the Cal-Sag Channel. At Lockport, the mixture of water leaving the system has been in the CAWS roughly 11 days.

In contrast to the “gates closed” season, water at the extreme upstream end of the NSC is new when the structure at Wilmette is open. Travel time down the NSC is slow, however, so that age increases to six days above the Northside WRP. From Northside to Lockport, the age follows the pattern described previously although the age is less due to the larger volumetric flow through the system. At Lockport, the mixture of water leaving the system has been in the CAWS nine days.

As in the NSC, water in the upper reaches of the Cal-Sag Channel is more than 20 days old during the “gates closed” season (February 2012, Figure 5.9). And as with the NSC, the age plummets rapidly with the introduction of new water from a WRP, this time the Calumet plant near km 50. Age increases with distance down the Cal-Sag Channel, then plummets a second time due to mixing with water moving down the CSSC. The portion of the figure below km 20 is the same on this axis and on the Lockport to NSC axis. Water leaving the system at Lockport has been in the CAWS roughly 11 days during the gates closed season. When water is discharged through the O’Brien Lock and Dam, water immediately downstream of the structure has negligible age (July 2012, Figure 5.10). Transport is slow, however, above the Calumet outfall. Water immediately above the outfall has an age of roughly ten days. From km 50 to Lockport, the previously-described pattern repeats. At Lockport, the mixture of water leaving the system has been in the CAWS nine days.

Water in the region of Lake Calumet can attain significant age due to restricted circulation and absence of major inflows. At a location immediately above O’Brien Lock and Dam (Figure 5.11), age increases from commencement of the simulation on January 1 through to the opening of the structure circa June 1, which corresponds to decimal year 0.4 on the  $x$ -axis. Roughly 150 days into the simulation, water upstream of O’Brien has an age in excess of 100

days. Age plummets when the structure is open but, at this location, age does not achieve its minimum of ten to 20 days until August, more than 200 days from commencement of the simulation. When the gates are closed in October, age increases, once again, to more than 100 days.

Water within Lake Calumet demonstrates some of the greatest age in the CAWS (Figure 5.12). The lake has no significant tributaries and no inflows from WRP's or CSO's although there is certainly some distributed inflow from the local drainage area. The major source of new water is exchanged through the passage that joins the lake to the Little Calumet River and Lake Michigan. As a consequence of limited exchange, age in the lake increases from the commencement of the simulation, on January 1, until the structure is opened at O'Brien. At this time, the age of water in Lake Calumet is roughly 130 days. Opening the structure does little to increase exchange with the lake but introduces new water in the Little Calumet which refreshes the lake. At the minimum, however, age at this location is 90 days and increases once again when the structure at O'Brien is closed.

#### *A Demonstration of eDNA Fate and Transport Simulation Capabilities*

The following example demonstrates how this water quality model can be implemented to simulate fate and transport of eDNA in the CAWS and to facilitate understanding how hydrologic conditions affect target marker concentrations. For the purpose of this example, a target marker concentration of 60 copies/L is assumed to exist in hydrologic inflows to the CAWS from Lake Michigan. No other sources of eDNA are assumed to be present. The simulation will show what the downstream concentrations would be under such a scenario and how far downstream such a load might be detected.

Results of the example are summarized in Figure 5.13, which shows two snap-shots of the target marker concentrations in the Lake Calumet grid. Figure 5.13a shows concentrations in the Lake Calumet grid on Julian day 152, at the end of the gates closed season. Concentrations are about 60 copies/L at the head of CRA, near the Lake Michigan boundary, but the concentration decreases to less than 20 copies/L about half way between Lake Michigan and CRB. This distribution of eDNA in the system is the result of the combined effects of the eDNA decay rate and the time and distance required for transport from the Lake Michigan boundary to CRB. While the gates at TJ O'Brien Lock and Dam are closed, movement of eDNA in CRA is controlled by the effects of tide and dispersion. The target marker concentrations in Lake Calumet is very close to zero copies/L.

Figure 5.13b shows target marker concentrations in the Lake Calumet grid on Julian day 273, near the end of the gates open season. During the gates open season, the sluice gates at TJ O'Brien Lock and Dam remain open so that water from Lake Michigan can be diverted to flush the CAWS. When the gates are left open, the hydrologic regime in the Lake Calumet grid is altered. The hydrologic regime goes from one that is dominated by the effects of tide and dispersion to one that is dominated by the effects of advection. Advection carries the eDNA further into the CAWS from the Lake Michigan Boundary. This greatly increases the extent of to which eDNA is distributed in the Lake Calumet grid. Concentrations greater of 30-40

copies/L can be seen at the O'Brien Lock and Dam and concentrations as high as 20 copies/L can be seen in the canal to Lake Calumet (CLK).

Simulation results can be expressed either in terms of the target marker concentration or in terms of the probability of detecting a target marker. Figure 5.14 expresses results of the above simulation in terms of the probability of detecting the silver carp target marker using cPCR with eight replicates. For the purpose of illustration, this example assumes a concentration of 60 copies/L at the CRA boundary with Lake Michigan. This corresponds to a probability of detection equal to approximately 0.08 at the boundary. Figure 5.14a shows that, during the gates closed season, as one moves downstream from the boundary, the probability of detecting eDNA decreases rapidly, and is less than 0.01 half way between Lake Michigan and CRB. During the gates open season, the dominant hydrologic transport process is advection, and – given the assumed load at the CRA boundary with Lake Michigan – the probability of detecting eDNA in the Lake Calumet grid increases greatly. Probabilities of detection are as high as 0.07 in the upstream portions of CRA and as high as 0.03 in CRU, just above the TJ O'Brien Lock and Dam. This example illustrates the importance of understanding the hydrologic influences in the CAWS before making inferences from eDNA monitoring program results.

## **6. Loading Rates for Potential Sources of eDNA**

Bighead carp and silver carp eDNA detected in monitoring samples from the CAWS may be attributed either to a primary source (live fish) or to one of six secondary sources, including CSOs, navigation, Lake Michigan inflows, bird feces, recreational fishing derbies, and commercial fishing nets. This section of the report describes a Bayesian MCMC simulation methodology to infer eDNA loading rates for potential sources of eDNA in the CAWS. A loading rate is an estimate of the number of copies of eDNA that are contributed to the CAWS per unit of time. Spatial and temporal estimates of loading rates are essential for understanding the sources of eDNA detected in monitoring samples. The results of the Bayesian MCMC simulation are used to support probabilistic statements about the strength of eDNA sources in the CAWS and the origin of eDNA detected in monitoring samples.

This section of the report begins with a general description of a loading rate function and also the Bayesian MCMC simulation methodology. Four applications of Bayesian MCMC are subsequently described. The first application is undertaken to calibrate two SSFTM transport parameters. The parameters are calibrated to data on total dissolved solids (TDS) concentrations in the CAWS. These parameters must be estimated before the SSFTM can be used to simulate target marker concentrations. The second and third applications of Bayesian MCMC are performed to evaluate the relative strength of each secondary source and to determine the probable origin of eDNA in monitoring samples. These applications assume that no primary source is present in the CAWS. The fourth application of Bayesian MCMC estimates the quantity of live silver carp that would be needed to sustain observed target marker concentrations in the CAWS in the absence of secondary sources.



### *Loading Rate Functions*

A unique loading rate function is defined for each distinct Asian Carp eDNA loading source to the CAWS. However, each separate eDNA loading function must be parameterized to complete its definition. When a value is estimated for the parameter(s) of a given loading function, then the corresponding loading rate (with units of copies of eDNA per unit time) for that source of eDNA can be computed in terms of its magnitude and distribution throughout the CAWS. The loading rate,  $L$  (copies  $\text{sec}^{-1}$ ) is a function of a loading factor,  $F$ , and a parameter,  $\pi$ , which represents the target marker copies contributed to the CAWS per unit loading factor:

$$L = \pi \cdot F$$

The basis for each loading function is its loading factor, and they were developed to be as physically representative as possible of the understood processes and available data which characterize each distinct source of eDNA. For example, as described in Section 4 of this report, the loading factor for CSOs is the seasonally averaged discharge ( $\text{m}^3 \text{sec}^{-1}$ ). Hence, the parameter of the CSO loading function,  $\pi_{\text{CSO}}$ , has units of copies  $\text{m}^{-3}$  to yield appropriate units for the computed CSO loading rate. For each modeled source of eDNA to the CAWS, Table 6.1 succinctly describes its loading factor and loading rate function parameter, including their respective units, as implemented and interfaced with the SSFTM. Each loading factor is consistent with the description in Section 4 of this report, but it has been seasonally averaged for use with the SSFTM. Table 6.2 lists receiving reaches for each potential secondary source and indicates whether or not the loading factor for that source varies by season and/or by year. Loading factors vary by reach or season depending on what data were available to estimate loading factors.

### *Bayesian Markov Chain Monte Carlo (MCMC)*

MCMC is a formal Bayesian approach for estimating the posterior probability distribution of the specified adjustable model parameters, in this case, the eDNA loading rate function parameters. It treats the specified adjustable model parameters as random variables, and relies upon Bayes' Theorem to compute their joint posterior probability distribution. Bayes' Theorem effectively communicates that the posterior distribution is proportional to the product of the prior distribution, prescribed based on the modeler's best judgment, expert opinion, or literature estimates, among possible others, and the likelihood function (i.e., conditional distribution), which encapsulates the conditioning process with the observed dataset. The idea behind MCMC is that while one wants to compute a probability density,  $p(\mathbf{p}|y)$ , where  $\mathbf{p}$  and  $y$  represent the vector of adjustable model parameters and the observed data, respectively, there is the understanding that such an endeavor may be impracticable. Additionally, simply being able to generate a large random sample from the probability density would be equally sufficient as knowing its exact form. Hence, the problem then becomes one of effectively and efficiently generating a large number of random draws from  $p(\mathbf{p}|y)$ . It was discovered that an efficient means to this end is to construct a Markov chain, a stochastic process of values that unfold in time, with the following properties: (1) the state space (set of possible values) for the Markov chain is the same as that for  $\mathbf{p}$ ; (2) the Markov chain is easy to simulate from; and (3) the Markov chain's equilibrium distribution is the desired probability density  $p(\mathbf{p}|y)$ . By constructing such a

Markov chain, one could then simply run it to equilibrium (and this period is often referred to as the sampler “burn-in” period) and subsequently sample from its stationary distribution. A Markov chain with the above mentioned properties can be constructed by choosing a symmetric proposal distribution and employing the Metropolis acceptance probability (Metropolis et al. 1953) to accept or reject candidate points. A more complete description of Bayesian MCMC can be found in Gelman *et al.* (2004).

The Differential Evolution Markov Chain MCMC sampler (ter Braak 2006) is used to integrate the steady state water quality model deployed to the CAWS, the eDNA concentration estimates derived from the monitoring program, and the defined and parameterized loading rate functions to yield random draws from the probability distributions implied by the modeling (i.e., the forward model, the observed data, the defined and parameterized loading rate functions, the loading rate function parameters, their prior information, the likelihood function, ...) for the eDNA loading rate function parameters and hence the eDNA loading rates to the CAWS. The DE-MC sampler combines salient features of the global optimization method Differential Evolution (DE) (Storn and Price 1995, 1997) with Bayesian MCMC. Briefly, with DE-MC, multiple chains are run in parallel with the chains learning from each other by way of jump proposals that are generated by taking the difference of two randomly selected chains from the current population. The probability of selecting the jump proposal is determined by using the Metropolis algorithm (Metropolis et al., 1953). The DE-MC MCMC sampler is by design parsimonious in terms of its number of input parameters and it has been demonstrated to be efficient with respect to its burn-in requirements and reliable with regard to its capacity to traverse multimodal densities (ter Braak 2006).

An overview of the Bayesian MCMC procedure is provided in Figure 6.1. The eDNA concentrations derived from the monitoring samples, the steady-state water quality model, and the defined and parameterized loading functions are integrated, via MCMC simulation, to yield random draws from the probability distributions for the loading rate function parameters for each of the modeled sources of eDNA to the CAWS. In Figure 6.1, the output from the MCMC displays, for illustrative purposes, random draws from the probability distribution for just one of the secondary source loading rate function parameters; viz. the Lake Michigan inflows eDNA concentration estimate which has units of eDNA copies per cubic meter. It is emphasized that upon completion of the analysis methodology encapsulated in Figure 6.1, one would have random draws from the distribution for each of the modeled loading rate function parameters, which in aggregate result in the capacity to make probabilistic statements regarding the relative strength of the modeled sources of eDNA to the CAWS and also the relative importance of each source in the monitoring samples based on the simulated concentrations from the optimized water quality model for the CAWS.

#### *Implementation of Bayesian MCMC to Estimate SSFTM Input Parameters*

Two SSFTM input parameters must be estimated before it can be used to infer eDNA loading rates to the CAWS. These variables, given by  $E$  and  $\alpha$ , control the exchange of material across box model interfaces.  $E$  accounts for effects such as tidal mixing and density differences, and  $\alpha$  controls advective mass transport. The SSFTM input parameters were calibrated using the DE-MC MCMC sampler and observed TDS data collected in the CAWS during the gates open

seasons for the years 2009 – 2012. These two parameters can vary spatially, and two zones are currently prescribed for parameterizing  $E$  and  $\alpha$  in the SSFTM. Parameters  $E_1$  and  $\alpha_1$  are estimated for the CSSC grid (Figure 5.3) and parameters  $E_2$  and  $\alpha_2$  are estimated for the Lake Calumet grid (Figure 5.4).

The two primary DE-MC MCMC sampler input parameters; viz., (1) the population size,  $N$ , and (2) the threshold frequency,  $\gamma$ , per evolution, with which the proposal distribution chain weighting parameter is randomly reset to a value of one in attempts to mitigate against potential entrapment in local minima, were set to 8 and 0.3, respectively. Uninformative uniform priors were specified for  $E_1$ ,  $E_2$ ,  $\alpha_1$ , and  $\alpha_2$  with lower and upper bounds of (0.01, 10,000) and (0, 1), respectively. Random samples were taken from the prior distributions to initialize the population. Out of bounds proposal dimensions were specified to remain at their current location. The forward model in this case is a composite model consisting of four distinct gates open season model runs for four years (2009 – 2012). Simulated TDS concentrations from each of these four models was compared with corresponding observations of TDS, resulting in a total of 66 comparisons of TDS observations (13 observations for the 2009, 2010, and 2011, and 27 observations for 2012). A squared deviation likelihood function was employed.

Observations of the population mean RMSE values, computed, updated, and reported upon at the end of each evolution, underscored model optimization as the population evolved over the course of the simulation, and the eventual convergence to a final minimized RMSE value range that is representative of the exploration of the target equilibrium posterior distribution for the four specified random variables; viz.,  $E_1$ ,  $\alpha_1$ ,  $E_2$ , and  $\alpha_2$ . One of the primary outputs of the Bayesian MCMC simulation is a set of posterior probability distributions for  $E$  and  $\alpha$ . Figure 6.2 presents plots characterizing the marginal posterior probability distributions for the four SSFTM input parameters. These posterior probability distributions for  $E$  and  $\alpha$  are associated with the optimized SSFTM whose calibration involved comparing simulated and observed TDS concentrations. Figure 6.3 shows how well simulated TDS concentrations match their observed counterparts. These estimates for  $E_1$ ,  $\alpha_1$ ,  $E_2$ , and  $\alpha_2$  are used in the applications of the SSFTM to estimate eDNA source loading rates.

### *Implementation of Bayesian MCMC to Estimate eDNA Source Loading Rates*

Bayesian MCMC simulation is implemented to estimate loading rate function parameters. Its application simultaneously results in model optimization and the capacity to compute random draws from the unknown probability distributions implied by the modeling methodology for each defined loading rate function parameter. And with the noted random draws from the probability distributions for each of the loading rate function parameters, obtained via the MCMC supervised simulation process, one can then compute and make formal probabilistic-based statements, by location, regarding (i.) the relative strength of the sources of eDNA to the CAWS and also (ii.) the relative importance of each source in the monitoring samples based on the simulated eDNA concentrations from the optimized water quality model for the CAWS. For example, item (i.) is determined, by location, simply by computing the frequency across all of the MCMC supervised simulation derived random draws from the optimized model for the rank (i.e., first, second, third, ...), in terms of magnitude, associated with each given source's computed aggregate eDNA load. And item (ii.) is presented by computing, also by location, the

mean contribution from each source to the eDNA concentration values simulated from the optimized model based on all of the MCMC supervised simulation derived random draws.

Bayesian MCMC is a computationally intensive exercise which requires numerous simulations (on the order of thousands) to calibrate the SSFTM. And it is for this reason that the computationally efficient mass balance SSFTM box model for the CAWS, rather than the HFFTM, was used to support inference of the eDNA loading rates. It is emphasized that the simulated concentration estimates from the SSFTM are consistent, temporally, and also spatially, with the eDNA concentration estimates that were derived from the monitoring program samples.

Observed concentrations are derived from data on the frequency of positive eDNA monitoring samples using a procedure that updates the concentration after each monitoring event. Because the specified prior distribution for the observed eDNA concentration has a large range and the frequency of positive detections tends to be consistently low, the posterior distributions tend to overestimate eDNA concentrations during the first few monitoring events. Two criteria for determining whether or not a median observed eDNA concentration estimate should be included in the Bayesian MCMC likelihood function calculations were established to control for this effect. These criteria are that 1) the observed eDNA concentration estimate is based on at least three iterations of the Bayesian updating procedure explained in Section 3 of this report, and 2) no concentration may be used twice unless it has been subsequently updated following a monitoring event in that season. There were 69 silver carp target marker concentration estimates that satisfied these requirements. Table 6.3 shows the median observed silver carp concentration estimates by reach, year, and season that served as the available observations to infer, via MCMC, the eDNA loading rates by source.

To ensure extraction of the maximum information possible from the observation dataset imparted to the Bayesian MCMC simulation supervised analysis process, eight consistently parameterized SSFTMs, each with boundary condition forcing terms representative for the respective period, are run in series to model the eight system states (i.e., (1) 2009 “gates open”, (2) 2009 “gates closed”, (3) 2010 “gates open”, (4) 2010 “gates closed”, (5) 2011 “gates open”, (6) 2011 “gates closed”, (7) 2012 “gates open”, and (8) 2012 “gates closed”). The final eDNA SSFTM is in fact a composite model consisting of these eight SSFTM box models for the CAWS executed in series. The Bayesian MCMC simulation employed a squared deviation likelihood function. And since there was very little if any outside information available, uninformative prior information was specified for the loading rate function parameters.

The results of three separate Bayesian MCMC simulations are described in this section. The first simulation estimates the loading rate function parameters for all six potential secondary sources of eDNA. The loading rate parameters estimated from this simulation are subsequently used in developing the probabilistic model of Asian carp presence in the CAWS. The second simulation is similar to the first, but excludes CSOs as a potential secondary source. The purpose of this simulation is to analyze sensitivity of simulation results by dropping CSOs as a secondary source in the first simulation. The motivation for dropping CSOs is discussed below. The third simulation estimates what quantity of silver carp would be needed in the CAWS to sustain the observed target marker concentrations in the absence of secondary sources. Additional results and related technical details associated with each of these three unique MCMC

supervised simulations are available in a Appendix 5. Appendix 5 is separate from this report because it has not been formatted for distribution, but it is available from the authors by request.

*a. Inference of secondary source loading rate function parameters, including CSOs*

The purpose of this MCMC simulation is to estimate loading rate function parameters for secondary sources of eDNA to the CAWS. With exception of CSOs, each secondary source is defined by a single loading rate function. CSOs are defined by nine loading rate functions, one for each reach that receives CSO discharges (see Table 6.2). Simulation results described in this report include: 1) an estimate of the loading function parameter for each secondary source; 2) a probabilistic ranking of secondary sources in terms of total contribution of eDNA to each CAWS reach; and 3) an estimate of the probability that eDNA detected in a monitoring sample originated from any one secondary source. Estimates of the fourteen loading function parameters are summarized in Table 6.4 and are further characterized by probability distributions plotted in Appendix 5. Figures 6.4 and 6.5 presents a comparison of simulated eDNA concentrations from the optimized water quality model together with their observed counterparts for all eight seasons. It is underscored to the reader that to the best of our knowledge there is no body of published eDNA simulation-based work available to draw upon to provide a summary statement regarding the quality of the calibration (e.g., as “excellent”, “very good”, “good”, “fair”, “poor”, etc.) via the fits shown in Figures 6.4 and 6.5.

Secondary sources can be ranked in terms of how much eDNA each source contributes to the CAWS to characterize their relative importance. Table 6.5 lists the probability that each secondary source occupies a particular rank. For example, the probability that CSOs are the largest source of eDNA to the CAWS is 0.623 and the probability that navigation (NAV) is the largest source is 0.377. These appear to be the dominant sources of eDNA in the CAWS. The probability that other secondary sources occupy any one of the remaining ranks is more difficult to discern because these probabilities tend to be evenly distributed among the remaining ranks. However, the probability that piscivorous bird feces is the source increases with the rank order, suggesting that this may be among the smallest of the secondary sources. Appendix 5 reports results of a probabilistic ranking for each CAWS reach. Results are largely consistent with those described here, but vary from reach to reach because not all reaches receive load from all secondary sources. For example, piscivorous birds and commercial navigation are the only secondary sources that contribute eDNA load directly to CR5, FBA, and CR6.

The ability to detect eDNA that originates from any one secondary source in a monitoring sample depends on many variables, such as the location of monitoring relative to the source, the strength of each source, and environmental factors influencing fate and transport of eDNA such as hydrology and kinetics. The detectability of a secondary source is evaluated by computing the mean relative contribution, by source, to the total simulated eDNA concentration values in each of the nineteen modeled main CAWS reaches, based on simulations using all of the MCMC derived random draws from the optimized water quality model. It is underscored to the reader that the values reported in Tables 6.6-6.9 are the computed means from the underlying relative contribution distributions associated with each source derived from the random draws associated with the optimized model. These are formal probability based values, derived via Bayesian MCMC simulation, and not simply the result of a single forward model call. Tables 6.6 and 6.7

report the probability of detecting eDNA from any one secondary source in any one reach for the gates open and gates closed seasons, respectively. These probabilities can also be calculated for spatial and temporal aggregations of the results, as in Tables 6.8 and 6.9, which report results on an annual basis by reach and for the entire CAWS, respectively.

Tables 6.6-6.7 reveal seasonal differences in the detectability of eDNA from each potential secondary source. For example, the probability that eDNA detected in an NSC monitoring sample originated from piscivorous bird feces is 0.0334 during the gates open season and 0.0005 during the gates closed season. This can be explained by differences in the population of piscivorous birds during the two seasons. Similarly, the probability of detecting eDNA attributed to Lake Michigan inflows (LMI) in the CSSC section of the CAWS is much lower during the gates closed season than the gates open season. The lower probability can be explained by the fact that the gates are closed, but this probability is not 0 during the gates closed season because leakage at the sluice gates is a normal part of system operation during the gates closed season.

Tables 6.6 and 6.7 reveal spatial differences in the probability of detecting eDNA from any particular secondary source. For example, recreational fishing derbies occur upstream of CR5 on the Cal-Sag Channel and Calumet River. Therefore, recreational fishing derbies are not a potential secondary source of eDNA in reaches located upstream of CR4. Similarly, eDNA associated with inflows from Lake Michigan are most likely to be detected in NSC, CRM, and CRA. This probability dissipates rapidly as one moves downstream. Commercial navigation exerts its largest influence in CR5, the Cal-Sag Channel, and the Calumet River. CSOs exert their largest influence in the CSSC upstream of CR5. CSOs are not a potential secondary source upstream of O'Brien Lock and Dam during the 2009-2012 monitoring period. Finally, the probability of detecting eDNA from piscivorous birds appears to be relatively low throughout the CAWS during both the gates open and gates closed seasons.

*b. Inference of secondary source loading rate function parameters, excluding CSOs*

This section describes results of a second Bayesian MCMC simulation that is identical to the first simulation in all respects, but excludes CSOs. The objective here is to explore the sensitivity of optimization results. CSOs have been targeted for this sensitivity analysis for two reasons. CSO discharges are highly sporadic in nature, but the SSFTMs inputs and outputs represent averages over a season. While simulated concentrations from the SSFTM are compatible with the time and space scales of the eDNA concentration estimates derived from the monitoring program, it is not well suited to simulate the temporal dynamics of CSO discharges. Since the MCMC results from the previous section indicated that a large fraction of the eDNA could be attributed to CSOs, this second MCMC simulation provides an additional opportunity for eDNA data interpretation. A second motivation for exploring the sensitivity of results to CSO discharges is that the QAPP that governs eDNA monitoring does not permit sample collection to occur for several days after a CSO event (USACE 2012). CSO discharges are associated with high flow events and, when they occur, the system tends to flush itself out quickly. Therefore, eDNA from CSOs may represent only a small fraction of the eDNA observed in monitoring samples despite the relative magnitude of its overall contribution of eDNA to the system.

The probabilistic rank of secondary sources in terms of their total contribution of eDNA to the CAWS is presented in Table 6.10. As with the previous simulation, probabilistic rankings are reported by reach in Appendix 5. These results suggest that commercial navigation is probably the largest contributor of eDNA to the entire CAWS (the probability is 0.986). Piscivorous birds and commercial fishing nets are tied for second and recreational fishing derbies are probably the smallest contributor. A comparison of these results with those presented in Table 6.5 reveals that the effect of removing CSOs is to reverse the trend in computed probabilities for piscivorous bird feces. In other words, DNA attributed to CSOs in the preceding simulation now appears to be attributed to piscivorous birds. The probabilistic rank of commercial fishing nets, recreational fishing derbies, and Lake Michigan inflows is similar to the previous simulation.

The probability that eDNA detected in monitoring samples originated from any one secondary source is reported for this simulation in Tables 6.11 – 6.14. These tables can be compared to results from the previous simulation (Tables 6.6 – 6.9) to gauge the sensitivity of this analysis to exclusion of the CSO loading function. Overall, the effect is to greatly increase the probability of detecting eDNA from piscivorous bird feces in eDNA monitoring samples. For the gates open season, the probability detecting eDNA from piscivorous birds, averaged over all nineteen reaches, is about 0.15. For the gates closed season, the probability is approximately 0.008. The probabilities for the remaining sources differ somewhat from the previous simulation, but are similar.

Plots comparing the simulated eDNA concentrations from the optimized water quality model, together with their observed counterparts, are provided in Appendix 5. And plots of all the random draws for each separate loading rate function parameter, characterizing its probability distribution, are also provided in Appendix 5.

### *c. Inference of primary source loading rate function parameters*

The purpose of the third Bayesian MCMC simulation is to estimate the mass of Asian carp that would be needed to sustain the concentrations of eDNA observed in the CAWS in the absence of secondary sources. This simulation is implemented by specifying one loading rate function parameter in each of the nineteen modeled main CAWS reaches as a random variable equal to the mass of Asian carp in those reaches. Each parameter was initially characterized by a uniform probability distribution, indicating a complete lack of information about the mass and distribution of Asian carp in the CAWS. For the purpose of this MCMC simulation, it was assumed that the shedding rate was 14 million copies/kg/hour, that 80 percent of the target markers shed from a live fish decay at a rate of  $0.456 \text{ d}^{-1}$ , and that the remaining 20 percent decays at  $0.079 \text{ d}^{-1}$ .

Results are summarized in Figure 6.6 and Table 6.15. Figure 6.6 plots the total mass of live silver carp that would be needed to sustain the concentrations of the silver carp target marker above the electric fish barrier if no secondary sources were present. Table 6.15 tabulates the expected mass and 95 percent confidence bounds on the mass by reach, and summarizes these results for the CAWS. Results show that an expected 4.6 metric tons (t) of live silver carp would

be needed in the CAWS and that the 95 percent confidence bound on this estimate ranges from 3.68 t to 5.96 t. Marginal distributions for each loading rate parameter were derived from random draws of the simulation and are plotted for each reach in Appendix 5. These figures suggest that, if silver carp were the sole source of the target markers detected in monitoring samples, the fish would not be uniformly distributed in the CAWS.

This simulation treats live fish as the only potential source of eDNA detected in monitoring samples, assumes no prior information about the distribution of live fish in the CAWS, and assumes that the mass of live fish is constant over the eDNA monitoring period. Given prior information about the spatial and temporal distribution of live fish, it would be possible to revise these assumptions. For example, the prior probability distributions on the loading rate parameters could incorporate information about which habitats are more or less preferred by silver carp. Similarly, the SSFTM could incorporate information about swimming behavior.

## **7. High-Fidelity Simulation of eDNA Fate and Transport**

The first step in simulating eDNA fate and transport with the HFFTM was to create load and boundary conditions for each year of the eDNA monitoring period, from 2009 through 2012. Load and boundary conditions were based on the previously described loading factors and loading rates. Model runs were conducted for individual years with no carry-over from year to year. That is, each year was initialized with zero target marker concentration. A one-year simulation of the Lake Calumet section was conducted first, to provide boundary conditions at the O'Brien Lock and Dam. These boundary conditions were employed in the subsequent one-year simulation on the CSSC grid. Runs were conducted separately to examine fate and transport of eDNA from primary sources (fish) and secondary sources. Computed target marker concentrations were analyzed in multiple formats including seasonal averages along major system axes, time series for each major reach, and seasonal averages by reach. Emphasis is placed here on the 2012 simulations since the loading factors are most accurate for this year and the target marker concentrations estimated from eDNA monitoring data incorporate the greatest number of possible field samples.

### *Loads and Boundary Conditions*

#### *a. Secondary source loads*

Loading rates for secondary sources were obtained from the MCMC modeling conducted with the SSFTM. Values were selected from the 50<sup>th</sup> percentile of the cumulative distribution of marginal loading rates for each source (Figure 7.1). Six distinct sources, including CSOs, were identified. CSOs were differentiated by reach, however, resulting in fourteen secondary source loading rates (Table 7.1). Secondary source loads were assumed to consist entirely of the “slow” eDNA fraction and were assigned a decay rate of  $0.079 \text{ d}^{-1}$ , the central value in a uniform distribution fit to the results obtained from the laboratory experiments.

The loading rates were specified in complementary units to the loading factors. The product of loading rate and loading factor was the eDNA load, in copies  $\text{d}^{-1}$ , provided to the



model. The location and timing of the loads varied according to the source. Lake Michigan loads were input at the location of three Lake Michigan interfaces: Wilmette, Chicago River Control Structure, and the mouth of the Calumet River. Loads were proportional to the volumetric flow rate computed by the hydrodynamic model and were updated on an hourly basis. Bird loads were distributed to surface cells in the computational grids in proportion to their surface area. The loading rate during the gates closed season was considered to be 10% of the loading rate during the gates open season, to reflect differences in bird population and activity. CSO loads were input to model cells adjacent to CSO locations and varied on a daily basis depending on reported daily CSO volumes. Navigation loads were updated daily and were distributed uniformly across reaches, depending on reported traffic patterns. Loads from fishing derbies were updated daily and distributed across reaches and backwaters, depending on records of recreational activity. Loads from fishing nets were updated daily and were input to model cells corresponding to locations of fishing activity.

Loading summaries (Table 7.2) indicate navigation and CSOs were the largest secondary sources of eDNA, during 2012, to the portion of the system represented on the CSSC grid. Lake Michigan, fishing derbies, and fishing nets were the largest secondary sources to the Lake Calumet portion during the 2012 gates open season. During the 2012 gates closed season, navigation, fishing derbies, and fishing nets were equivalent, dominant, sources to the Lake Calumet portion. These results describe the relative magnitude of the various secondary sources in computational grid when aggregated by season. However, HFFTM simulations and other results of this study indicate that the relative importance of secondary sources varies over space and time within the CAWS.

*b. Primary sources loads*

The primary source mass in each reach required to generate the observed target marker concentrations was estimated by the MCMC procedure with the steady-state box model. The mass was constant across all years and seasons. Primary source mass for the high-fidelity model was selected as the 50<sup>th</sup> percentile of the cumulative distribution of marginal mass values (Table 7.3). The mass in each reach was multiplied by the unit shedding rate, 14 million copies hr<sup>-1</sup> kg<sup>-1</sup> fish, to obtain the eDNA load which was distributed evenly to each surface cell in the reach. Loads were split into “fast” (80%) and “slow” (20%) fractions with decay rates of 0.462 d<sup>-1</sup> and 0.079 d<sup>-1</sup>, respectively. These rates represent central values of uniform distributions fit to the results obtained from the laboratory experiments.

The largest primary source masses, and consequently loads, are in reaches CR3, CRE, and CR4. Consideration of mass alone can be deceptive, however, since the masses and loads are distributed across reaches of differing extent and volume. When the masses are normalized by volume, FBA stands out as having the greatest primary source mass per unit volume. A secondary tier of roughly equivalent values exists in reaches NSC, BCR, MXZ, CR3, and CRV.

## *Secondary Source Simulation Results*

### *a. Axial distribution*

Seasonal-average computed target marker concentration from secondary sources is shown along three system axes: Lockport to North Shore Channel (Figures 2, 3), Lockport to O'Brien Lock and Dam (Figures 7.4, 7.5), and O'Brien Lock and Dam to Lake Michigan (Figures 7.6, 7.7). Generalizations about the relative roles of various secondary sources are difficult to draw from the results. The results indicate the dominant secondary sources vary according to location and season. In some portions of the system, there is no clearly predominant secondary source. Nevertheless, some consistent properties are apparent. Navigation is a predominant secondary source from Lockport to the junction of the CSSC and Cal-Sag Channel, 20 km upstream (Figures 7.2, 7.3). The potential influence of Lake Michigan varies with season. When the gates are open, secondary sources in the Lake may dominate below Wilmette, in the vicinity of the Chicago River Control Structure (Figure 7.3), and through much of the reach from O'Brien to Lake Michigan (Figure 7.7). Loads from bird droppings are a consistently lesser source throughout the system. At times, the potential exists for a significant fraction of the eDNA to result from contamination due to fishing nets (Figures 7.2 – 7.4).

### *b. Temporal reaction*

Time series of computed target marker concentration resulting from secondary sources are presented for selected reaches in two formats: as concentration from each source and as the fraction contributed by each source to the total target marker concentration. The figures reinforce the principle that the predominant source varies with location and time. The figures also demonstrate that, in some instances, no predominant source can be identified. In the NSC (Figure 7.8), CSOs are the predominant secondary source until the structure is opened at Wilmette (circa Day 150) after which Lake Michigan prevails. When the structure is closed (circa Day 285), fishing nets become the predominant source. The relative roles of CSOs and nets at the end of the 2012 simulation illustrate the influence of random processes (hydrology) and anthropogenic activities (monitoring events). CR2 (Figure 7.9) presents an example of a reach in which a consistent predominant secondary source is difficult to identify. Predominance switches, with a frequency on the order of ten days, between four secondary sources. The lengthy extent of the CSSC represented by CR4 (Figure 7.10) shows a similar lack of consistent predominant source. The time series confirm the conclusion from the longitudinal plots that navigation is the predominant secondary source in the vicinity of Lockport (Figure 7.11).

The time series confirm the dominant role of Lake Michigan as a potential secondary source in the portion of the Calumet River represented by CRA (Figure 7.12) although navigation loads may be significant at times. Other secondary sources assume larger roles with distance downstream until, in the large extent of the Cal-Sag Channel represented by CRE (Figure 7.13), almost any source can be dominant at any time although there is a tendency for navigation to be more significant during the gates closed season and for fishing derbies to be more significant when gates are open.

The time series illustrate reaches that are off the system axes. In BCR (Figure 7.14), CSOs are the predominant secondary source whenever the hydrology is sufficiently wet to generate a discharge at the pumping station located at the head of the creek. Otherwise, fishing nets, Lake Michigan, and navigation are potential predominant sources. Fishing derbies and fishing nets are the predominant potential secondary sources in Lake Calumet (Figure 7.15). Both of these are anthropogenic sources. Absent these sources, Lake Calumet presents a rare instance in which bird droppings could be a significant secondary source.

*c. Comparison with observed target marker concentrations*

The comparison of model results with observations is by reach and season. The observed concentrations were derived as described in Section 3. Briefly, uniform, uninformed prior concentrations were assumed in each reach and for each season at the beginning of 2009. The concentrations were updated based on the results of successive sampling events. The process resulted in characteristic target marker concentrations for each reach and season. As a result of the sporadic sampling process, the characteristic concentrations in each reach potentially represent different sampling periods and numbers of samples. For comparison with the 2012 model results, we adopted a screening process which required at least three 2012 sampling events per reach and season. Eleven reaches in the gates open season and eight reaches in the gates closed season met these criteria. Observations in these reaches reflected multiple sampling events during 2012 but also incorporated information from the uninformed priors and from sampling previous to 2012. For comparison with the observations, model results were volumetrically averaged, at hourly intervals, across all cells in each reach. Descriptive statistics – mean, median, 5<sup>th</sup> and 95<sup>th</sup> percentile – were derived from these hourly values for the gates open and gates closed seasons.

For the 2012 gates open season, computed target marker concentrations are greatest in LKC and adjacent segments (Figure 7.16). Qualitatively, the model median concentrations agree with the observations in this vicinity. The greatest observed concentrations are in the NSC and adjoining reaches down to MXZ, however. Computed medians fall short of observations in these reaches. During the gates closed season, the predominance of the two regions, Lake Calumet vs. North Shore Channel is reversed (Figure 7.17). The greatest observations are in the LKC vicinity and predominate over NSC and CR1. Computed medians universally fall short of corresponding observations.

Several issues cloud the comparison of observed and computed median concentrations described above. The first is the different bases of the observations and computations. The observations represent characteristic values influenced by all sampling events from 2009 through 2012. The computations are influenced solely by loading and transport during the two 2012 seasons. A second issue is the range of potential characteristic values. The observed median is a single value when a range of potential values might be more descriptive. A third issue is uncertainty in the loads. The MCMC procedure which estimated the loads produced, in fact, a range of loads from which the 50<sup>th</sup> percentile was selected for model use. Greater or lesser loads than the values employed are feasible. A second view of the observations versus computations incorporates the range from 5<sup>th</sup> to 95<sup>th</sup> percentile of observations and computations. During the gates open season, the model range overlaps the observed range for most reaches (Figure 7.18).

In only two reaches, CRM and CRB, are the computations and observations distinctly different. The discrepancy suggests an inadequacy in loading. Greater or lesser loading rates should be selected from the potential range although the excess of observations over computations in CRM allows for the existence of a source not considered here. During the gates closed season, the computed range overlaps with the observed range in all reaches (Figure 7.19) indicating the transport processes, loads, decay rates, and other model processes and parameterizations result in computed concentrations which reflect the characteristic observed values.

### *Primary Source Simulation Results*

#### *a. Axial distribution*

Seasonal-average computed target marker concentration from primary sources is shown along three system axes: Lockport to North Shore Channel (Figures 7.20, 7.21), Lockport to O'Brien Lock and Dam (Figures 7.22, 7.23), and O'Brien Lock and Dam to Lake Michigan (Figures 7.24, 7.25). Computed concentration of each fraction (fast, slow) ranges within an order of magnitude in the reaches from Lockport to NSC and Lockport to O'Brien. The order of magnitude variation is narrow compared to the range resulting from various secondary sources. Concentrations of the fast fraction predominate over the slow fraction indicating that the disparity in loading, four-to-one in favor of the fast fraction, is more influential in determining relative concentration than the disparity in decay rates. The fast fraction decays nearly six times faster than the slow fraction. Variations along the axes largely reflect dilution from WRPs and other inflows. Along the Lockport to NSC axis, for example, the influences of the North shore WRP, near km 75, and the Stickney WRP, near km 40, are evident. Seasonal differences are most evident in the vicinity of the control structures. Computed concentration between Wilmette (km 80) and the North Shore WRP (km75) is roughly an order of magnitude greater during gates closed than gates open (Figure 7.20 vs. 7.21). Variation of similar origin, although of lesser magnitude, is evident between the Calumet WRP, near km 50, and the O'Brien Lock and Dam, near km 56 (Figure 7.22 vs. 7.23).

Computed concentration along the axis from O'Brien to Lake Michigan ranges within two orders of magnitude for each fraction. The greater range along this axis is due to dilution by lake water. Variation between the gates open and gates closed seasons (Figures 24 vs. 25) is most evident in the immediate vicinity of the connection to the lake.

#### *b. Temporal reaction*

The time series of computed concentration in many reaches are flat, consistent with the constant loading from the constant primary source mass in each reach. This phenomenon is typified in CR4 (Figure 7.26) and LKC (Figure 7.27). Reaches near control structures e.g. NSC (Figure 7.28) and inflows e.g. BCR (Figure 7.29) reflect the diluting influence of freshwater flows.

*c. Comparison with observed target marker concentrations*

The comparisons of eDNA computed from primary sources to observations are presented in the same formats as the comparisons to computations from secondary sources. The computed concentrations from primary sources are larger than concentrations based on secondary sources. As a result, comparisons with observations near the NSC during gates open season (Figure 7.30) and throughout the system during gates closed season (Figure 7.31) are superior to the comparisons based on secondary sources.

The eDNA computations based on primary sources are subject to the same influences and constraints with regard to uncertainties in observations and loadings as the eDNA computations based on secondary sources. When the ranges of computations and observations are included in the comparisons (Figures 7.32, 7.33), the ranges overlap in most reaches, indicating the loads from primary sources, in combination with transport processes, decay rates, and other model processes and parameterizations, result in computed concentrations which largely reflect the characteristic observed values. Interestingly, disagreement between computations and observations recurs in reaches CRM and CRB during the gates open season. Neither the primary nor secondary sources explain the high concentrations observed in CRM. Both loading sources produce computed concentrations in excess of the observations in CRB. The primary sources also result in excess concentrations in CLK during gates open season and in CRV during gates closed season. Likely all of these discrepancies could be addressed through adjustment of the primary source loads within the range of potential values. However, the consistent discrepancies in CRM and CRB suggest the observations in these reaches should be reviewed.

*Comparison of HFFTM Simulation Results with SSFTM Simulation Results*

Seasonal, median target marker concentrations computed by the HFFTM are compared with results from the SSFTM for secondary sources (Figures 7.34, 7.35) and primary sources (Figures 7.36, 7.37). From a qualitative viewpoint, concentrations computed by the HFFTM for secondary sources often fall short of concentrations computed by the steady-state model. By contrast, concentrations from the HFFTM for primary sources are roughly equivalent to and occasionally higher than concentrations from the steady state model. The visual impression is borne out by correlation coefficients. The  $R^2$  value for seasonal median concentrations computed by the two models is 0.43 for secondary sources compared to 0.77 for primary sources.

The SSFTM is based on the following properties:

- The spatial scale for computation is equivalent to the spatial scale of reaches.
- The temporal scale for computation is seasonal, gates open or closed.
- The temporal scale for loading is seasonal, for secondary sources.
- There is no temporal variation in primary loads.

The HFFTM is based on the following properties:

- The spatial scale for computation is the grid cell, roughly 30 x 60 x 2 m.
- The temporal scale is the discrete time step in the solution algorithm for the transport equation, on the order of minutes.
- The temporal scale for loading is daily, for most secondary sources.

- There is no temporal variation in primary loads.

Computations from the HFFTM can be readily aggregated by reach and season. However, when the computations are based on temporally-varying secondary source loads, the concentrations will differ from the steady-state model. These comparisons indicate the concentrations computed by the HFFTM resulting from secondary source loads will be less than the concentrations computed by the steady-state model for the same loads. When the loads have equivalent time scales, however, as for primary sources, the aggregated concentrations from the HFFTM agree well with the steady-state model.

#### *Summary of Conclusion based on HFFTM Simulation Results*

The median secondary source loading rates derived through the MCMC procedure were implemented in the HFFTM. The resulting computed concentrations indicated the predominant source of eDNA varies with location and season. For many reaches, a predominant source was difficult to identify. Some prevailing characteristics were noticeable, however:

- During the gates open season, Lake Michigan is the predominant source in the adjoining reaches: NSC, CRM, CRA. During the gates closed season, Lake Michigan remains a significant, but not necessarily predominant source in CRM and CRA.
- Navigation can be a predominant eDNA source in the region immediately above Lockport, denoted as reaches CR6, FBA, and CR5.
- The region surrounding Lake Calumet is largely free of CSOs. In this region, (reaches CRB, CLK, LKC, CRU, CRV) fishing derbies and fishing nets can be predominant sources.
- CSOs represent a significant source of eDNA in the reaches that receive large discharges, especially during gates closed season e.g. NSC, BCR, MXZ, CR3
- Birds do not appear to be a predominant eDNA source in any reach. They represent a significant fraction of computed eDNA only in LKC during gates open season, which coincides with our assumed period of high population density and activity.

In a comparison of median computed and observed eDNA, by season and reach, the model often falls short of the observations. Best results are obtained for the region around Lake Calumet. Less demanding comparisons indicate that the 90% range of model concentrations overlaps with the 90% range of observations in most reaches and seasons.

Computed results from primary sources contrast with the results from secondary sources. The computed medians often equal or exceed the observations. The 90% range of model concentrations overlaps with the 90% range of observations in most reaches and seasons.

Comparisons between eDNA computed by the HFFTM and by the steady-state model parallel the comparisons between the HFFTM and the observations. That is, agreement is better for the primary sources than for the secondary sources. We suggest the superior agreement for

the primary source loads is due to the employment of steady loads in the HFFTM. Agreement between the two models deteriorates when steady loads are used in the steady-state model and temporally-varying loads are used in the HFFTM.

Agreement between computed and observed eDNA concentrations based on secondary source loads could likely be improved by selecting optimal loads from the range of feasible values rather than arbitrarily selecting the median load.

## **8. Prior Probabilities of Target Species Presence**

A prior probability on target species presence is required for development and implementation of a model to estimate the probability of target species presence. One approach might be to assume no prior information on the matter and adopt a uniform prior distribution to characterize uncertainty in target species presence. This non-informative prior distribution suggests that the target species presence is just as likely as not. Alternatively, one could make a subjective probability statement that reflects an individual or corporate degree of belief based on an intimate knowledge of the system. For example, it is known that the CAWS is protected by an electric barrier and that no members of the target species have been seen in the CAWS. Thus, one might assign a relatively low probability to target species presence and a relatively high probability to target species absence. A third possibility is to make an objective probability statement based on an analysis of available data. This is the approach used in this report to analyze Asian carp presence in the CAWS. Data on conventional fisheries surveillance effort is used to update an uninformed prior probability of target species presence to a posterior probability. This posterior probability then serves as an input to the probabilistic model, where it characterizes uncertainty in target species presence prior to accounting for results of the eDNA monitoring program. This section of the report summarizes conventional fishing effort and describes how the prior probability of target species presence can be evaluated using that data.

### *Conventional Fisheries Surveillance in the CAWS*

ILDNR has carried out a conventional Asian carp surveillance program in the CAWS since 2010. The conventional approach to surveillance is to set fishing gear at those locations where it is believed the target species may be lurking. ILDNR provided information on the date, location, type, and level of FRS, RR, and PIS fishing effort in the CAWS. FRS and PIS gear sets were described in a detailed database for the years 2011 – 2013 (no fishing effort occurred in 2009, records of FRS and PIS gear sets were not available for 2010). Aggregate summaries of RR fishing effort were obtained from MRWG reports (MRWG 2012, MRWG 2013). Four basic types of fishing gear have been used in the course of conventional surveillance. Tables 8.1 – 8.4 summarize conventional fishing effort as reported by ILDNR. Gear types include: 1) commercial fishing nets (including gill nets, trammel nets, commercial seines and deep gill nets fished up to three hours), 2) electrofishing boats, 3) trap nets, and 4) deep gill nets fished longer than three hours. The level of effort reported in Tables 8.1- 8.4 is described using units appropriate for each gear type. Commercial fishing net effort is expressed in terms of the length of net fished (100 meters). Electrofishing effort is described in terms of the length of pedal time (hours). Trap net effort is described in terms of net days. Effort using deep gill nets fished longer than three hours is described in terms of 100 meter hours.

ERDC estimated 2010 fishing effort and determined the location of each gear set in relation to the hydrodynamic grid using the data provide by ILDNR. ERDC estimated the level of 2010 fishing effort using 2011 data provided in MRWG reports. MRWG (2012) reports 23.8 miles (383.02 100-meters) of commercial fishing nets were set in the course of FRS monitoring between June and September, 2010. The corresponding FRS effort between June and September 2011 is 474.12 100-meters. The 2010 effort was imputed by taking the gear set records from June through September 2011 and weighting the level of effort by 0.80785 (the ratio of 383.02 and 474.12). A similar approach was used to impute 2010 electrofishing effort. MRWG (2012) reports that there were 519 15-minute electrofishing transects (129.75 hours) run between June and November 2010. During 2011, there were 561 15-minute electrofishing transects (140.25 hours) run between June and November, 2011. The 2010 fishing effort was imputed by taking the 2011 electrofishing records from between June and November and weighting them by 0.9251 (the ratio of 519 and 561). Tables 8.5 and 8.6 incorporate the estimates of 2010 fishing effort into the tables summarizing commercial gill and trammel net effort and electrofishing effort.

ERDC determined the location of each gear set in relation to the hydrodynamic grid of the CAWS by geo-referencing gear set records to hydrodynamic grid cells using the latitude and longitude reported in the ILDNR database. If the coordinates of a gear set record place the set outside the hydrodynamic grid, but within 100 meters of a grid cell, the gear set was assigned to the nearest grid cell. In many cases, geo-referencing located the gear set more than 100 meters from the grid. In other cases, no latitude and/or longitude were reported in the record. In such cases, ERDC assigned an approximate location for the gear set based on the fixed or random site name and location codes. In the best of such cases, the gear set could be placed on a transect half way between the preceding and subsequent samples, or matched to another fixed or random site record for which the location was reported in another database record or in MRWG reports (MRWG 2012, MRWG 2013). In other cases, ERDC located the gear set at the geographic center of a reach based on descriptive information provided with each record.

### *Single Sample Gear Detection Probabilities*

Information on fishing effort is used in this study to estimate the probability that the target species is present in the CAWS upstream of the electric fish barrier. This calculation requires an estimate of the single sample gear detection probability for each gear type. The single sample detection probability is the probability that one unit of fishing effort will catch at least one specimen of a target species at a specific site. This probability varies from one site to another and depends on a wide variety of factors. For example, these factors may include the shape and complexity of the search area, habitat characteristics, size or volume of the search area, as well as characteristics and density of the target species.

Butler et al. (2014) describe how single sample gear detection probabilities can be estimated for hoop nets and electrofishing boats targeting bighead carp and silver carp, respectively. These authors estimated single sample detection probability at seven sites on the Illinois River downstream of the Dresden Island pool. No single sample detection probabilities could be estimated upstream of the electric fish barrier because no specimens of the target species were captured. Butler et al. (2014) also describe how the probability of detecting a target



species can be estimated from single sample detection probabilities. The probability of capturing a target species,  $F$ , at a site can be estimated given information about the level of fishing effort,  $E$ , and the single sample detection probability,  $s$ :  $F = 1 - (1 - s)^E$ . It follows that the level of fishing effort required to achieve a probability,  $F$ , of capturing at least one specimen of the target species at the site can be estimated:  $E = \log(1 - F)/\log(1 - s)$ . Butler et al. (2014) also show that detection probabilities are positively correlated with catch per unit effort (CPUE), which is a proxy for target species density.

Butler et al. (2014) discussed how their results might be applied to estimate how much fishing effort is needed to achieve a 95 percent probability of detecting the target species at sites located upstream of the electric fish barrier. Single sample detection probabilities could not be estimated at sites upstream of the electric fish barrier because no specimens were captured during sampling events. Therefore, the authors contemplated using the lowest estimated single sample detection probabilities from downstream of the barrier as an estimate at sites above the barrier. The lowest estimates of detection probabilities were 0.07 per net night for bighead carp targeted with hoop nets and 0.17 per quarter hour of pedal time for silver carp targeted with electrofishing boats. However, the authors emphasized that these single sample detection probabilities are likely to greatly overestimate those above the electric barrier because, if the target species is present, it is most likely present at a much lower density than at locations below the electric barrier.

### *Calculating the Prior Probability of Target Species Presence*

The prior probability of target species presence used in the probabilistic model is actually the posterior probability from a preliminary calculation that is made using the single sample detection probability and data on fishing effort. This preliminary calculation also requires an initial prior statement about the degree of belief in the null hypothesis that the target species is present. This initial prior probability is then updated using Bayes rule to calculate the posterior probability of the fish being present using the lack of capture as evidence. A simple event tree, shown in Figure 8.1, provides a useful way of thinking about these probabilities. The vertices of the tree describe random variables, the labels on the branches of the tree describe potential states (or values) of those variables, and the conditional probabilities of those states are given in parentheses.

The fishing expedition is an experiment designed to inform prior beliefs about the state of a random variable, SPECIES\_PRESENT, which can take one of two values, *True* or *False*. The strength of the prior belief in the state of the random variable can be expressed as a probability,  $p_1$ . Alternatively, SPECIES\_PRESENT = *False* has probability  $\overline{p_1} = (1 - p_1)$ . The second random variable, CATCH, describes the outcome of the experiment, whether or not at least one specimen of the target species is caught. Given SPECIES\_PRESENT = *True*, the probability of capturing at least one specimen,  $q_1 = F$ , can be calculated from the single sample detection probability,  $s$ , and level of fishing effort,  $E$ . Alternatively, if the target species is not present, the probability of capturing a specimen,  $q_2$ , is 0 and the probability of not capturing a specimen is 1. Then, the probability that the target species is present at the site given that no fish were caught during the expedition can be derived using Bayes rule:

$$p(\text{SPECIES\_PRESENT} = \text{True} \mid \text{CATCH} = \text{False}) = \frac{p_1(1 - q_1)}{p_1(1 - q_1) + (1 - p_1)}$$

The prior probability is updated to a posterior probability after each fishing expedition. It should be noted that some assumptions are required to implement this method. Recruitment and mortality must be balanced and there must be no net immigration or emigration from the site during the period over which sampling occurs.

The following example will illustrate how this approach can be applied. Suppose that fisheries managers claim no prior knowledge about whether or not a target species is present at a search site. The corresponding initial prior probability on target species presence is 0.5. Now suppose that ten units of fishing effort will be expended on five separate fishing expeditions to assess whether or not the target species is present and that the best estimate of the single sample gear detection probability is 0.07. The cumulative probability of detecting the species given that it is present is  $q_1 = F = 0.516$ . After the first expedition, the posterior probability that the species is present,  $p(\text{SPECIES\_PRESENT} = \text{True} \mid \text{CATCH} = \text{False})$ , is 0.326. This posterior becomes the prior for the second expedition during which another ten gear sets are made. If the species is not detected again, then the posterior probability,  $p(\text{SPECIES\_PRESENT} = \text{True} \mid \text{CATCH} = \text{False})$ , is further reduced to 0.19. The sequence of priors and posteriors over the five fishing expeditions are summarized in Table 8.7 and in Figure 8.2. If the target species has not been detected after five fishing expeditions, then the probability that the target species is absent from the site increases to 0.974. This example illustrates how fisheries managers can increase their confidence in the absence of an invasive fish species from the CAWS by repeatedly targeting the species. Although this approach sounds simple, implementation is fraught with the challenge of estimating single sample gear detection probabilities.

### *Challenges to Implementation and Approach*

One challenge to implementing this method is the difficulty of obtaining a single sample detection probability at the site where no specimen of the target species has been caught. A logical solution to this problem would be to transfer a single sample detection probability estimated at a site characterized by similar size, shape, complexity, and habitat characteristics. A single sample gear detection probability estimated at one site can be applied at another site if all of the factors influencing that probability are identical, including target species density. It is likely that these requirements will be difficult to satisfy in practice. However, there may be ways of accounting for differences between sites. For example, a single sample gear detection probability might be scaled to account for differences in the size or volume of the search area, the complexity of the habitat, or prior beliefs about species density. Approximate estimates of the single sample gear detection probability can be used in heuristic analyses to provide insights into the probability that the target species is present at a specified density and the levels of fishing effort that would be needed to achieve some level of confidence about target species presence at that density.

For the purpose of developing the probabilistic model, the following approach is used to estimate the single sample gear detection probability in a CAWS reach. The single sample gear detection probability,  $s$ , is the ratio of target species mass (kg) to the volume ( $\text{m}^3$ ) of the search

site as determined using the hydrodynamic grid. This implies that the probability of catching a specimen of the target species is directly proportional to the target species density at the search site. For example, the probability of detecting a target species that is present at a density of  $1 \text{ kg m}^{-3}$  with one unit of fishing effort is 0.001. Figure 8.3 illustrates how the single sample detection probability varies by CAWS reach over a range of potential target species mass. For example, if a target species mass of 30 kg is presumed, the single sample gear detection probability ranges from  $2.88\text{E-}06$  to  $1.18\text{E-}04$ . This approach results in single sample gear detection probabilities that are several orders of magnitude less than those estimated by Butler et al. (2014). No distinctions have been made for gear types or target species. An implicit assumption is that fish are randomly distributed in the reach and that there is no avoidance of or attraction to the gear. Single sample gear detection probabilities account for effects of target species density, but not for the effects of target species, gear type, or habitat characteristics. While these single sample gear detection probabilities are not ideal, they are useful for the purpose of developing the probabilistic model and demonstrating its application in this report. However, these single sample gear detection probabilities should be revised as better estimates become available in the future.

Prior probabilities of target species presence were calculated for the probabilistic model considering fishing effort during the period 2009-2012 because it coincides with the hydrodynamic modeling period. For development purposes, three sets of prior probabilities were calculated using different subsets of the effort data. These subsets are described in Table 8.8. The first subset considers only commercial gill and trammel net effort, the second subset considers only electrofishing effort, and the third considers all fishing effort. Prior probabilities of target species presence are reported for each subset of effort data in Tables 8.9 – 8.11. These probabilities are calculated for a range of target shedding units from less than 1 kg to an arbitrary maximum of 20,000 kg in each CAWS reach. For target shedding units less than about 1000 kg, the probabilities remain close to the initial prior probability, 0.5. This suggests that fishing effort has not been sufficient to influence beliefs about target species presence at low density. As the target species density increases with the number of shedding units, the probabilities decrease. This pattern is strongest in those reaches where fishing effort has been relatively high (e.g., NSC, CR1, CR2, LKC). For example, in Table 8.11 the probability that 19,000 - 20,000 kg of the target species is present in the NSC is 0.096, which is much lower than the initial prior probability. The trend indicates that the conventional surveillance program has successfully increased the probability that large quantities of the target species are absent in the NSC.

## **9. A Bayesian Network for Inference about the Presence of Live Asian Carp**

The probabilistic model developed in this report integrates all of the information developed in previous sections of this report to provide a coherent framework for making inferences from eDNA monitoring results. A Bayesian network is a graphical model of a joint probability distribution over some set of random variables. The nodes of the graph are random variables, the edges between nodes signify causal influence between linked variables, and the strength of these influences is expressed by forward conditional probabilities (Pearl 1988). Mathematically, a Bayesian network is a factorization of a joint probability distribution that can be written:

$$P(X_1, X_2, \dots, X_n) = \prod_{i=1}^n P(X_i | X_{pa(i)})$$

The notation  $pa(i)$  means  $X$  is a parent of node  $i$  and the notation  $P(X_i | X_{pa(i)})$  means the probability that  $X$  is in state  $i$  given the state of parent nodes. Nodes with parents are parameterized by conditional probability tables (CPTs) that give, for every possible state of the variable, a probability of being in that state given the state of all parent node variables. Nodes without any parents are called roots and are parameterized by unconditional probability distributions.

The motivation for developing a Bayesian network model is the desire to perform inference about some hypothesis. Bayesian networks support both predictive and diagnostic inference. In predictive applications, the objective is to reason from cause to effect and so assess the probability of a particular outcome given knowledge about the state of ancestral nodes. The ability to solve predictive inference problems is particularly useful when dealing with complex systems about which understanding of causal effects is limited or direct observation of system states is difficult. In such cases, the state of the system must be inferred from uncertain information about site conditions. Diagnostic inference is reasoning from effects to causes and the objective is to predict the probability that an ancestor node is in a particular state given evidence about the descendent node. When there are multiple possible causes for an effect, this form of reasoning can be used to predict the probabilities of potential causes, a process known as “explaining away”. According to Kjaerulff and Madsen (2008), the ability to explain away the causes of an effect is unique to Bayesian networks.

Inference is accomplished by first applying information to the model in the form of either hard evidence or soft evidence. Hard evidence is knowledge that a particular variable is in a particular state and that the probability of being in all of the other possible states is zero. Entering hard evidence is called instantiation (Kjaerulff and Madsen 2008). Soft evidence is uncertain knowledge about a variable. When hard or soft evidence is entered into a node to reflect observations about a variable in the system, the objective is to compute the posterior probabilities for all the variables in the network. The posterior probability is simply the probability that the hypothesis variables in a network are in a particular state given the observed state of evidence variables. This process of updating the probabilities in the network is accomplished using Bayes’ theorem, which has previously been described in Section 2. Information on updating of probabilities in Bayesian networks using exact or approximate algorithms can be found in Kjaerulff and Madsen (2008), Koller and Friedman (2009), and Darwiche (2009). The ability to perform mathematically exact calculations of the probabilities efficiently is one of the primary advantages of Bayesian networks. Bayesian networks have been widely used to support statistical inferences about environmental problems. Some examples of environmental applications are reviewed in Schultz et al. (2011).

### *The Bayesian Network*

The purpose of the Bayesian network developed in this report is to make statistical inferences about the presence of live Asian carp in the CAWS. The network is illustrated in Figure 9.1. There is potentially one network for each reach from which eDNA samples are

collected. The network contains 22 random variables that are represented by nodes. Each node is parameterized using conditional probability tables (CPTs) developed from a combination of equations, experiments, simulation outputs, and hydrographic or environmental observations from the CAWS. The CPTs in each network contain 6.7 million conditional probabilities. The motivation for developing this Bayesian network is the desire to perform probabilistic inference about the presence of live Asian carp using as evidence the results from the eDNA monitoring program and conventional surveillance efforts. Each of the variables in the network is summarized and described in Table 9.1. The structure of the graph can be explained starting at the terminal node and proceeding up, against the direction of the edges. The following subsections describe each node or group of nodes in the network, starting with the terminal node in the graph.

*a. Fraction of positive hits (FOPH)*

The terminal node in the graph is the fraction of monitoring samples testing positive for the target marker (FOPH). FOPH depends on what Asian carp species is being targeted in monitoring samples (SPECIES, *Bighead* or *Silver*) and the concentration of eDNA in the monitored water body (TOTAL\_CONC, copies/L). The FOPH node is parameterized by calculating the probability that a target marker is detected with some frequency given the ambient concentration of the target marker in the water column. The probabilities are calculated by sampling from the model of target marker detection rates, described in Section 2 of this report. The CPT is constructed as described in Section 3 of this report. A set of realizations are generated at each potential concentration and the results,  $p[\text{ASSAY} = \text{POS} \mid C_M]$ , are binned into potential frequencies of positive detection to calculate the fraction of observing the evidence given the target marker concentration,  $p[e \mid C_M = c]$ .

*b. Species (SPECIES)*

The Bayesian network is developed for inference about two species of Asian carp, bighead carp and silver carp. Networks for the two species reflect differences in the sensitivity of target markers to detection and sequencing methods used in the laboratory. For the reasons outlined in Section 2 of this report, it is more difficult to confirm the detection of the bighead carp target marker by sequencing than to confirm the detection of the silver carp target marker. This difference tends to make the silver carp marker much easier to detect in monitoring samples than the bighead carp marker.

*c. Total concentration (TOT\_CONC)*

The total concentration (TOTAL\_CONC, copies/L) variable is the target marker concentration in the sample reach. The node is parameterized using a CPT constructed from an equation:  $\text{TOTAL\_CONC} = \text{TOT\_PRIM\_CONC} + \text{TOT\_SEC\_CONC}$ . The variable TOT\_PRIM\_CONC is the concentration attributed to primary sources (copies/L) and TOT\_SEC\_CONC is the concentration attributed to secondary sources (copies/L).

*d. Secondary source concentration (TOT\_SEC\_CONC)*

The secondary source concentration (TOT\_SEC\_CONC, copies/L) is the target marker concentration in the sample reach attributed to secondary sources. There are six secondary sources, including piscivorous birds, Lake Michigan inflows, CSOs, recreational fishing derbies, commercial fishing nets, and commercial navigation. TOT\_SEC\_CONC is parameterized by generating a set of production runs using the HFFTM. The production runs are processed to create a time series of median concentration for each source and reach. The TOT\_SEC\_CONC node is parameterized by creating a CPT to characterize uncertainty in the total secondary source concentration. The TOT\_SEC\_CONC node is dependent on the slow decay rate (K\_SLOW, day<sup>-1</sup>), the hydrologic season (SEASON, *Gates Open* or *Gates Closed*), and the ALL\_ACTIVE node, which characterizes the prior degree of belief that secondary source loads are contributors of eDNA to the CAWS.

Production runs were completed by simulating the target marker concentration from each secondary source over a four-year period and assuming a slow decay rate. All secondary source loads are assumed to decay in accordance with the slow decay rate. One production run was completed for each possible value of the slow decay rate (0.038, 0.079, 0.120 d<sup>-1</sup>). Loading rates used in the production runs were selected to provide convenient units for input and to be large enough that the patterns of transport in the CAWS could be determined through representative computed concentrations. The secondary sources and loading rates employed in the production runs were:

- Commercial fishing nets – one million copies / 100 m net fished / day
- Piscivorous birds – one million copies / m<sup>2</sup> / day
- Commercial navigation – ten million copies / boat hour
- Recreational fishing derbies – ten million copies / recreational boat day
- CSOs – one million copies / m<sup>3</sup>
- Lake Michigan inflows – one million copies / m<sup>3</sup>

The concentrations estimated by production runs are scalable. Therefore, the concentration resulting from any other (proposed) loading rate can be obtained by multiplying the production run concentration by the ratio of the proposed loading rate to the production run loading rate.

Production runs for secondary sources were four years in duration, 2009 – 2012. Each secondary source run was conducted in two parts in order to transfer boundary conditions from the Lake Calumet grid to the CSSC grid. Complete data to describe loading factors for recreational fishing derbies and navigation was available for 2012 only. Therefore, 2012 loading factors were used to represent the processes generating secondary source loads for all four years. Bird loads were considered constant across all years. Seasonal variations in loading due to variations in avian population and activity were considered subsequently by scaling the model results to the seasonal variation in loading rate. Loading factors for fishing nets, combined sewer overflows, and Lake Michigan inflows were available for all four years and employed in the model runs.

Production runs were organized into 19 data files, one for each major reach. Each of these 342 data files consisted of a table showing the hourly median target marker concentration from each secondary source and each decay rate. No attempt was made to determine in what

upstream reach the target marker was released. These 342 data files were subsequently used to construct the CPT for the TOT\_SEC\_CONC node. HFFTM concentration estimates were divided by the nominal loading rate used in production runs to represent the unit concentration response in a reach to a change in the unit loading factor for each secondary source. This unit concentration response can be scaled by a unit loading rate or a loading factor to estimate the effect of a secondary source on the target marker concentration.

Six potential unit loading rates were chosen for each secondary source. These included 0, and five loading rates spanning five orders of magnitude in the range of Bayesian MCMC estimated loading rates. One table of hourly median secondary source concentrations was generated for every 46,656 combinations of loading rates. The concentrations were summed to calculate the secondary source concentration from all source combined and then binned by SEASON and K\_SLOW into 44 concentration intervals ranging from 0 to 3500 copies/L. The fraction of hourly concentrations in each bin is the probability of the total secondary source concentration occurring given the six secondary source loading rates, the season, and the slow decay rate.

*e. Secondary source activity (ALL\_ACTIVE)*

The ALL\_ACTIVE node characterizes the degree of belief in that secondary sources contribute eDNA to the CAWS. The ALL\_ACTIVE node has two potential states: *True* and *False*. If the node state is *True*, the secondary source loading rates are consistent with those estimated by Bayesian MCMC in Section 5. If the state of the ALL\_ACTIVE node is *False*, the secondary source loading rates are 0. Loading rates for secondary sources cannot be varied individually in the network because they were estimated simultaneously and; therefore, are not independent. The ALL\_ACTIVE node is parameterized with a uniform prior distribution, reflecting lack of knowledge about whether or not secondary sources actually contribute bighead carp and silver carp eDNA to the waterway.

*f. Slow decay rate (K\_SLOW)*

As described in Section 4 of this report, target markers shed from a primary source can be divided into two fractions, one that decays relatively rapidly and another that decays relatively slowly. For the purpose of this analysis, it is assumed that target markers that are mobilized and subsequently released by secondary sources into the CAWS decay at the slower rate because it is believed that those target markers that decay at the faster rate would have decayed either before or during mobilization by the secondary source. The K\_SLOW node has three potential states representing a range of possible decay rates: 0.038, 0.079, and 0.120 d<sup>-1</sup>.

*g. Season (SEASON)*

There are two hydrologic seasons in the CAWS: *Gates Open* and *Gates Closed*. Hydrology is the principal force influencing the transport of target markers released from both primary and secondary sources. When sluice gates controlling flows between Lake Michigan and the CAWS are open, flows in the CAWS tend to increase and substances tend to be

transported faster and further from their source. Gates between the CAWS and Lake Michigan are open from approximately June 1 to October 15 and are closed from October 15 to June 1.

*h. Total primary concentration (TOT\_PRIM\_CONC)*

Total primary concentration (TOT\_PRIM\_CONC, copies/L) is the concentration in the sample reach attributed to primary sources. The node is parameterized using an equation. TOT\_PRIM\_CONC is the product of its two parent variables, EQUIV\_NOM\_SHEDUNITS and PRIM\_NOM\_CONC. EQUIV\_NOM\_SHEDUNITS is the number of shedding units (kg) that would be needed to produce the total primary source concentration in the sample reach assuming a nominal shedding rate of 14 million copies/hour/kg. PRIM\_NOM\_CONC is the target marker concentration in the sample reach that would be attributed to a single shedding unit in an upstream reach if that shedding unit were present.

*i. Primary nominal concentration (PRIM\_NOM\_CONC)*

Primary nominal concentration (PRIM\_NOM\_CONC, copies/L) is the concentration that would be attributed to a single shedding unit in an upstream reach if that shedding unit were present. The node is parameterized using an equation that is the weighted sum of the primary fast concentration (PRIM\_FAST\_CONC, copies/L) and the primary slow concentration (PRIM\_SLOW\_CONC, copies/L):

$$\text{PRIM\_NOM\_CONC} = \text{FRACT} \cdot \text{PRIM\_FAST\_CONC} + (1 - \text{FRACT}) \cdot \text{PRIM\_SLOW\_CONC}.$$

The fast and slow concentrations are weighted by FRACT and 1-FRACT, respectively. FRACT is the fraction of target markers shed by a primary source that decays in a manner consistent with the fast decay rate.

*j. Primary concentration (PRIM\_FAST\_CONC, PRIM\_SLOW\_CONC)*

The concentration of the target marker that is shed by a primary source can be divided into two fractions. One fraction decays at a faster rate and the other fraction decays at a slower rate. These two nodes are parameterized by post processing a set of production runs generated using the HFFTM. Production runs for primary source (live fish) loads were completed for three fast decay rates (0.266, 0.463, 0.660 d<sup>-1</sup>) and three slow decay rates (0.038, 0.079, 0.120 d<sup>-1</sup>). Each run was four years in duration, 2009 – 2012, and was completed in two parts. First, the Lake Calumet portion of the grid was run. Computed concentrations at the O'Brien Lock and Dam from this run were saved and used as boundary conditions for a subsequent run on the CSSC grid.

Primary source loads from each reach were modeled as unique variables in the HFFTM so that the origin (source reach) of eDNA detected downstream could be determined. The CEQUAL-ICM code was enhanced by increasing the number available contaminants to nineteen so that, with backwater areas combined with their adjacent main-stem reach, the fate and transport of eDNA from all nineteen source reaches could be modeled in a single simulation run. The nominal primary source loading rate used in production runs was 14 million copies hr<sup>-1</sup> per



shedding unit. The production run assumed one shedding unit per computational grid cell (average size is 2,418 m<sup>3</sup>). The load to each cell was multiplied by the ratio of local cell volume to average cell volume in order to provide a uniform initial concentration throughout each reach. The output from each model run was organized into 19 files, one for each major reach. Each file comprised a table showing, at hourly intervals, the concentration in that reach resulting from a primary source in each of 19 reaches.

Output files from the production runs were post-processed to construct the CPTs for the PRIM\_FAST\_CONC and PRIM\_SLOW\_CONC nodes. The hourly concentrations of target markers attributed to each source reach were binned into eight concentration intervals including 0, and seven order of magnitude intervals spanning from less than 1E-6 to greater than 1E1. The relative frequency of hourly concentrations in each bin is the probability of the median fast or slow concentration being in each possible state. Probabilities were conditioned on SEASON, source reach (LURK\_REACH), and decay rate.

*k. Equivalent nominal shedding units (EQUIV\_NOM\_SHEDUNITS)*

Equivalent nominal shedding units (EQUIV\_NOM\_SHEDUNITS, kg) is the number of shedding units that would be needed to explain the concentration in the TOT\_PRIM\_CONC node given the concentration that would be generated in the sample reach by a single shedding unit residing in one of the reaches upstream (PRIM\_NOM\_CONC). This node is required because primary source production runs have been completed using a nominal shedding rate of 14 million copies kg<sup>-1</sup> hr<sup>-1</sup>. The node is parameterized using an equation:

$$\text{EQUIV\_NOM\_SHEDUNITS} = \text{ACTUAL\_SHEDUNITS} \cdot \frac{\text{SHEDRATE}}{14 \times 10^6}$$

Where, ACTUAL\_SHEDUNITS is the actual number of shedding units in the upstream reach and SHEDRATE is the actual shedding rate.

*l. Shedding rate (SHEDRATE)*

The shedding rate (SHEDRATE, copies kg<sup>-1</sup> hr<sup>-1</sup>) is the number of copies of target marker produced by a primary source. The node is parameterized using a lognormal probability distribution using data from Klymus et al. (2014) as described in Section 4. The CPT in the SHEDRATE node is constructed by discretizing uncertainty in shedding rate, which is characterized by a lognormal probability distribution, LN(16.2354, 0.6615).

*m. Actual shedding units (ACTUAL\_SHEDUNITS)*

The actual number of shedding units (ACTUAL\_SHEDUNITS, kg) is the number of shedding units in an upstream reach. The node is parameterized using a CPT that is conditioned on a single parent node: SPECIES\_PRESENT. When the state of node SPECIES\_PRESENT is *True*, ACTUAL\_SHEDUNITS has a uniform probability distribution over its potential states. This indicates that one or more shedding units are located in an upstream reach, but the actual number of shedding units is highly uncertain. When the state of “SPECIES\_PRESENT” is

*False*, ACTUAL\_SHEDUNITS is in state 0 with probability 1. This indicates that there are no shedding units in upstream reaches.

n. *Species present* (SPECIES\_PRESENT)

The node SPECIES\_PRESENT describes whether or not fish are present in a reach upstream of the sample reach. The node takes one of two possible states: *True* and *False*. This node is parameterized using a CPT in which the conditional probabilities are estimated from data on single sample detection probabilities and fishing effort by gear type, accounting for all conventional surveillance efforts over the period 2009-2012. The node is dependent on three parent nodes: TARGET\_SHEDUNITS, LURK\_REACH, and GEARTYPE.

TARGET\_SHEDUNITS is the number of shedding units potentially present in an upstream reach (the number of shedding units one is looking for) and LURK\_REACH is the reach of the CAWS where the TARGET\_SHEDUNITS are potentially located. The GEARTYPE node describes what type of gear was used in the course of conventional surveillance efforts.

The CPT for this node is developed by calculating  $p(\text{SPECIES\_PRESENT} = \textit{True} \mid \text{CATCH} = \textit{False})$  for every combination of parent node states as outlined in Section 4.5. The conditional probabilities are calculated accounting for fishing effort in each reach. Since the each reach is calculated independently, this implies that all shedding units are present in a single upstream reach (LURK\_REACH). This is in contrast to the possibility that the shedding units might be dispersed among more than one upstream reach. This limitation could be overcome through further development of the Bayesian network. The conditional probabilities in the CPT account for all fishing effort from 2010, the year surveillance began, through 2012. This includes fishing effort from FRS monitoring program and the RR program, as described in Section 4. Fishing effort from 2013 has not been included in this analysis because it occurred after the last hydrologic year represented in the CE-QUAL-ICM.

Parameterization of the SPECIES\_PRESENT node requires knowledge of the single sample gear detection probability. Butler et al. (2013) have estimated single sample gear detection probabilities for hoop nets targeting bighead carp and to electrofishing boats targeting silver carp in selected sections of the Illinois River below Dresden Lock and Dam. These estimates are not necessarily applicable above the electric fish barrier because, if target species are present, they are present at much lower density. Habitat characteristics are also very different. For the purpose of this study, the single sample gear detection probability (SSGDP) in a reach is estimated by the ratio of TARGET\_SHEDUNITS (kg) to REACH\_VOLUME (m<sup>3</sup>):

$$\text{SSGDP} = \frac{\text{TARGET\_SHEDUNITS}}{\text{REACH\_VOLUME}}$$

TARGET\_SHEDUNITS is the number of shedding units (kg) for which SPECIES\_PRESENT is being evaluated and REACH\_VOLUME is the volume of LURK\_REACH (m<sup>3</sup>). The probability of catching a target species that is present in a reach with a density of 0.001 kg/m<sup>3</sup> given one unit of fishing effort is 0.001, or one-in-a-thousand. No distinctions have been made for gear types or target species in estimating the SSGDP. This approach assumes that the fish are randomly distributed in the reach and that there is no avoidance of or attraction to the gear.

*o. Target shedding units (TARGET\_SHEDUNITS)*

The target shedding units node (TARGET\_SHEDUNITS, kg) is the number of shedding units for which  $p(\text{SPECIES\_PRESENT})$  is being evaluated. The node is parameterized assuming a uniform probability distribution over 31 discrete states from 0 to 20,000 kg. The parameterization implies no prior information about how many fish might be present in the target reach.

*p. Lurk reach (LURK\_REACH) and search area (SEARCH\_AREA)*

The target reach (LURK\_REACH) is the location where the target shedding units might be located and where  $p(\text{SPECIES\_PRESENT})$  is being evaluated. The target shedding units may be located in any one of 19 CAWS reaches; however, as described above, it is assumed that all of the target shedding are in one reach. LURK\_REACH is dependent on a single parent node, labeled SEARCH\_AREA, which is the area where over which  $p(\text{SPECIES\_PRESENT})$  is being evaluated. The node has five potential states that describe the location of the LURK\_REACH in relation to the sample reach, where eDNA monitoring samples are collected: *Upstream*, *Local*, *Downstream*, *Above Barrier*, and *Entire CAWS*. *Upstream* means any reach upstream of the sample reach, including the sample reach. *Local* means strictly in the sample reach. *Downstream* means any reach downstream of the sample reach. *Above Fish Barrier* means any reach above the electric fish barrier regardless of its relationship to the sample reach. *Entire CAWS* means any reach upstream of Lockport Lock and Dam, regardless of its relationship to the sample reach. In most cases, the SEARCH\_AREA node should be instantiated to either *Upstream* or *Local* because eDNA monitoring samples provide very little information suitable for inference about the presence of shedding units downstream of the sample reach. The LURK\_REACH node is parameterized using a CPT in which the conditional probabilities are calculated from the volume of the LURK\_REACH divided by the volume of the SEARCH\_AREA. The SEARCH\_AREA node is parameterized using a uniform probability distribution.

*Statistical Inference about the Presence of Silver Carp from eDNA Monitoring Data*

The Bayesian network provides a structure in which to make statistical inferences about the presence of a primary source in the CAWS using results of the eDNA monitoring program. The network computes the posterior probability that some quantity of the target species is present in or upstream of the sample reach given that no specimens of the target species have been captured in the course of conventional fisheries surveillance in those reaches. Posterior probabilities can be computed by applying information about the target species and the fraction of eDNA monitoring samples testing positive for the target marker. The Bayesian network can be used for inference only as long as no specimens of the target species have been captured in the course of conventional surveillance. There is one Bayesian network parameterized for each reach from which the monitoring samples have been obtained. Inference in any one sample reach must be done using the network that is parameterized for that reach.

The following set of variables will help improve the quality of inference if they are instantiated to define a scenario. These include SEASON, TARGET\_SHEDUNITS, SEARCH\_AREA, and GEAR\_TYPE. SEASON describes the hydrologic season during which the monitoring samples were collected. TARGET\_SHEDUNITS describes the number of shedding units for which the posterior probability is to be evaluated. SEARCH\_AREA describes the location of the area where the primary source may be located in relation to the sample reach. Although each Bayesian network has been parameterized so that several different search areas can be defined, it is best to instantiate the SEARCH\_AREA node to *Upstream*, which includes the sample reach where eDNA monitoring data have been collected. GEAR\_TYPE describes the type of fishing effort to consider in computing the prior probability of target species presence.

The node labeled ALL\_ACTIVE describes the *a priori* belief that secondary sources are an actual contributor of eDNA to the CAWS. The possible states are *True* and *False*. This node should remain un-instantiated for inference. ECALS studies have confirmed that the target marker is associated with each of the secondary sources considered in this report and could be released into the water column. However, those processes have not been observed or documented and the loading rates have not been measured. Therefore, ALL\_ACTIVE has been parameterized assuming that  $p(\text{ALL\_ACTIVE} = \text{True}) = 0.5$ , which suggests that secondary sources are as likely as not to be a contributor of eDNA to the CAWS. It is possible that some observers may believe more or less strongly that secondary sources can contribute eDNA to the CAWS. Since the conclusions of this study are sensitive to those beliefs, the sensitivity of this study's conclusions is examined in relation to parameterization of the ALL\_ACTIVE node.

Inference using the Bayesian network proceeds by specifying which node represents the hypothesis and which node represents the evidence. The hypothesis of greatest interest is SPECIES\_PRESENT, which takes the state *True* if the target species is present and *False* if the target species is not present. Evidence to evaluate the hypothesis is provided by the eDNA monitoring program and conventional fisheries surveillance. Since conventional fishing effort has already been accounted for in computing the CPT of the SPECIES\_PRESENT node, only the FOPH node can be varied. The FOPH node describes the fraction of eDNA monitoring samples testing positive for the target marker in the sample reach. The posterior probability that the hypothesis is true,  $p(\text{SPECIES\_PRESENT} = \text{True} | e)$ , is computed using the Bayesian network by instantiating the TARGET\_SPECIES and FOPH nodes. If the posterior probability is greater than 0.5, the evidence is in favor of the null hypothesis  $\text{SPECIES\_PRESENT} = \text{True}$ . Alternatively, if  $p(\text{SPECIES\_PRESENT} = \text{True} | e) < 0.5$ , the evidence is against the hypothesis.

Evidence for or against a hypothesis may be strong or weak. Bayes factor measures the weight of evidence by the change in odds in favor of the hypothesis going from the prior to the posterior (Lavine and Schervish 1999). Bayes factor,  $B$ , is the ratio of the posterior odds in favor of a hypothesis,  $H$ , given the evidence,  $e$ , to the prior odds in favor of the hypothesis:

$$B = \frac{p(H = \text{True}|e)/(1 - p(H = \text{True}|e))}{p(H = \text{True})/(1 - p(H = \text{True}))} = \frac{p(e|H = \text{True})}{1 - p(e|H = \text{True})}$$

Bayes factor characterizes the weight of evidence in favor of the null hypothesis,  $H = True$ , and against an alternate hypothesis,  $H = False$ . Bayes factors are attributed to Jeffreys (1935, 1961), who created the following scale for their interpretation (Kass and Raftery 1995):

< 1	Against the null hypothesis, in favor of the alternate hypothesis.
1-3.2	In favor of the null hypothesis, but barely worth a mention.
3.2-10	Substantial.
10-100	Strong.
> 100	Decisive.

An evaluation using Bayes factor is similar to conventional (Fisherian) hypothesis testing. A comparison between the methods is not necessarily straight forward, but Efron and Gous (2001) show that, for a one-sided hypothesis test under a Gaussian distribution,  $B = 3.2$  corresponds roughly to rejecting the null hypothesis with a critical level of  $\alpha = 0.025$ . In general, Jeffery's Bayes factor scale is regarded as providing a more conservative test of the null hypothesis than Fisher's hypothesis test (Kass and Raftery 1995, Efron and Gous 2001).

Bayes factor indicates the direction and magnitude of the effect that evidence would have on a posterior. For example, assume the odds ratio under a prior system of beliefs is 2, indicating that the null hypothesis is twice as likely as the alternate hypothesis. Upon consideration of some new evidence, the prior probability is updated to a posterior probability and a posterior odds ratio can be calculated. Assume the posterior odds ratio is 10. Bayes factor is the ratio of the posterior odds to the prior odds, which in this case is equal to 5. Since Bayes factor is greater than 1, the evidence is in favor of the null hypothesis. Higher values of Bayes factor indicate that evidence is more strongly in favor of the null hypothesis. In this case, the evidence is "substantially" in favor of the null hypothesis because Bayes factor is greater than 3.2. Although evidence may be substantially or strongly in favor of a null hypothesis, a posterior probability may still indicate that the null hypothesis is less likely than the alternate hypothesis. This situation indicates that the evidence has not overcome the prejudice of prior belief.

Conclusions of this study are sensitive to prior probabilities specified in the model. This report explores the sensitivity of posterior probabilities and Bayes factors to prior probabilities specified in the ALL\_ACTIVE node, which describes the degree of belief that secondary sources are a contributor of eDNA to the CAWS. The sensitivity of posterior probabilities in the SPECIES\_PRESENT node are analyzed using the sensitivity function, described in Kjaerulff and van der Gaag (2000) and Kjaerulff and Madsen (2008, p. 282). Bayes factors were re-computed over the range of prior probabilities on ALL\_ACTIVE to determine the prior probability on ALL\_ACTIVE = True at which Bayes factor indicates that eDNA provides substantial evidence in favor of the hypothesis that the target species is present.

#### *Statistical Inference for Silver Carp in Lake Calumet*

This section of the report demonstrates statistical inference using the Bayesian network and interpretation of results for a single sample reach, LKC (Lake Calumet). The null hypothesis being tested is  $H_0$ : SPECIES\_PRESENT = True and the alternate hypothesis is  $H_A$ : SPECIES\_PRESENT = False. Prior probabilities in the hypothesis node (SPECIES\_PRESENT)

have been calculated using information on the level of conventional fishing effort from 2009-2012 (Table 8.8). The network can only be used for inference if no specimen of the target species has been captured during the course of conventional monitoring. In this demonstration, posterior probabilities are calculated iteratively over a range of target shedding units and seasons to illustrate sensitivity to these variables. All results are for a mass of silver carp potentially located in LKC or in one of the reaches upstream (CRA, CRB, CLK).

Evidence to update the prior probabilities in the SPECIES\_PRESENT node is provided by the eDNA monitoring program. For consistency with the hydrologic simulation period, the level of conventional fishing effort, and the characterization of secondary source loading factors, this demonstration considers only eDNA monitoring results from 2009-2012. However, if it is assumed that year to year variability in hydrodynamics and secondary source loading factors have been adequately characterized, this Bayesian network can also be used to evaluate monitoring periods other than 2009-2012. This would be accomplished by re-parameterizing the SPECIES\_PRESENT node to reflect the level of fishing effort during the monitoring period and calculating the frequency of positive eDNA monitoring samples for the target species over that same period. When selecting a monitoring period, it is assumed that immigration and emigration of the target species are balanced during that period.

Figure 9.2 illustrates how the results of statistical inference can be interpreted. The  $x$ -axis is the fraction of eDNA monitoring results testing positive for eDNA. The  $y$ -axis is the  $p(\text{SPECIES\_PRESENT} = \text{True})$ . The green dashed line denotes the prior probability of fish presence, based strictly on information about the level of conventional fishing effort. The blue solid line plots the posterior  $p(\text{SPECIES\_PRESENT} = \text{True})$ . As the fraction of eDNA monitoring samples increases, so does the posterior. The red line plots the probability of the alternate hypothesis,  $p(\text{SPECIES\_PRESENT} = \text{False})$ . There are three critical frequencies of positive detection on the  $x$ -axis that divide the  $x$ -axis into the four regions shown in the figure (A, B, C, and D):

- A: The posterior is less than the prior. In this case, the eDNA evidence reduces the degree of belief that the target species is present.
- B: The posterior is greater than the prior, but less than 0.5. This indicates that eDNA evidence increases the degree of belief that the target species is present, but it is still more likely than not the target species is absent.
- C: The fraction of positive eDNA monitoring samples increases the posterior probability to a value greater than 0.5, indicating that it is more likely than not that the target species is present.
- D: Bayes factor is greater than 3.2, indicating that eDNA evidence is substantially in favor of the presence of the target species.

Prior probabilities are updated to posterior probabilities by applying evidence to the FOPH node. Results of statistical inference in LKC are illustrated in Figure 9.3 for silver carp varying the hydrologic season and the number of shedding units targeted. Results depend on the

hydrologic season because this affects how eDNA moves through the system. Results depend on the number of target shedding units because the single sample detection probabilities used in parameterizing the CPT for the SPECIES\_PRESENT node are density dependent. If the sample reach has been the subject of conventional fishing effort, the prior  $p(\text{SPECIES\_PRESENT} = \text{True})$  will tend to be lower for higher numbers of target shedding units and closer to 0.5 for lower numbers of target shedding units. For any given frequency of positive detections, lower priors will have lower posteriors.

The results of inference are summarized in Figure 9.3. Figures 9.3(A) and (B) show results for the gates open season and a target mass of 1-5 kg and in Figure 9.3(B) for a target mass of 10-11 t (metric tons), respectively. Each figure is interpreted by plotting an imaginary vertical line at the frequency of positive detection and then reading the posterior probability from the y-axis. For samples collected during the gates open season between 2009-2012, the fraction of eDNA monitoring samples testing positive for the silver carp target marker in Lake Calumet was 0.067.

*Season: Gates open; Target shedding units: 1-5 kg:* The posterior  $p(\text{SPECIES\_PRESENT} = \text{True})$  given the observed FOPH is 0.481, which is less than the prior of 0.5. Because the posterior is less than the prior, evidence provided by eDNA monitoring has reduced the degree of belief that the target species, silver carp, are in or a reach upstream of LKC. These results suggest that it is less likely than not that 1-5 kg of silver carp are present in LKC or a reach upstream of LKC. The FOPH at which Bayes factor indicates that eDNA monitoring would provide substantial evidence in favor of the null hypothesis,  $\text{SPECIES\_PRESENT} = \text{True}$ , is 0.90.

*Season: Gates open; Target shedding units: 10-11 t:* The posterior  $p(\text{SPECIES\_PRESENT} = \text{True})$  given the observed FOPH is 0.349, which is greater than the prior of 0.322. Because the posterior is greater than the prior, evidence provided by eDNA monitoring has increased the degree of belief that 10-11 t of silver carp are present in LKC or a reach upstream of LKC. These results suggest that it is less likely than not that 10-11 t of the target species are present in LKC or a reach upstream of LKC. The FOPH at which Bayes factor indicates that eDNA monitoring would provide substantial evidence in favor of the null hypothesis,  $\text{SPECIES\_PRESENT} = \text{True}$ , is 0.90.

The hydrologic conditions in Lake Calumet are altered by closure of the sluice gates at O'Brien Lock and Dam, which is located at the base of CRU. When gates are open, the water moves in and out of Lake Calumet much more freely. When gates are closed, Lake Calumet tends to be more stagnant. This would tend to make sources of the target marker located outside of the reach more difficult to detect and those located inside the reach easier to detect. Figures 9.3(C) and 9.3(D) show results for the gates closed season. For eDNA monitoring samples collected during the gates closed season, the fraction of eDNA monitoring samples testing positive for the silver carp target marker was 0.154.

*Season: Gates closed; Target shedding units: 1-5 kg:* The posterior  $p(\text{SPECIES\_PRESENT} = \text{True})$  given the observed FOPH, 0.154, is 0.60, greater than the prior, 0.5. Because the posterior is greater than the prior, the evidence provided by

eDNA monitoring increases the degree of belief that 1-5 kg of the target species is present in LKC or a reach upstream of LKC. These results suggest that it is more likely than not that 1-5 kg of live silver carp are present in LKC or in a reach upstream. Bayes factor indicates that eDNA monitoring results would provide substantial evidence in favor of the null hypothesis, Fish present = *True*, when  $FOPH \geq 0.55$ .

*Season: Gates closed; Target shedding units: 10-11 t:* The posterior  $p(\text{SPECIES\_PRESENT} = \textit{True})$  given the observed FOPH, 0.154, is 0.465, greater than the prior, 0.322. Because the posterior is greater than the prior, the evidence provided by eDNA monitoring increases the degree of belief that 10-11 t of the target species is present in LKC or a reach upstream of LKC. These results suggest that it is less likely than not that 10-11 t of live silver carp are present in LKC or in a reach upstream. Bayes factor indicates that eDNA monitoring results would provide substantial evidence in favor of the null hypothesis, Fish present = *True*, if  $FOPH \geq 0.5$ .

The four regions delineated by three critical frequencies of positive detection are summarized in Table 9.2.

As the fraction of eDNA monitoring samples testing positive for the target marker increases, the weight of that evidence in favor of the null hypothesis also increases. This relationship is illustrated in Figure 9.4, which plots Bayes factor on the frequency of positive eDNA monitoring samples. Figure 9.4 (A) shows that, during the gates open season, a frequency of positive eDNA monitoring samples greater than 0.9 is needed to meet the criteria for being substantially in favor of the null hypothesis. During the gates closed season, the criterion is satisfied when the frequency of positive detections is greater than 0.55. Figure 9.4 (B) shows that this relationship does not vary much with TARGET\_SHEDUNITS.

This demonstration shows the effect of two variables on the posterior probability of SPECIES\_PRESENT. Smaller quantities of shedding units are more difficult to capture using conventional surveillance and more difficult to detect through eDNA monitoring. Therefore, priors and posteriors are relatively close to an uninformed prior probability of 0.5 and, as TARGET\_SHEDUNITS increases, the prior and the posterior probabilities tend to be lower. Hydrologic influences can have a dramatic effect on the ability to detect eDNA in a sample reach and, in the CAWS, these influences are strongly related to whether or not the sluice gates controlling inflows from Lake Michigan are open or closed. The hydrologic effects will vary from reach to reach. In Lake Calumet, the posterior  $p(\text{SPECIES\_PRESENT} = \textit{True})$  tends to be higher for any given fraction of eDNA monitoring samples testing positive for a target marker.

#### *Sensitivity of Posterior Probabilities to Parameterization of the ALL\_ACTIVE Node*

Sensitivity analysis examines what effect a change in one or more parameters of a model would have on results of the model. The parameters of a Bayesian network are the conditional probabilities in CPTs that characterize prior beliefs in the states of random variables. An important variable in the Bayesian network developed for this project is ALL\_ACTIVE, which describes the prior degree of belief that concentrations of the target marker above the electric barrier can be explained by secondary sources. Field studies have unambiguously



demonstrated that bighead carp and silver carp eDNA can be detected in bird feces, in sewer outfalls, on commercial fishing nets, and on boat hulls (ECALS 2014). However, the process by which these sources might contribute eDNA to the waterway has not been observed directly and the strength of these sources has not been measured. Therefore, the ALL\_ACTIVE node has been parameterized for the nominal case using a non-informative prior probability of 0.5 to reflect uncertainty in whether secondary sources are actually contributing eDNA to the system.

This sensitivity analysis explores how posterior probabilities would change with parameterization of the ALL\_ACTIVE node given the observed frequencies of positive detection for the silver carp target marker. The ALL\_ACTIVE node has two potential states: *True* and *False*. If ALL\_ACTIVE = *True*, secondary sources contribute copies of the target marker to the system at rates consistent with those estimated in Section 6 using Bayesian Markov chain Monte Carlo. If ALL\_ACTIVE = *False*, secondary sources do not contribute eDNA to the system. Sensitivity analysis is completed using the sensitivity function described by Kjaerulff and van der Gaag (2000). Figure 9.4 (A) illustrates the results of sensitivity analysis for 1-5 kg of the target species and Figure 9.4 (B) illustrates the results of sensitivity analysis for 10-11 t of the target species. The solid line plots the posterior  $p(\text{SPECIES\_PRESENT} = \textit{True})$  for the gates open season and the dashed line plots the posterior for the gates closed season.

The nominal value of  $p(\text{ALL\_ACTIVE} = \textit{True})$  is 0.5. The results of statistical inference for the nominal parameterization of the ALL\_ACTIVE node and the observed rates of target marker detection can be found in Figure 9.4 for each hydrologic season. Results for each season can be found by reading the  $p(\text{SPECIES\_PRESENT} = \textit{True})$  at which an imaginary vertical line at  $p(\text{ALL\_ACTIVE} = \textit{True}) = 0.5$  intersects the curve for that season. Lower values of  $p(\text{ALL\_ACTIVE} = \textit{True})$  are associated with greater skepticism that secondary sources contribute copies of the target marker to the system; therefore  $p(\text{SPECIES\_PRESENT} = \textit{True})$  approaches 1 as  $p(\text{ALL\_ACTIVE} = \textit{True})$  decreases to 0. The stronger the degree of belief that secondary sources are contributing copies of the target marker to the system, the higher the value of  $p(\text{ALL\_ACTIVE} = \textit{True})$ . As  $p(\text{ALL\_ACTIVE} = \textit{True})$  increases from 0.5 to 1, the posterior  $p(\text{SPECIES\_PRESENT} = \textit{True})$  decreases relative to the nominal case. The effect is stronger for the gates open season than for the gates closed season. The effect is also stronger for larger numbers of shedding units. While the posterior  $p(\text{SPECIES\_PRESENT} = \textit{True})$  decreases as  $p(\text{ALL\_ACTIVE} = \textit{True})$  increases, it never reaches a value of 0. Thus, even if it were certain that secondary sources were a source of the target marker to the system, conclusions about the presence of the target species would remain uncertain.

#### *Sensitivity of Bayes Factor to Parameterization of the ALL\_ACTIVE Node*

A sensitivity analysis can also be carried out with respect to Bayes factor to explore how changes in parameterization of the ALL\_ACTIVE node would influence the interpretation of evidence from eDNA monitoring. This analysis takes the observed frequency of positive detections during the period 2009-2012 in LKC as given, and illustrates how the interpretation of that evidence depends on prior beliefs about secondary sources as contributors of eDNA to the system. Results are illustrated in Figure 9.6, which plots Bayes factor over a range of prior beliefs. There are three possible interpretations of the evidence, depending on prior beliefs: 1) the evidence is substantially in favor of the hypothesis SPECIES\_PRESENT = *True*; 2) the

evidence is in favor of the hypothesis, but barely worth a mention; and 3) the evidence is against the hypothesis.

Individuals who are skeptical that point sources contribute eDNA to the system have low priors on the  $p(\text{ALL\_ACTIVE} = \text{True})$  parameter. These individuals would interpret the evidence as being substantially in favor of target species presence. The sensitivity analysis indicates what the prior  $p(\text{ALL\_ACTIVE} = \text{True})$  would have to be in order to arrive at this conclusion based on the evidence from eDNA monitoring. For TARGET\_SHEDUNITS equal to 1-5 kg, Bayes factor is greater than 3.2 during the gates open season when the prior  $p(\text{ALL\_ACTIVE} = \text{True}) < 0.125$  and during the gates closed season when the prior probability on ALL\_ACTIVE = True is less than 0.2. For TARGET\_SHEDUNITS equal to 10-11 t, Bayes factor is greater than 3.2 during the gates open season when the prior  $p(\text{ALL\_ACTIVE} = \text{True}) < 0.175$  and during the gates closed season when the prior probability on ALL\_ACTIVE = True is less than 0.26. Individuals with prior  $p(\text{ALL\_ACTIVE} = \text{True})$  below these levels would interpret eDNA evidence as being in favor of the presence of the target species, silver carp.

An individual who does not have strong prior beliefs about whether or not secondary sources contribute eDNA to the system has prior  $p(\text{ALL\_ACTIVE} = \text{True})$  between the point at which Bayes factor equals 3.2 and the point at which Bayes factor equals 1. As shown in Figure 9.6, the upper limits of this range vary considerably depending on SEASON and TARGET\_SHEDUNITS. For a TARGET\_SHEDUNITS of 1-5 kg, the upper limit of this range is 0.45 during the gates open season and about 0.8 for the gates closed season. For a TARGET\_SHEDUNITS of 10-11 t, the upper limit of this range is about 0.55 for the gates opens season, and one for the gates closed season. Individuals with prior probabilities in this range interpret the evidence from eDNA monitoring as being somewhat in favor of the presence of the target species, but not substantially.

Individuals who believe strongly that secondary sources are a contributor of eDNA to the system would interpret the evidence quite differently than individuals in the other two categories. These individuals are characterized as having a prior  $p(\text{ALL\_ACTIVE} = \text{True})$  above the critical levels described in the preceding paragraph. For these individuals, Bayes factor is less than one, indicating that the posterior  $p(\text{SPECIES\_PRESENT} = \text{True})$  is less than the prior and that eDNA evidence is interpreted as being against the presence of the target species. For these individuals, a larger fraction of eDNA monitoring samples would have to test positive for the target marker before this evidence would be interpreted as being in favor of the target species presence.

The ALL\_ACTIVE variable is a source of scientific uncertainty. While field studies have documented the association between target markers for bighead carp and silver carp with secondary sources described in this report, the contributions have not been observed or measured and many questions remain about the mechanisms by which distribution of the target markers occurs in the CAWS. The interpretation of evidence from eDNA monitoring depends on prior beliefs about the ALL\_ACTIVE variable. Because this variable has a strong influence on the interpretation of results from eDNA monitoring, it is a strong candidate for further research to reduce this uncertainty.

## *Results of the Probabilistic Model for Silver Carp*

This section of the report summarizes results of the probabilistic model for silver carp in six sample reaches: NSC, CRM, CR2, LKC, CRD, and CR5. These reaches were consistently sampled for eDNA during the period 2009-2012. Although reach CR5, was not consistently sampled after 2010, it has been selected because of its location immediately upstream of the electric fish barrier. As such, it provides a perspective on the entire CAWS because probabilities of target species presence are for both the sample reach and reaches upstream of the sample reach. The discussion of results in this report emphasizes silver carp because the silver carp target marker is much more commonly detected than the bighead carp target marker.

Results for the six sample reaches are presented in Figures 9.7-9.18. There are two figures for each sample reach, one for each season. Each figure includes four insets, each of which plots the prior and posterior  $p(\text{SPECIES\_PRESENT} = \textit{True})$ , and the posterior  $p(\text{SPECIES\_PRESENT} = \textit{False})$  for a specific number of TARGET\_SHEDUNITS. The prior and posterior can be read from the graph for any potential fraction of eDNA monitoring samples testing positive for the silver carp target marker on the  $x$ -axis. The fraction of eDNA monitoring samples testing positive for bighead and silver can be calculated for any period from 2009 – 2013 from the data provided in Table 3.1-3.4. For the purpose of this discussion, eDNA monitoring results are averaged over the period of 2009-2012 for consistency with the hydrologic simulation period.

As described in the preceding discussion of sensitivity analysis, results of the probabilistic model are sensitive to parameterization of the ALL\_ACTIVE node. The ALL\_ACTIVE variable describes whether secondary sources are in fact a contributor of the eDNA detected in monitoring samples. All results described in this section have been generated assuming a uniform probability distribution for the ALL\_ACTIVE node, meaning that ALL\_ACTIVE is as likely to be *True* as it is *False*. This is an appropriate stance given the collective uncertainty about this variable. However, for any one reader, the degree of belief about the state of this variable is likely to sway more strongly one way or the other. As demonstrated in the sensitivity analysis for LKC, a prior probability that is more heavily toward the state of this variable being *False* will result in higher posteriors and a prior probability that is weighted more heavily toward *True* will result in lower posteriors.

When reviewing the results described in this section, emphasis is placed on understanding the relationship between the prior and posterior probabilities of the null hypothesis, SPECIES\_PRESENT = *True*. The closer that the posterior (solid line) is to the prior (the cross-hatched line), the less impact evidence from eDNA monitoring has in terms of influencing beliefs about the presence of the target species. If the posterior is less than the prior, evidence is against the null hypothesis. If the posterior is greater than the prior, evidence supports the null hypothesis. The weight of evidence can be approximated by calculating Bayes factor from the prior and posterior probabilities of target species presence shown in each figure.

### *a. Lake Calumet (LKC)*

Results for LKC are illustrated for the gates open season in Figure 9.7 and for the gates closed season in 9.8. The fraction of positive monitoring samples for the period 2009-2012 was

0.067 for samples collected during the gates open season and 0.154 for samples collected during the gates closed season. Failure to detect the target marker in eDNA monitoring samples is represented by 0 on the  $x$ -axis. If the target marker is not detected in any monitoring samples, the posterior is less than the prior, indicating that the effect of eDNA evidence is to reduce the  $p(\text{SPECIES\_PRESENT} = \textit{True})$  relative to the prior. Failure to detect the target marker does not result in a posterior probability of 0 because the PCR assay has a high false negative rate at low concentrations. The posterior tends to increase rapidly as soon as the fraction of positive eDNA monitoring samples is greater than 0.

The posterior responds differently to the fraction of positive detections than at higher levels of TARGET\_SHEDUNITS than at lower levels of TARGET\_SHEDUNITS. At higher TARGET\_SHEDUNITS, the posterior  $p(\text{SPECIES\_PRESENT} = \textit{True})$  tends to increase more slowly in response to an increasing fraction of positive detections. This occurs because larger target species populations would tend to cause higher concentrations of the target marker, leading to a higher fraction of positive detections. Therefore, a lower detection rate provides evidence that a large population is absent.

A minimum fraction of eDNA monitoring samples is needed to support the conclusion that the TARGET\_SPECIES is more likely to be present than not. This fraction can be read from the  $x$ -axis where the two posteriors,  $p(\text{SPECIES\_PRESENT} = \textit{True})$  and  $p(\text{SPECIES\_PRESENT} = \textit{False})$ , are equal. For a TARGET\_SHEDUNITS equal to 1-5 kg, approximately 25 percent of eDNA monitoring samples would have to test positive to support the conclusion that the target species is probably present (see inset A). The minimum fraction increases at higher TARGET\_SHEDUNITS. For a TARGET\_SHEDUNITS equal to 5-6 t, any detection of eDNA in monitoring samples leads to an increase in the probability that the target species is present, but a minimum of 65 percent of eDNA monitoring samples would have to test positive to support the conclusion that 5-6 t of silver carp are present in or upstream of LKC (see inset C).

Figure 9.8 plots results of the probabilistic model that is parameterized for Lake Calumet during the gates closed season, when circulation in Lake Calumet becomes more limited. Results show that a smaller fraction of eDNA monitoring samples must test positive for the posterior  $p(\text{SPECIES\_PRESENT} = \textit{True})$  to be greater than 0.5. This can be attributed to reduced circulation in the lake during the gates closed season. There are relatively few secondary sources that may be contributing eDNA directly to the lake, and the amount of eDNA that might be coming from other reaches is reduced. Therefore, there are fewer alternate explanations for the presence of the eDNA.

Conclusions from the probabilistic model in Lake Calumet depend on the hydrologic season. During gates open season, the posterior probabilities are very close to the prior probabilities informed by conventional surveillance. Therefore, eDNA monitoring appears to have little influence on  $p(\text{SPECIES\_PRESENT} = \textit{True})$ . During the gates closed season, evidence from eDNA monitoring tends to support the hypothesis that silver carp are present, but based on Bayes factor this evidence is not substantially in favor of that hypothesis.

### *b. North Shore Channel (NSC)*

Hydrologic conditions in the NSC are substantially different from those in LKC because tides have little influence on the system. When sluice gates at the Wilmette Pump Station are open, flow from Lake Michigan into the NSC helps flush the system. During the gates closed season, the upper NSC acts more like a stagnant backwater and flows in the lower section of the reach are attributed to discharges from the North Shore Pump Station (NSPS). Results for the NSC are plotted in Figures 9.8 and 9.9 for the gates open season and the gates closed season, respectively. The figures show how evidence from eDNA monitoring would influence the probability of target species presence in the NSC over a range of potential detection rates. Prior probabilities of target species presence in the NSC are among the lowest in the CAWS because considerable fishing effort has been expended in the reach.

The silver carp target marker has been detected in 4.7 percent of eDNA monitoring samples during the gates open season, and 3.1 percent of eDNA monitoring samples during the gates closed season. Evidence observed in the course of eDNA monitoring results in the posterior  $p(\text{SPECIES\_PRESENT} = \text{True})$  being less than the prior during both the gates open and the gates closed seasons. During the gates open season, a detection rate of at least 0.125 is needed to increase the posterior to a level greater than 0.5, but the posterior remains close to 0.5 until the detection rate is 0.3 (see inset Figure 9.9 (A)). As the TARGET\_SHEDUNITS increases, the minimum detection rate needed to favor a conclusion that silver carp are present increases.

During the gates closed season, higher rates of target marker detection are needed to raise the posterior probability of target species presence above 0.5. Figure 9.10 (D), which illustrates probabilistic model results for 10-11 t of the target species in the NSC, shows that posterior remains less than 0.5 over all potential rates of target marker detection. This result can be explained by the large amount of conventional fisheries surveillance in the NSC. So much conventional fishing effort has been expended that no amount of target marker detection would result in the posterior favoring the hypothesis that 10-11 t of silver carp are present in the NSC. Overall, these results suggest that eDNA monitoring evidence leans against the presence of silver carp in the NSC.

### *c. Chicago River Main (CRM)*

The reach designated CRM extends from the Chicago River Controlling Works at the Lake Michigan boundary to the confluence of the Chicago River with the North Branch of the Chicago River. This reach is dominated by flows from Lake Michigan during the gates open season, and as with the upper NSC, forms a kind of backwater in the system during the gates closed season. The reach differs from others in that no fishing effort occurred in the reach during the period 2009-2012. As a result, no information is available to update the prior probability of target species presence before considering eDNA monitoring results and the prior probability of target species presence is 0.5. During the gates open period, 6.3 percent of eDNA monitoring samples tested positive for the silver carp target marker. During the gates closed season, 3.2 percent of monitoring samples tested positive for the silver carp target marker.

Figures 9.10 and 9.11 summarize results of the probabilistic model in CRM. The prior probability of target species presence is 0.5, and varying TARGET\_SHEDUNITS has no effect on this prior probability in CRM because there has been no conventional fishing effort in the reach. The frequency of positive detections is 0.063 during the gates open season and 0.032 during the gates closed season. During the gates open season, eDNA evidence results in the posterior being slightly greater than the prior, and during the gates closed season the eDNA evidence results in the posterior being about 20 percent less than the prior. These results suggest that evidence from eDNA monitoring in CRM leans slightly in favor of the presence of the target species during the gates open season, but against the presence of the target species during the gates closed season.

#### *d. Chicago River (CR2)*

Reach CR2 is a segment of the Chicago River extending from the confluence with the North Branch of the Chicago River to the confluence with Bubbly Creek. Results of the probabilistic model are summarized for CR2 in Figures 9.13 and 9.14. The detection rate for the silver carp target marker during the gates open season was 0.04 and during the gates closed season was 0.006. The posterior is greater than the prior during both seasons, indicating that evidence from eDNA monitoring leans towards the null hypothesis SPECIES\_PRESENT = *True*. Although the evidence leans in favor of target species presence, the increase in the posterior probability relative to the prior is not large enough to provide substantial evidence in favor of that hypothesis.

The interpretation of the plots in Figure 9.14 for the gates closed season deserves some discussion because the posterior is difficult to read directly from the plots. The frequency of positive detections during the gates closed season is 0.006, and, at this detection rate, it appears the posterior probability is less than the prior. However, this is a misinterpretation. The Bayesian network has been developed by discretizing random variables. The fraction of positive eDNA monitoring samples represented on the  $x$ -axis has been discretized into 21 intervals including 0 and twenty intervals of 0.05 between 0 and 1. To construct the plots, the posterior is calculated for each interval starting at 0 and at the midpoint of each subsequent interval. Therefore, in Figure 9.14(A), the line between (0, 0.185) and (0.025, 0.537) is an approximation of a curve. The posterior probability is calculated for the interval  $0 > x \geq 0.05$  and is 0.537. It should still be possible to read the posterior probabilities from the plot as long as this issue is taken into account.

#### *e. Calumet River (CRD)*

Reach CRD is a segment of the Calumet River downstream of O'Brien Lock and Dam that extends from its confluence with the Grand Calumet River to its confluence with the Little Calumet River (Figure . Results of the probabilistic model are summarized for reach CRD in Figures 9.15 and 9.16. During the gates open season, the target marker for silver carp was detected in 1.1 percent of samples. For each level of TARGET\_SHEDUNITS, the posterior is very similar to the prior, suggesting that detection of the target marker in up to 5 percent of samples has very little influence on  $p(\text{SPECIES\_PRESENT} = \textit{True})$ . Conclusions from the probabilistic model are different during the gates closed season. The target marker for silver

carp was detected in 2.9 percent of samples during the gates closed season. For a TARGET\_SHEDUNITS of 1-5 kg, this evidence increases the posterior 22 percent, from 0.5 to 0.61. This indicates that the eDNA evidence leans toward target species presence, but is not substantially in favor of that hypothesis. Evidence from eDNA monitoring has a similar effect at higher levels of TARGET\_SHEDUNITS, but the prior probabilities are lower because of fishing effort in the reach.

#### *f. Chicago Sanitary and Ship Canal (CR5)*

Reach CR5 extends from the confluence of the Chicago Sanitary and Ship Canal with the Cal-Sag Channel to the upstream boundary of the electric fish barrier. This reach is distinguished by its location just above the fish barrier and downstream of every other reach in the CAWS. This reach is influenced by all of the hydrologic forces upstream, but that is less important than the potential ability to inform statements about the presence of the target species in the CAWS as a whole. Posterior probabilities calculated from the Bayesian network represent the probability that the target species is located in the sample reach or in a reach upstream of the sample reach.

The detection rate for silver carp target markers in CR5 is 0.03 during the gates open season and 0.015 during the gates closed season. Any detection of silver carp eDNA in CR5 leads to an increase in the  $p(\text{SPECIES\_PRESENT} = \text{True})$  during both seasons. For smaller quantities of shedding units, posterior probabilities are greater than 0.5, but increases in  $p(\text{SPECIES\_PRESENT} = \text{True})$  are not substantially in favor of the null hypothesis. Figures 9.17(D) and 9.18(D) show that, for 10-11 t of the target species, posterior probabilities are less than 0.5, indicating that it is less likely than not that such a large quantity of the target species is present either in the sample reach or in one of the reaches upstream. Overall, the slope of the line plotting the posterior over the fraction of monitoring samples testing positive for eDNA is less than in reaches upstream. This suggests that, in terms of shaping beliefs about the presence of the target species in the CAWS, the detection of silver carp target markers in CR5 has less impact than detection in other reaches despite its location at the base of the system.

#### *Potential Improvements to the Bayesian Network*

Several opportunities to improve the Bayesian network exist. Presently, inference from eDNA monitoring data is carried out separately for each reach. It seems likely that there would be much benefit to conducting inference in multiple reaches simultaneously. However, constraints on memory presently limit the complexity of the network and the size of CPTs that can be compiled. The complexity of CPTs, the number of parent nodes and their number of potential states, is also limited by the amount of time required to build the tables. With regard to the graphical model described in this report, the TOT\_SEC\_CONC node has the largest CPT. This CPT is built from HFFTM production runs and already requires several days of processing time to build on a desktop computer (not including the time required to complete the HFFTM simulation), and each sample reach requires a unique CPT for this node. Processing time increases exponentially with the number of secondary sources and the number of potential loading rates. A related limitation of the model is the inability to perform inference under an explicit set of hydrologic conditions. Presently, the Bayesian network is set up to perform

inference for one of two seasons, gates open or gates closed. In most reaches, each seasons is characterized by a distinct hydrologic condition. However, hydrologic conditions also vary within seasons. For example, there are periods of very high flow and these tend to be associated with CSO discharges. The ability to distinguish between these conditions and periods of lower flows seems likely to produce great benefits in terms of the strength of inference. The various limitations described here could be overcome with additional development effort.

## 10. Conclusion

The over-arching objective of this study is to improve the ability of natural resource managers to understand and interpret results of the eDNA monitoring program in the CAWS. This has been accomplished by developing models, methods, and analyses that enable natural resource managers to draw inferences about the source(s) of Asian carp eDNA and the presence of live bighead carp and silver carp in the CAWS. In the course of developing these products, numerous other models and methods have been demonstrated along the way, yielding a variety of additional insights that have been described throughout this report. For example, these include methods to assess the reliability of an eDNA sampling program and to estimate target marker concentrations in the waterway.

A short list of general findings about Asian carp in the CAWS that emerged in the course of this study includes:

- The PCR assay used to detect bighead carp and silver carp target markers in the CAWS has a high false negative rate at low concentrations. This is attributed to processing and division of water samples.
- It is much more difficult to detect bighead carp target markers than silver carp target marker. This is attributed to differences in the self-annealing properties of the primers.
- Ambient concentrations of eDNA can be inferred from eDNA monitoring results analyzed using PCR (*i.e.*, presence/absence data).
- For the CAWS as a whole, the secondary sources that contribute the most eDNA to the system are probably CSOs and navigation. However, the relative importance of each secondary source varies by season and reach.
- Hydrologic conditions vary over space and time within the CAWS. Under certain hydrologic conditions, eDNA can be transported long distances from the point of its release in the CAWS.
- Information about the fraction of positive eDNA monitoring samples that test positive for a target marker can be used to update a prior probability of target species presence.
- Inferences from eDNA monitoring results vary by reach and season. However, taken as a whole, these results do not provide strong evidence in favor of the hypothesis that live Asian carp are present.



- There is a sustained source of Asian carp eDNA in the CAWS. If live silver carp were the only source of eDNA in the CAWS, between 3.8 and 5.9 metric tons of live fish would need to be distributed throughout the CAWS to sustain target marker concentrations that were observed during the period 2009 – 2012.

Many of the ideas, concepts, and methods described in this report are transferable to other locations and species, and provide general insights into the use of eDNA as a method of invasive species detection that are widely applicable. Similarly, the models developed in this report are transferable in the sense that they could be adapted and re-parameterized for other locations and species. The results of models specifically parameterized for bighead carp and silver carp in the CAWS during the four-year hydrologic period, 2009-2012, are specific to these species at this location during this time period. However, these models should provide a reasonably good basis for making generalizations outside of the simulation period as long as the hydrology and other factors likely to influence the distribution of eDNA in the CAWS remain similar from year to year. For example CSOs and navigation have been identified as most likely being the largest secondary sources of eDNA in the CAWS. Barring significant changes in the system over time, there is no reason why that would not also be true in 2013 and in future years. Similarly, the Bayesian network models described in this report have been parameterized for the period 2009-2012. These models update a prior probability of target species presence to a posterior probability, indicating whether or not evidence from eDNA monitoring has increased or decreased the probability of target species presence and whether target species presence is more likely than not. Natural resource managers can continue to use these models in the CAWS as long as the prior probabilities of target species presence are updated to reflect conventional fishing effort during the period of analysis.

## 11. Literature Cited

- Alaeddini, R., 2012, Forensic implications of PCR inhibition – A review, *Forensic Science International: Genetics* 6(2012): 297-305
- Asian Carp Regional Coordinating Committee (ACRCC), 2012, FY 2012 Asian Carp Control Strategy Framework, <http://www.asiancarp.us/documents/2012Framework.pdf> (Accessed July 16, 2013), February, p. 165.
- Battelle Memorial Institute (BMI), 2010, Revised Final Independent External Peer Review Report Environmental DNA (eDNA) Science and Methodology, Report to the US Army Corps of Engineers, Rock Island District, December 7, Unpublished Report ([http://www.usace.army.mil/Portals/2/docs/civilworks/Project%20Planning/eDNA\\_review.pdf](http://www.usace.army.mil/Portals/2/docs/civilworks/Project%20Planning/eDNA_review.pdf)) Accessed August 26, 2012.
- Benson, D.A., M. Cavanaugh, K. Clark, I. Karsch-Mizrachi, D.J. Lipman, J. Ostell, and E.W. Sayers, 2011, GenBank, *Nucleic Acids Research* 39(Database Issue):D32-D37.
- Besag, J. (2001). “Markov Chain Monte Carlo for Statistical Inference.” Center for Statistics and the Social Sciences, Working Paper No. 9, University of Washington, Seattle, Washington, April.
- Blume, L., J. Darling, M. Vazquez, and J.S. Chandler, 2010. Laboratory Audit Report: Lodge Laboratory, Department of Biological Sciences, University of Notre Dame, Report by the Great Lakes National Program Office, U.S. Environmental Protection Agency, Chicago, IL, February 5, ([http://people.cst.cmich.edu/mahon2a/MahonLab/Publications\\_files/2011%20Blume%20et%20al%20EPA%20Audit%20Report%20of%20eDNA%20process%205%20Feb%202009.pdf](http://people.cst.cmich.edu/mahon2a/MahonLab/Publications_files/2011%20Blume%20et%20al%20EPA%20Audit%20Report%20of%20eDNA%20process%205%20Feb%202009.pdf)), Accessed August 26, 2013.
- Cerco, C., S-C Kim, and M. Noel. (2010). “The 2010 Chesapeake Bay eutrophication model,” A Report to the U.S. Environmental Protection Agency Chesapeake Bay Program and to the U.S. Army Corps of Engineers Baltimore District. <http://www.chesapeakebay.net/publications>
- Changnon, S.A. and J.M. Changnon, 1996, History of the Chicago diversion and future implications, *Journal of Great Lakes Research*, 22(1996): 100-118.
- Chick, J.H., and M.A. Pegg, 2001, Invasive carp in the Mississippi River, *Science* 292: 2250-2251.
- Darling, J.A. and M.J. Blum, 2007, DNA-based methods for monitoring invasive species: A review and prospectus, *Biological Invasions* 9(2007): 751-765.

- Darling, J.A. and A.R. Mahon. 2011. From molecules to management: Adopting DNA-based methods for monitoring biological invasions in aquatic environments, *Environmental Research* 111(7): 978-988.
- Dejean, T., A. Valentini, A. Duparc, S. Pellier-Cuit, F. Pompanon, P. Taberlet and C. Miaud, 2011, Persistence of environmental DNA in freshwater ecosystems, *PLoS ONE* 6(8):e23398. Doi: 10.371/journal.pone.0023398
- Efron, B. and A. Gous, 2001, Scales of evidence for model selection: Fisher versus Jeffreys, *Institute of Mathematical Statistics Lecture Notes – Monograph Series*, 38(2001): 208-246
- Emelko, M.B., Schmidt, P.J., and Reilly, P.M., 2010, Particle and microorganism enumeration data: Enabling quantitative rigor and judicious interpretation, *Environmental Science and Technology* 44 (2010): 1720-1727.
- Environmental DNA Calibration Study (ECALS), 2013, Environmental DNA Calibration Study Interim Technical Review Report, US Army Corps of Engineers, January, [http://www.asiancarp.us/documents/ECALS\\_INTERIM.pdf](http://www.asiancarp.us/documents/ECALS_INTERIM.pdf), Accessed August 27, 2013.
- Environmental DNA Calibration Study (ECALS), 2014, Environmental DNA Calibration Study Third Interim Technical Review Report, US Army Corps of Engineers, *in preparation*.
- Ficetola, G.F., C. Miaud, F. Pompanon and P. Taberlet, 2008, Species detection using environmental DNA from water samples, *Biology Letters*, 4(2008): 423-425.
- Foote, A.D., P.F. Thomsen, S. Sveegaard, M. Wahlberg, J. Kielgast, L.A. Kyhn, A.B. Salling, A. Galatius, L. Orlando, M.T.B. Gilbert, 2012, Investigating the potential use of environmental DNA (eDNA) for genetic monitoring of marine mammals, *PLoS ONE* 7(8):e41781, doi:10.1371/journal.pone.0041781.
- Guilfoyle, M.P., Dorr, B.S., and Fisher, R.A., 2013, Documenting the Presence and Movements of Piscivorous Birds along the Illinois and Des Plaines Rivers and within the Chicago Area Waterway System (CAWS), Draft report prepared for the US Army Corps of Engineers Chicago District, IL (September).
- Gelman, Andrew, Carlin, John B., Stern, Hal S., and Rubin, Donald B. 2003. Bayesian Data Analysis, Second Edition. Chapman & Hall/CRC Texts in Statistical Science. ISBN-10: 158488388X.
- Goldberg, C.S., D.S. Pilliod, R.S. Arkle, and L.P. Waits, 2011, Molecular detection of vertebrates in stream water: A demonstration using Rocky Mountain tailed frogs and Idaho giant salamanders, *PLoS ONE* 6(7): e22746, doi: 10.1371/journal.pone.0022746.
- Gosset, W.S., 1907, On the error of counting with a haemocytometer, *Biometrika* 5 (1907): 351–360.

- Hahn, S., Bauer, S., and Klaassen, M., 2007, Estimating the contribution of carnivorous waterbirds to nutrient loading in freshwater habitats, *Freshwater Biology* 52(2007): 2421-2433.
- Holland, P.M., R.D. Abramson, R. Watson, and D.H. Geffland, 1991, Detection of specific polymerase chain reaction product by utilizing the 5'-3' exonuclease activity of *Thermus aquaticus* DNA polymerase, *Proceedings of the National Academy of Sciences, USA*, 88(1991): 7276-7280.
- Illinois Department of Natural Resources (ILDNR), 2011, *Bighead Carp in Illinois Urban Fishing Ponds*, Unnumbered report prepared by the ILDNR Aquatic Nuisance Species Program, <http://asiancarp.us/documents/BigheadCarpinIllinoisUrbanFishingPonds.pdf>, Accessed November 27, 2011.
- Jeffreys, H., 1935, Some tests of significance, Treated by the theory of probability, *Proceedings of the Cambridge Philosophy Society* 31: 203-222.
- Jeffreys, H., 1961, *Theory of Probability* (3<sup>rd</sup> Edition), Oxford, U.K., Oxford University Press.
- Jerde, C.L., A.R. Mahon, W.L. Chadderton, and D.M. Lodge, 2011, "Sight unseen" detection of environmental DNA for surveillance of aquatic organisms at low densities, *Conservation Letters* 4: 150-157.
- Jerde, C.L., W.L. Chadderton, A.R. Mahon, M.A. Renshaw, J. Corush, M.I. Budny, S. Mysorekar, and D.M. Lodge, 2013, Detection of Asian carp DNA as part of a Great Lakes basin-wide surveillance program, *Canadian Journal of Fisheries and Aquatic Science* 70(4): 522-526.
- Johnson, B., Heath, R., Hsieh, B., Kim, K., and Butler, L. (1991). "User's guide for a three-dimensional numerical hydrodynamic, salinity, and temperature model of Chesapeake Bay," Technical Report HL-91-20, Department of the Army Waterways Experiment Station, Vicksburg MS.
- Kass, R.E., and A. E. Raftery, 1995, Bayes factors, *Journal of the American Statistical Association* 90(430): 773-795.
- Kjaerulff, U. B. and L. van der Gaag, 2000, Making sensitivity analysis computationally efficient, *Proceedings of the Sixteenth Conference on Uncertainty in Artificial Intelligence*, June 30 – July 3, Stanford CA, Morgan Kaufman, San Francisco, p. 317-325
- Kjaerulff, U. B., and A. L. Madsen, 2008, *Bayesian Networks and Influence Diagrams: A Guide to Construction and Analysis*, Springer, New York, p. 318.

- Kolar, C.S., D.C. Chapman, W.R. Courtenay Jr., C.M. Housel, J.D. Williams, and D.P. Jennings, 2007, Bighead Carps: A Biological Synopsis and Environmental Risk Assessment, Special Publication No. 33, American Fisheries Society, Bethesda, MD, p. 204.
- Klymus, K., C. Richter, D. Chapman, and C. Paukert, 2013, ECALS: Loading Studies Interim Report July 2013, Interim Milestone Report to Asian Carp Regional Coordinating Committee, Unpublished, p. 21.  
<http://www.asiancarp.us/documents/ECALSloadingreportJuly2013.pdf> (accessed May 27, 2014).
- Koller, D., and N. Friedman, 2009, *Probabilistic Graphical Models: Principles and Techniques*, MIT Press, Boston, MA, p. 1231.
- Lance, R., et al., 2013, Milestone Report on ECALS eDNA degradation rate studies, <http://www.asiancarp.us/documents/ECALSdegradationreport.pdf> (accessed May 27, 2014).
- Lavine, M. and M.J. Schervish, 1999, Bayes factors: What they are and What they are not, *The American Statistician* 53(2): 119-122.
- Levy-Booth, D.J., R.G. Campbell, R.H. Gulden, M.M. Hart, J.R. Powell, J.N. Klironomos, K.P. Pauls, C.J. Swanton, J.T. Trevors, K.E. Dunfield, 2007, Cycling of extracellular DNA in the soil environment, *Soil Biology & Biochemistry* 39(2007): 2977-2991.
- Lodge, D.M., C.R. Turner, C.L. Jerde, M.A. Barnes, W.L. Chadderton, S.P. Egan, J.L. Feder, A.R. Mahon, M.E. Pfrender, 2012, Conservation in a cup of water: Estimating biodiversity and population abundance from environmental DNA, *Molecular Ecology* 21(2012): 2555-2558.
- Marlin, J.C., 2003, *Barge Transport of Illinois River Sediment from Peoria to Chicago*, Report TR-037, Waste Management and Research Center, University of Illinois, Urbana-Champaign (April), p.21.
- Marlin, J. C., 2004, "Long Distance Transport of Illinois River Dredged Material for Beneficial Use in Chicago." Proceedings of the Western Dredging Association twenty-fourth Technical Conference and Thirty-Sixth Texas A&M Dredging Seminar. July 6-9, 2004. pp. 177-186, ([http://www.istc.illinois.edu/special\\_projects/il\\_river/long-distance-il-river-sediment-transport.pdf](http://www.istc.illinois.edu/special_projects/il_river/long-distance-il-river-sediment-transport.pdf), accessed May 30 2014).
- Matsui, M., Honjo, M., and Z. Kawabata, 2001, Estimation of the fate of dissolved DNA in thermally stratified lake water from the stability of exogenous plasmid DNA, *Aquatic Microbial Ecology* 26(2001): 95-102.

- Merkes, C.M., McCalla, S.G., Jensen, N.R., Gaikowski, M.P., Amberg, J.J., 2014, Persistence of DNA in carcasses, slime and avian feces may affect interpretation of environmental DNA data. *PLoS ONE* 9(11): e113346. doi: 10.1371/journal.pone.0113346
- Metropolis, N., A.W. Rosenbluth, M.N. Rosenbluth, A.H. Teller, and E. Teller. 1953. Equation of state calculations by fast computing machines. *Journal of Chemical Physics* 21(1953): 1087-1092.
- Metropolitan Water Reclamation District of Greater Chicago (MWRD), 2008, *Description of the Chicago Waterway System for the use Attainability Analysis*, MWRD Research and Development Department Report 08-15R, March, p.23.
- Monitoring and Response Work Group (MRRWG), 2012, 2011 Asian Carp Monitoring and Rapid Response Plan Interim Summary Reports, Asian Carp Regional Coordinating Committee, April.
- Monitoring and Response Work Group (MRWG), 2013a, 2012 Asian Carp Monitoring and Rapid Response Plan Interim Summary Reports, Asian Carp Regional Coordinating Committee, April.
- Monitoring and Response Work Group (MRWG), 2013b, Monitoring and Response Plan for Asian Carp in the Upper Illinois River and Chicago Area Waterway System, Asian Carp Regional Coordinating Committee, May.
- Monitoring and Response Work Group (MRWG), 2013c, MRRWG Environmental DNA Database, Excel Spreadsheet, unpublished.
- Olson, Z. H., J.T. Briggler, R.N. Williams, 2012, An eDNA approach to detect eastern hellbenders (*Cryptobranchus a. alleganiensis*) using samples of water, *Wildlife Research* 39(2012): 629-636,
- Rasmussen, J. L., H.A. Regier, and R.E. Sparks, 2011, Dividing the waters: The case for hydrologic separation of the North American Great Lakes and Mississippi River Basins, *Journal of Great Lakes Research* 37(3): 588-592.
- Scherer, N.M., Gibbons, H.L, Stoops, K.B., Muller, M., 1995, Phosphorous loading of an urban lake by bird droppings, *Lake and Reservoir Management*, 11(4): 317-327.
- Schultz, M.T., Borrowman, T.D., and Small, M.J., 2011, Bayesian Networks for Modeling Dredging Decisions, ERDC/EL TR-11-14, Engineer Research and Development Center, US Army Corps of Engineers, Vicksburg, MS.
- Stohlgren, T.J., and J.L. Schnase, Risk analysis for biological hazards: What we need to know about invasive species, *Risk Analysis* 26(1): 163-173.

- Storn, R. and K. Price. 1995. Differential Evolution — a simple and efficient adaptive scheme for global optimization over continuous spaces. International Computer Science Institute, Berkeley, TR-95-012.
- Storn, R. and K. Price. 1997. Differential Evolution — a simple and efficient heuristic for global optimization over continuous spaces. *Journal of Global Optimisation* 11: 341–359.
- Takahara, T., T. Minamoto, H. Yamanaka, H. Doi, and K. Zen'ichiro, 2012, Estimation of fish biomass using environmental DNA, *PLoS ONE* 7(4): e35868 doi: 10.1371/journal.pone.0035868.
- Takahara, T. T. Minamoto, H. Doi, 2013, Using environmental DNA to estimate the distribution of an invasive fish species in ponds, *PLoS ONE* 8(2): e56584. doi: 10.1371/journal.pone.0056584.
- ter Braak, C.J.F. 2006. A Markov Chain Monte Carlo version of the genetic algorithm differential evolution: easy Bayesian computing for real parameter spaces. *Stat. Comput.* 16, 239-249.
- Thomann, R. (1972). *Systems analysis & water quality management*. Environmental Science Service Division, New York.
- Thomsen, P.F., J. Kielgast, L.L. Iversen, P.R. Moller, M. Rasmussen, and E. Willerslev, 2012a, Detection of a diverse marine fish fauna using environmental DNA from seawater samples, *PLoS ONE* 7(8):e41732, doi:10.1371/journal.pone.0041732.
- Thomsen, P.F., J. Kielgast, L.L. Iversen, C. Wiuf, M. Rasmussen, M.T.P. Gilbert, I. Orlando, and E. Willerslev, 2012b, Monitoring endangered freshwater biodiversity using environmental DNA, *Molecular Ecology* 21(2012): 2565-2573.
- Untergasser, A., Nijveen, H., Rao, X., Bisseling, T., Geurts, R., and Leunissen, J.A.M, 2007, Primer3Plus, an enhanced web interface to Primer3, *Nucleic Acids Research*, 2007 35: W71-W74; doi:10.1093/nar/gkm306
- US Army Corps of Engineers, 2012, Quality Assurance Project Plan: eDNA Monitoring of Invasive Asian Carp in the Chicago Area Waterway System, USACE Chicago District Chicago, May (<http://www.asiancarp.us/documents/USACE-eDNA-QAPP.pdf>) Accessed August 26, 2013.
- US Army Corps of Engineers, 2014, Great Lakes and Mississippi River Basin Study (GLIMRS) Report, <http://glmr.is.anl.gov/glmris-report/> (accessed May 30, 2014).
- US Fish and Wildlife Service, 2014, Bighead & Silver Carp eDNA Early Detection Results, <http://www.fws.gov/midwest/fisheries/eDNA/Results-chicago-area.html> (accessed May 30, 2014)

US Geological Survey, 2013, Non-Indigenous Aquatic Species Database (<http://nas.er.usgs.gov/>) (accessed August 9, 2013).

Wilcox, T.M., K.S. McKelvey, M.K. Young, S.F. Jane, W.H. Lowe, A.R. Whiteley, and M.K. Schwartz, 2013, Robust detection fo rare species using environmental DNA: The importance of primer specificity, *PLoS ONE* 8(3): e59520.  
Doi:10:1371/journal.pone.0059520.

Willerslev, E., Hansen, A.J., Poinar, H.N., 2004, Isolation of nucleic acids and cultures from fossil ice and permafrost, *Trends in Ecology & Evolution* 19(2004):141-147.



*This page left intentionally blank.*

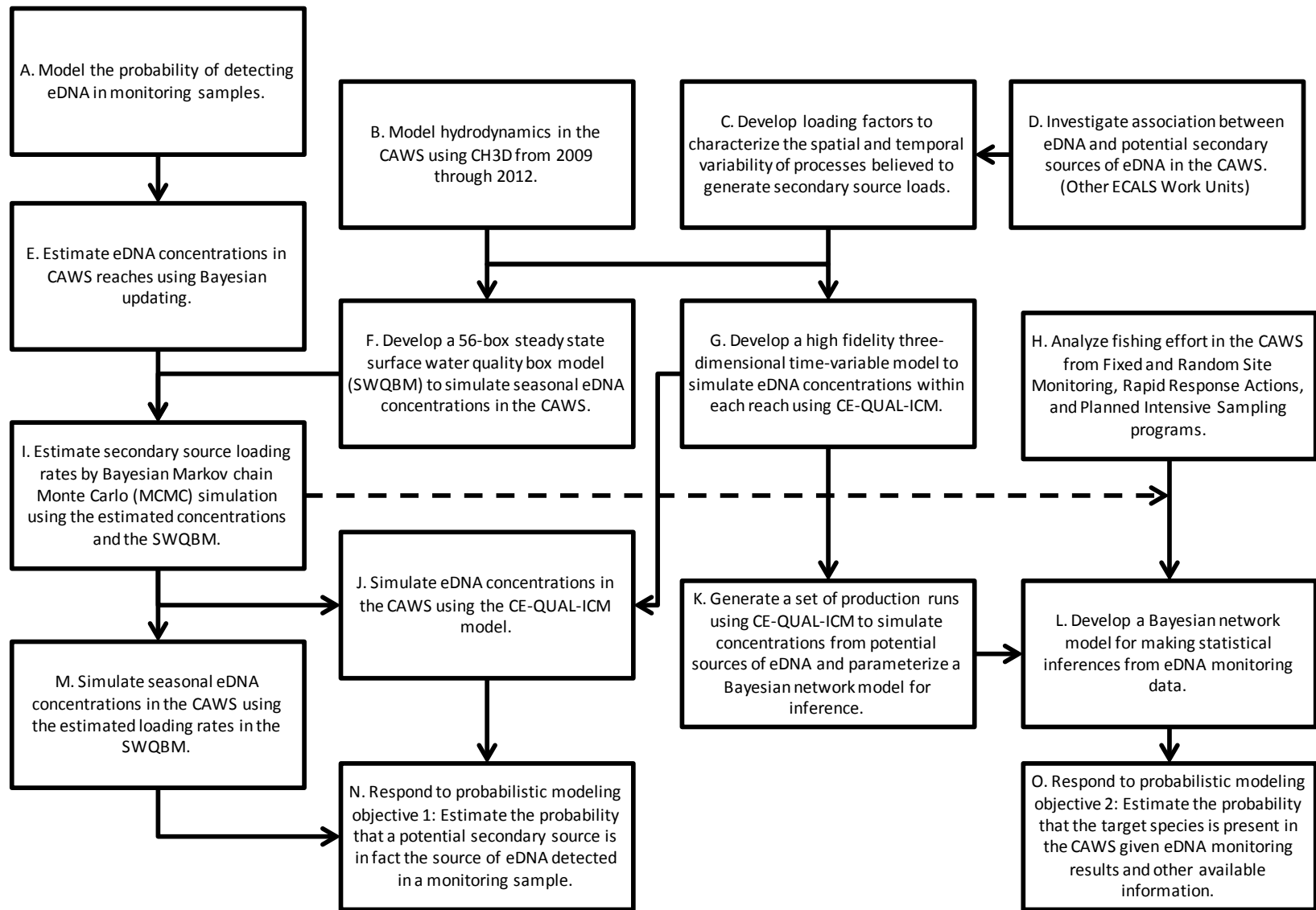


Figure 1.1: Schematic flowchart describing how the probabilistic modeling objectives have been addressed by the ECALS project.

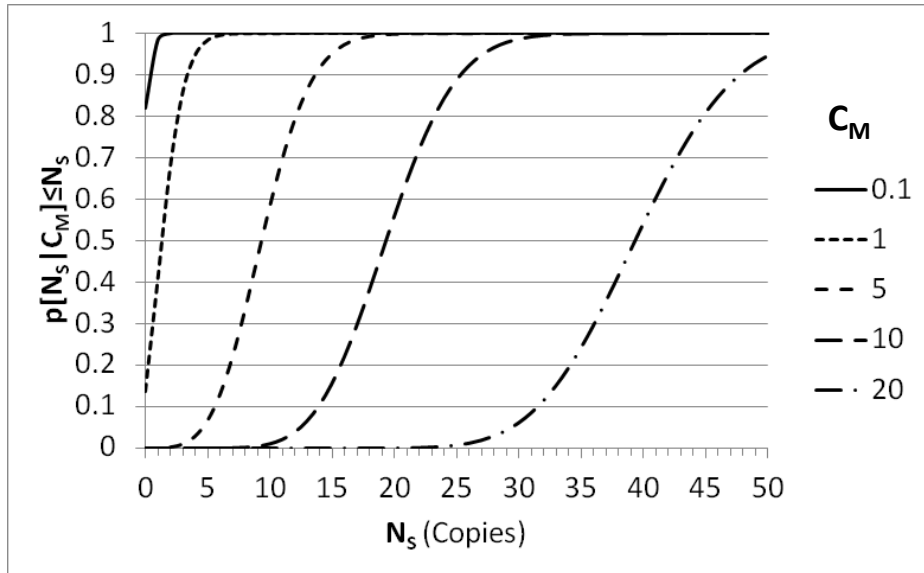


Figure 2.1: Probability of capturing no more than  $N_s$  markers in one two-liter sample of source water with concentration,  $C_M$ .

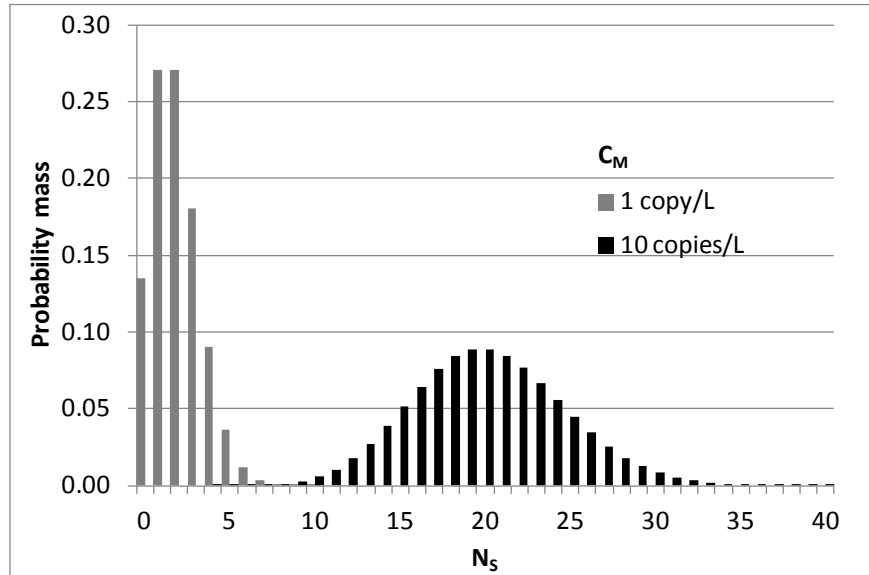


Figure 2.2: Probability mass functions showing the number of target marker copies in a two liter sample of water taken from a monitored water body for two selected concentrations, C<sub>M</sub>.

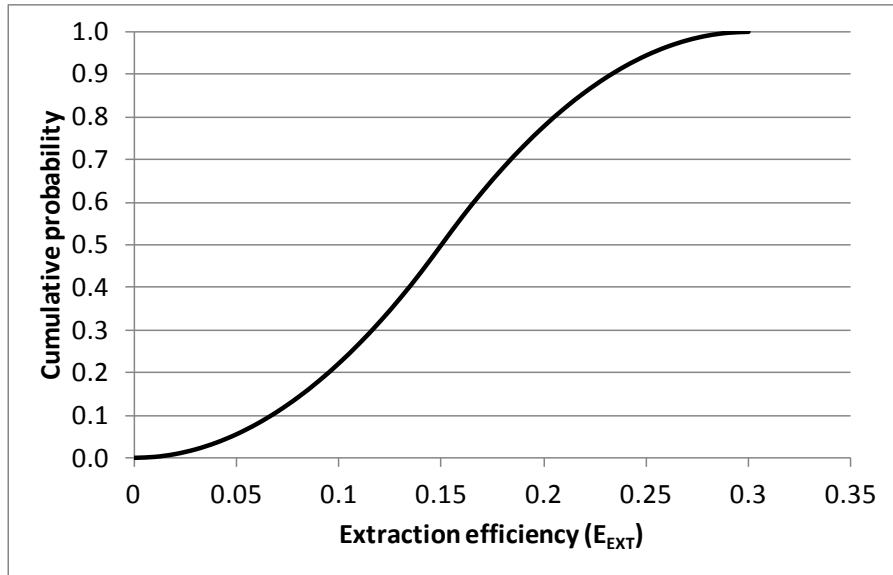


Figure 2.3: Triangular distribution function characterizing uncertainty in extraction efficiency,  $E_{EXT}$ .

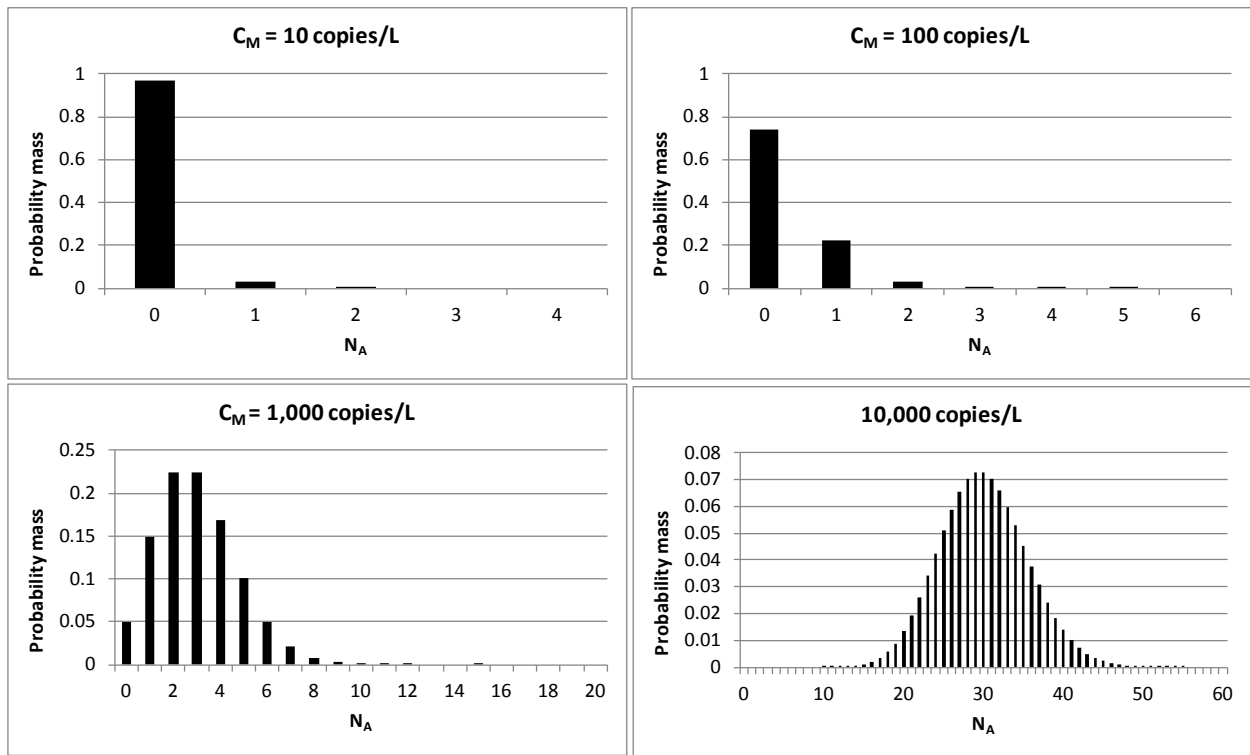


Figure 2.4: Relative frequency of target marker counts in a PCR replicate,  $N_A$ , for selected values of source water concentration,  $C_M$ .

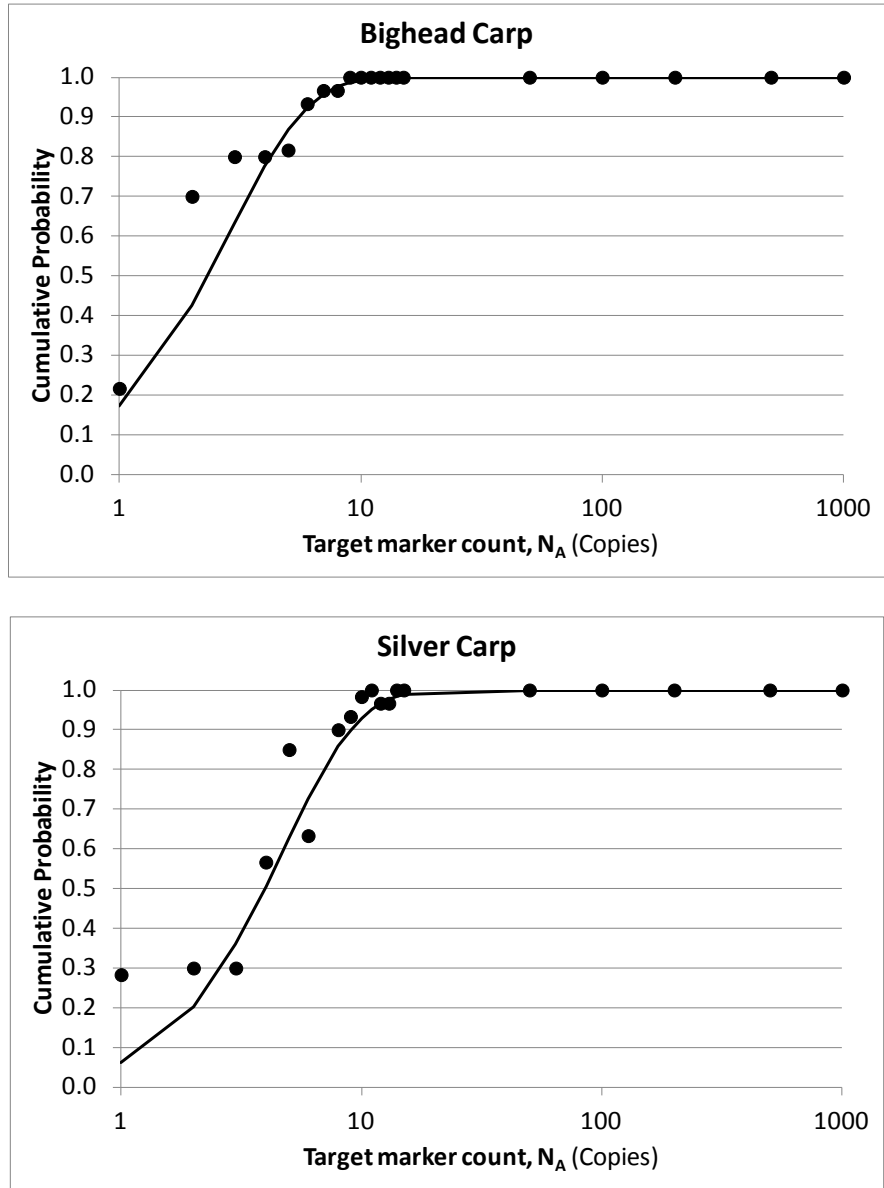


Figure 2.5: Probability of detecting bighead carp and silver carp target markers in a cPCR assay with one replicate.

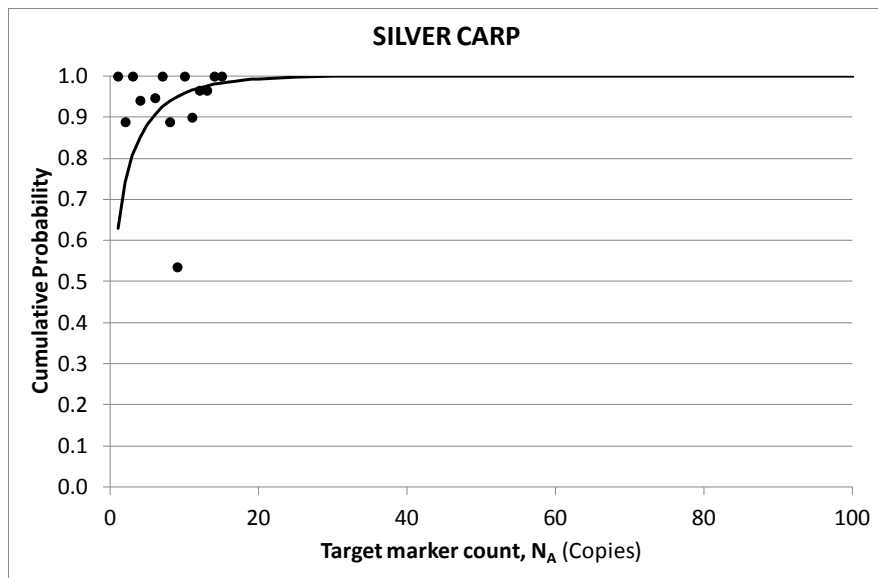
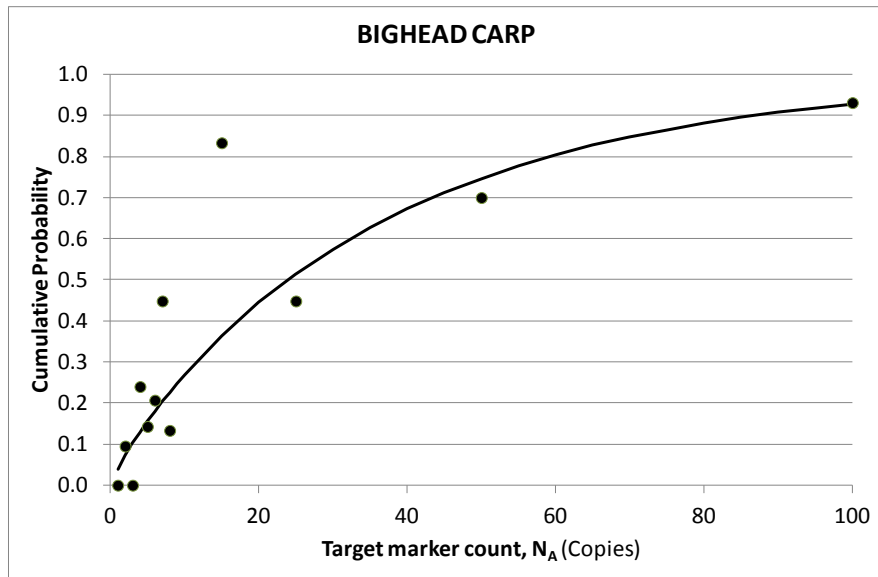


Figure 2.6: Probability of successfully sequencing target markers following positive detection using cPCR.



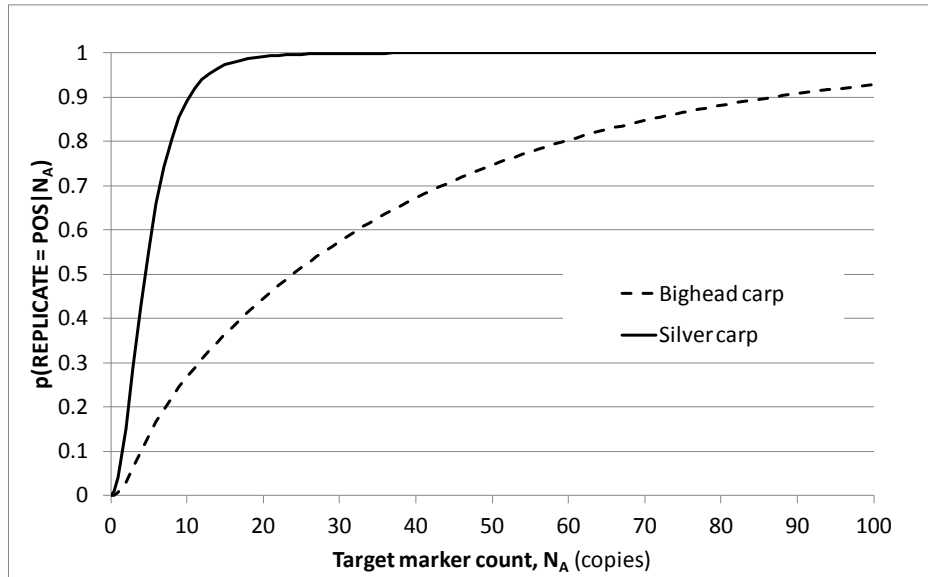


Figure 2.7: Joint probability of detecting and successfully sequencing bighead carp and silver carp target markers as a function of target marker counts,  $N_A$ , in cPCR replicates.

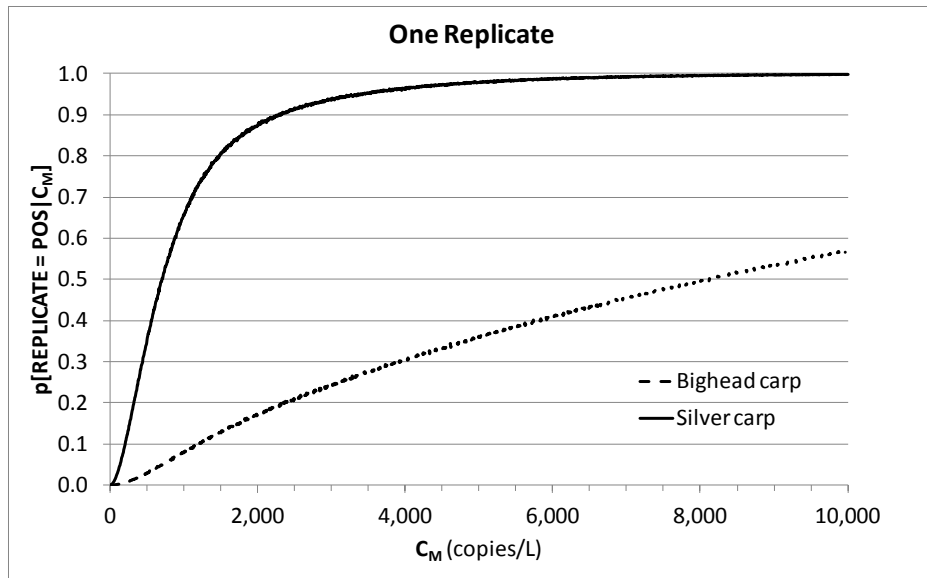


Figure 2.8: Probability of detecting and successfully sequencing bighead carp and silver carp target markers in a single cPCR replicate as a function of source water concentration,  $C_M$ .

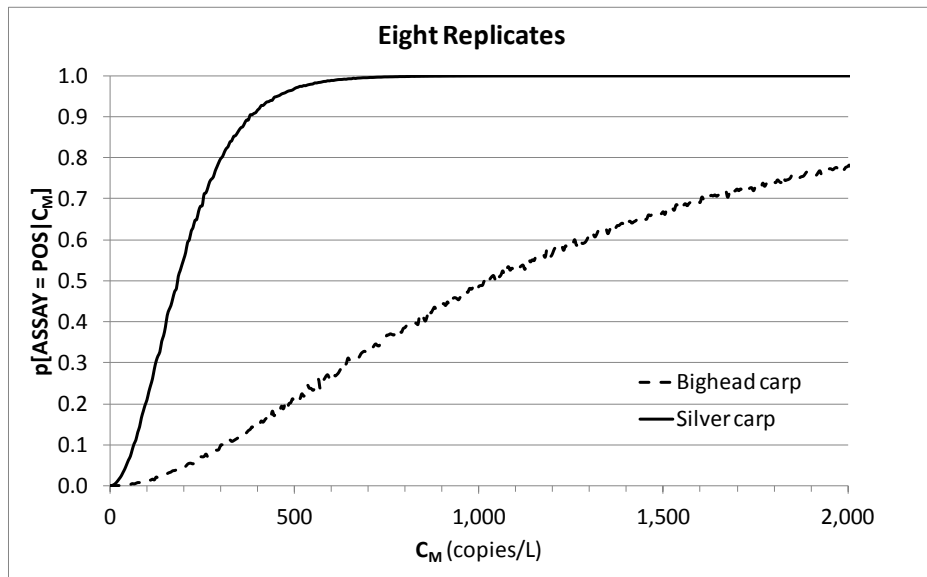


Figure 2.9: Probability of detecting and successfully sequencing bighead carp and silver carp target markers in a cPCR assay consisting of eight replicates as a function of source water concentration,  $C_M$ . Note the difference in the  $x$ -axis scale compared to Figure 2.8.

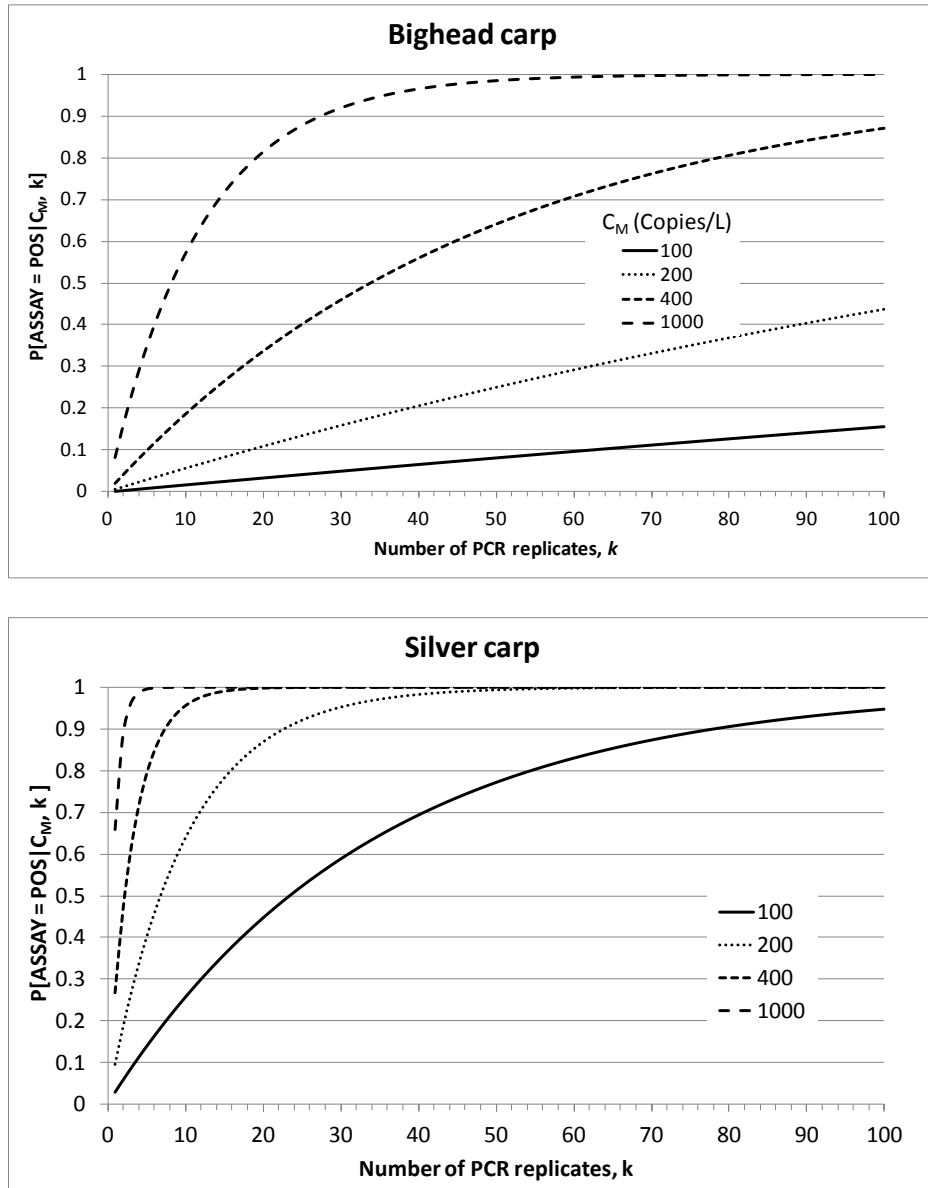


Figure 2.10: Probability the cPCR assay is positive for bighead carp and silver carp as a function of selected source water target marker concentrations (copies/L) and replicates used in PCR.

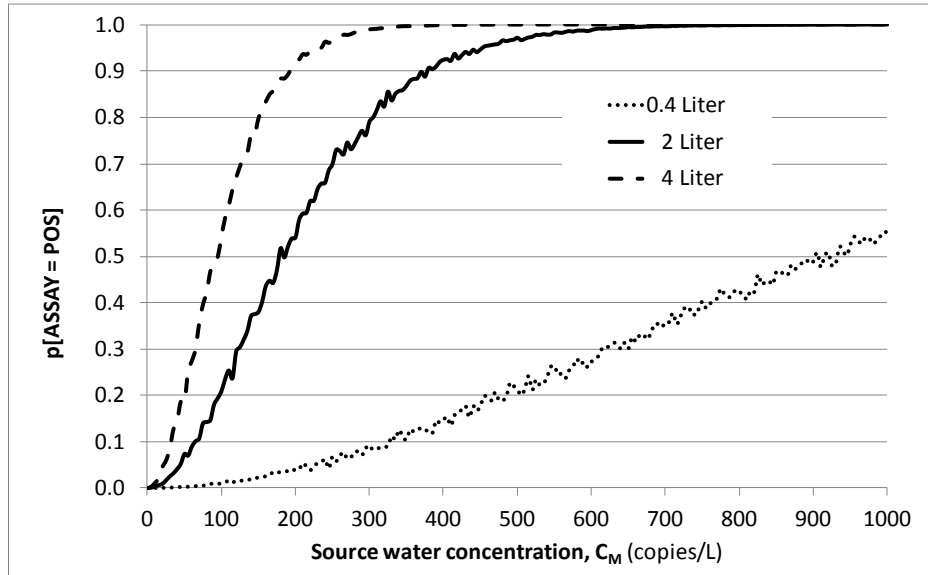


Figure 2.11: Effect of sample volume on the probability of detecting silver carp. This analysis assumes that eight replicates are used in the cPCR assay.

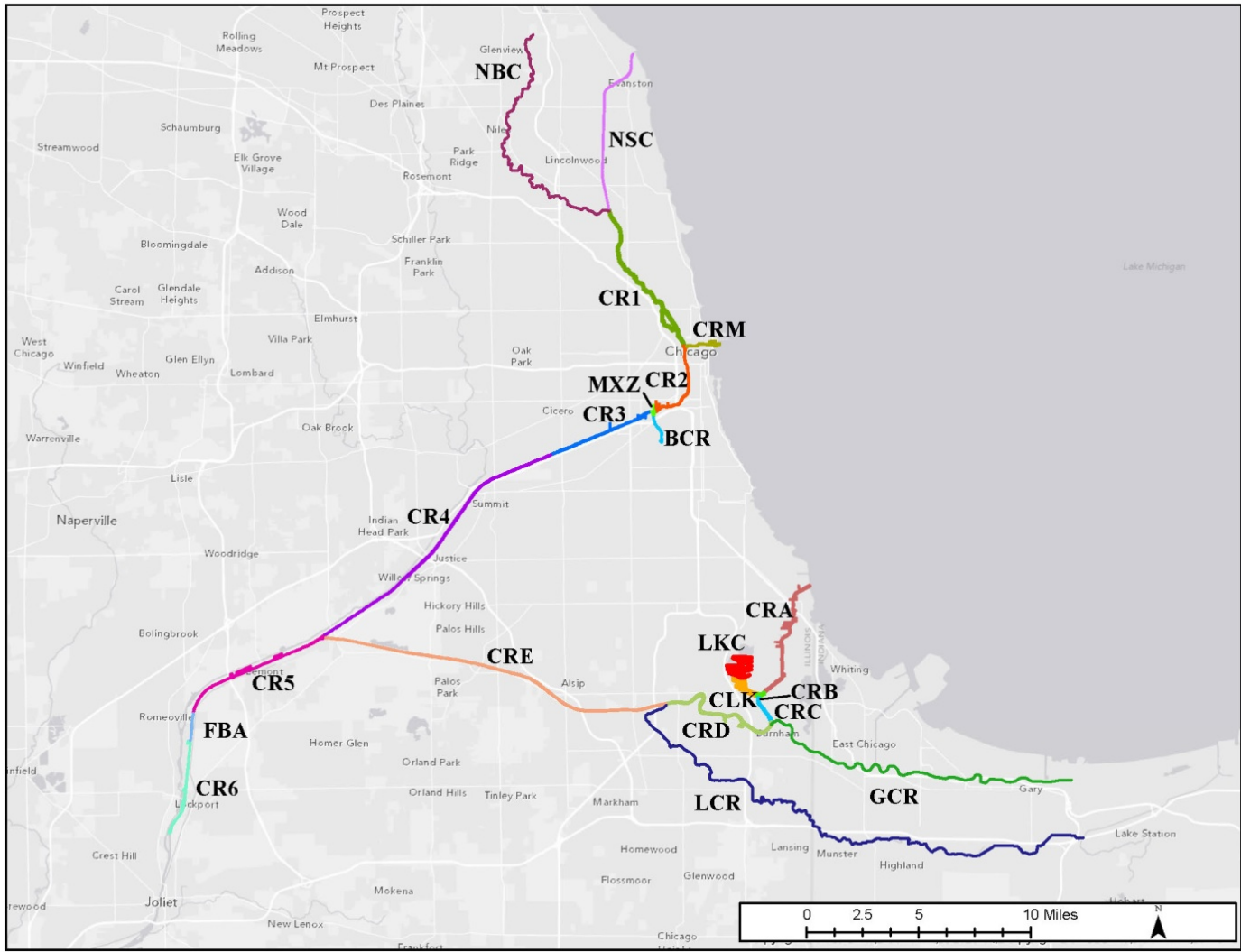
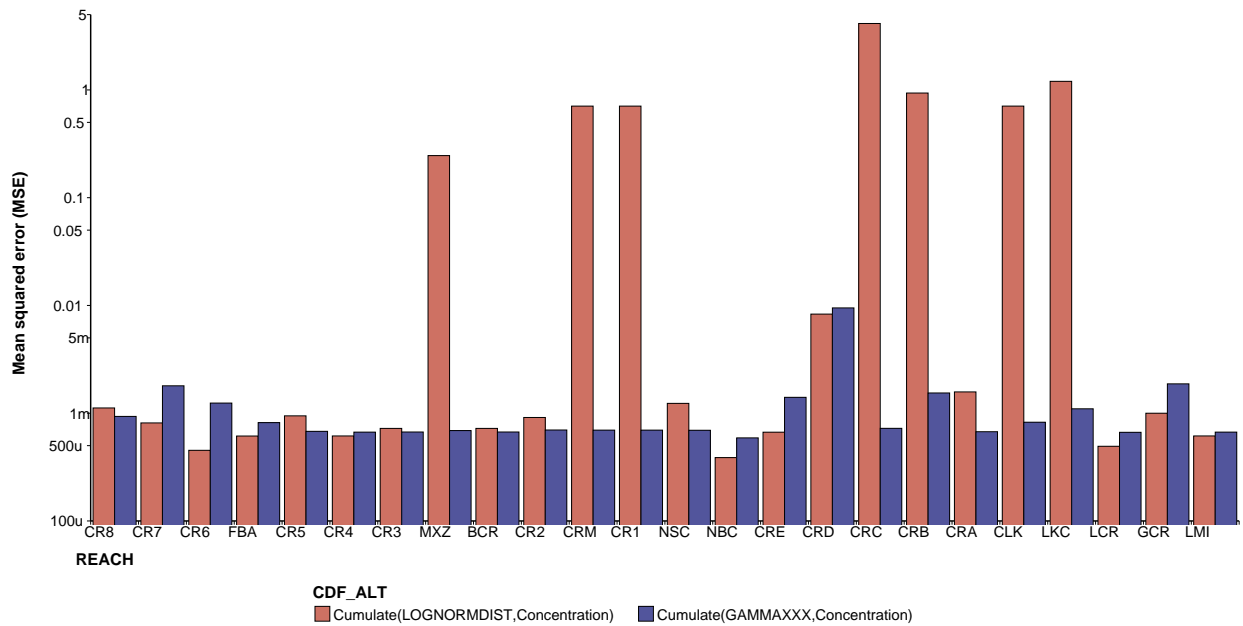
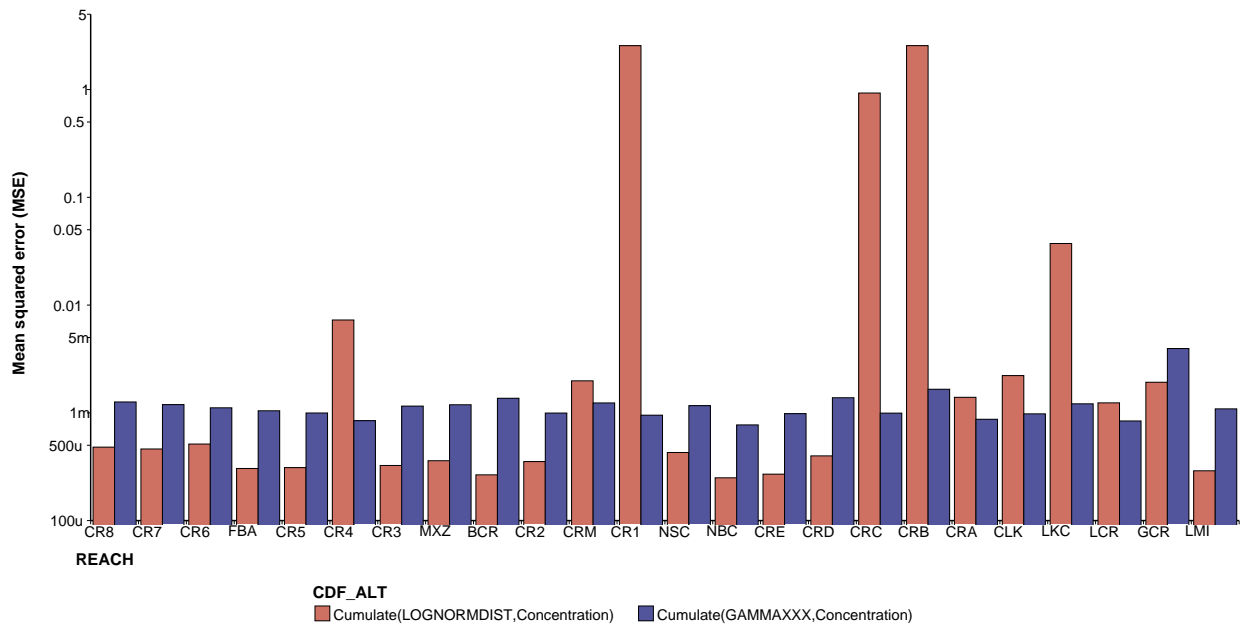


Figure 3.1: Main stem reaches of the CAWS between Lake Michigan and Lockport Lock and Dam. Since creation of this figure, CRC has been divided into CRU, upstream of O’Brien Lock and Dam, and CRV, downstream of O’Brien Lock and Dam.



a) Bighead carp



b) Silver carp

Figure 3.2: Fit of lognormal and gamma distributions to PMFs evaluated using mean squared error for a) bighead carp and b) silver carp. The y-axis shows the sum of mean squared error (MSE) over all probability distributions fit in the reach.

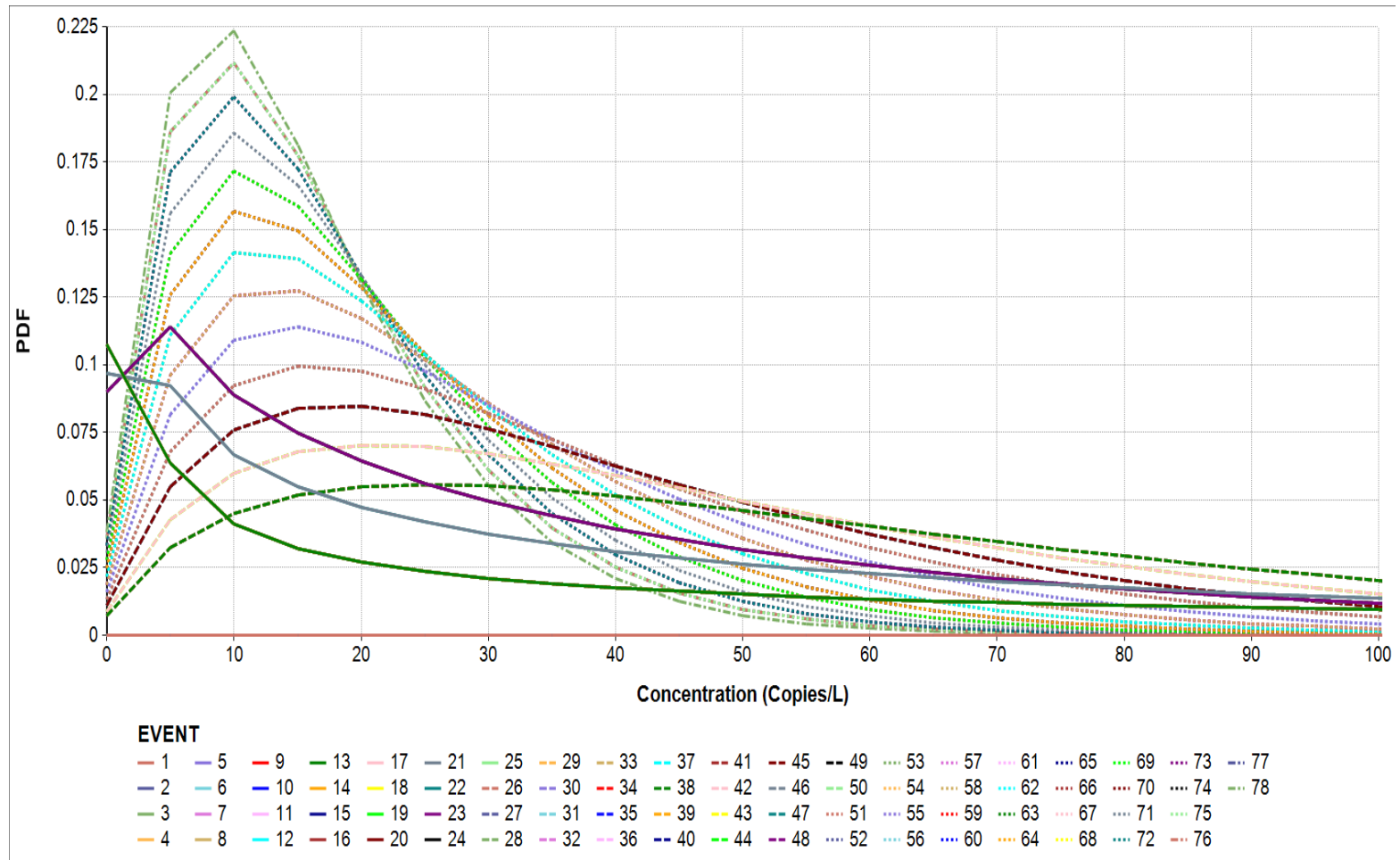


Figure 3.3: Probability density functions characterizing uncertainty in target marker concentrations for bighead carp in the North Shore Channel (NSC).



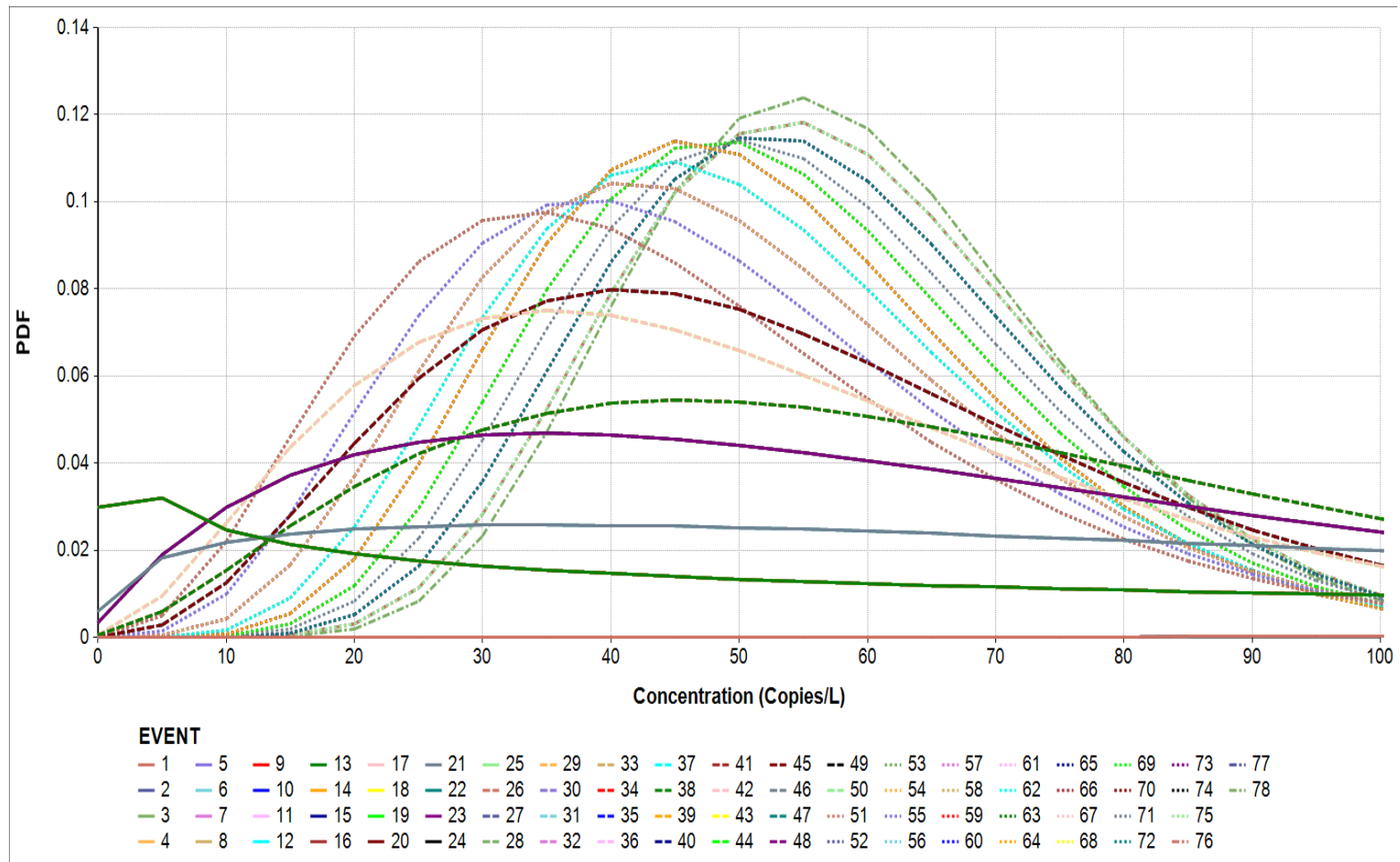


Figure 3.4: Probability density functions characterizing uncertainty in target marker concentrations for silver carp in the North Shore Channel (NSC).

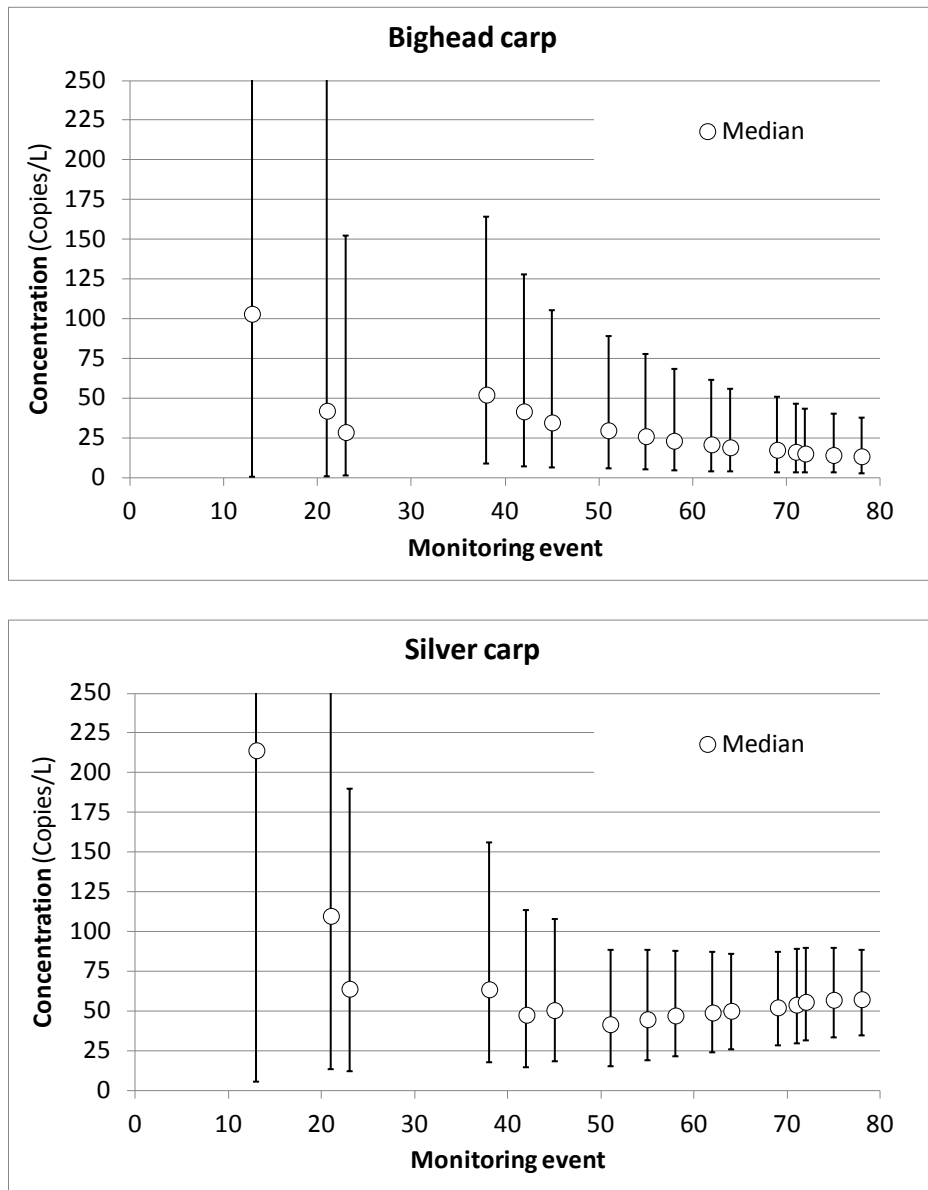
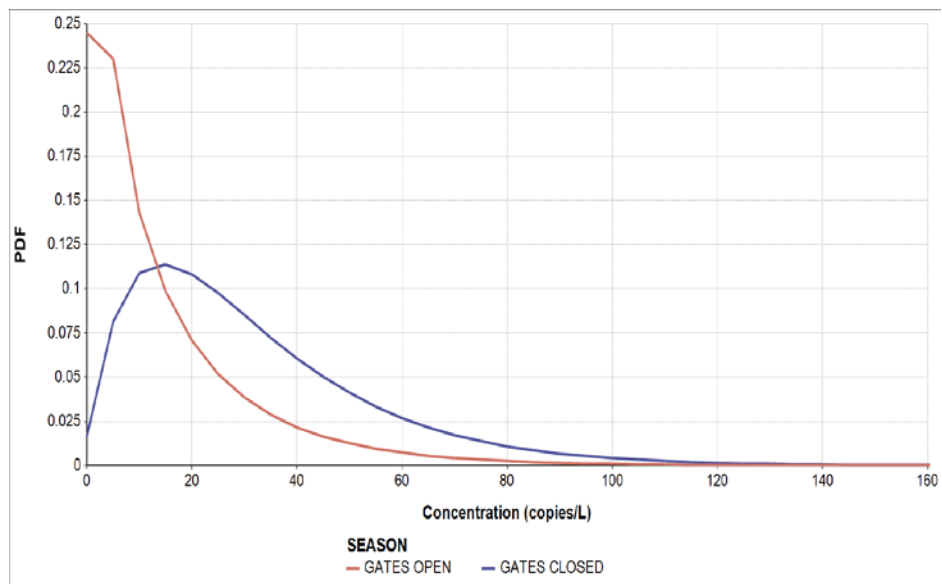
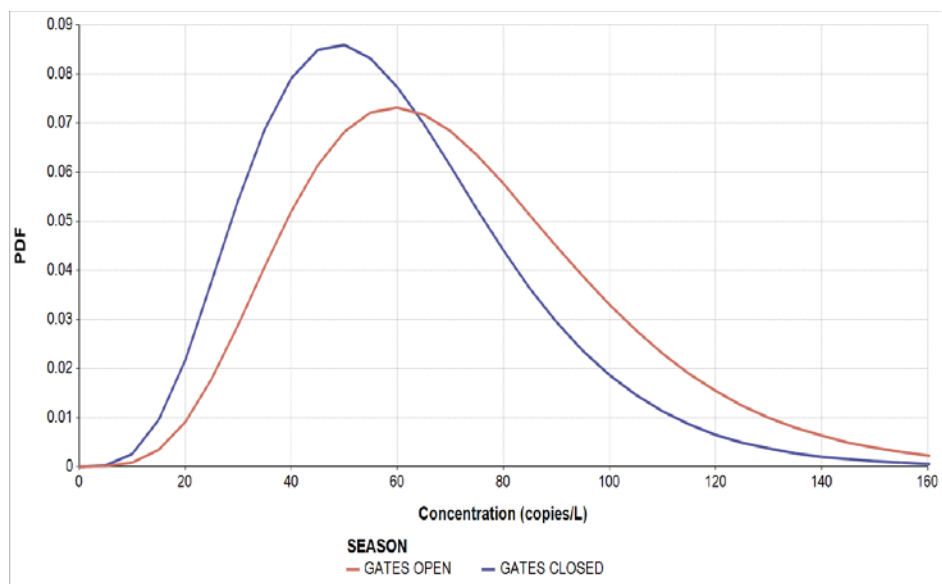


Figure 3.5: Median target marker concentration and 90 percent confidence bounds for bighead carp and silver carp in the NSC.



a) Bighead carp



b) Silver carp

Figure 3.6: Seasonal concentration estimates for *a)* bighead carp and *b)* silver carp in the NSC.

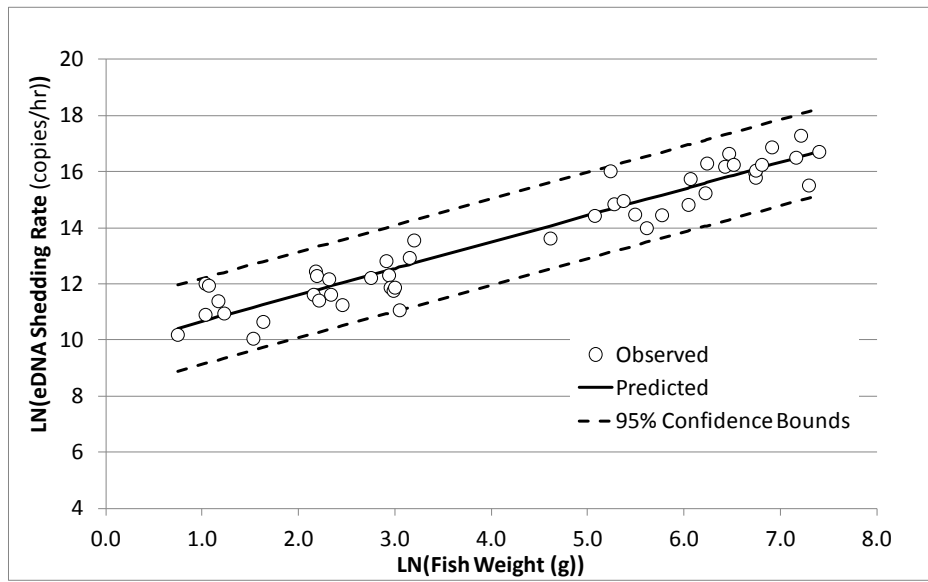


Figure 4.1: eDNA Shedding rate (copies/hr) from juvenile and sub-adult fish. Data from Klymus et al. (2013).

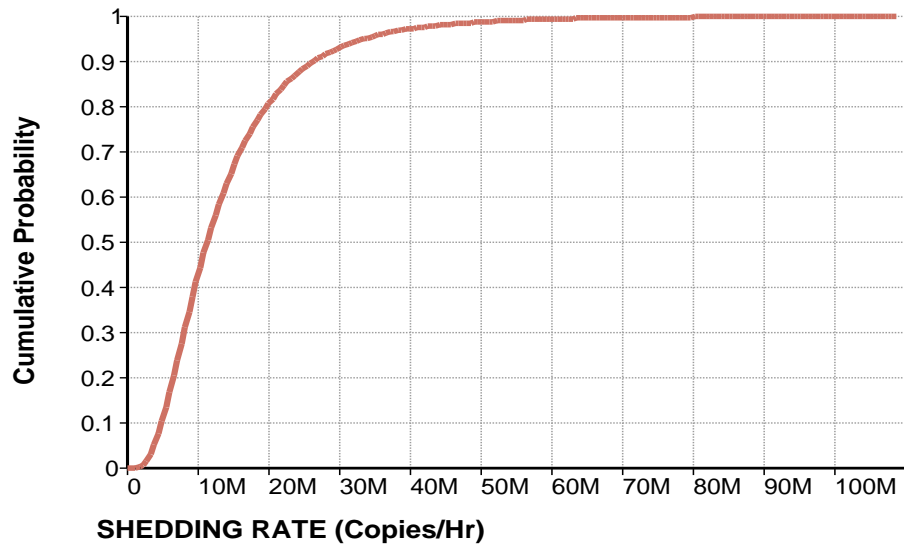


Figure 4.2: Uncertainty in the shedding rate from one kg of juvenile and sub-adult fish.

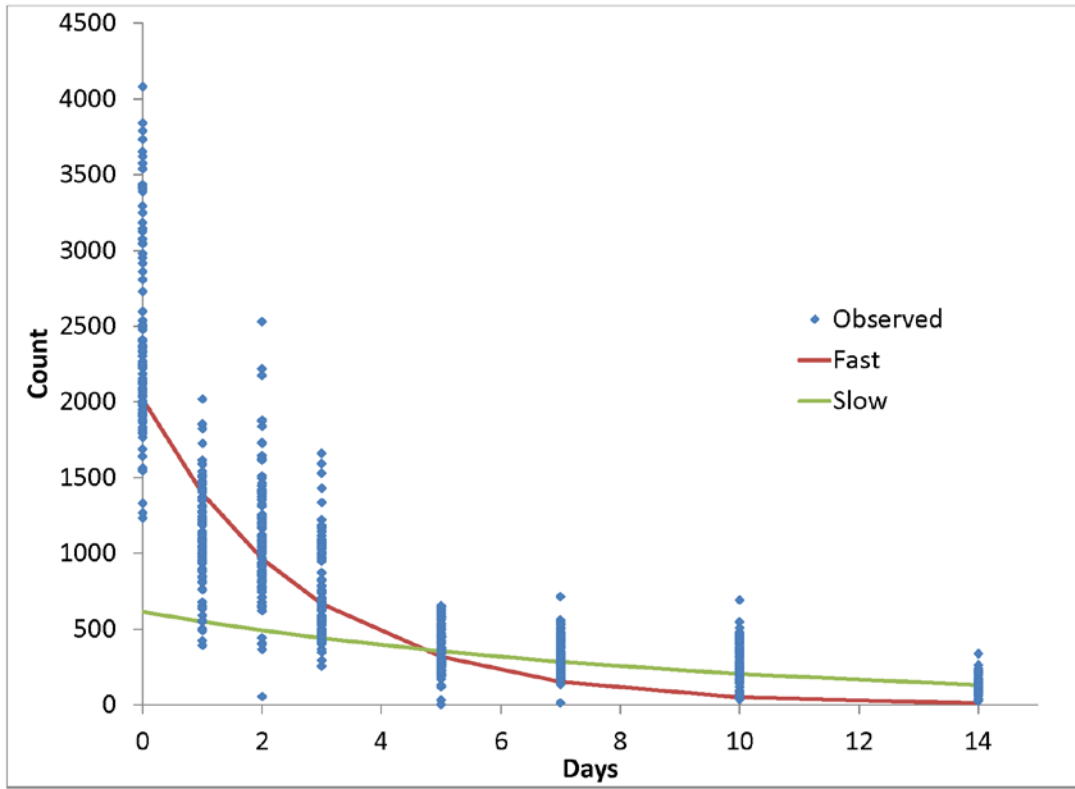
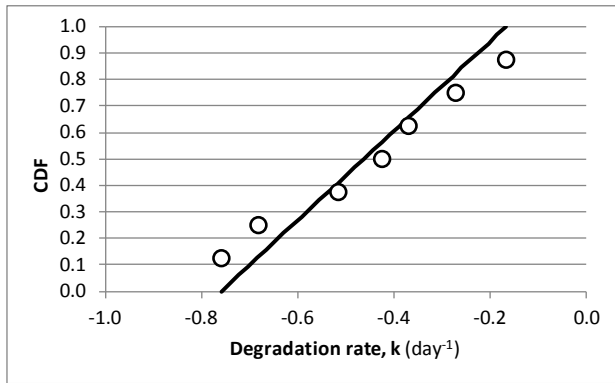
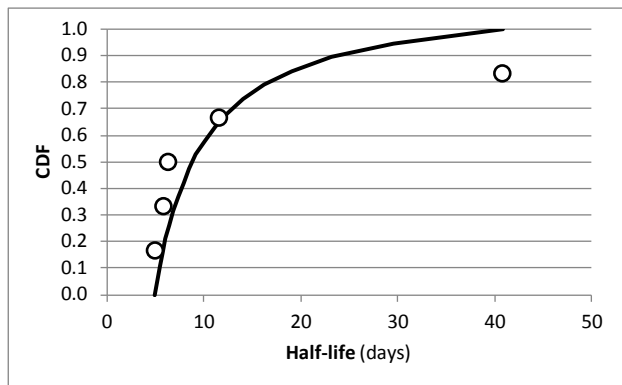
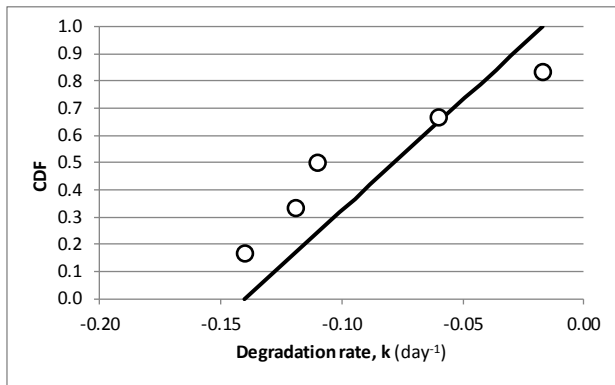


Figure 4.3a: Fast and slow degradation rate curves fitted to experimental data.



a) Degradation rate for the fast fraction.



b) Degradation rate for the slow fraction.

Figure 4.3: Uncertainty in degradation rates expressed in terms of a decay rate,  $k$  ( $\text{day}^{-1}$ ) and half-life.

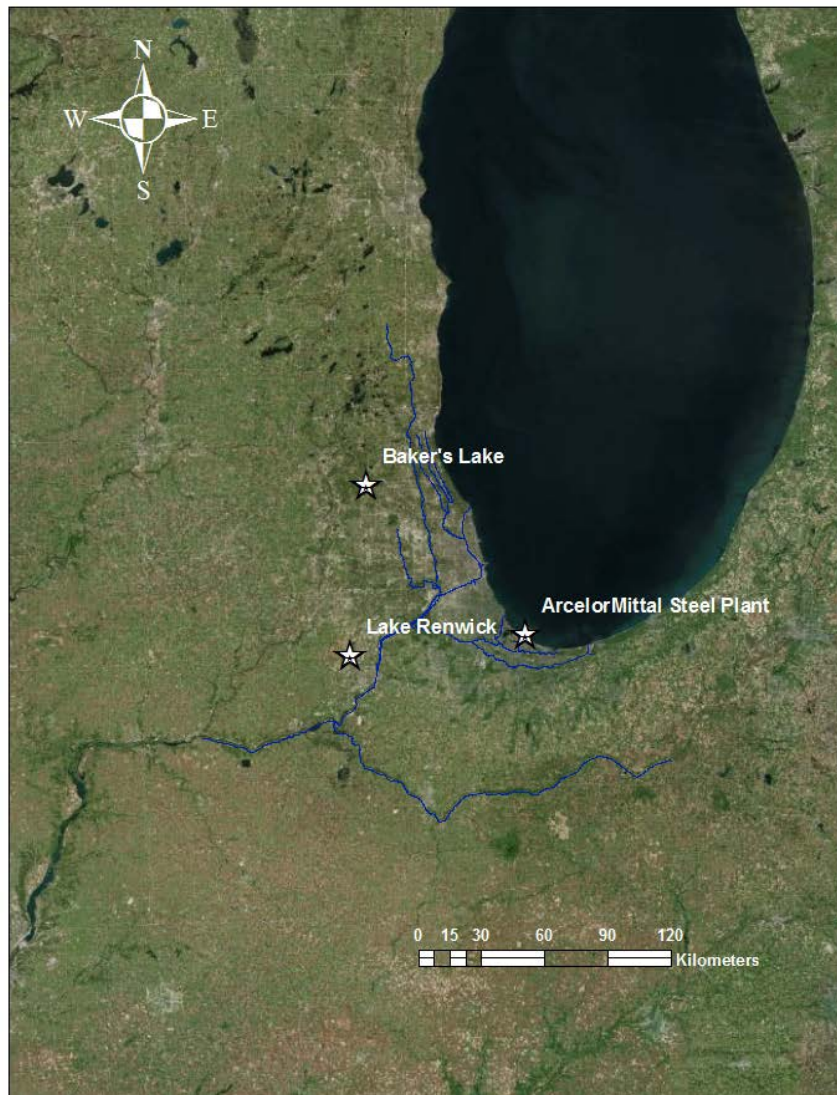


Figure 4.4: Location of three large cormorant colonies in the CAWS.





Figure 4.5: Locations of combined sewer overflows (CSOs) discharging into the CAWS.

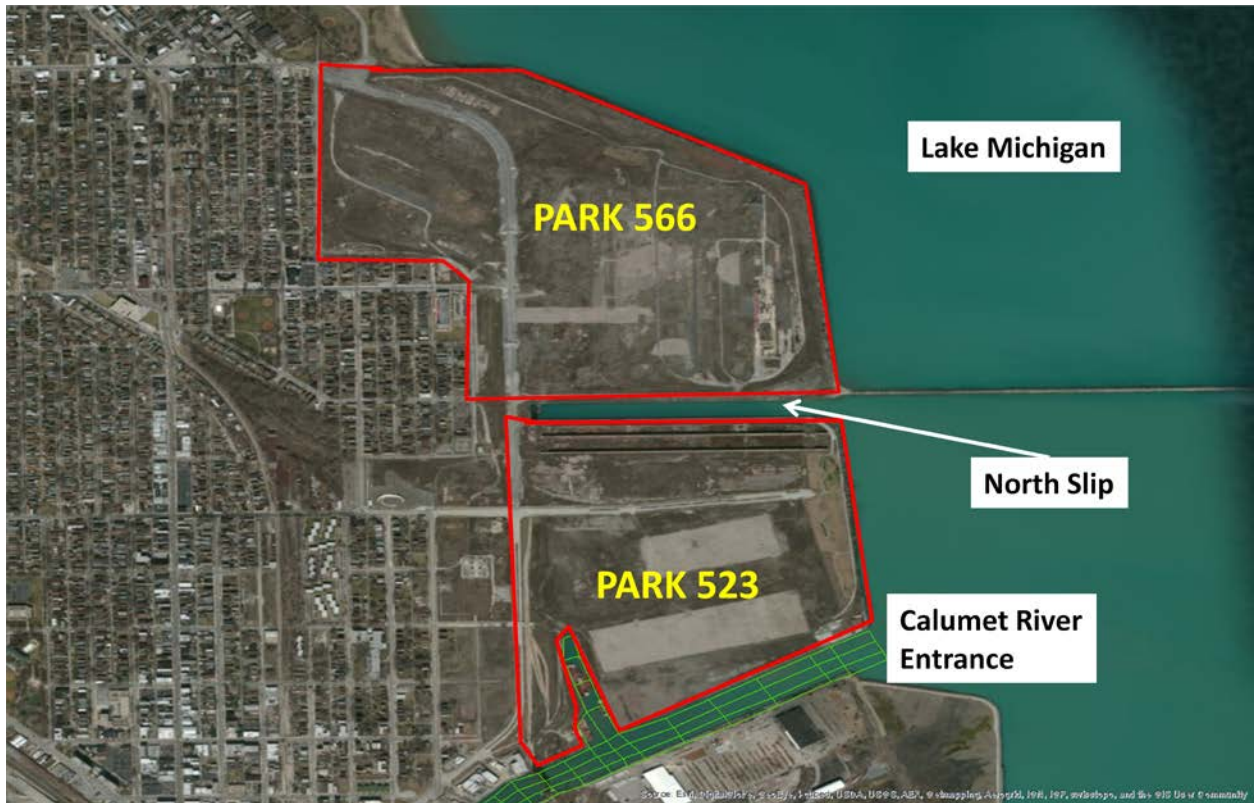


Figure 4.6: Mud-to-Parks Program sediment deposition sites on the shores of Lake Michigan.



Figure 5.1: Plan view of computational grid extending from Lockport to Wilmette and to O'Brien Lock and Dam.

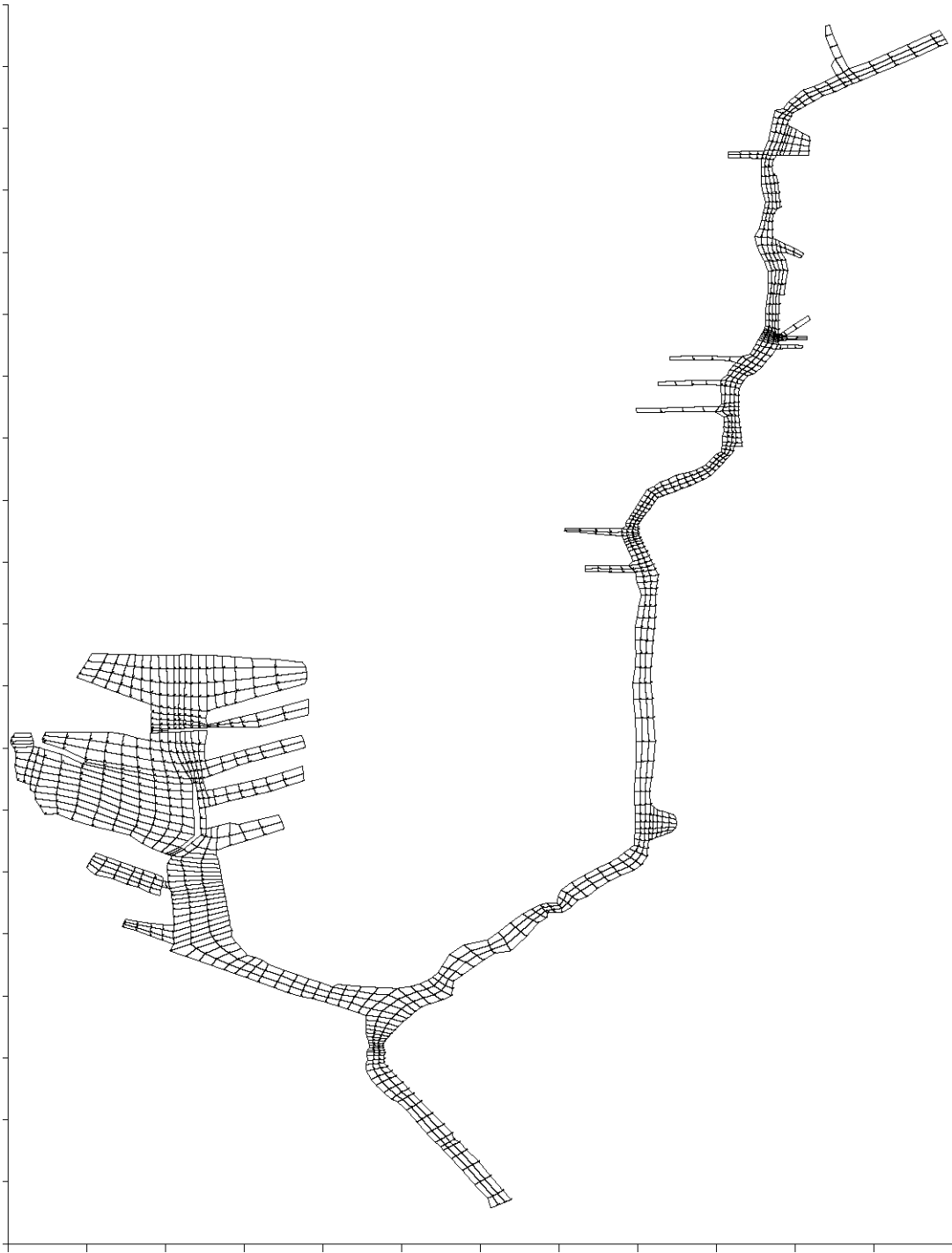


Figure 5.2: Plan view of computational grid extending from O'Brien Lock and Dam to Lake Michigan, including Lake Calumet.

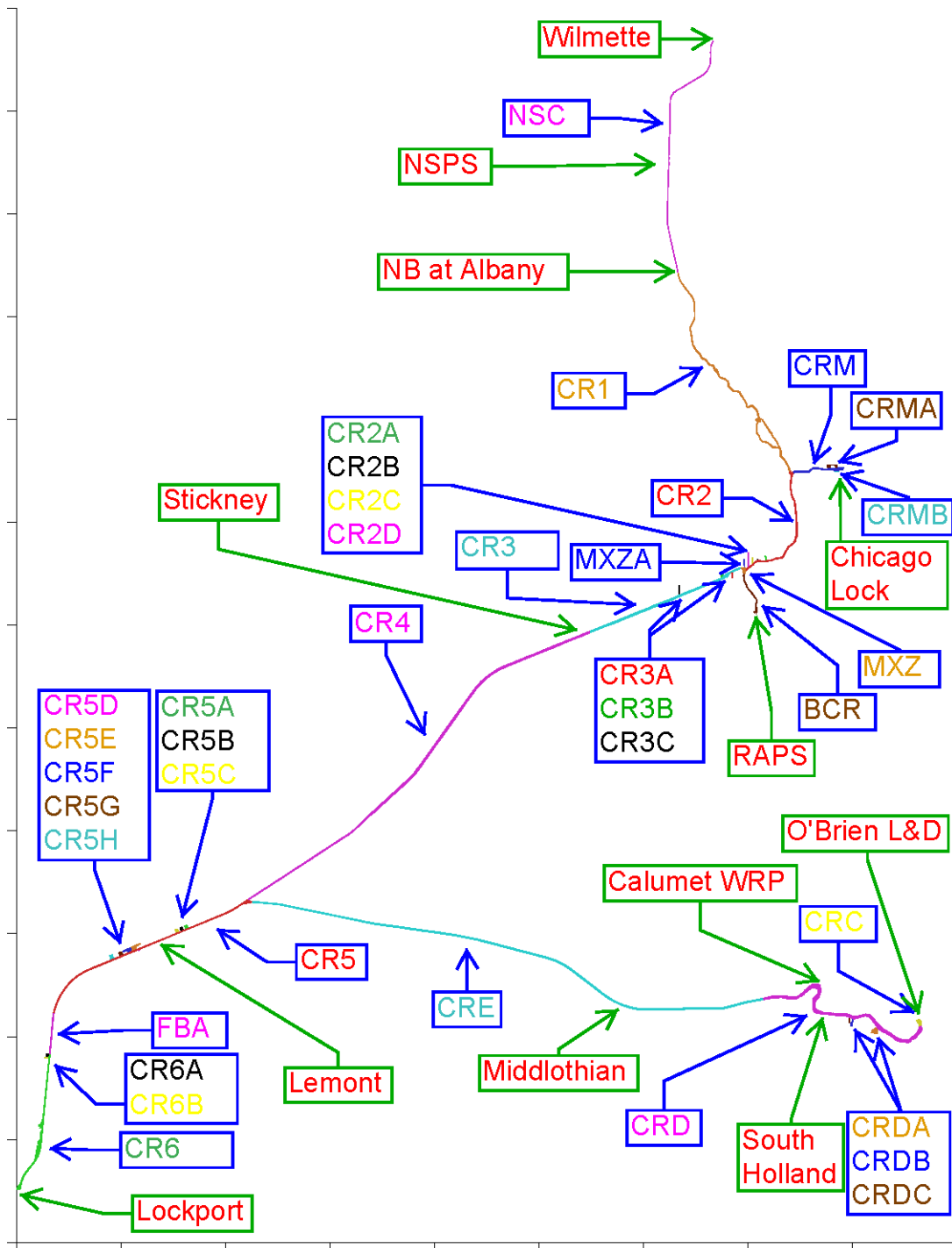


Figure 5.3: Plan view of reaches in steady-state model. Reach designations are in blue rectangles. Green rectangles indicate inflows and boundary conditions. (Note: the steady-state model includes Lake Calumet which is shown on a separate figure to improve resolution.)

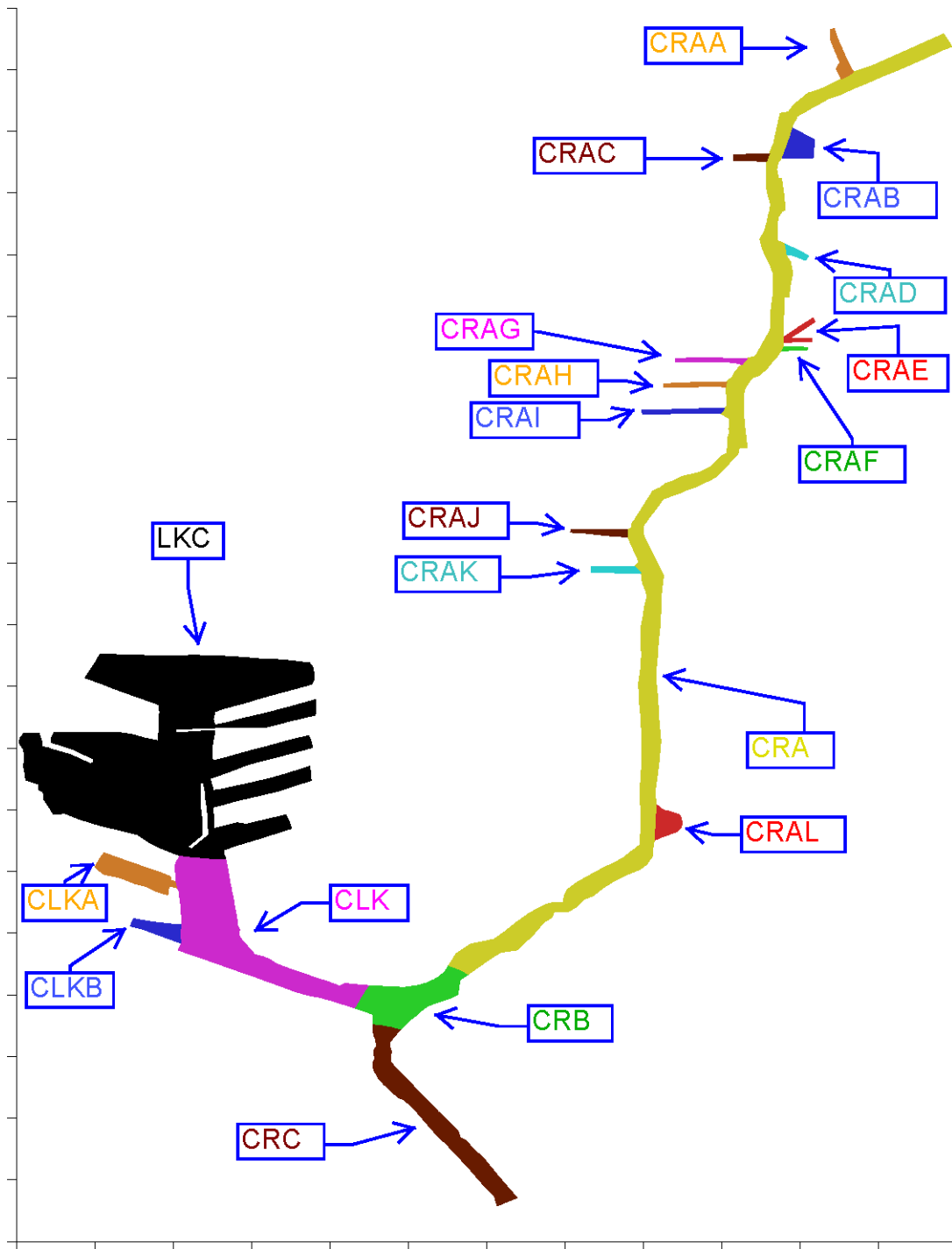


Figure 5.4: Plan view of Lake Calumet portion of steady-state model. Reach designations are in blue rectangles. (Note: the steady-state model includes the entire system. Lake Calumet is shown separately to improve resolution.)

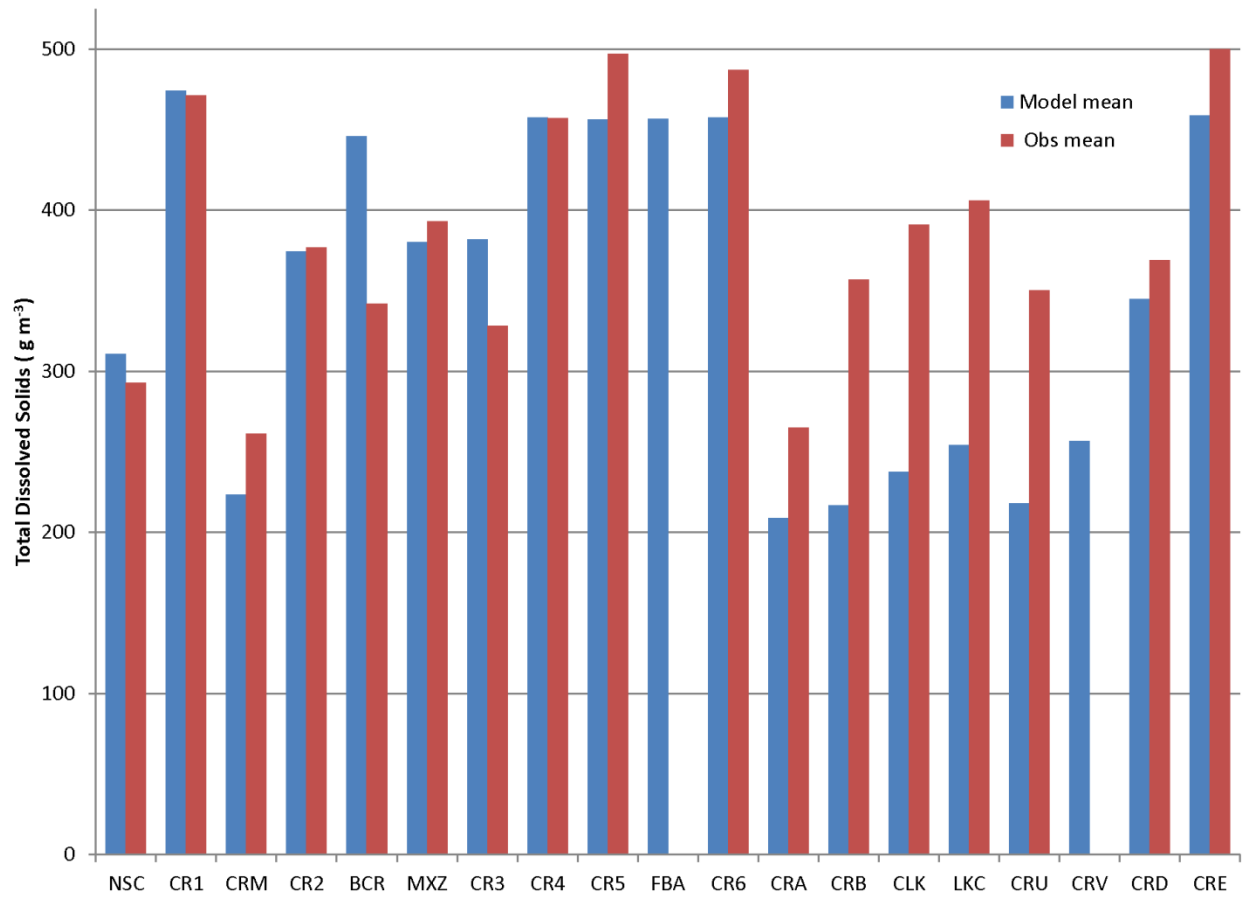


Figure 5.5: Computed and observed TDS concentrations during the 2012 gates open season. Mean values are shown for reaches illustrated in Figures 5.3 and 5.4.

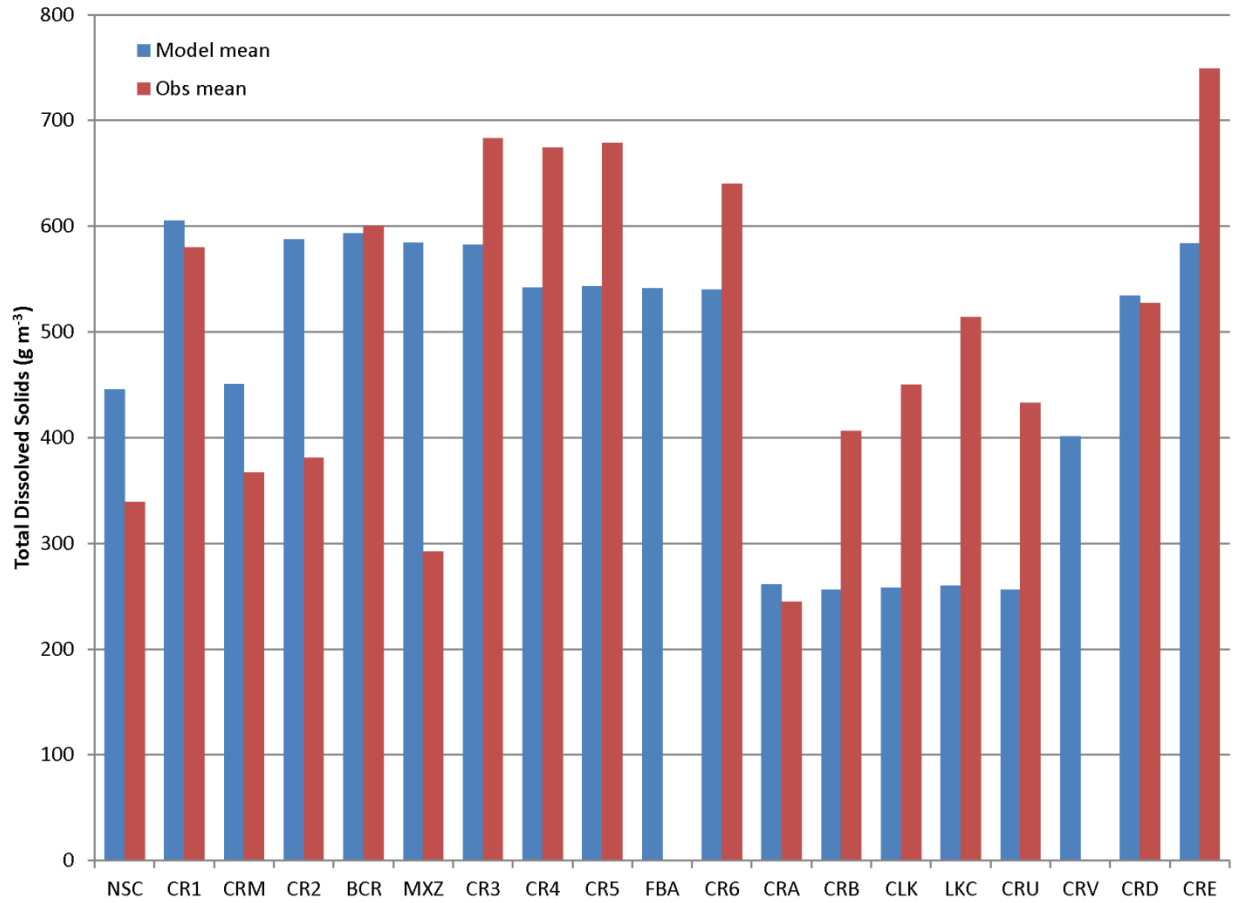


Figure 5.6: Computed and observed TDS concentrations during the 2012 gates closed season. Mean values are shown for reaches illustrated in Figures 5.3 and 5.4.



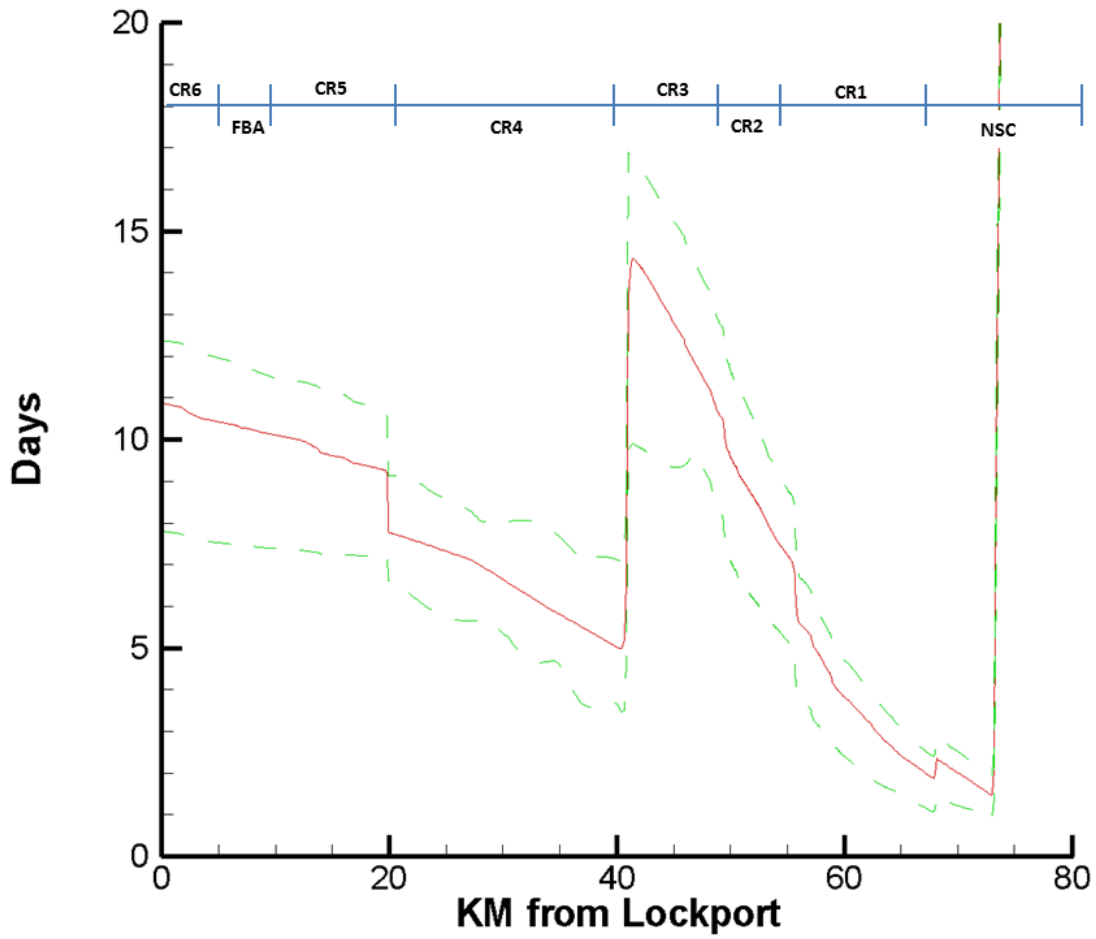


Figure 5.7: Computed age along the axis from Lockport to Wilmette during February 2012 (gates closed). The solid red line shows mean age over the month. The dashed green line shows maximum and minimum age during the month. The horizontal bar at the top of the figure identifies the CAWS reach, as described in Figure 5.3.

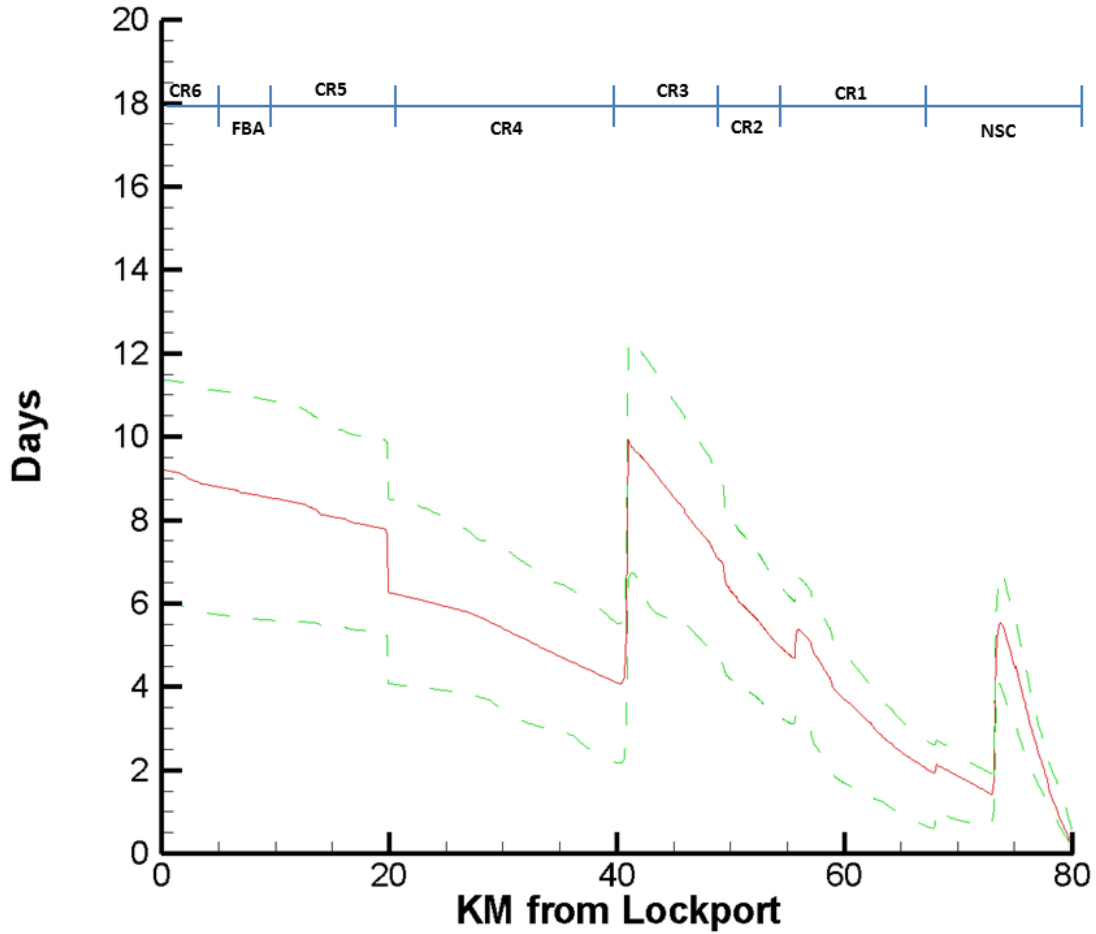


Figure 5.8: Computed age along the axis from Lockport to Wilmette during July 2012 (gates open). The solid red line shows mean age over the month. The dashed green line shows maximum and minimum age during the month. The horizontal bar at the top of the figure identifies the CAWS reach, as described in Figure 5.3.

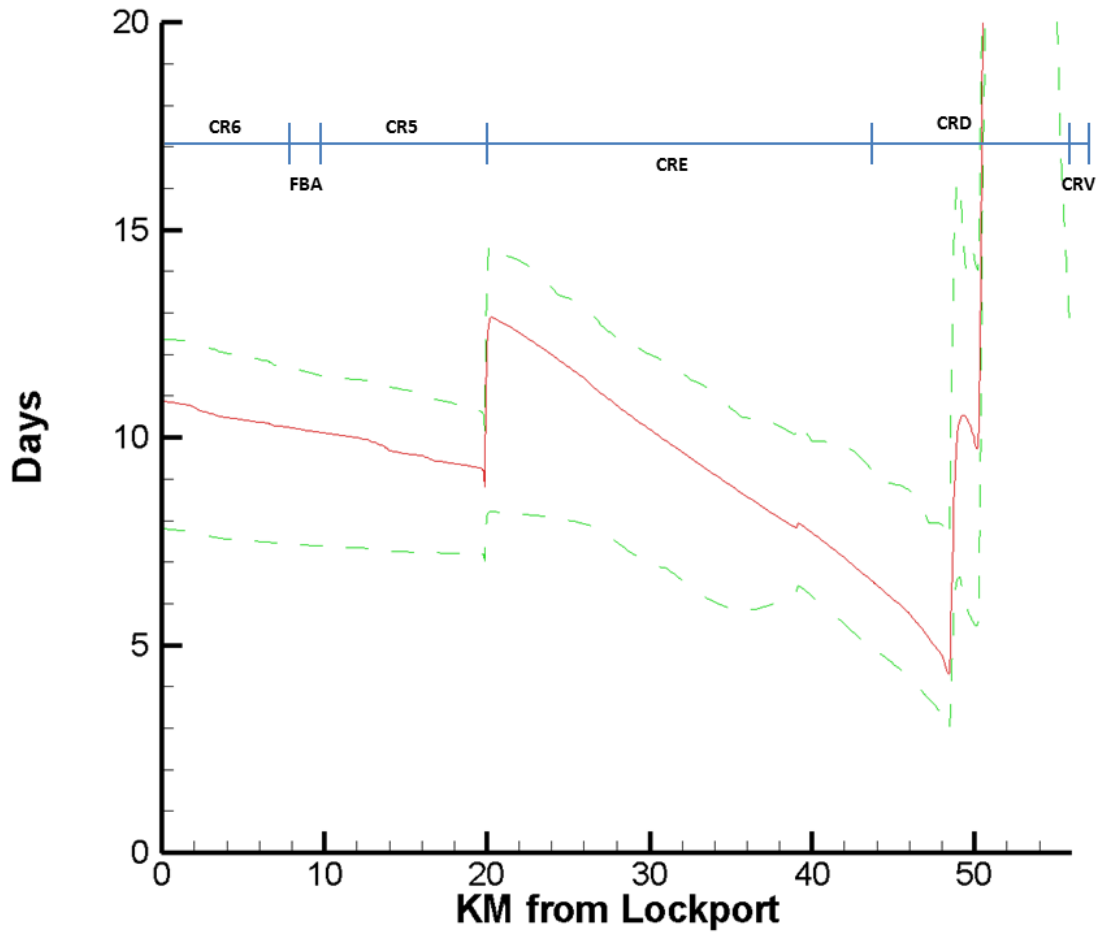


Figure 5.9. Computed age along the axis from Lockport to O'Brien L&D during February 2012 (gates closed). The solid red line shows mean age over the month. The dashed green line shows maximum and minimum age during the month. The horizontal bar at the top of the figure identifies the CAWS reach, as described in Figures 5.3 and 5.4.

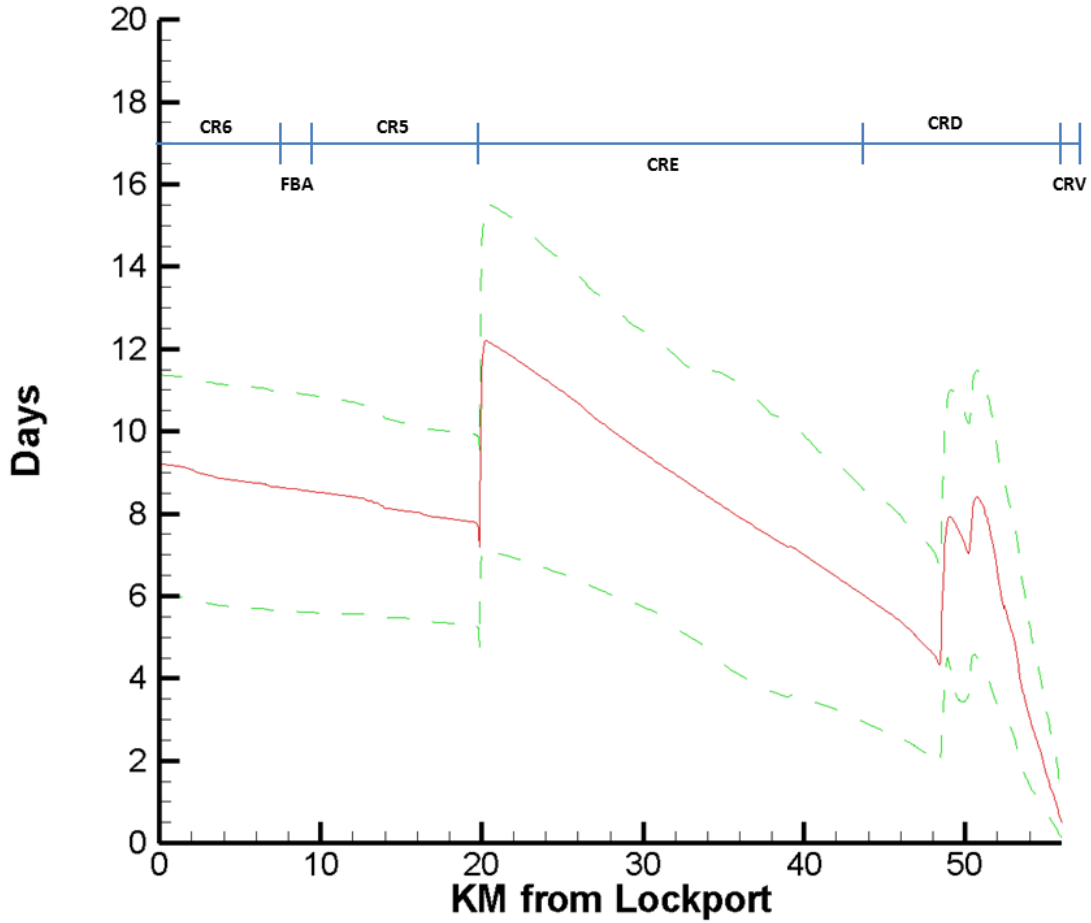


Figure 5.10. Computed age along the axis from Lockport to O'Brien L&D during July 2012 (gates closed). The solid red line shows mean age over the month. The dashed green line shows maximum and minimum age during the month. The horizontal bar at the top of the figure identifies the CAWS reach, as described in Figures 5.3 and 5.4.

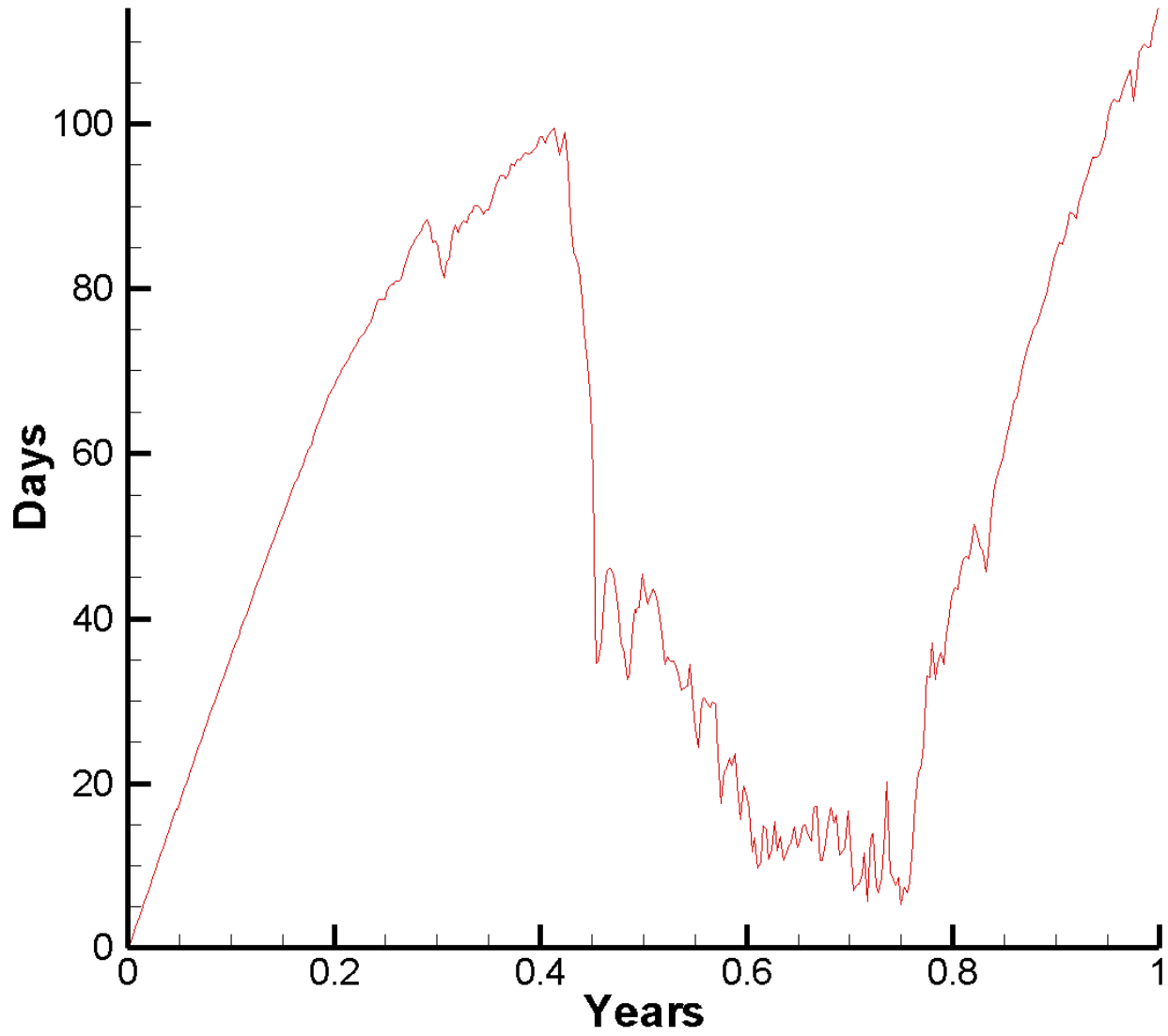


Figure 5.11. Computed age during the year 2012 at a location immediately above the O'Brien Lock and Dam.

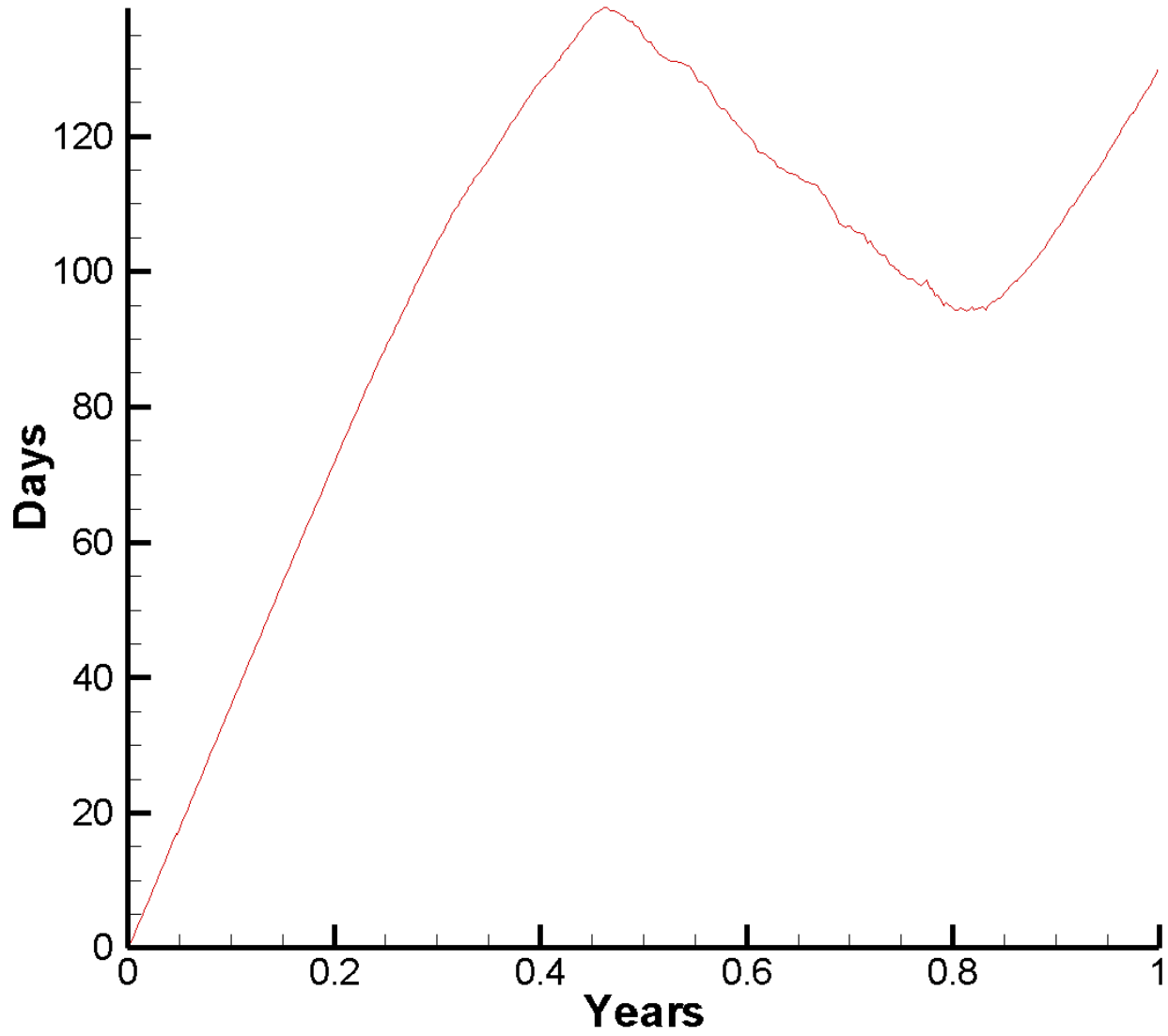
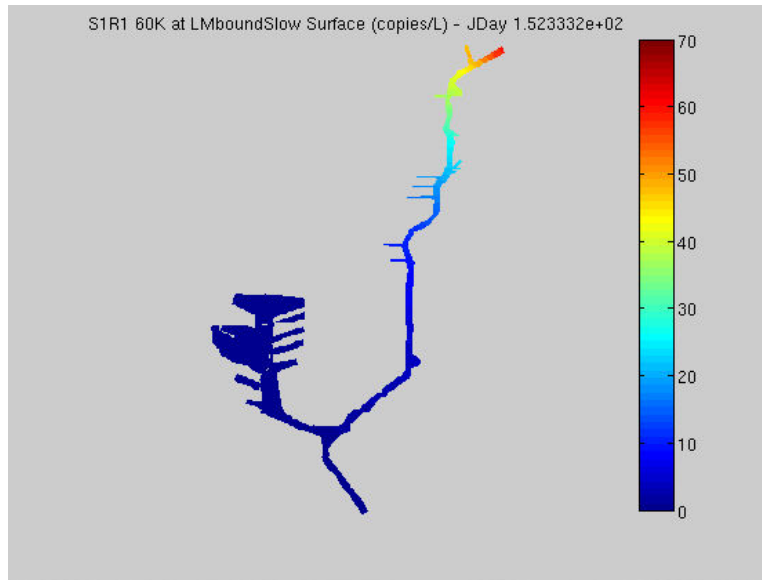
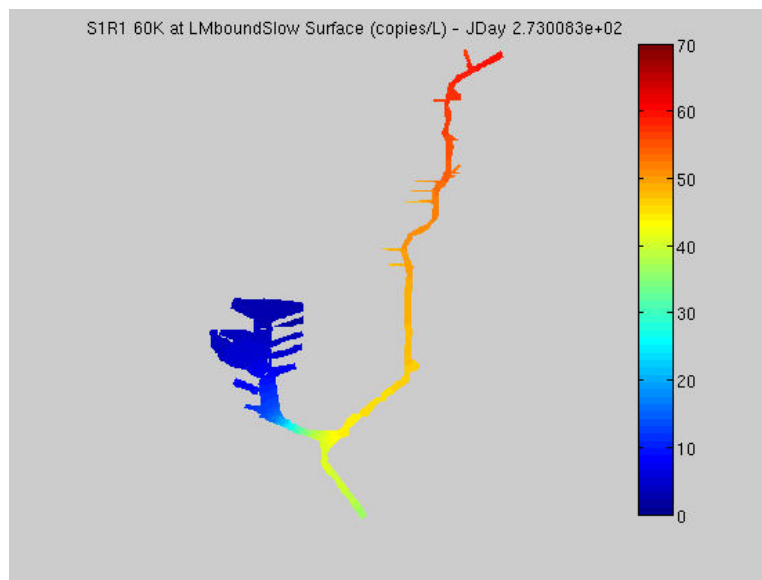


Figure 5.10. Computed age during the year 2012 at a location in the interior of Lake Calumet.

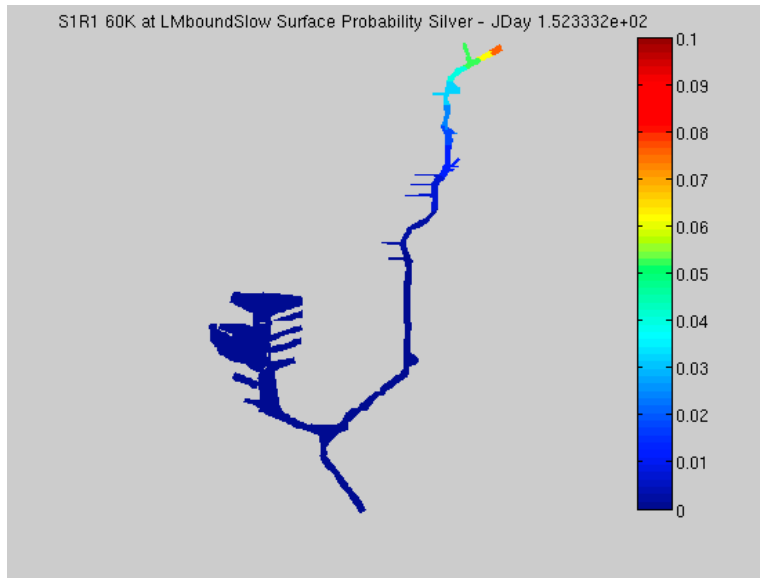


a) Concentrations of eDNA (copies/L) at the end of the gates closed season.

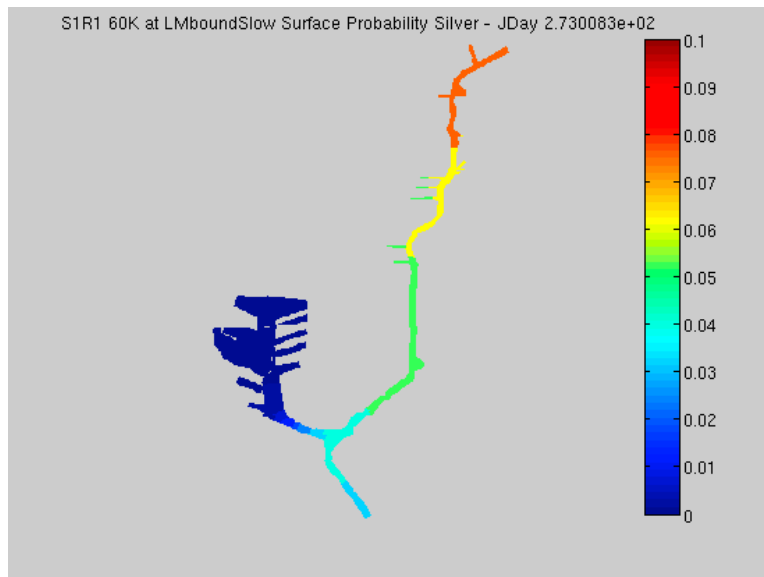


b) Concentrations of eDNA (copies/L) at the end of the gates open season.

Figure 5.13: Illustrative simulation of eDNA fate and transport for load at the CRA boundary with Lake Michigan. These figures show that, under the assumed loading conditions of this scenario, target marker concentrations in Lake Calumet may vary as a result of seasonal differences in hydrodynamics.



a) Probability of detecting silver carp eDNA at the end of the gates closed season.



b) Probability of detecting silver carp eDNA at the end of the gates open season.

Figure 5.14. Illustrative simulation results showing the probability of detection silver carp eDNA given an assumed concentration of 60 copies/L at the CRA boundary with Lake Michigan.



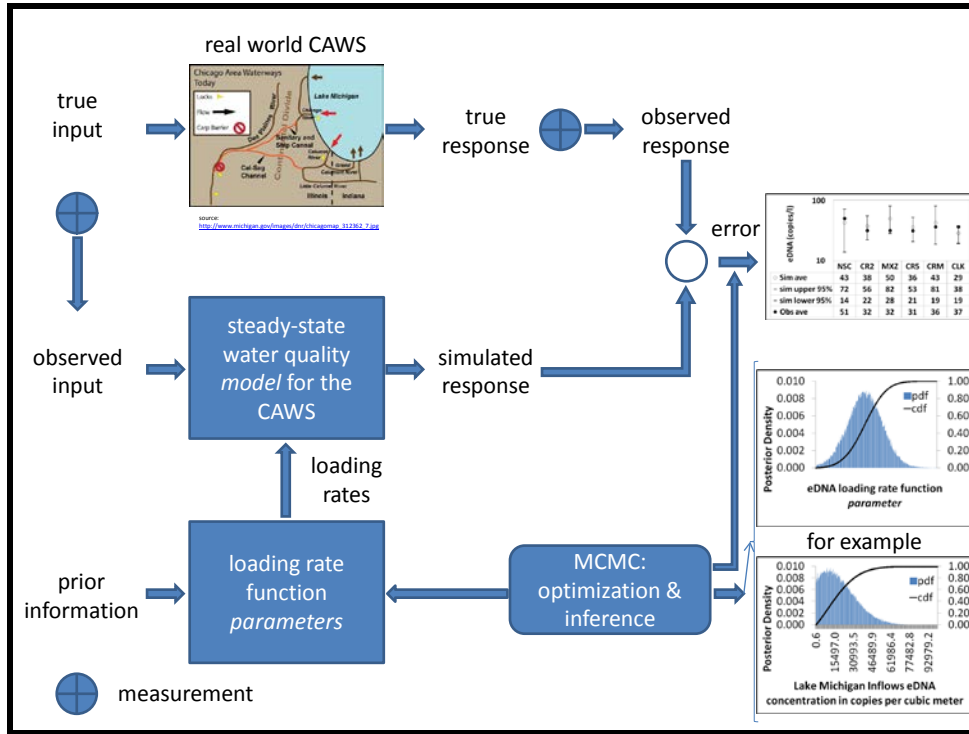


Figure 6.1: Diagram depicting the formal probabilistic simulation-based analysis methodology that was employed to infer modeled secondary source loading rates which uses the eDNA concentrations derived from the monitoring samples, the steady-state water quality model, the defined and parameterized secondary source loading functions, and Bayesian MCMC.

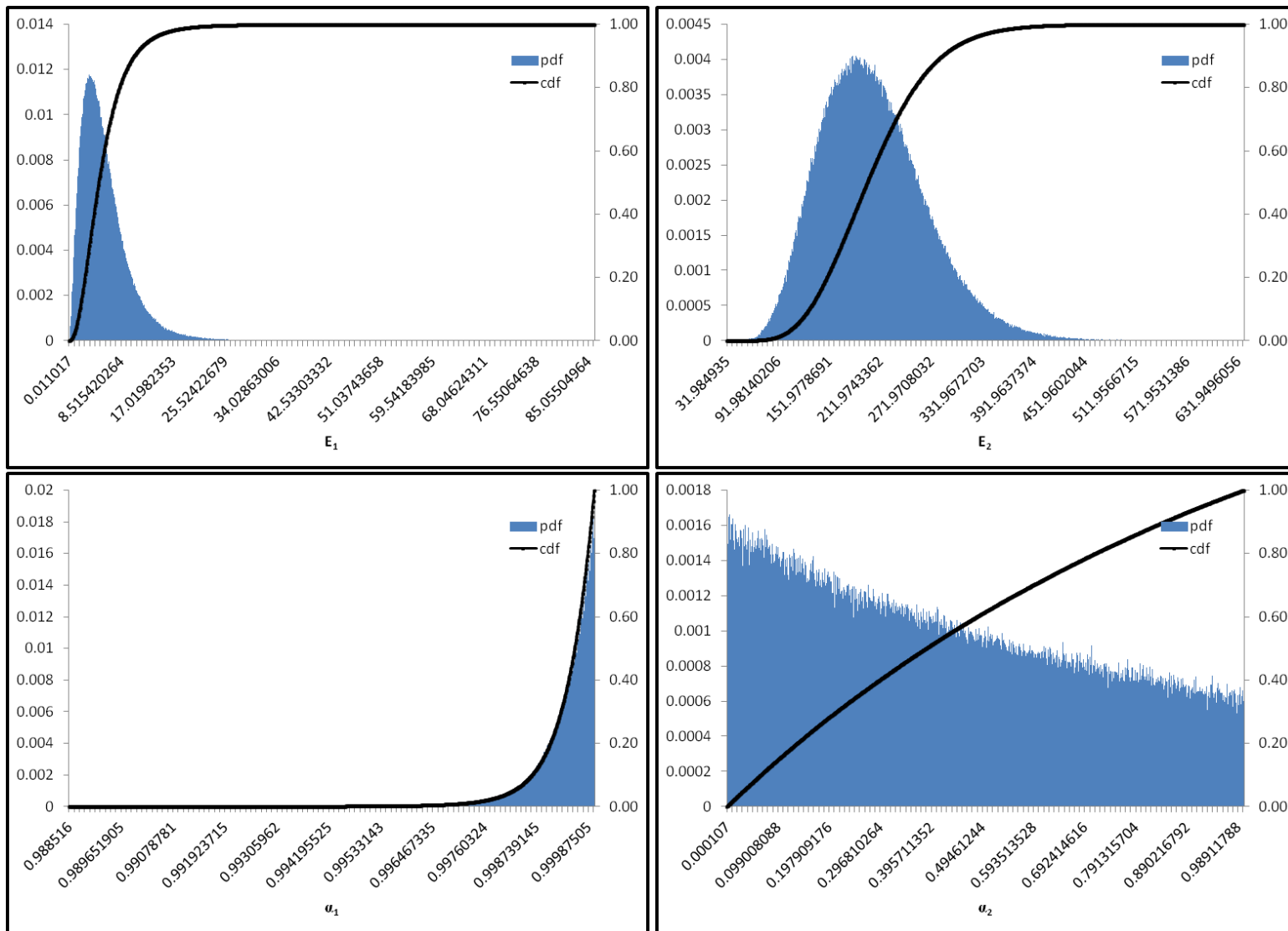
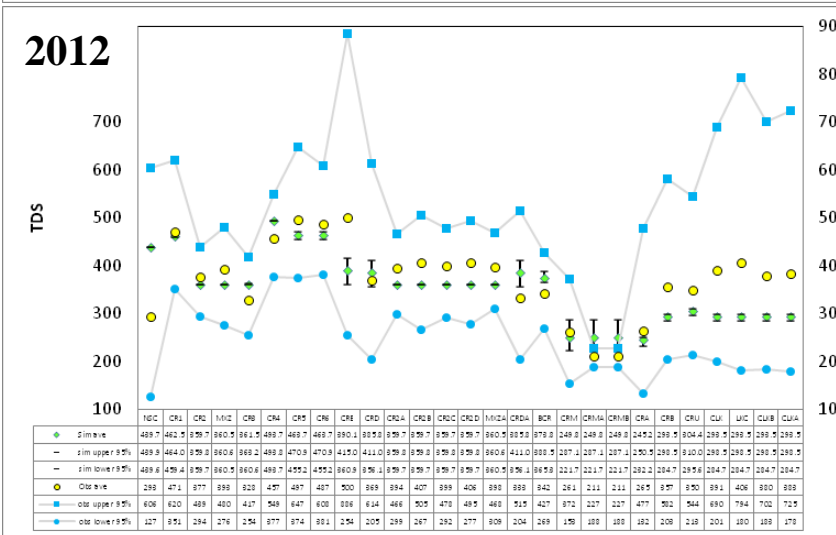
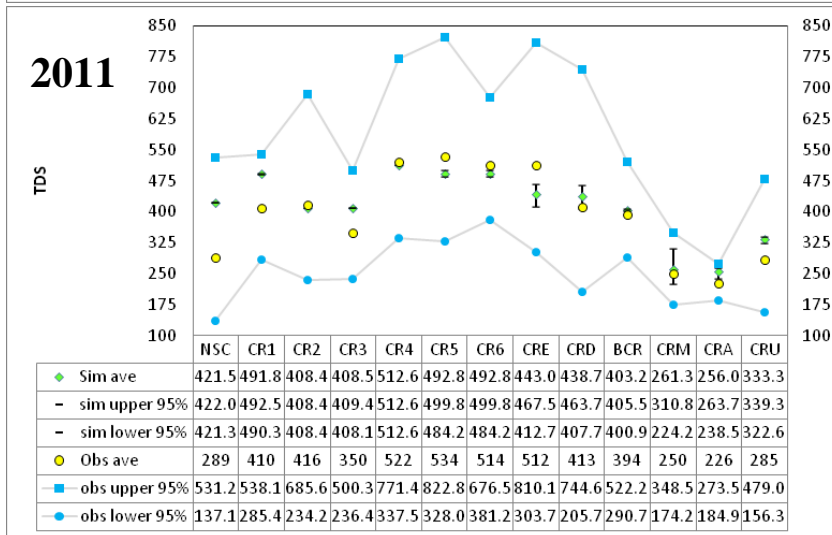
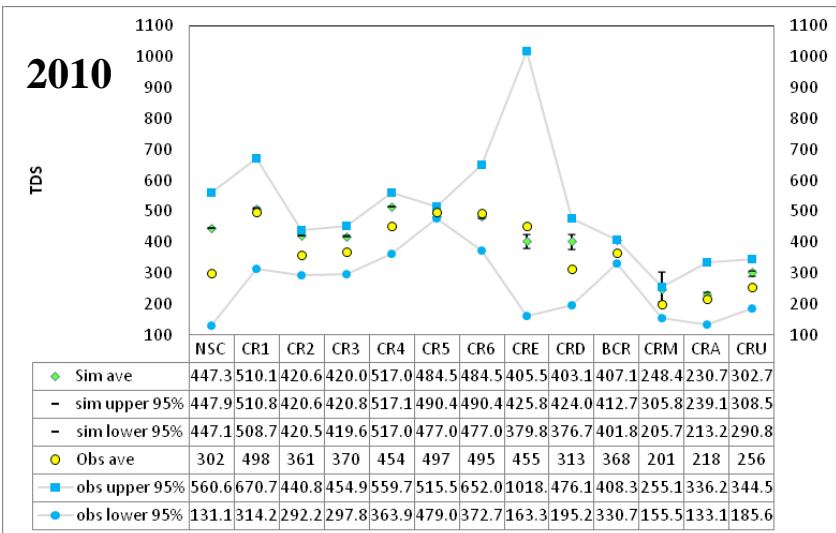
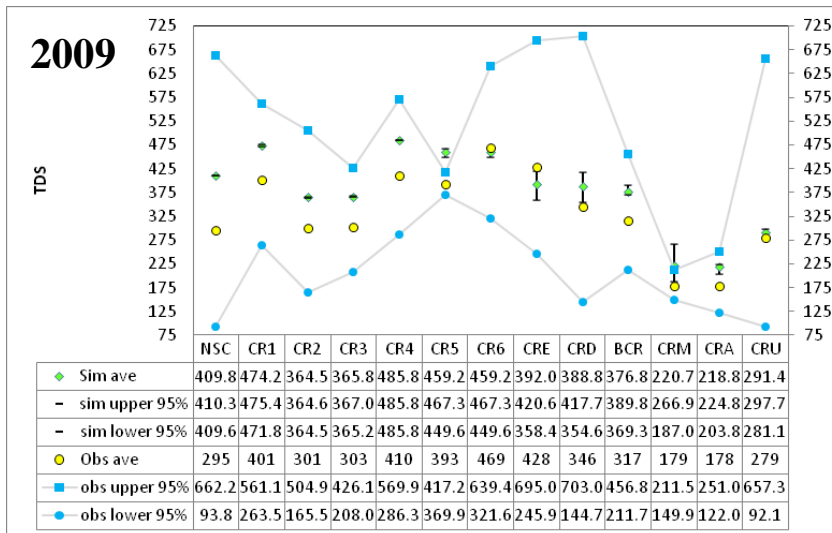
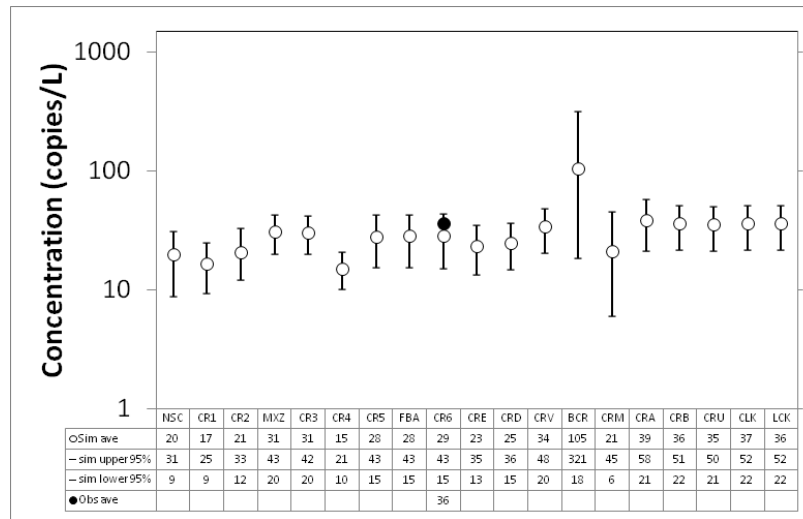
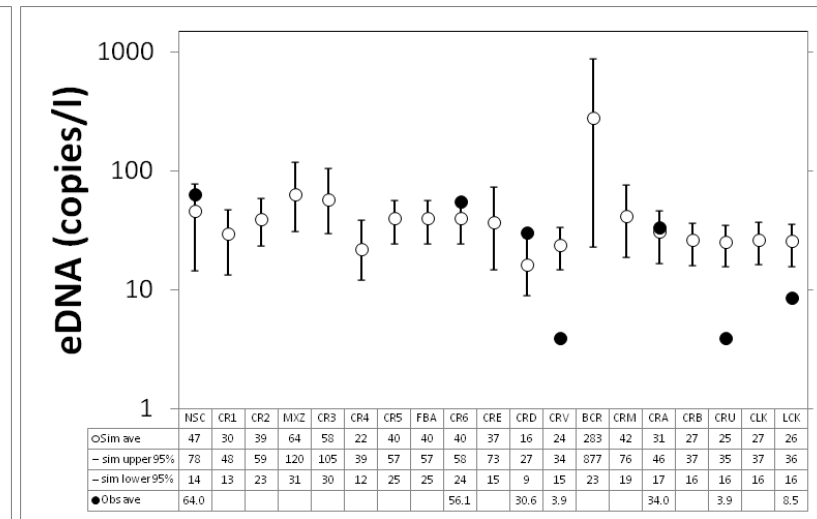


Figure 6.2: Histogram of the post burn-in monitoring period random draws for the box model parameters  $E_1$ ,  $E_2$ ,  $\alpha_1$ , and  $\alpha_2$ .

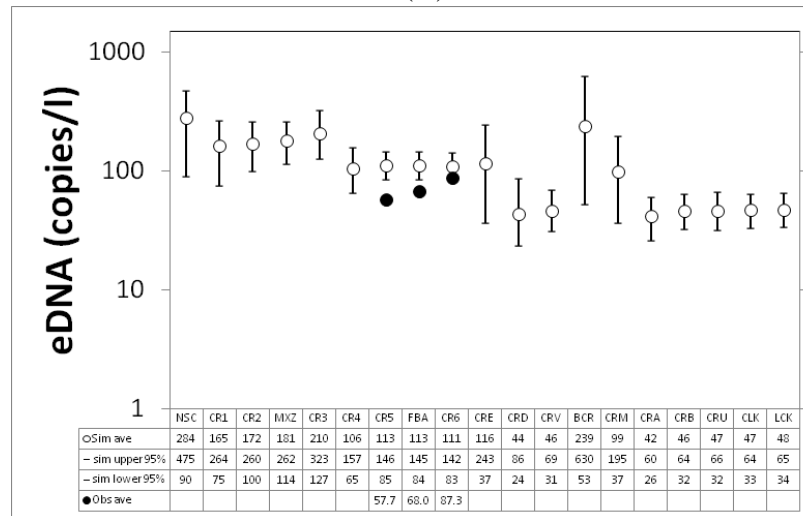




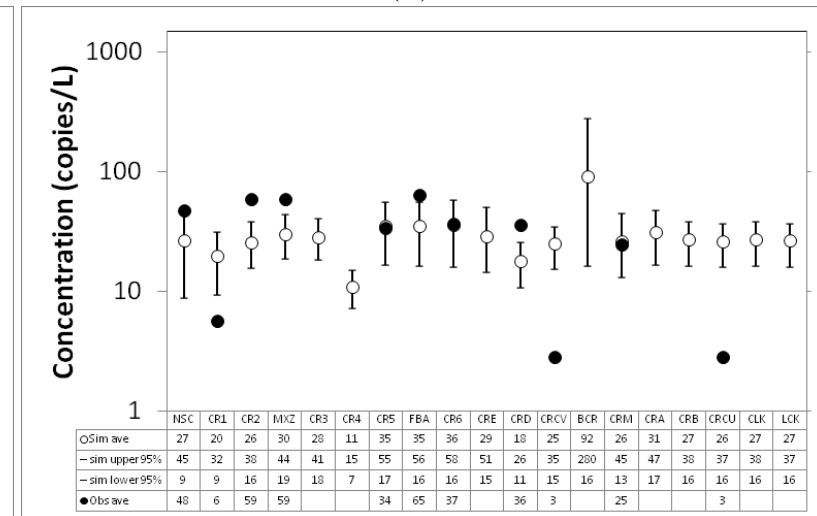
(A)



(B)

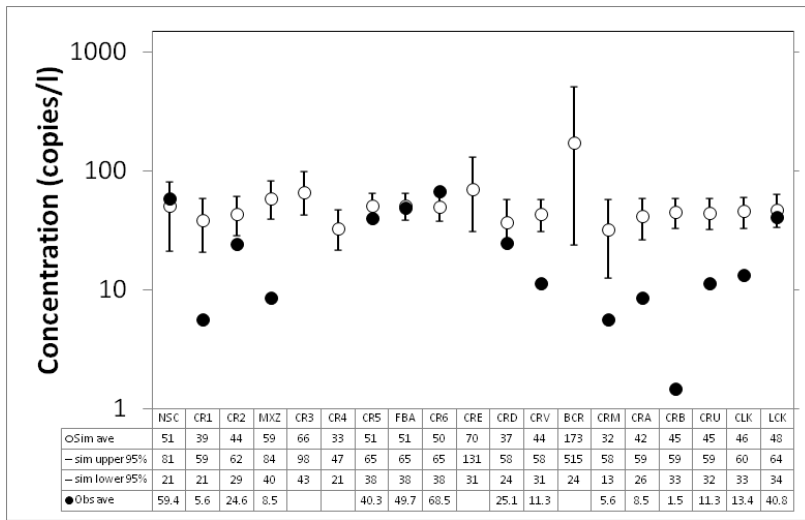


(C)

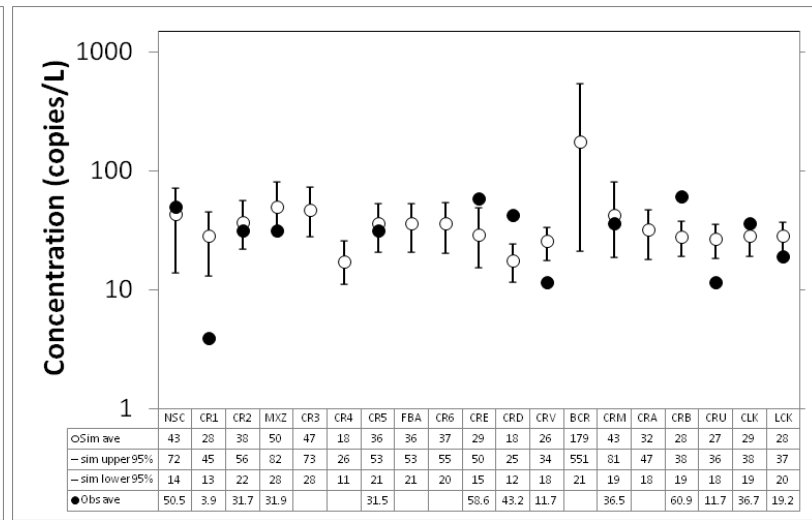


(D)

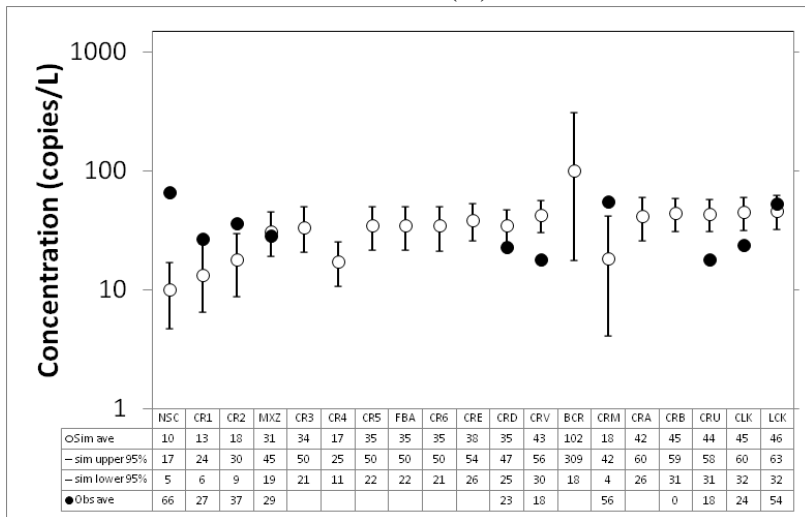
Figure 6.4: Comparison of simulated and median observed eDNA concentrations for 2009 gates open (A), 2009 gates closed (B), 2010 gates open (C), and 2010 gates closed (D).



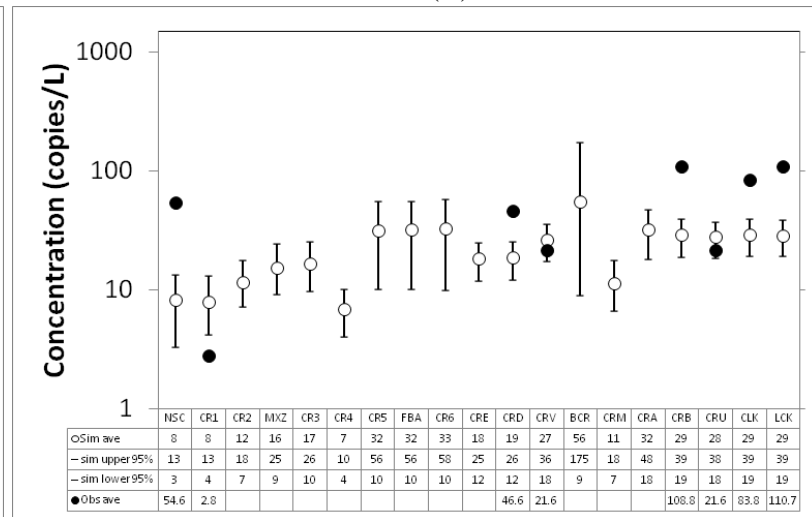
(A)



(B)



(C)



(D)

Figure 6.5: Comparison of simulated and observed eDNA concentrations for 2011 gates open (A), 2011 gates closed (B), 2012 gates open (C), and 2012 gates closed (D).

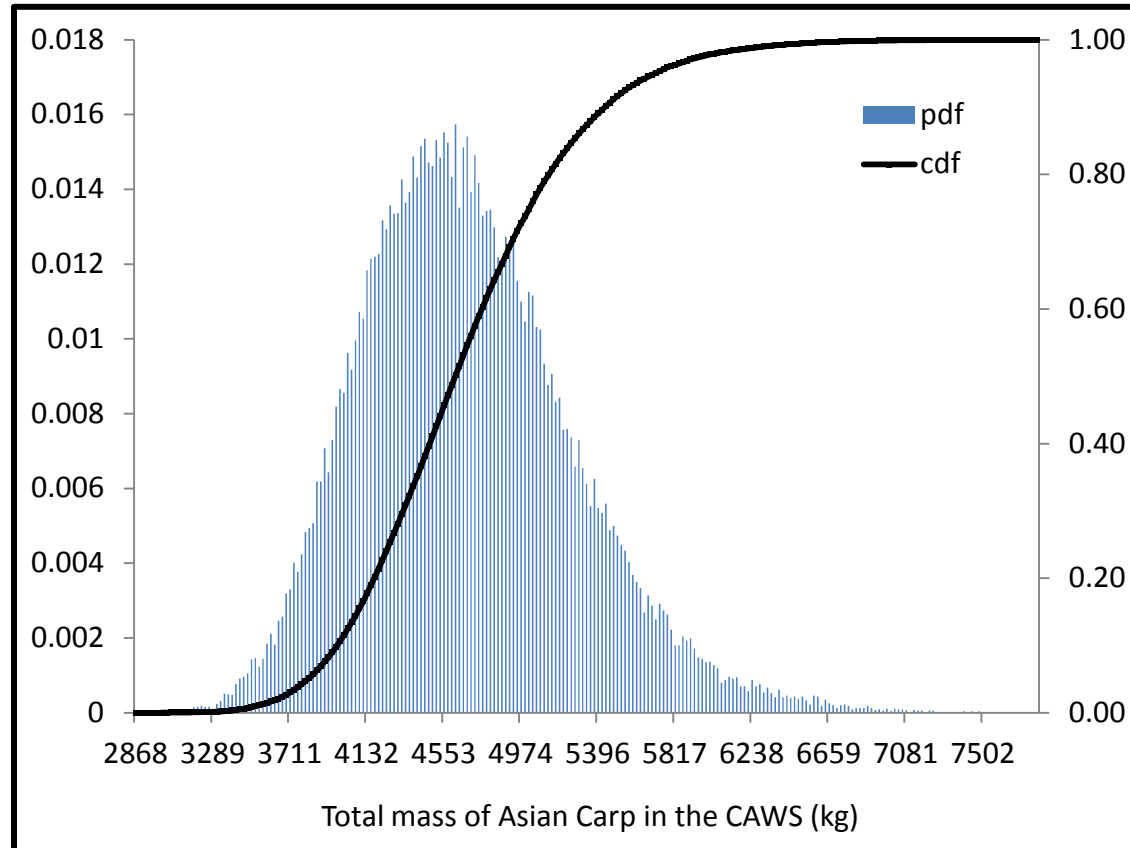


Figure 6.6: Plot of the sums of the random draws associated with the optimized model representative of the probability distribution for the total mass, in kilograms, of Asian Carp (silver) in the CAWS.

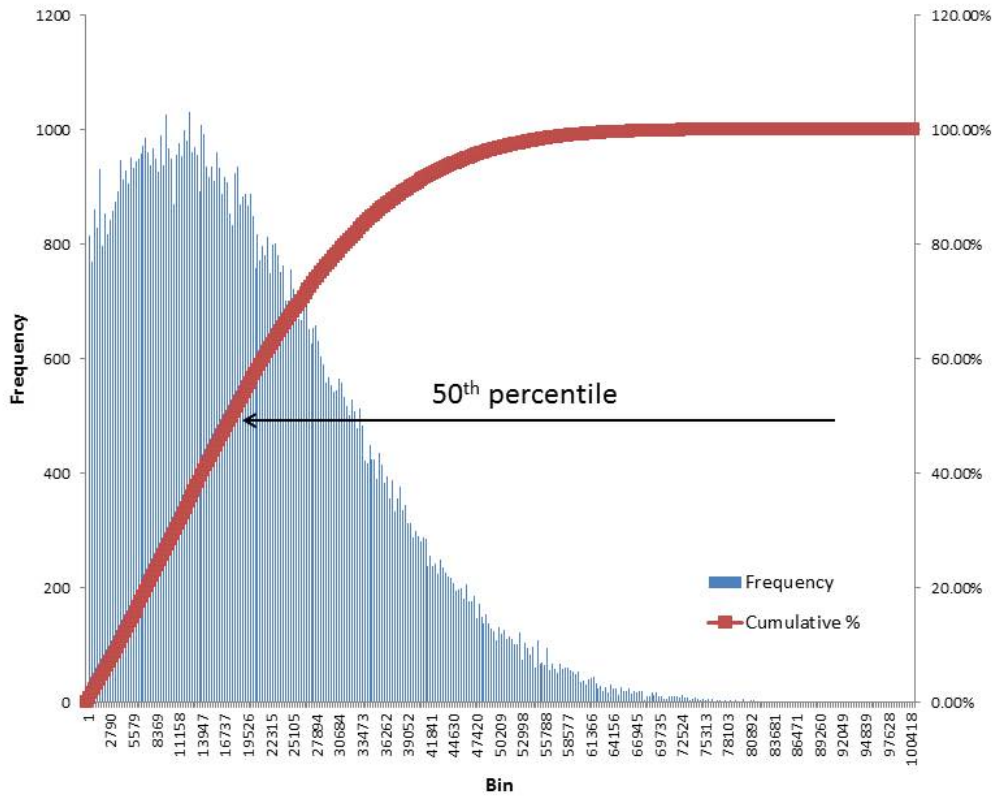


Figure 7.1. Selection of 50<sup>th</sup> percentile loading rate from MCMC results. In this figure, the eDNA concentration in Lake Michigan was derived as 17,700 copies / m<sup>3</sup>.

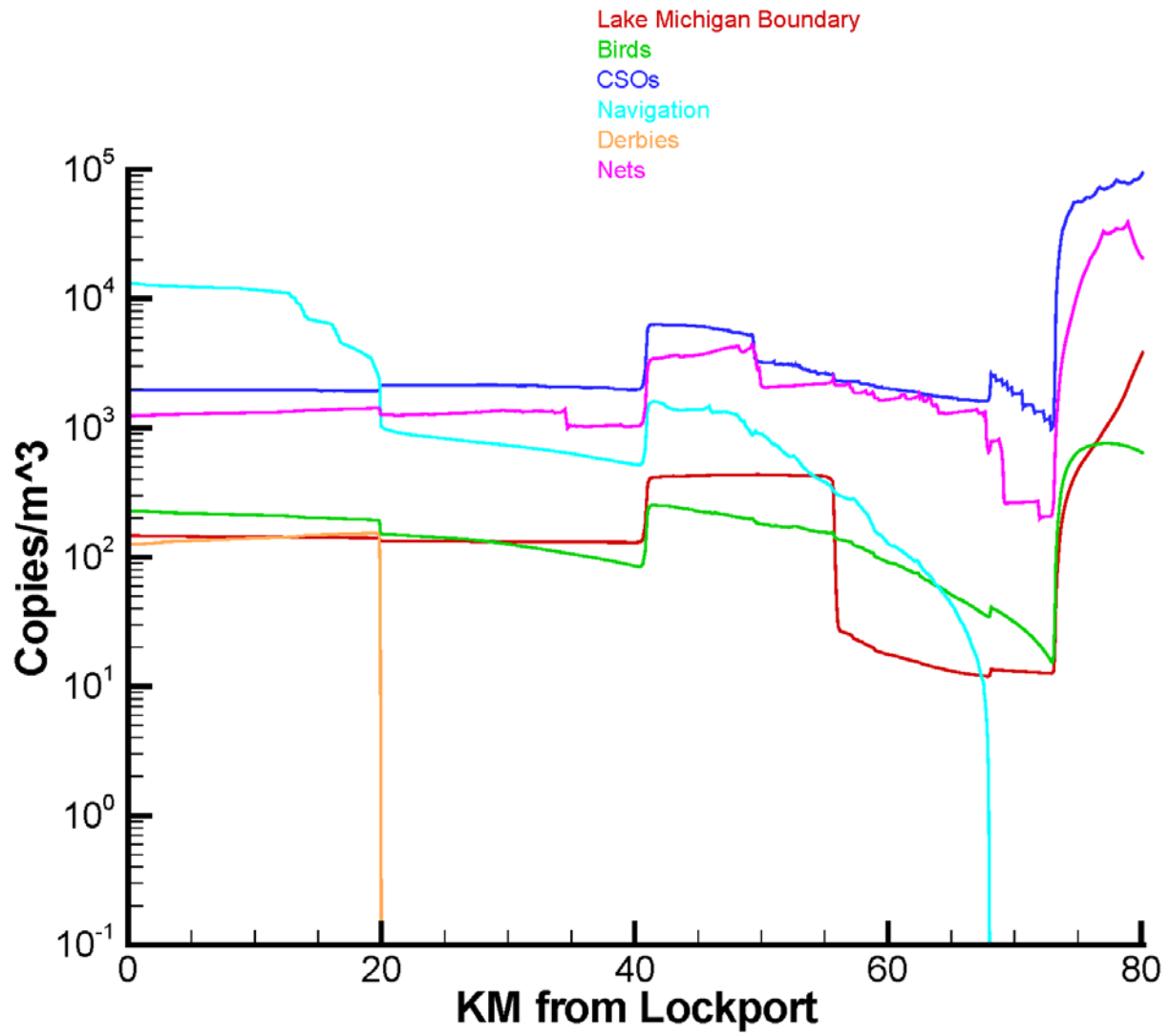


Figure 7.2. Seasonal-average computed eDNA concentration from secondary sources. Lockport to North Shore Channel during “gates closed” season.



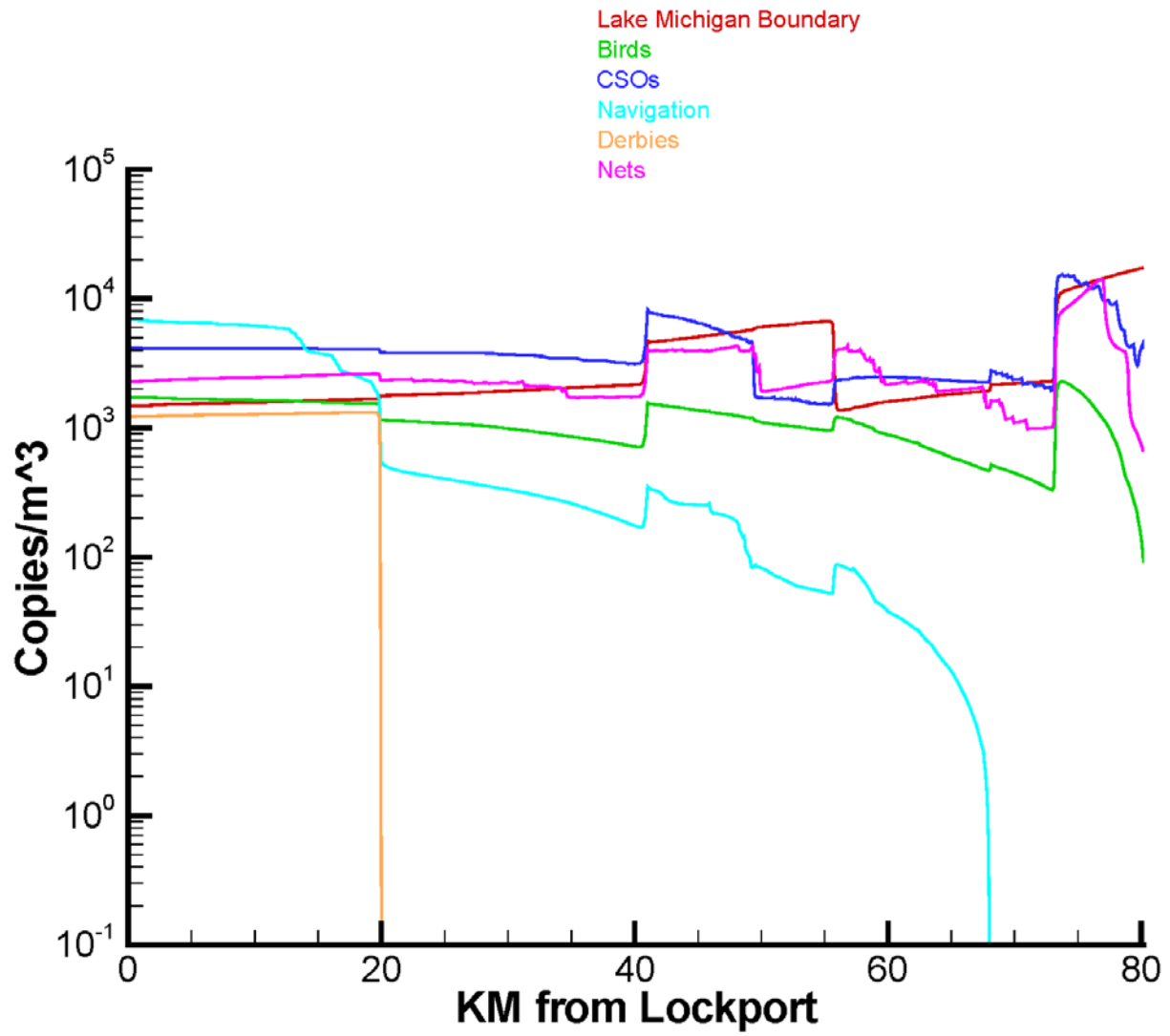


Figure 7.3. Seasonal-average computed eDNA concentration from secondary sources. Lockport to North Shore Channel during “gates open” season.

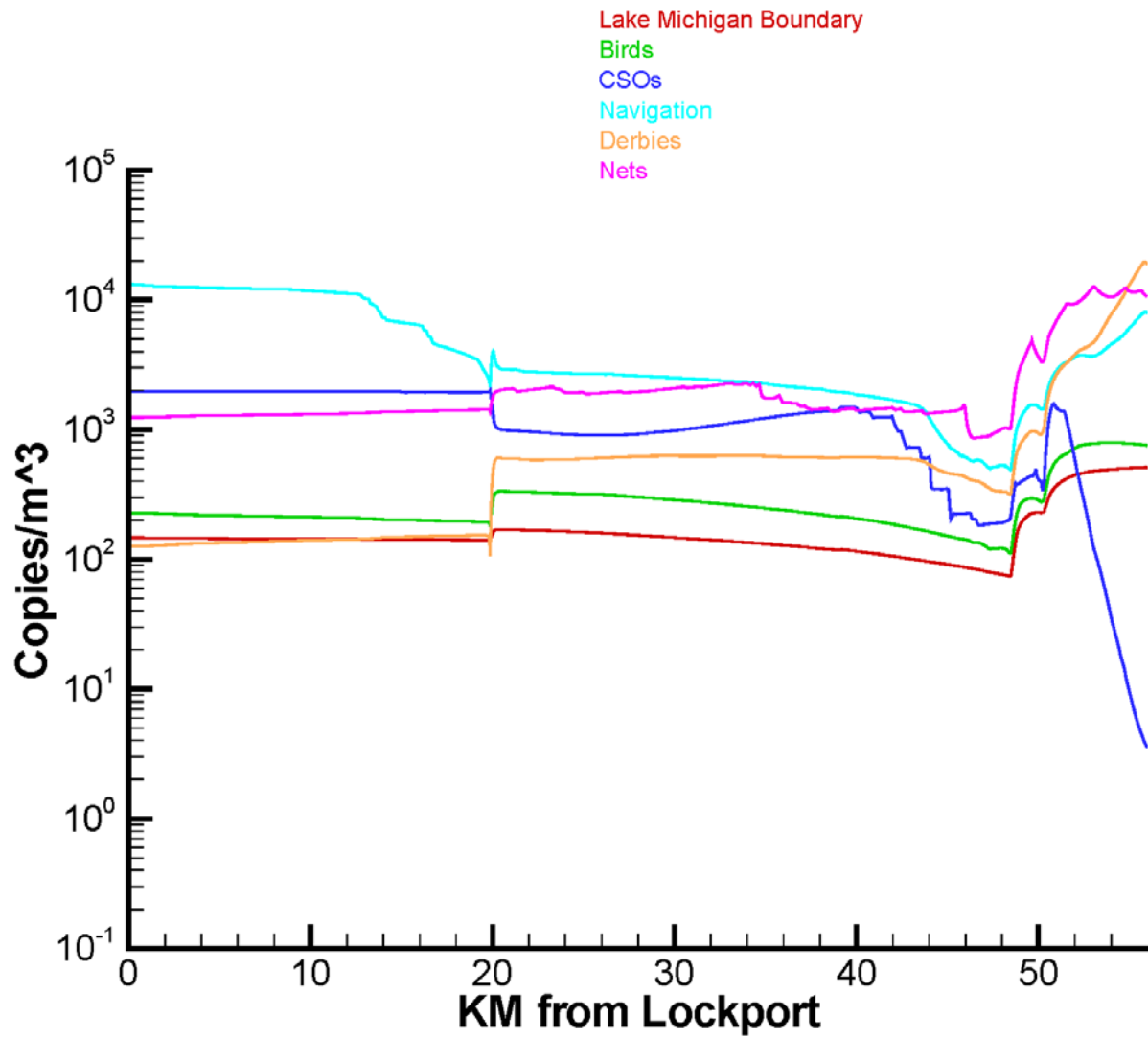


Figure 7.4. Seasonal-average computed eDNA concentration from secondary sources. Lockport to O'Brien during "gates closed" season.

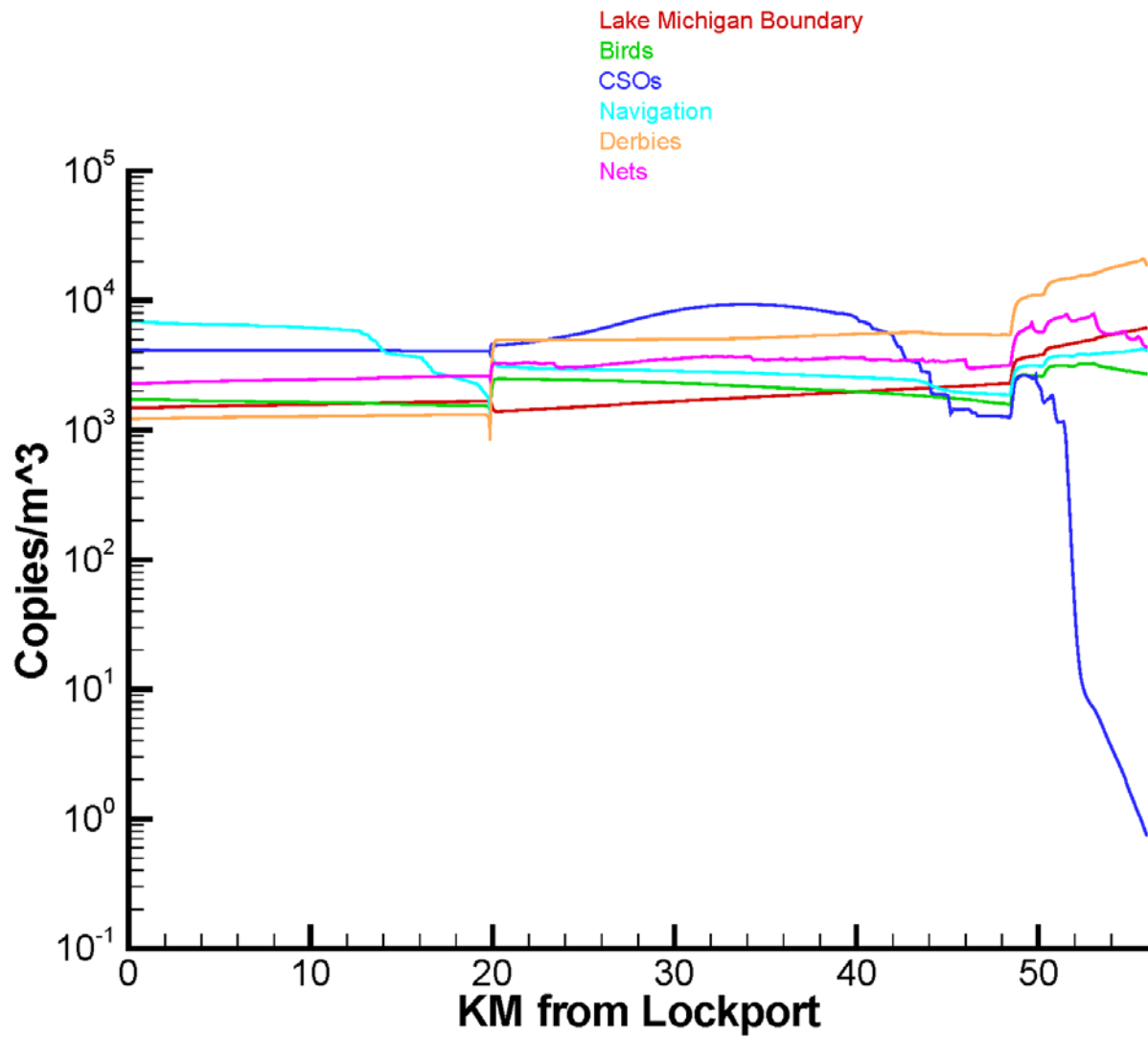


Figure 7.5. Seasonal-average computed eDNA concentration from secondary sources. Lockport to O'Brien during "gates open" season.

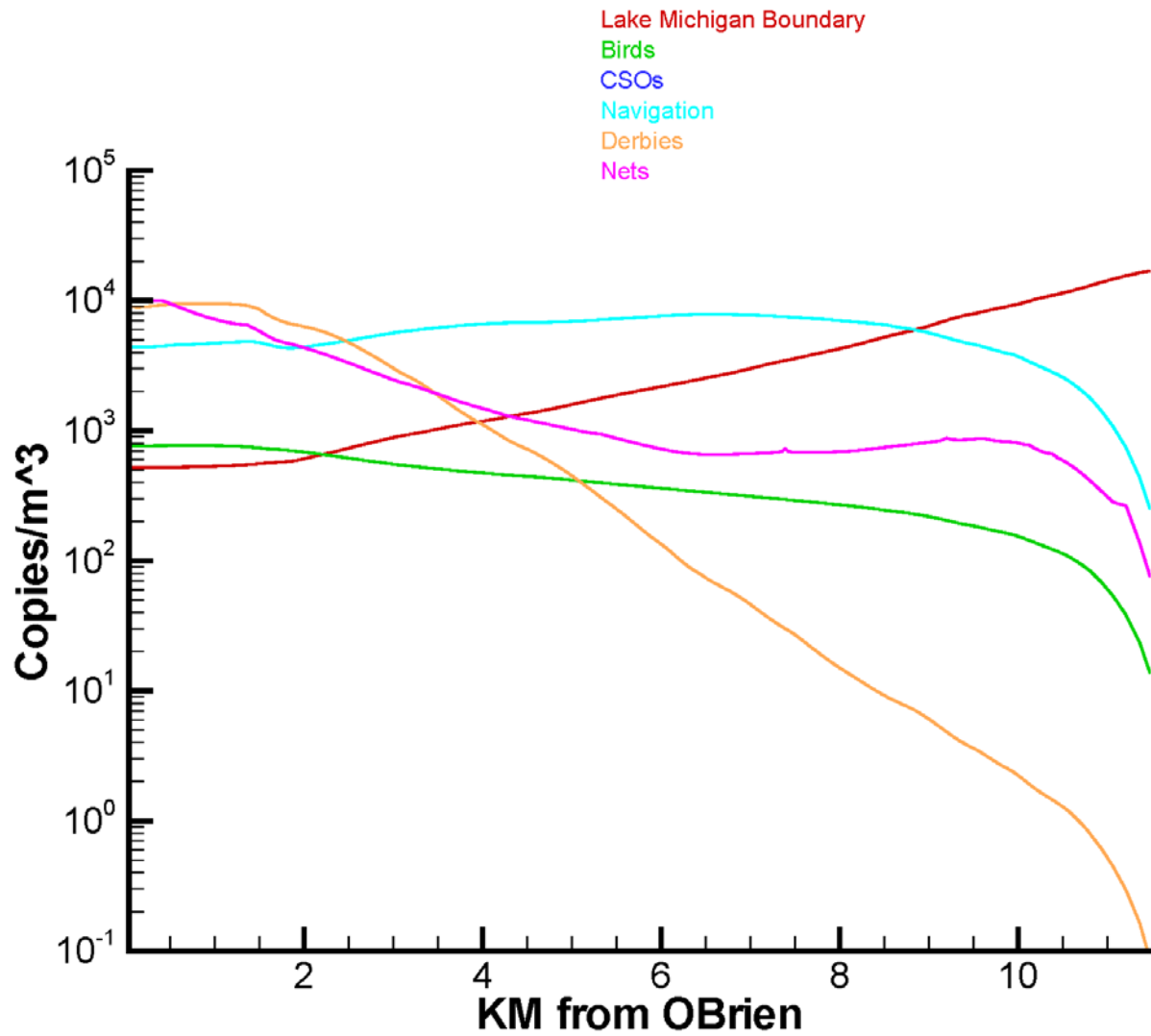


Figure 7.6. Seasonal-average computed eDNA concentration from secondary sources. O'Brien to Lake Michigan during "gates closed" season.

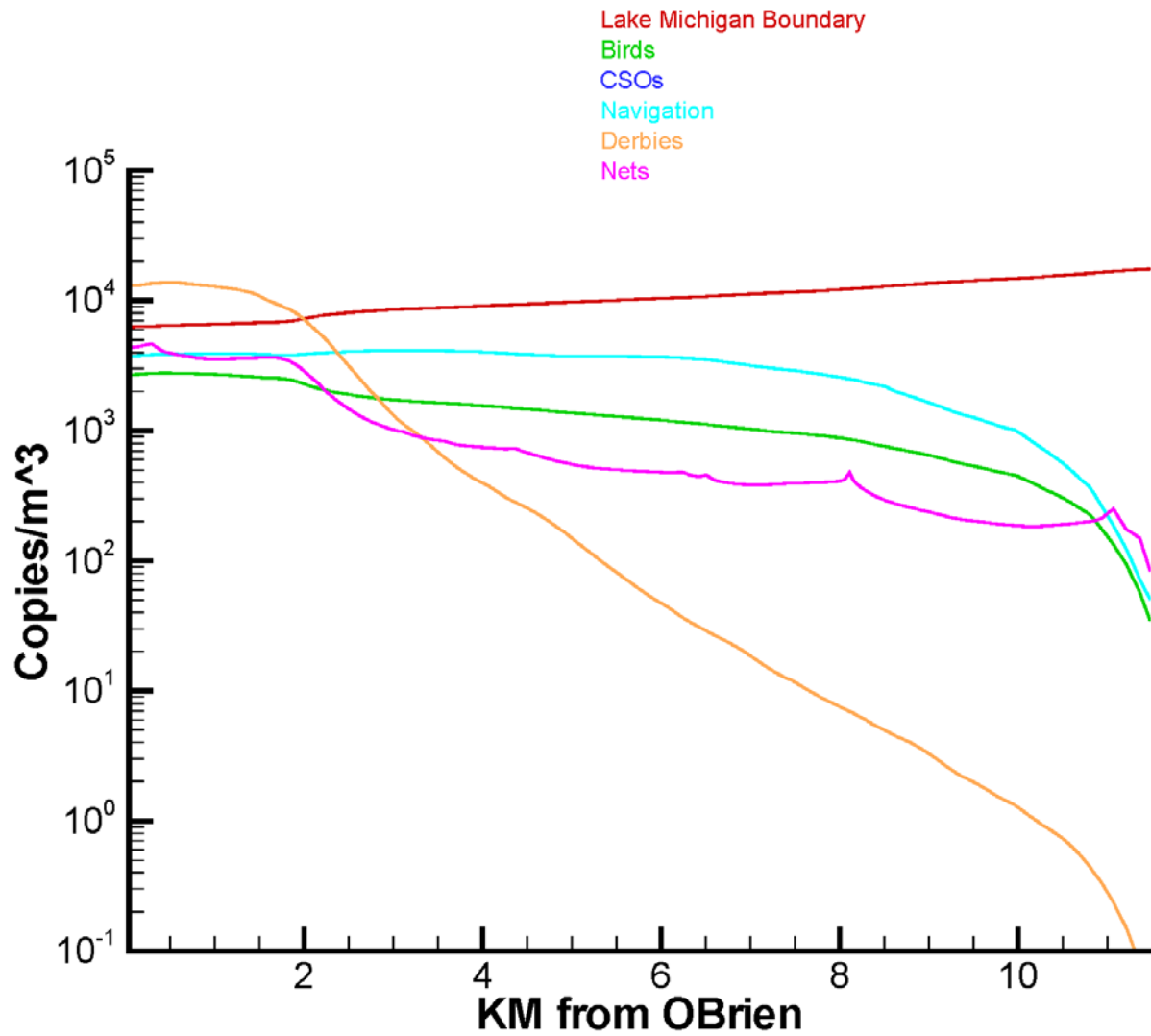


Figure 7.7. Seasonal-average computed eDNA concentration from secondary sources. O'Brien to Lake Michigan during "gates open" season.

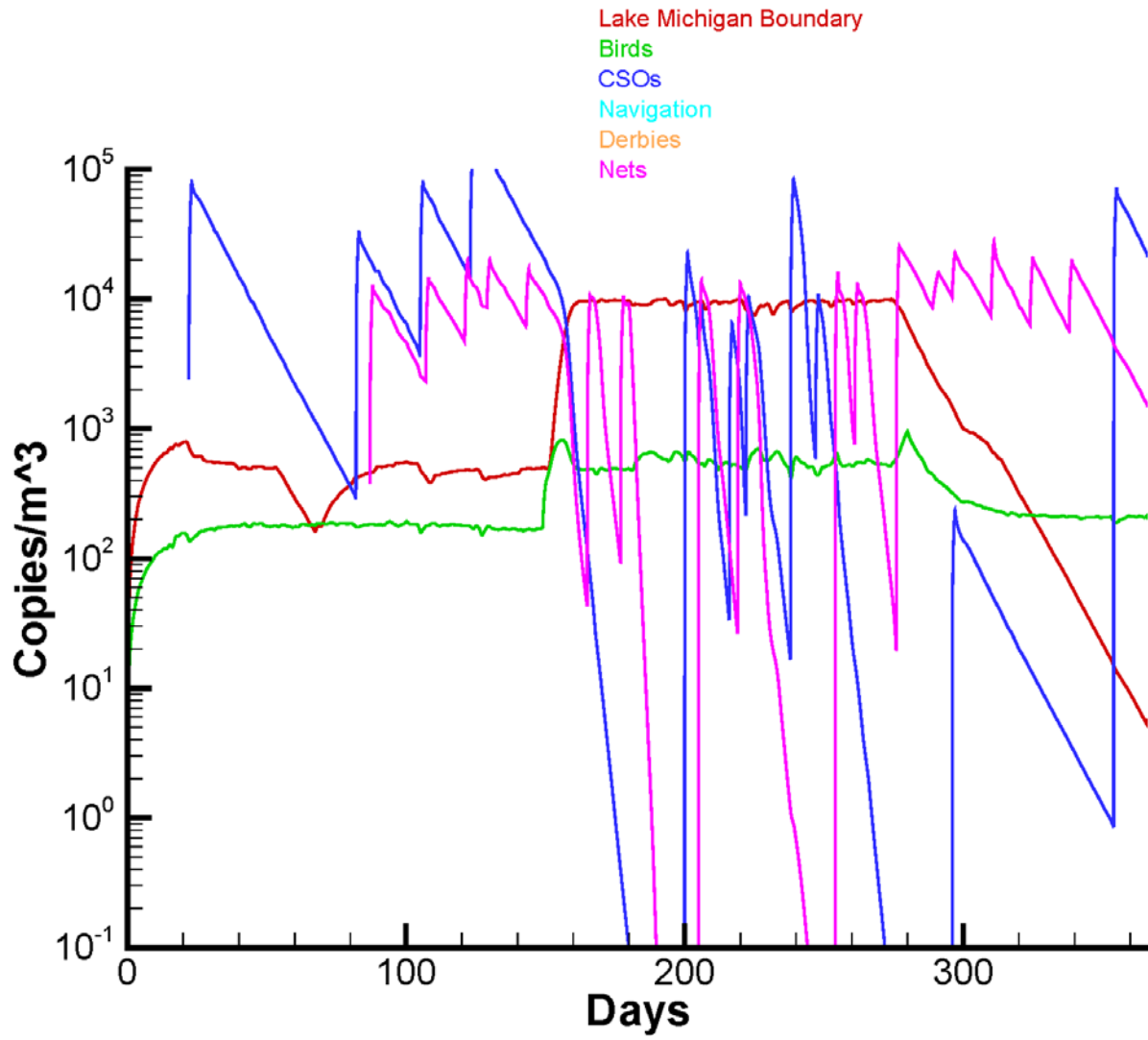


Figure 7.8. Time series of computed eDNA concentration resulting from secondary sources. Reach NSC (North Shore Channel).

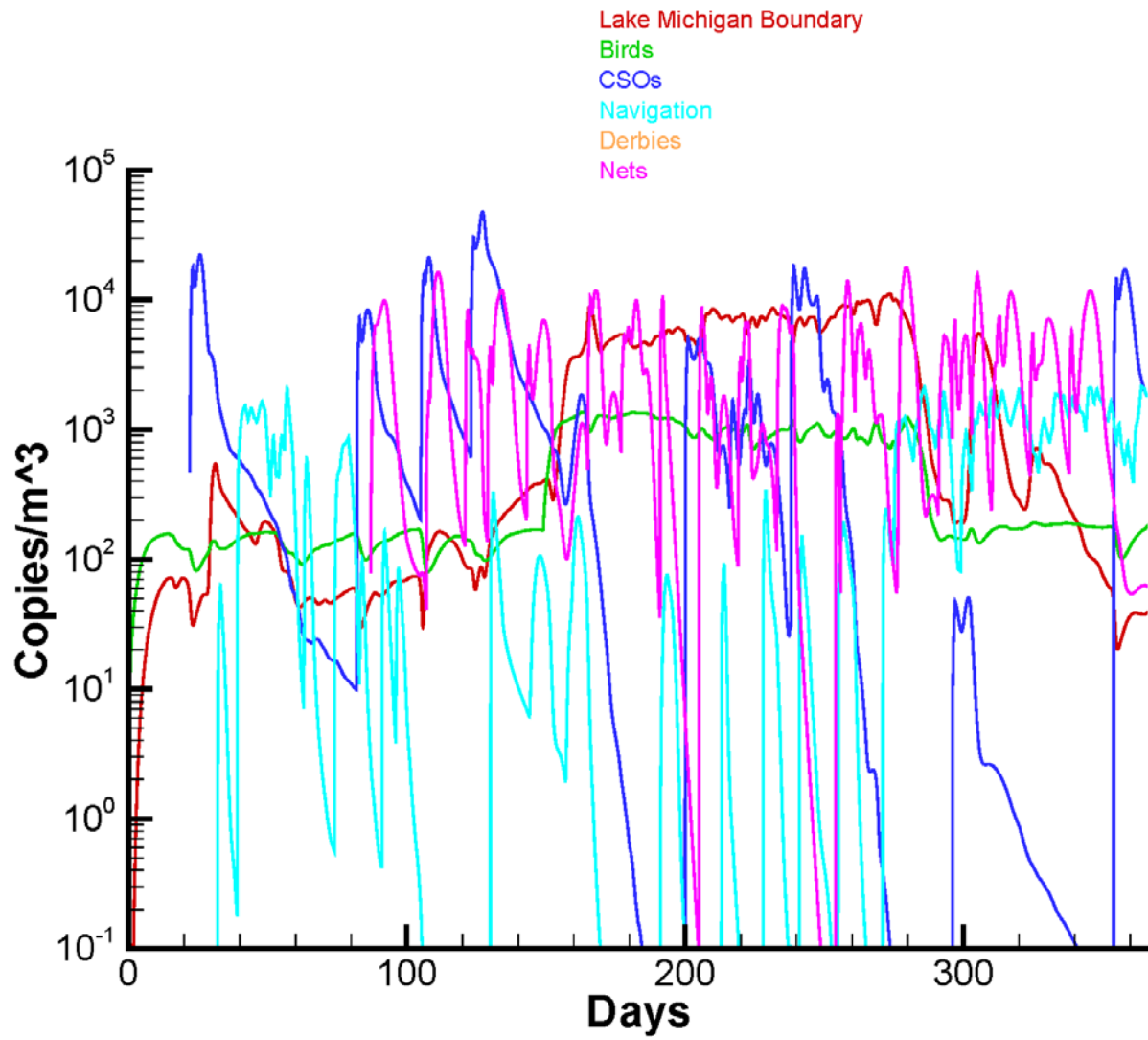


Figure 7.9. Time series of computed eDNA concentration resulting from secondary sources. Reach CR2 (near the eastern end of the Chicago Sanitary and Ship Canal).

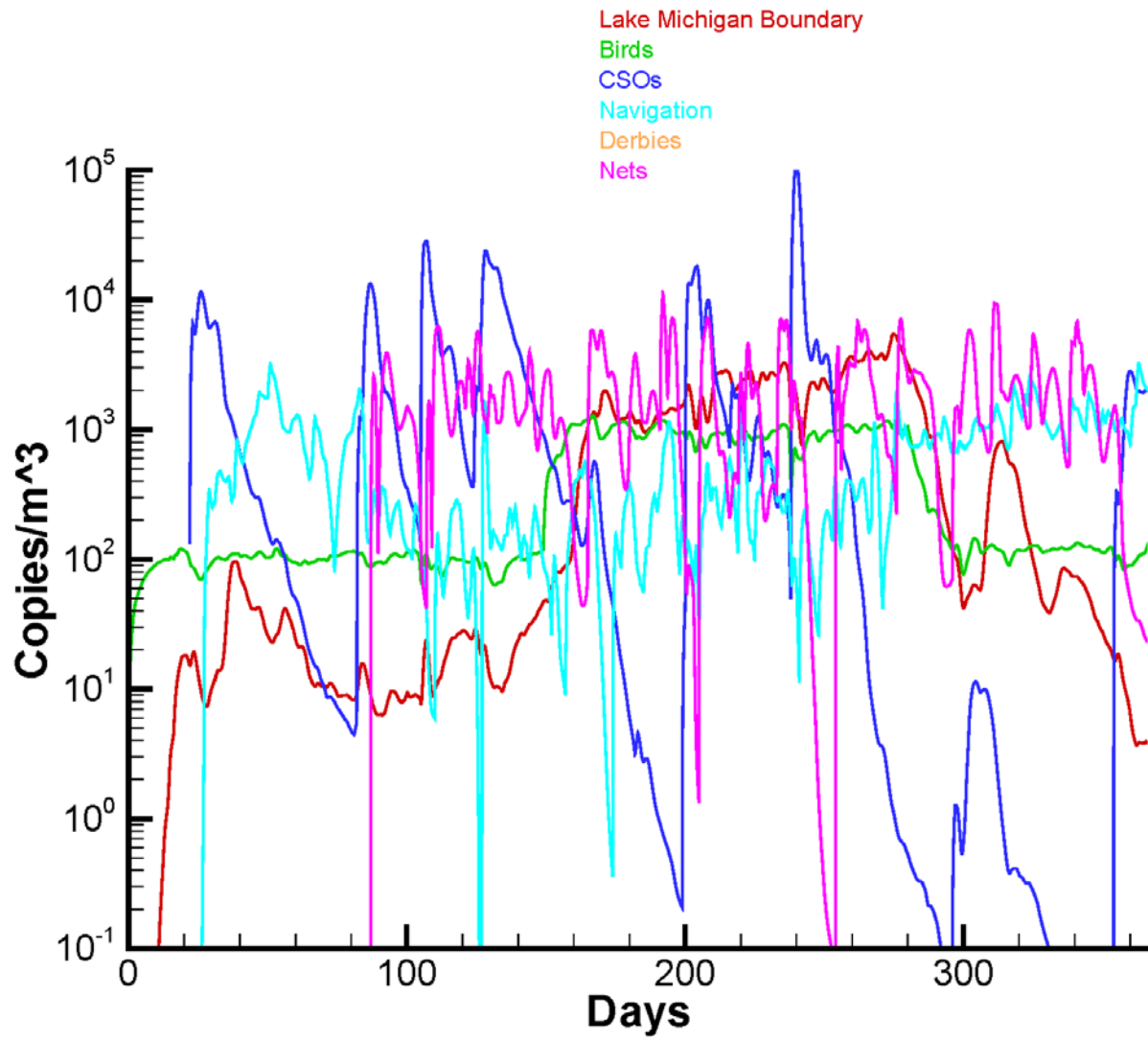


Figure 7.10. Time series of computed eDNA concentration resulting from secondary sources. Reach CR4 (mid-section of Chicago Sanitary and Ship Canal).



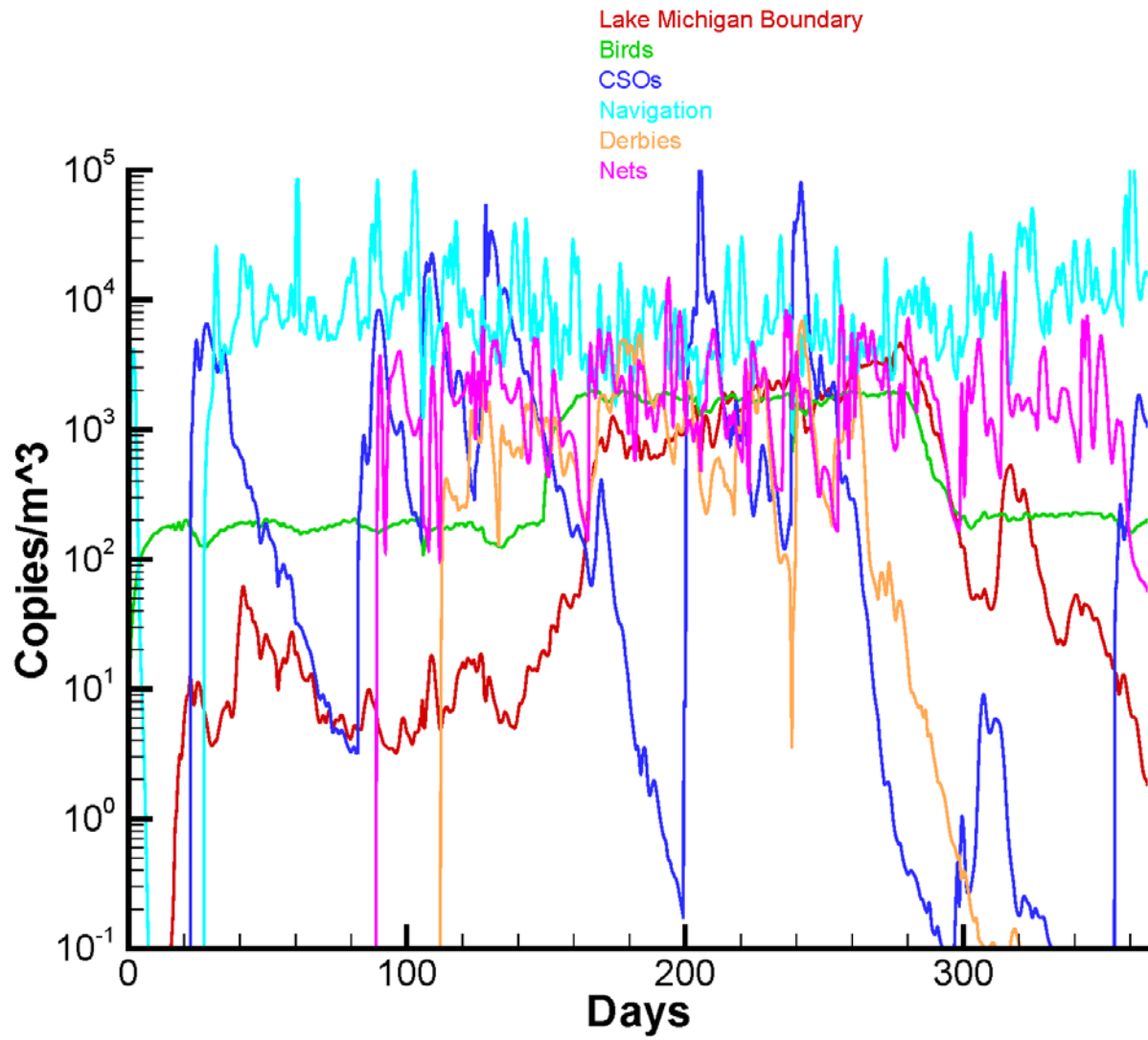


Figure 7.11. Time series of computed eDNA concentration resulting from secondary sources. Reach CR6 (adjacent to Lockport).

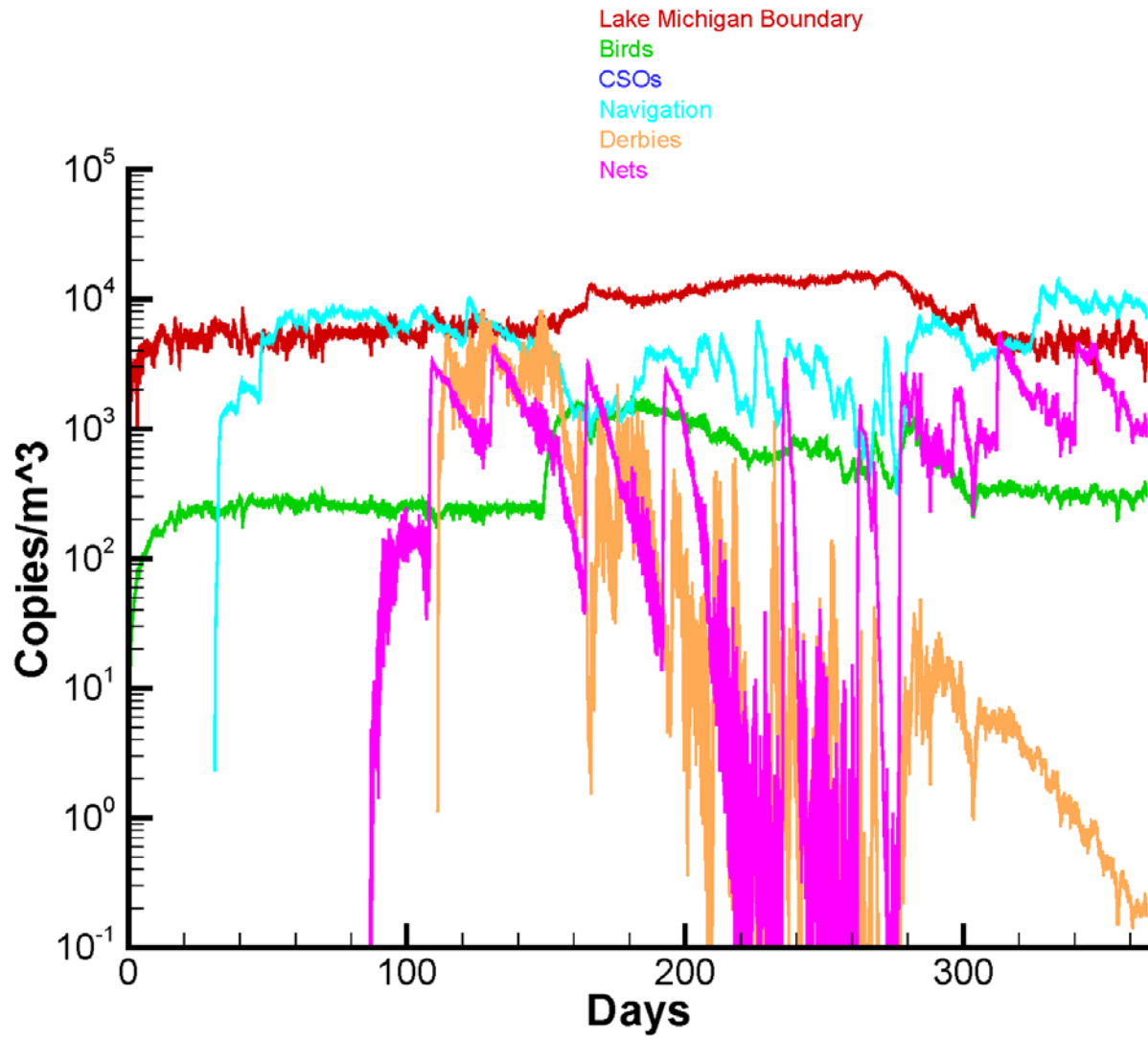


Figure 7.12. Time series of computed eDNA concentration resulting from secondary sources. Reach CRA (adjacent to Lake Michigan).

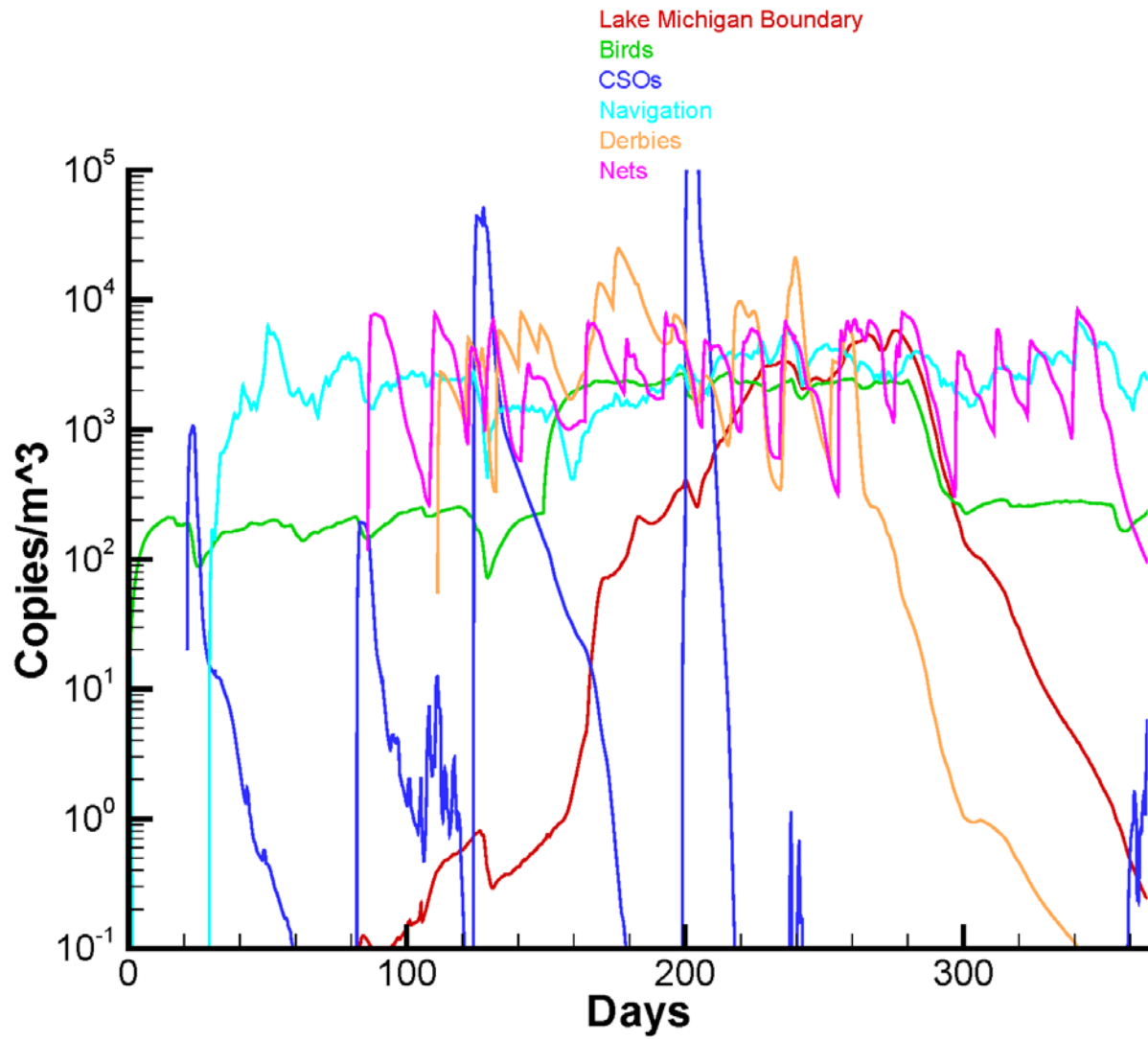


Figure 7.13. Time series of computed eDNA concentration resulting from secondary sources. Reach CRE (main section of the Cal-Sag).

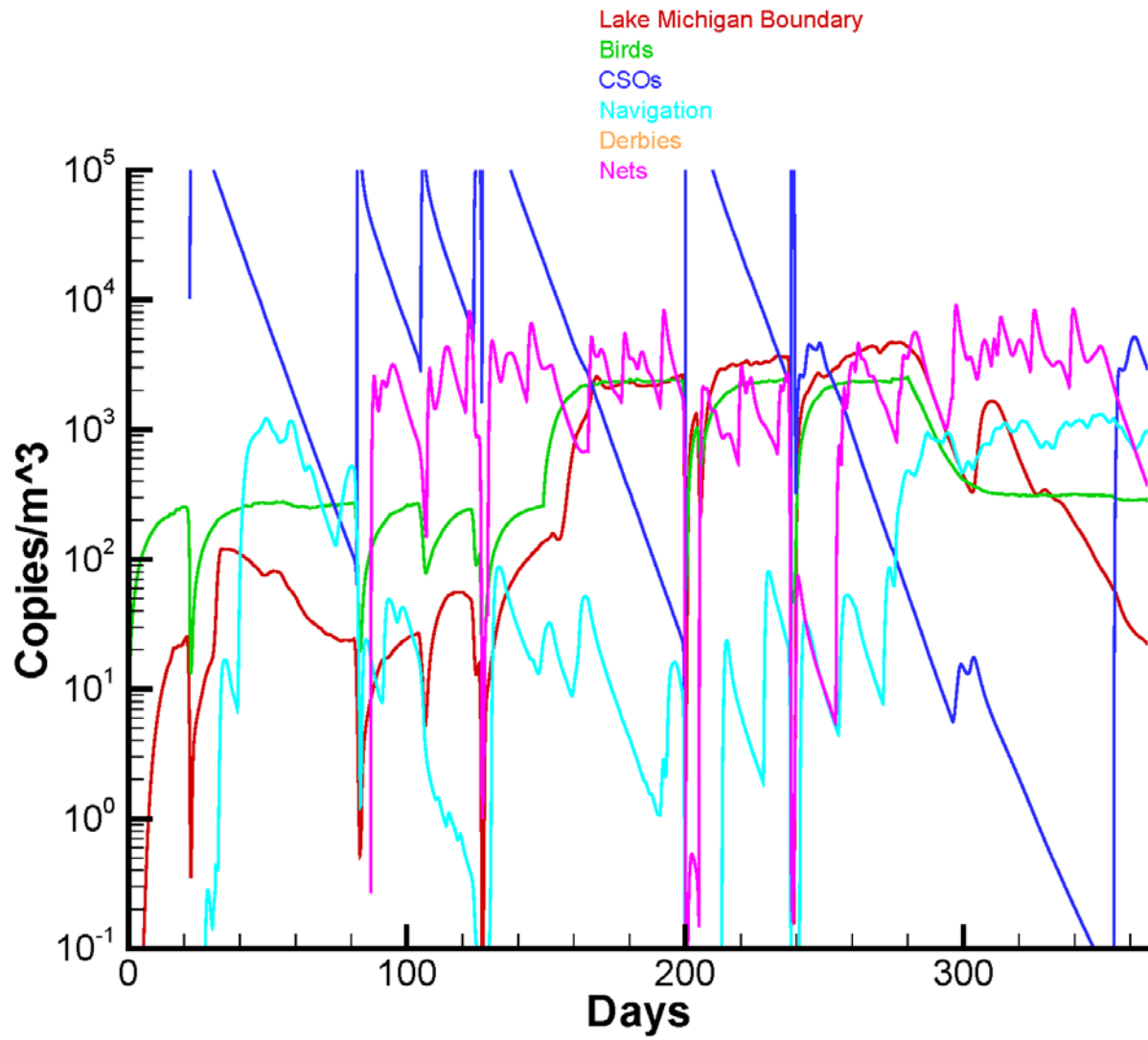


Figure 7.14. Time series of computed eDNA concentration resulting from secondary sources. Reach BCR (Bubbly Creek).

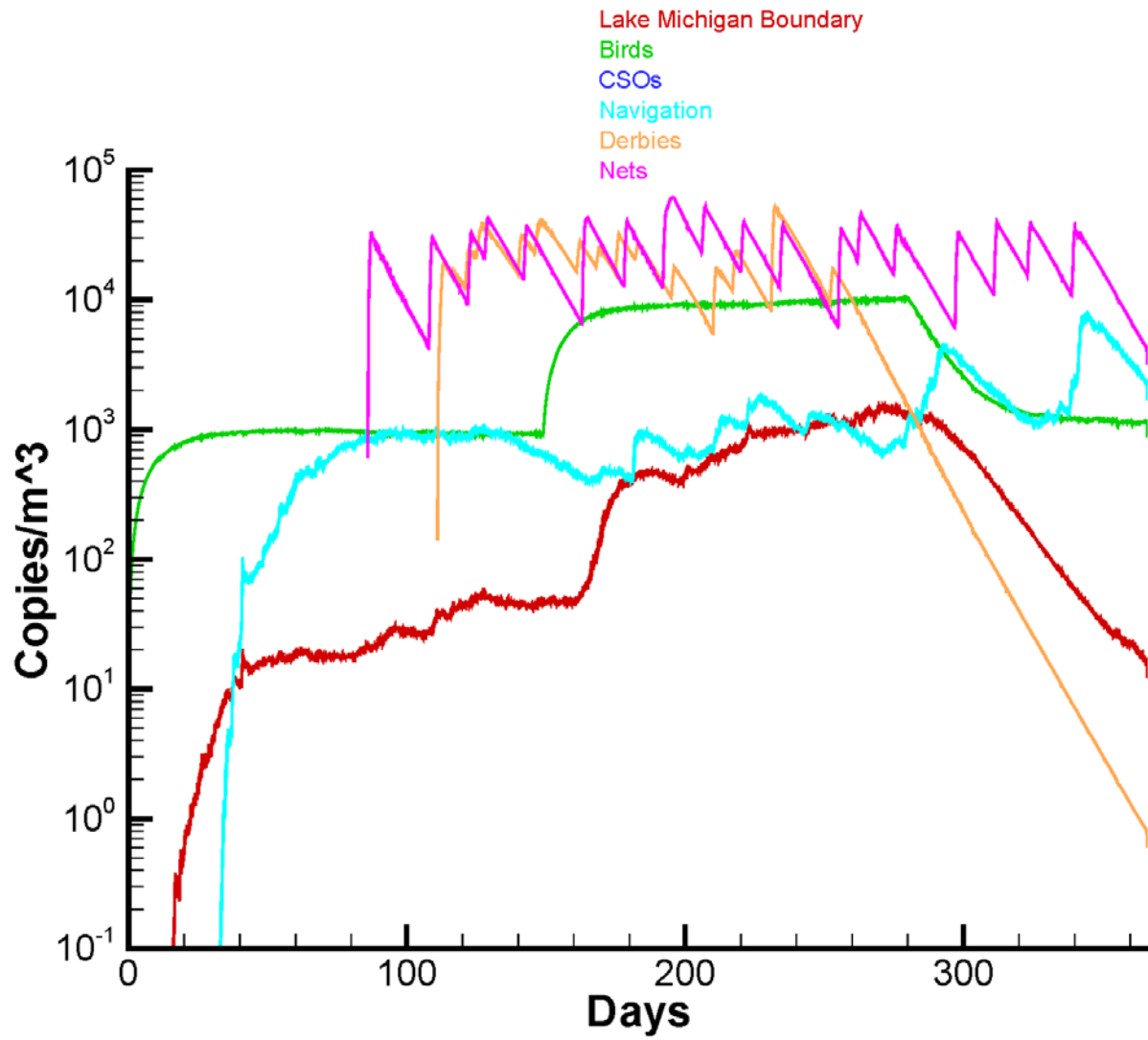


Figure 7.15. Time series of computed eDNA concentration resulting from secondary sources. Reach LKC (Lake Calumet).

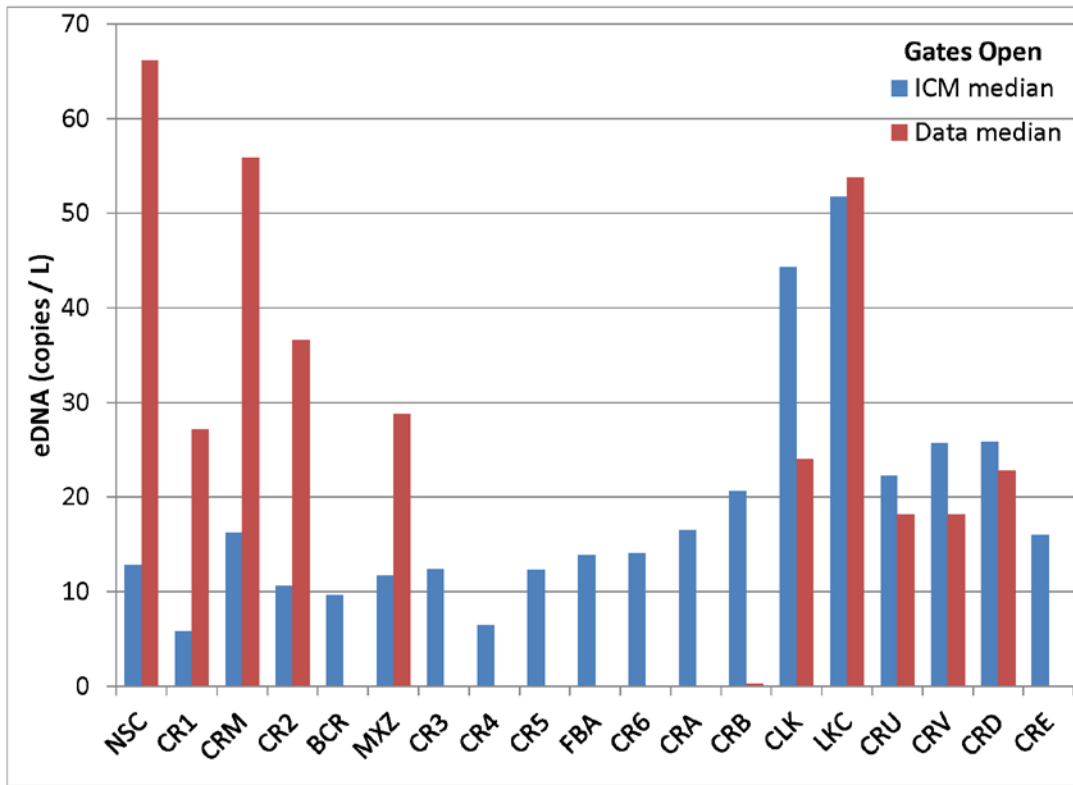


Figure 7.16. Median computed eDNA from secondary sources in all reaches compared to the median of observations in reaches for which data is available. “Gates open” season.

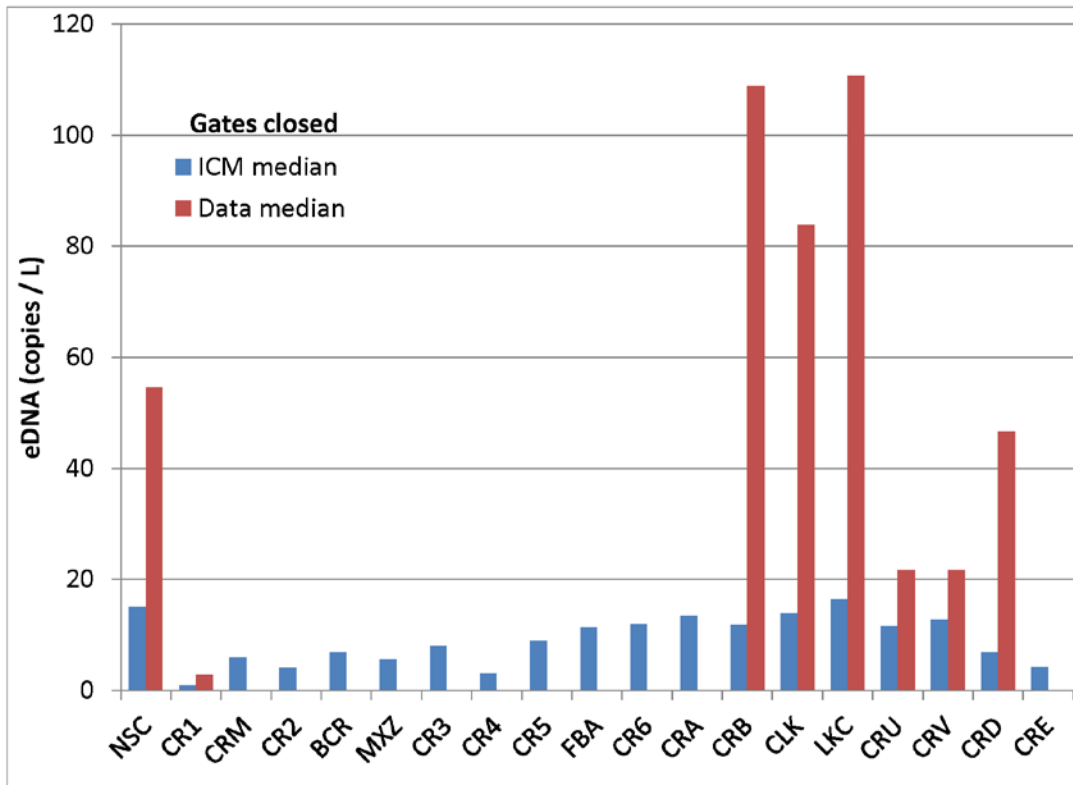


Figure 7.17. Median computed eDNA from secondary sources in all reaches compared to the median of observations in reaches for which data is available. “Gates closed” season.

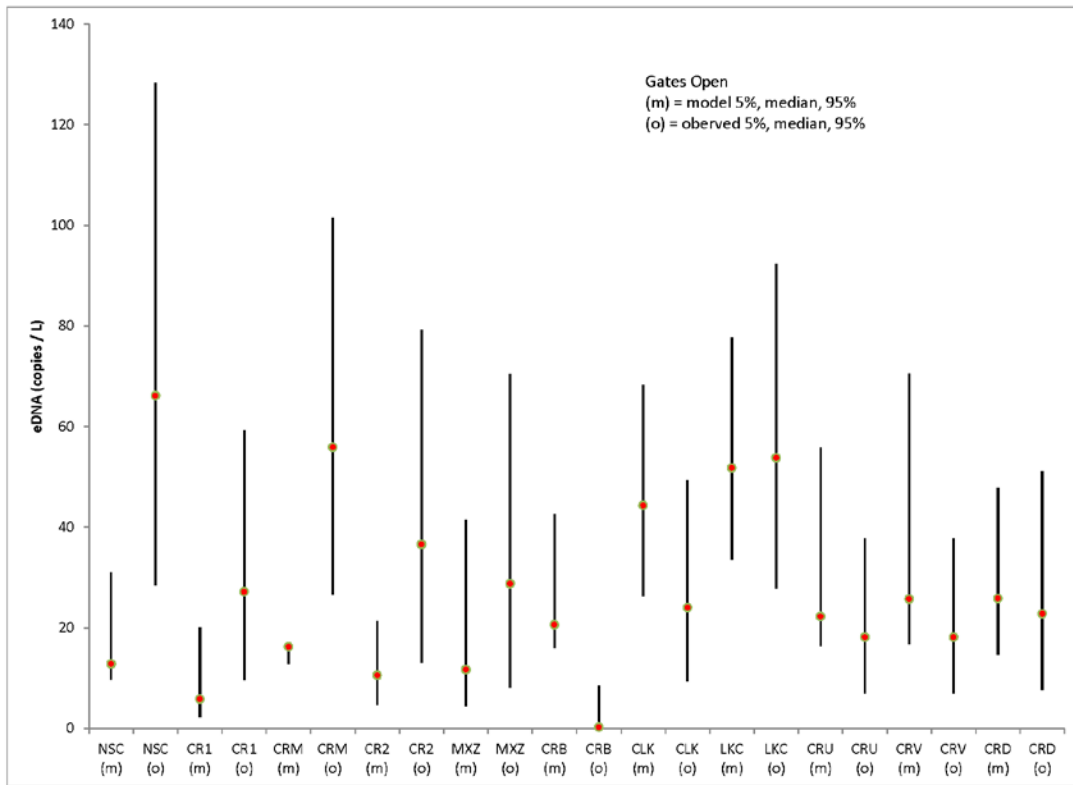


Figure 7.18. Median and 90% range for computed eDNA from secondary sources and for observations. Comparison is restricted to reaches with observations. “Gates open” season.



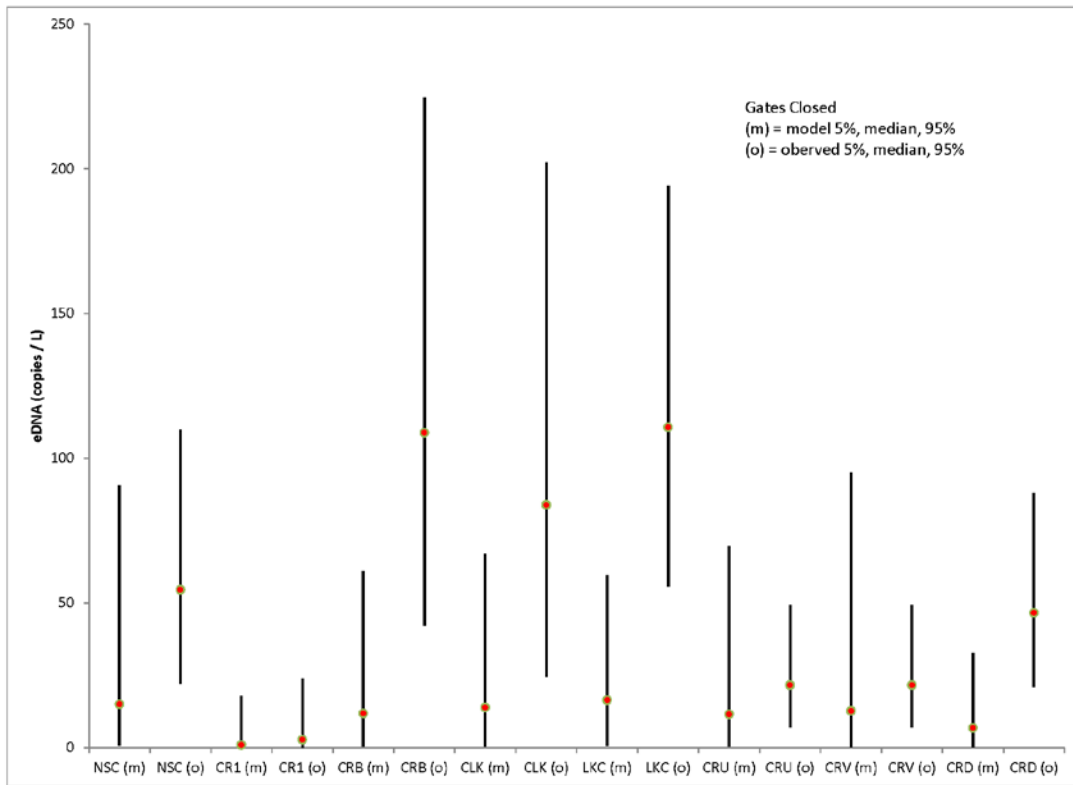


Figure 7.19. Median and 90% range for computed eDNA from secondary sources and for observations. Comparison is restricted to reaches with observations. “Gates closed” season.

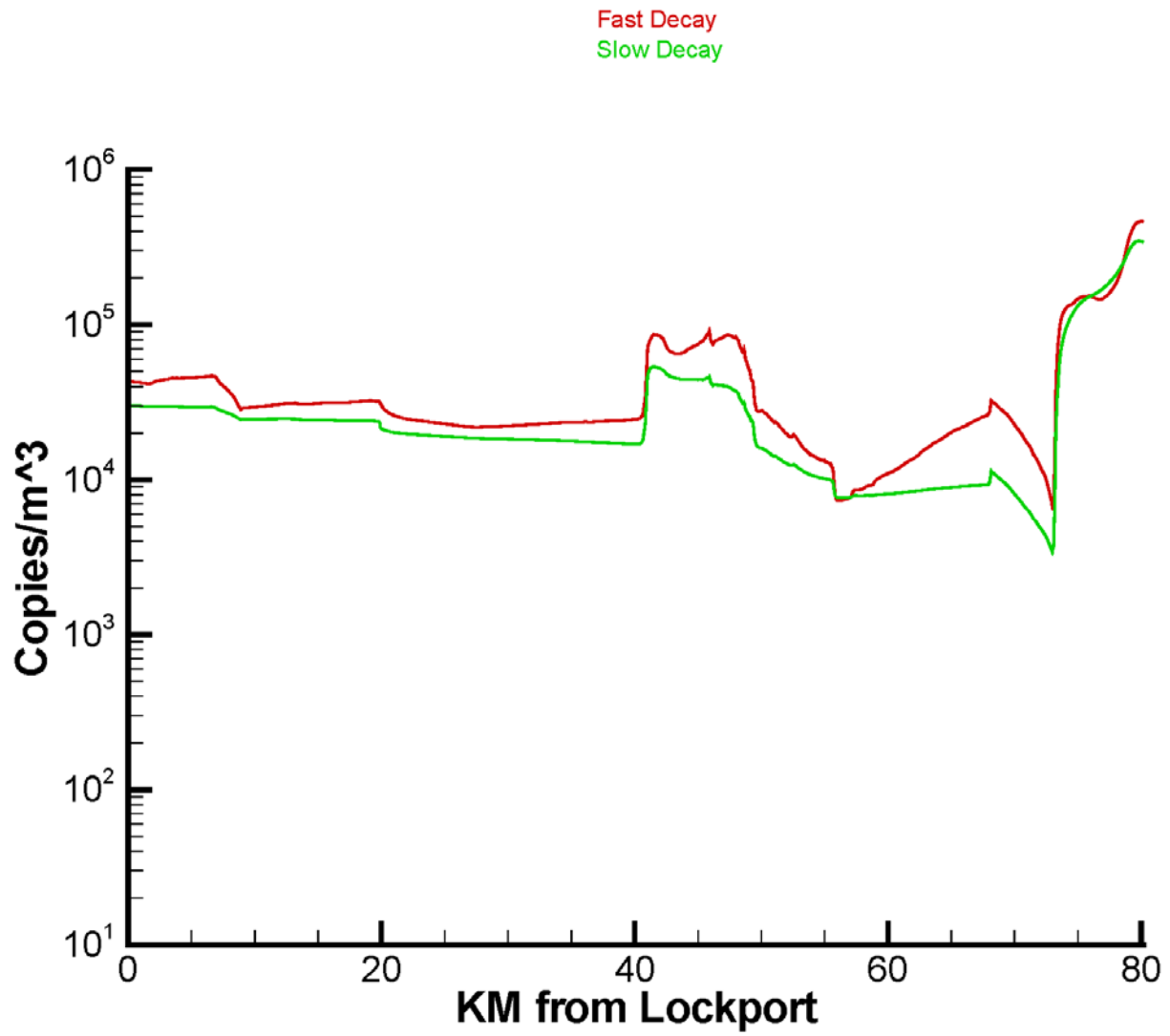


Figure 7.20. Seasonal-average computed eDNA concentration from primary sources. Lockport to North Shore Channel during “gates closed” season.

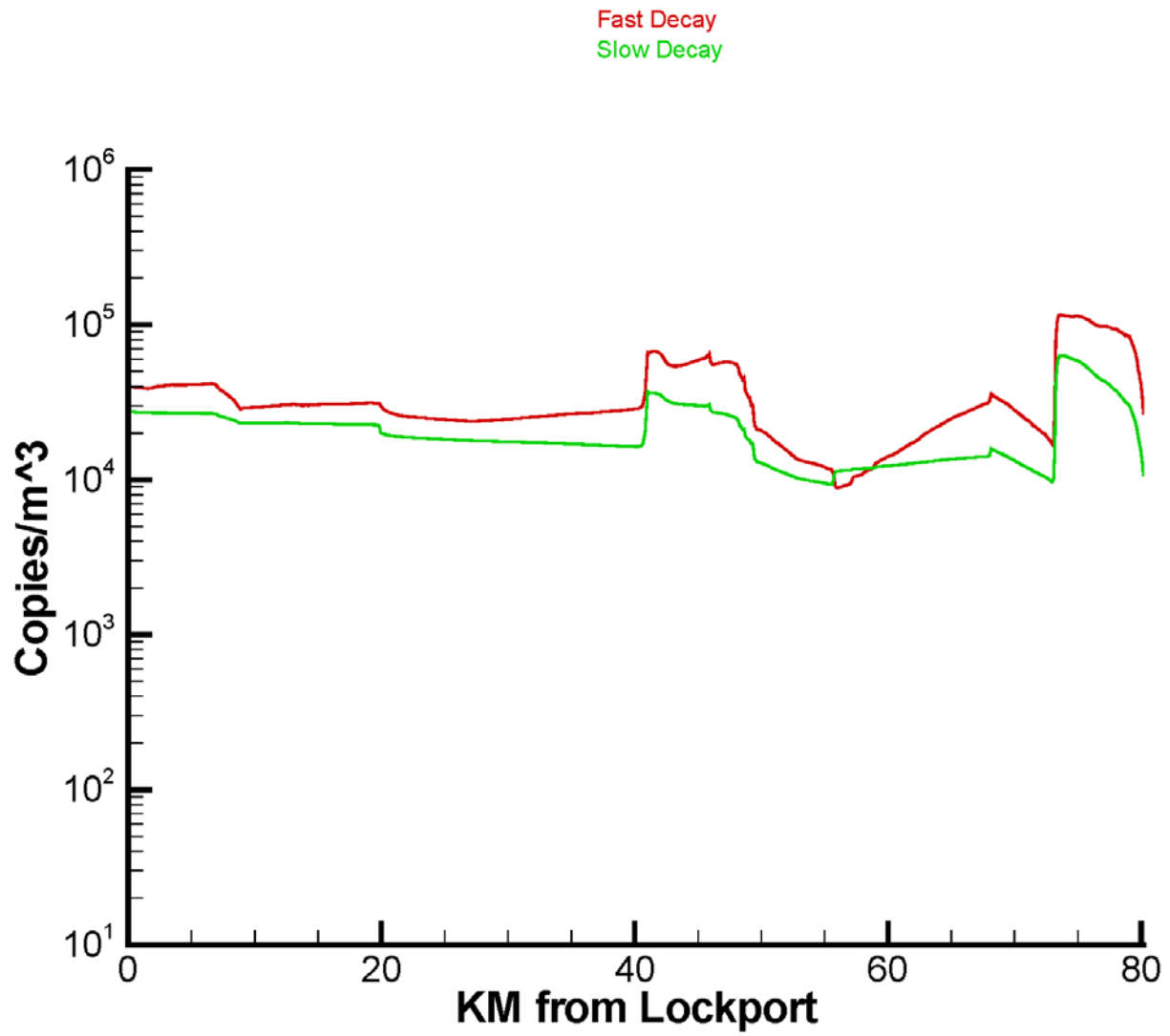


Figure 7.21. Seasonal-average computed eDNA concentration from primary sources. Lockport to North Shore Channel during “gates open” season.

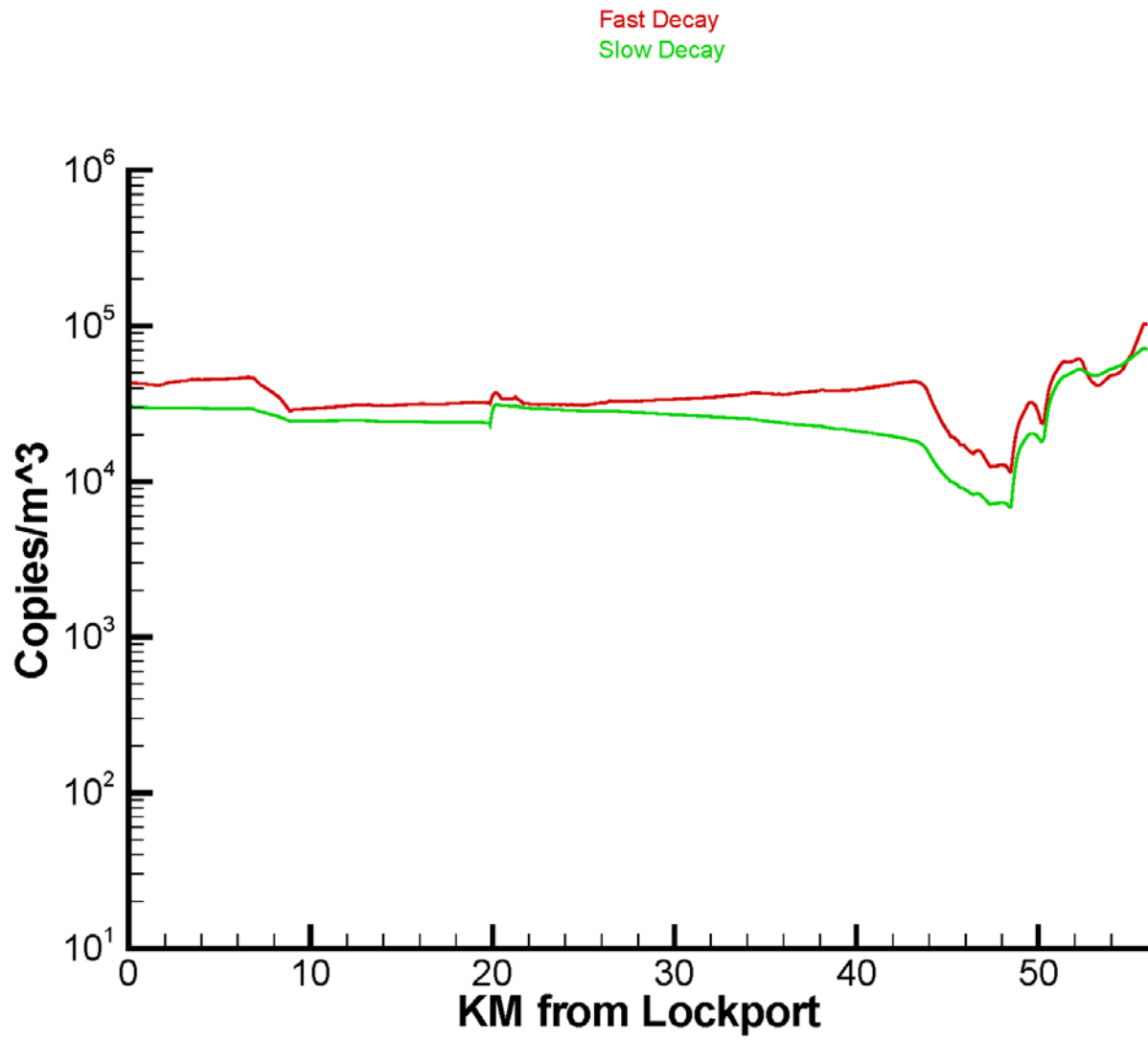


Figure 7.22. Seasonal-average computed eDNA concentration from primary sources. Lockport to O'Brien during "gates closed" season.

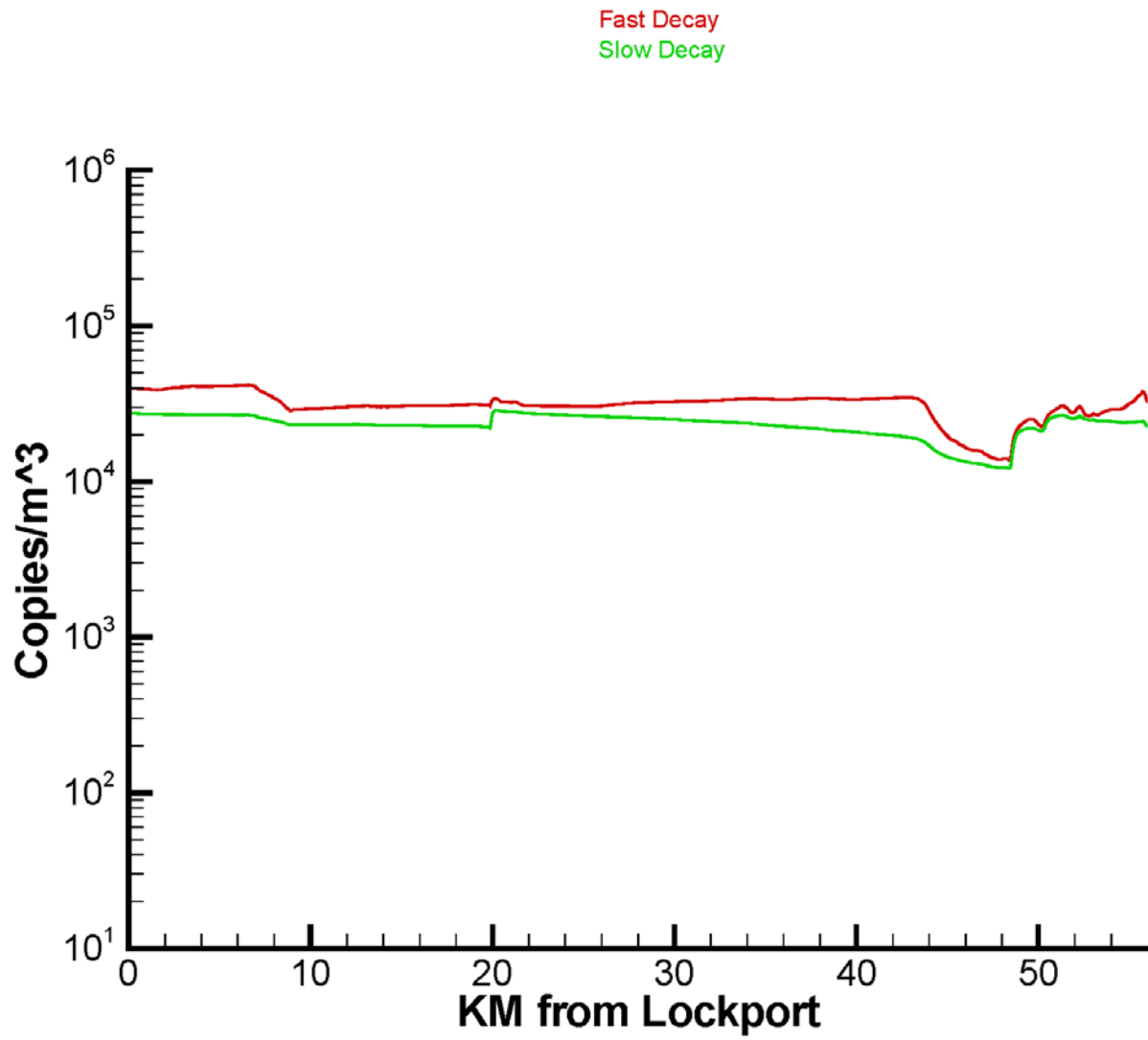


Figure 7.23. Seasonal-average computed eDNA concentration from primary sources. Lockport to O'Brien during "gates open" season.

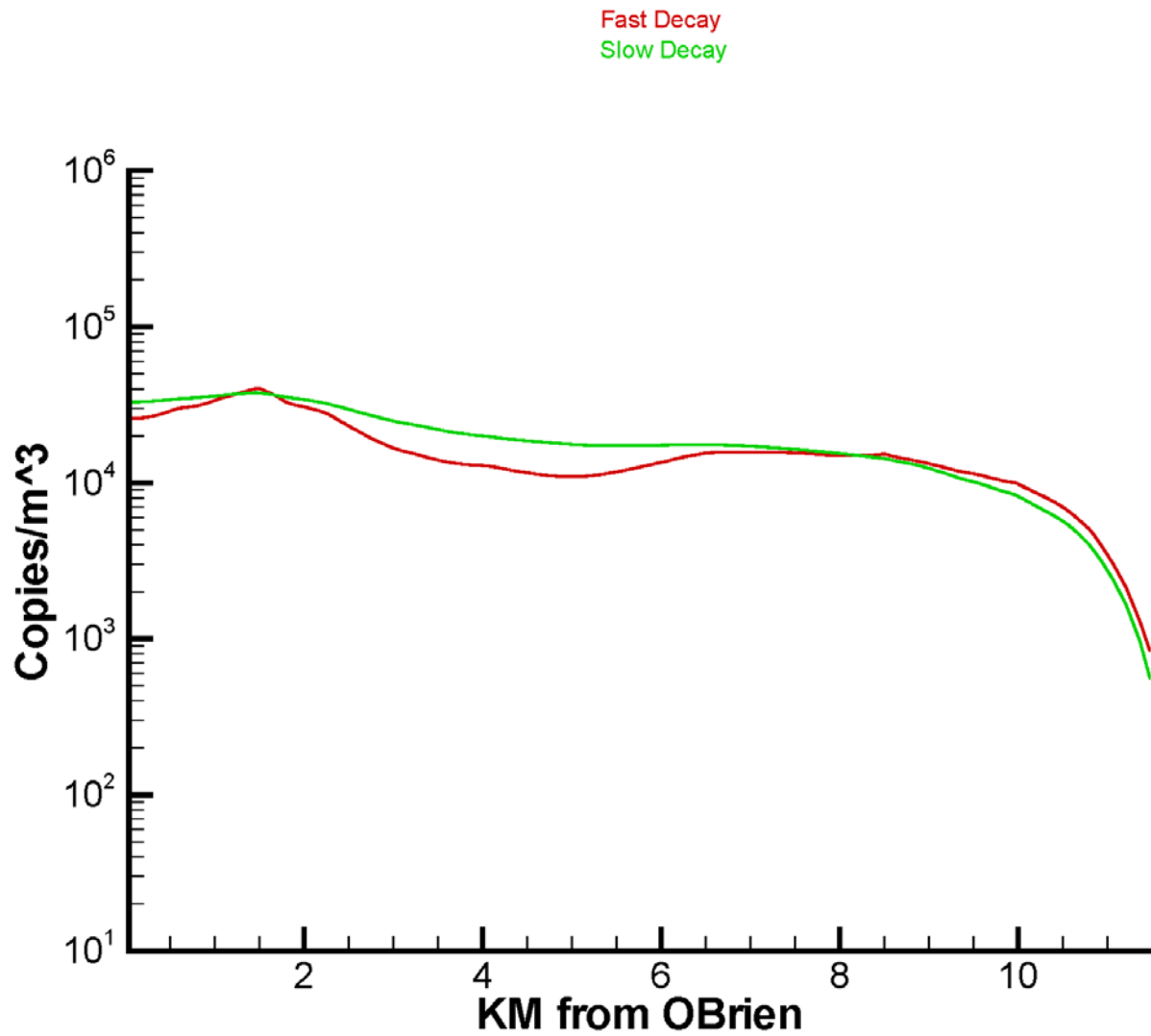


Figure 7.24. Seasonal-average computed eDNA concentration from primary sources. O'Brien to Lake Michigan during "gates closed" season.

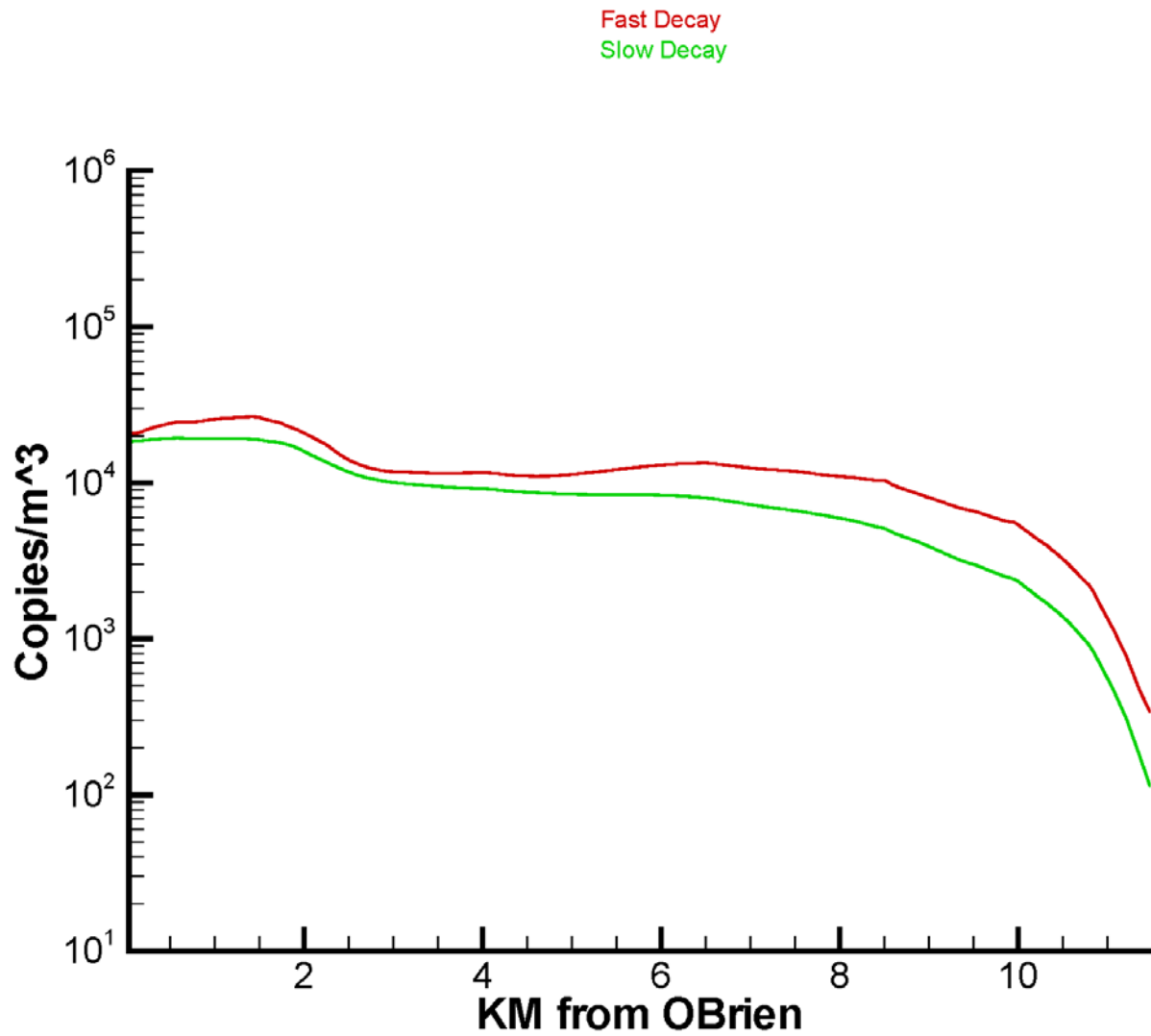


Figure 7.26. Seasonal-average computed eDNA concentration from primary sources. O'Brien to Lake Michigan during "gates open" season.

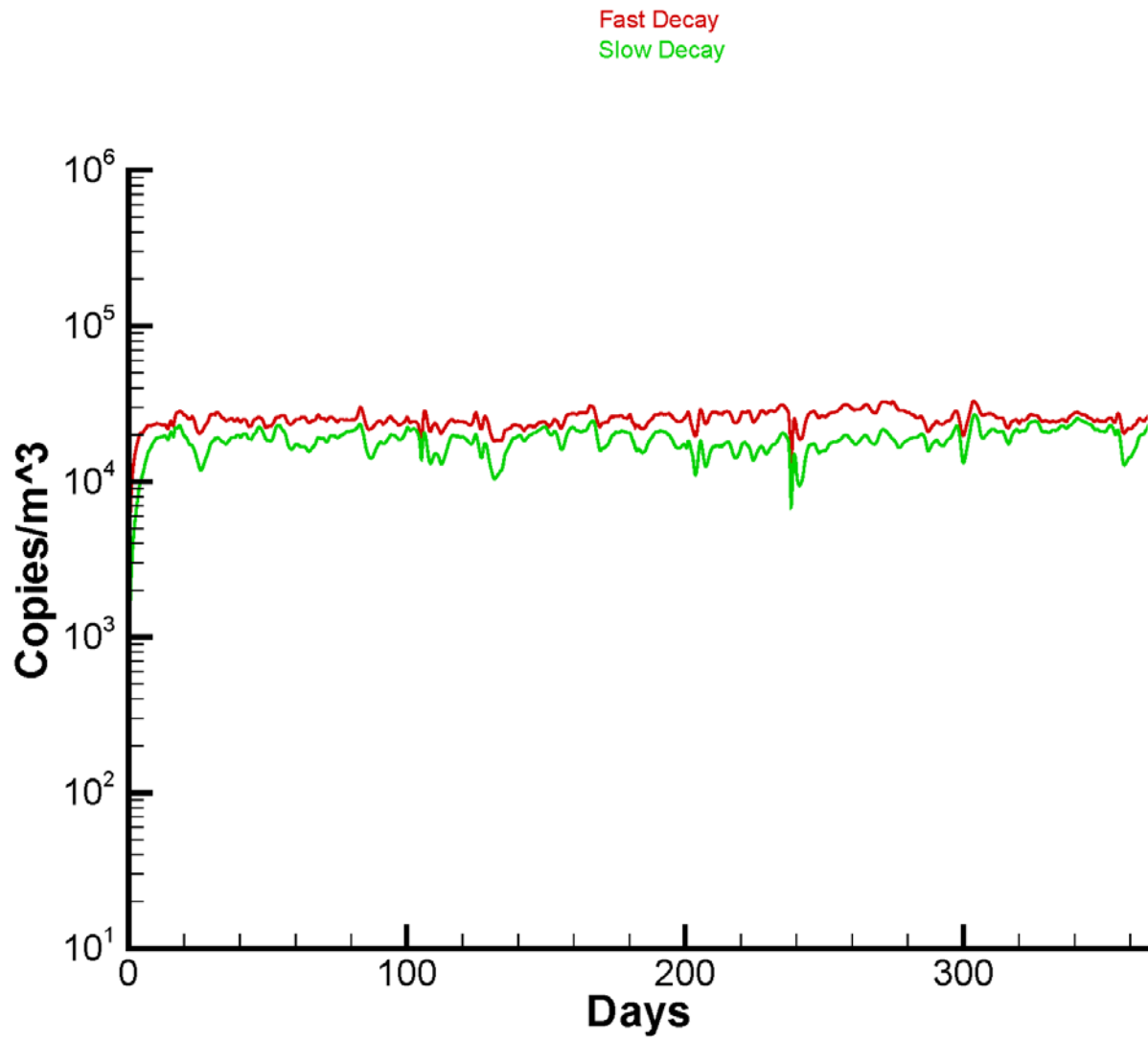


Figure 7.26. Time series of computed eDNA concentration resulting from primary sources. Reach CR4 (mid-section of Chicago Sanitary and Ship Canal).



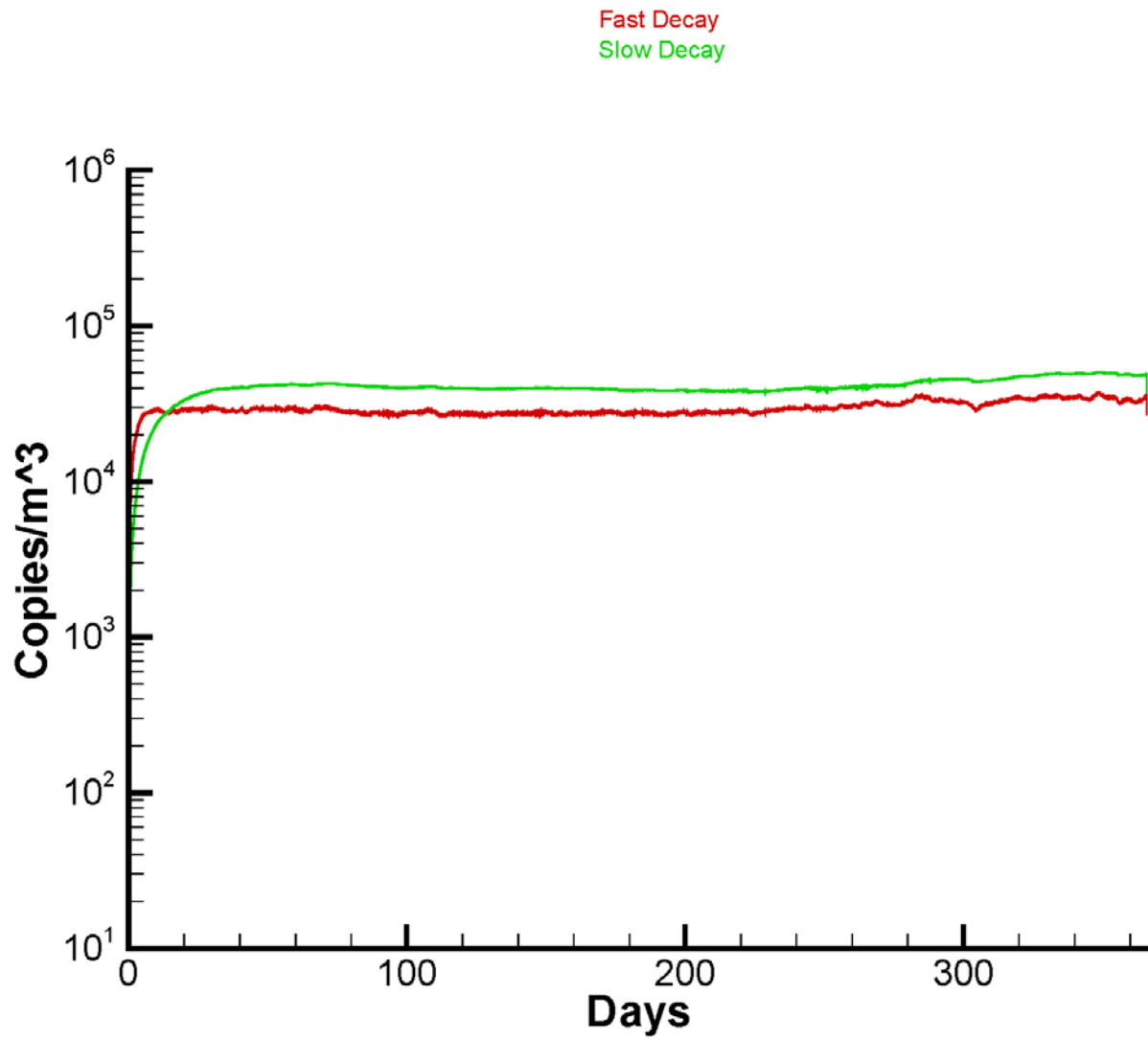


Figure 7.27. Time series of computed eDNA concentration resulting from primary sources. Reach LKC (Lake Calumet).

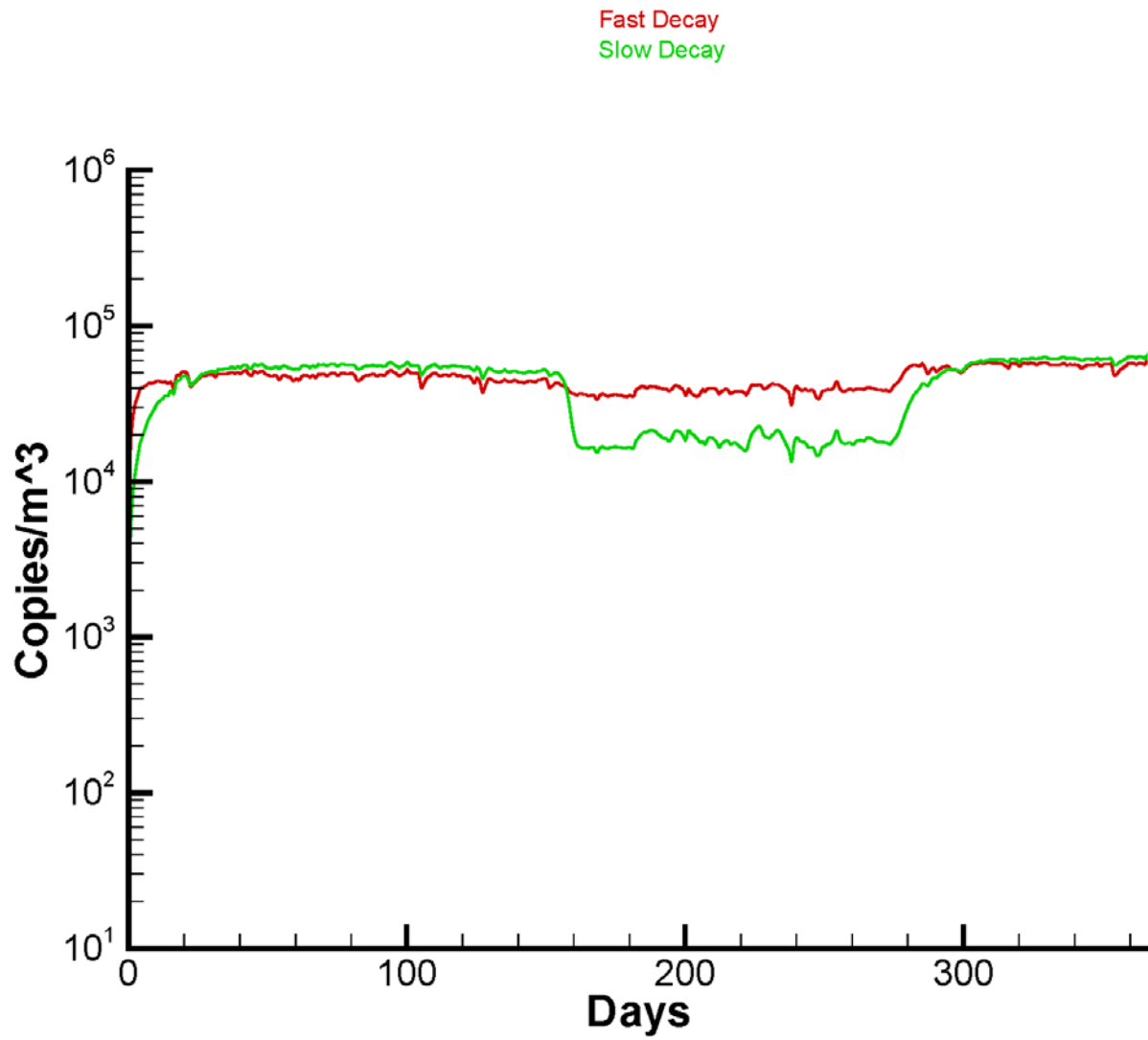


Figure 7.28. Time series of computed eDNA concentration resulting from primary sources. Reach NSC (North Shore Channel).

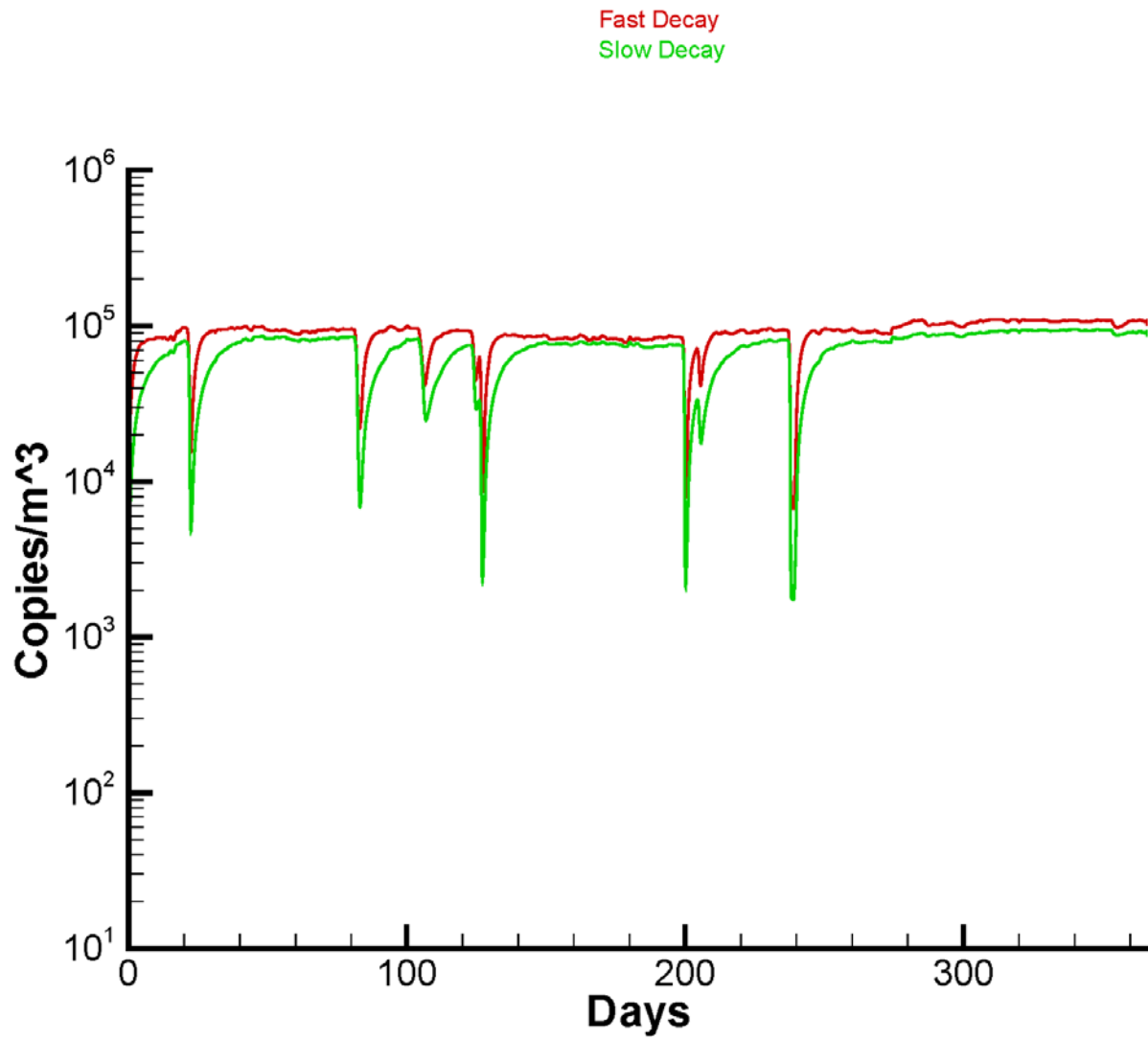


Figure 7.29. Time series of computed eDNA concentration resulting from primary sources. Reach BCR (Bubbly Creek).

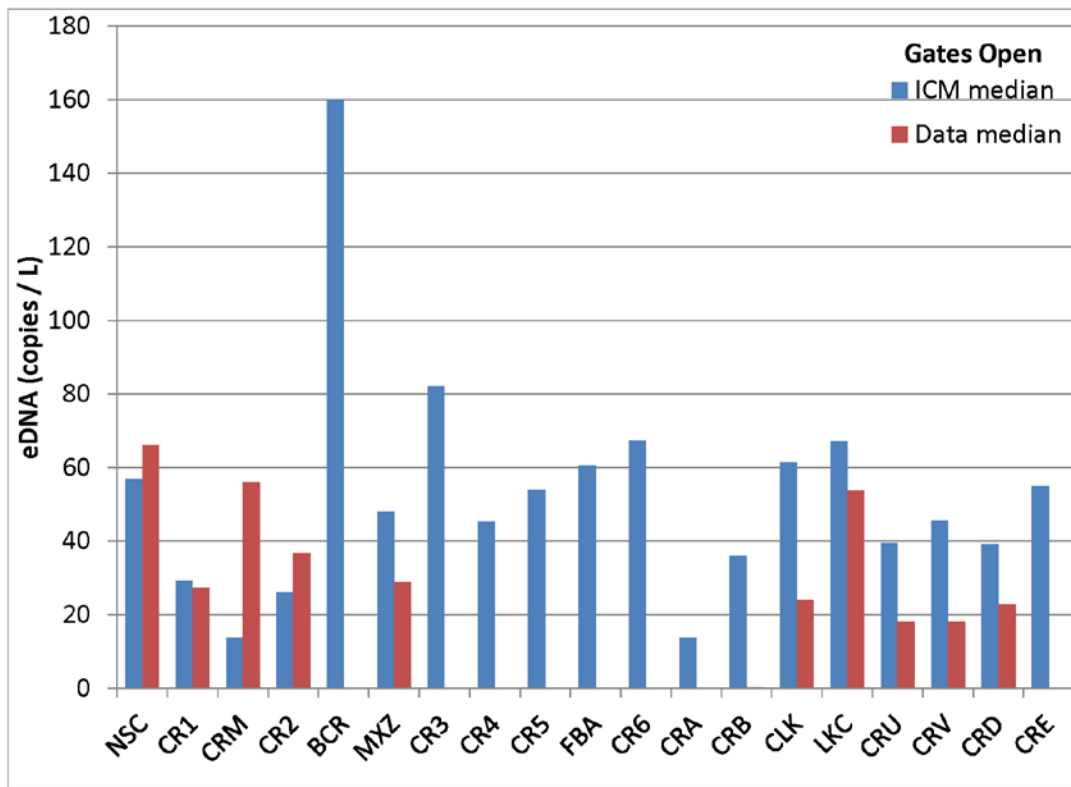


Figure 7.30. Median computed eDNA from primary sources in all reaches compared to the median of observations in reaches for which data is available. “Gates open” season.

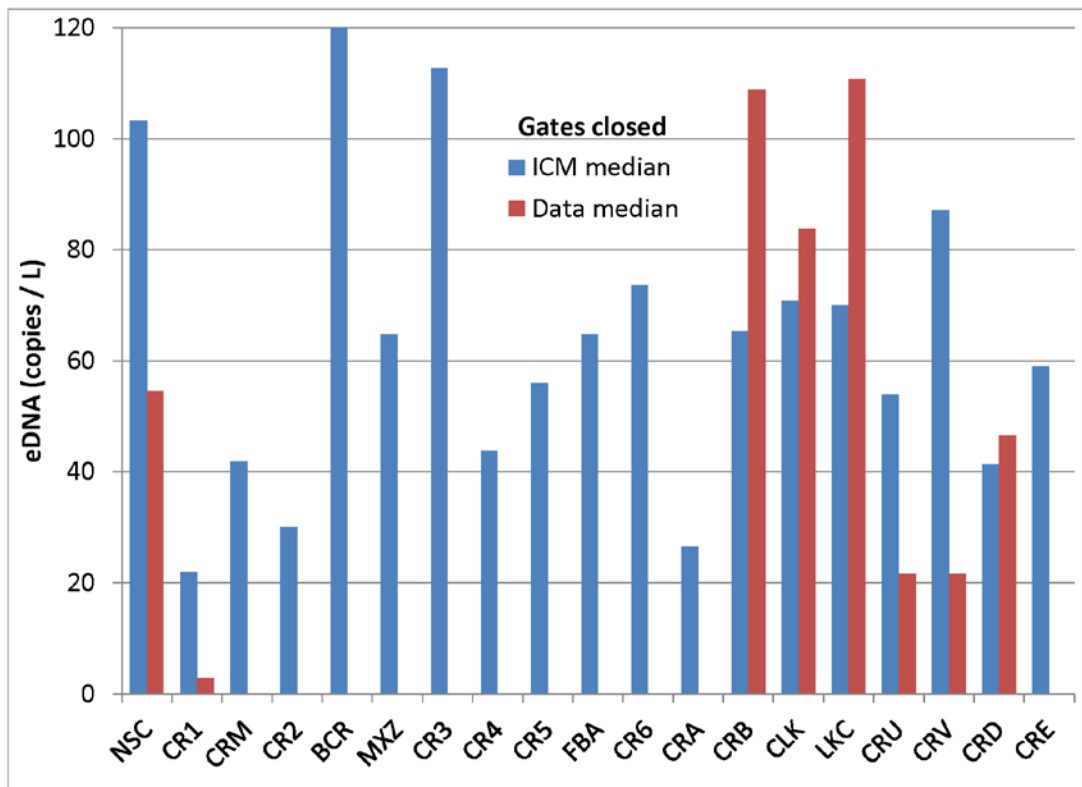


Figure 7.31. Median computed eDNA from primary sources in all reaches compared to the median of observations in reaches for which data is available. “Gates closed” season.

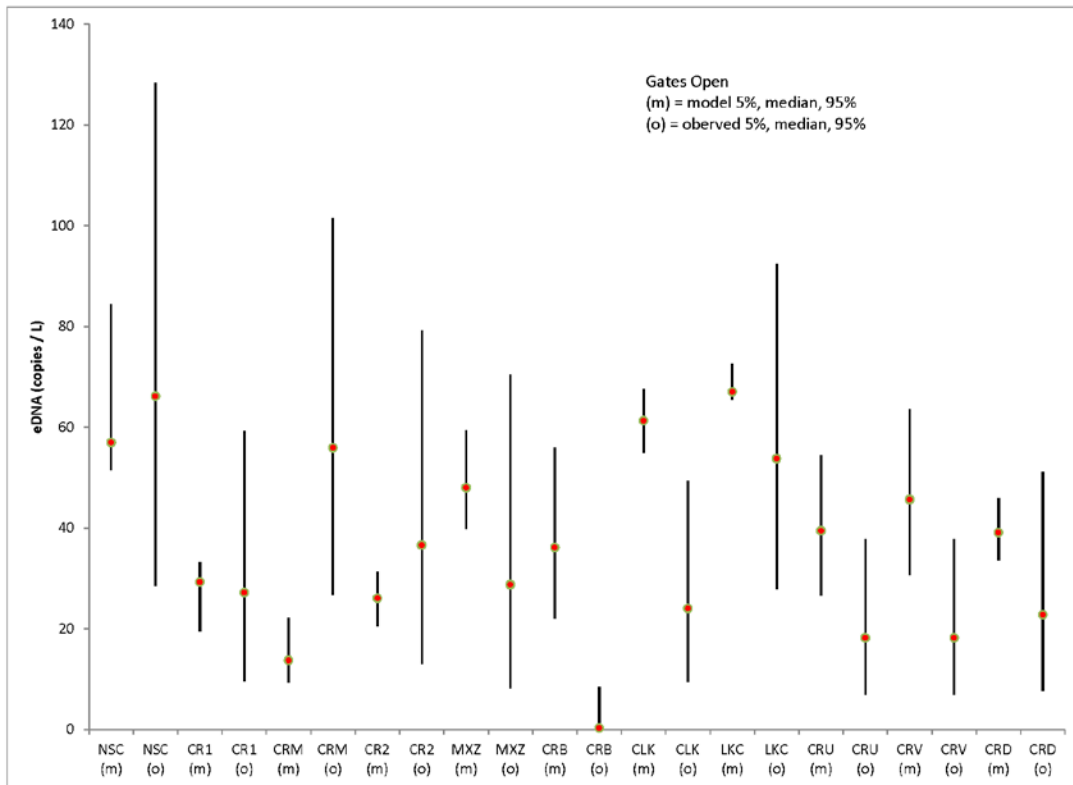


Figure 7.32. Median and 90% range for computed eDNA from primary sources and for observations. Comparison is restricted to reaches with observations. “Gates open” season.

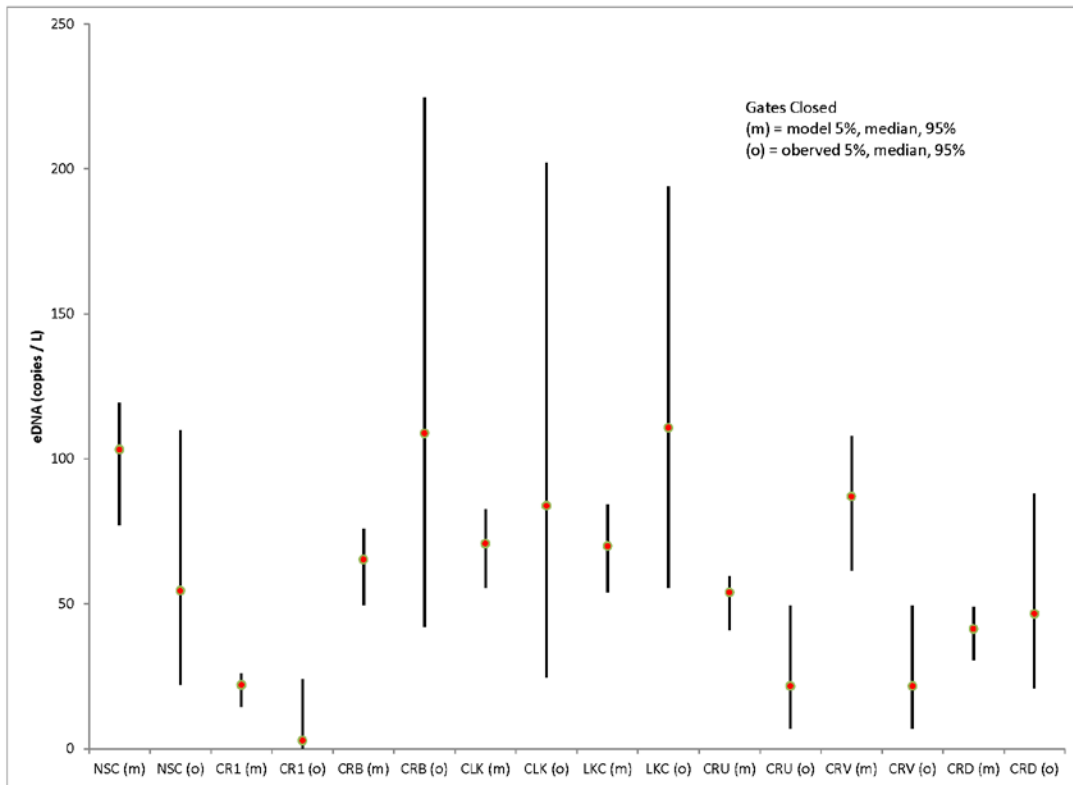


Figure 7.33. Median and 90% range for computed eDNA from primary sources and for observations. Comparison is restricted to reaches with observations. "Gates closed" season.

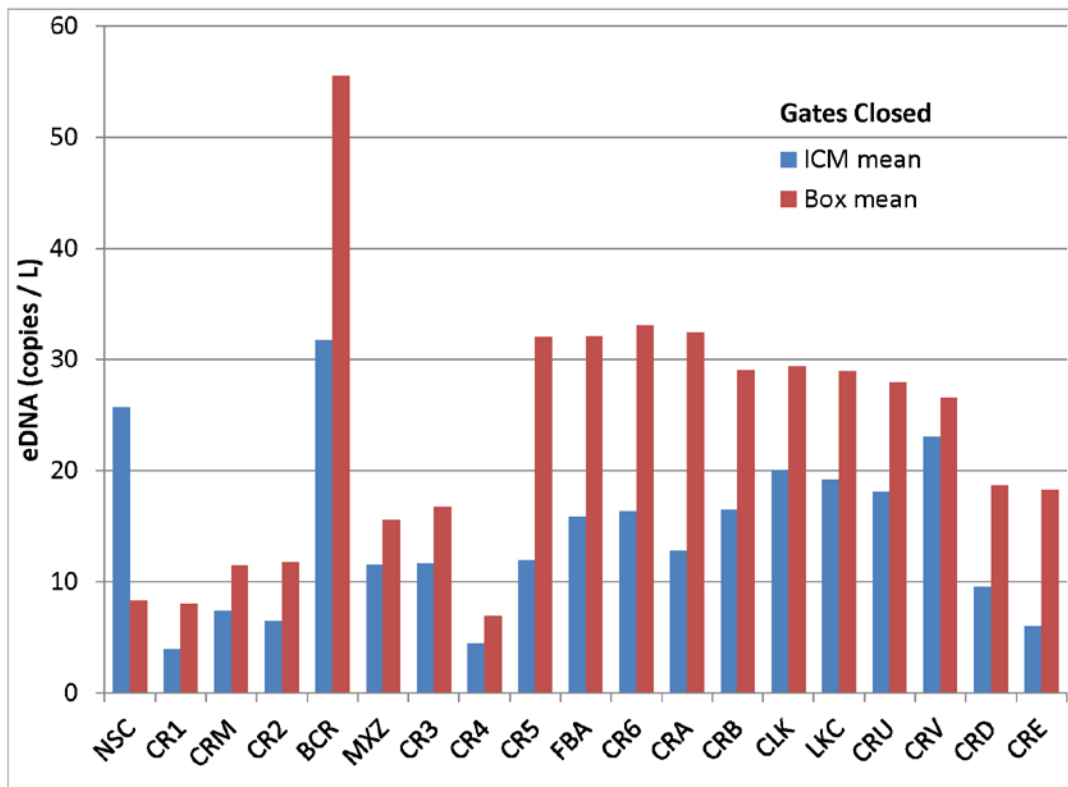


Figure 7.34. Median computed eDNA from the HFFT model compared to the box model. Secondary sources during the “gates closed” season.



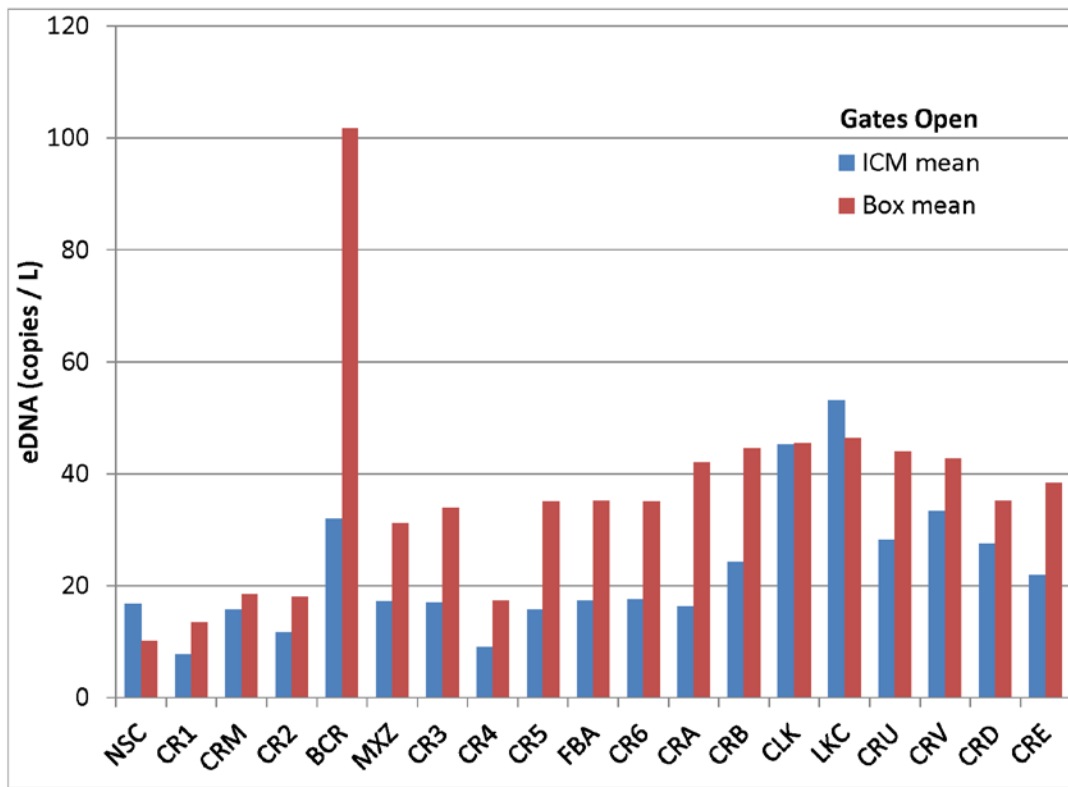


Figure 7.35. Median computed eDNA from the HFFT model compared to the box model. Secondary sources during the “gates open” season.

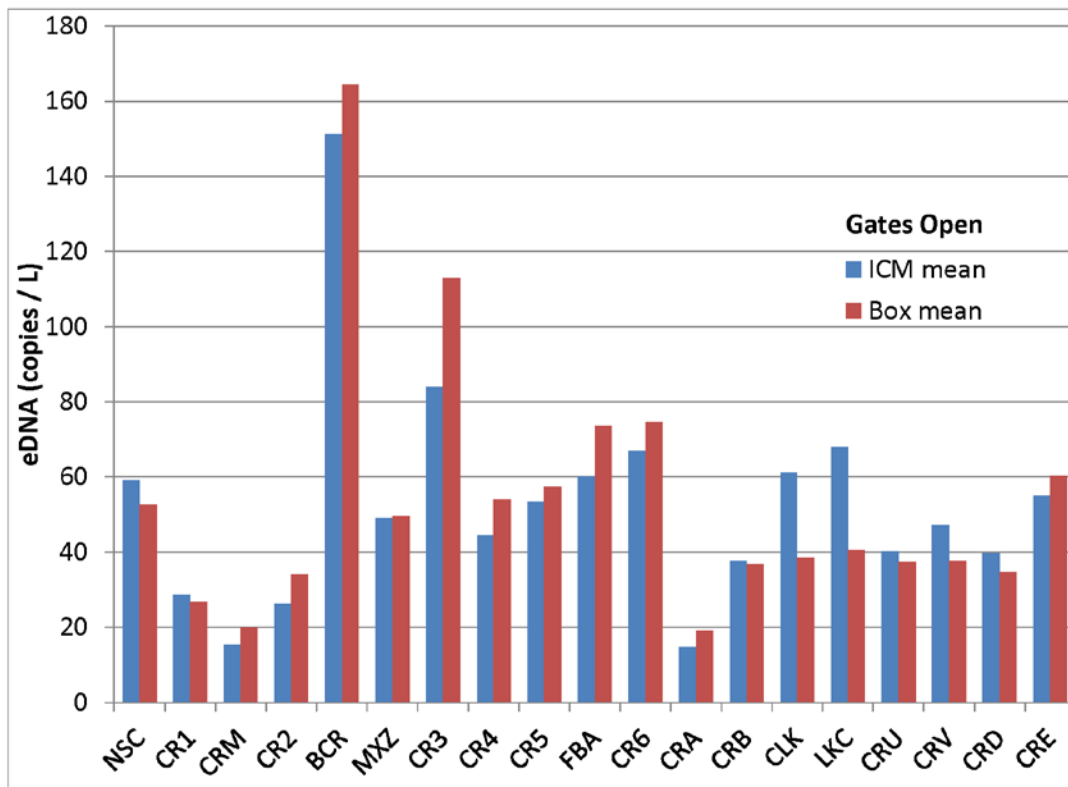


Figure 7.36. Median computed eDNA from the HFFTM compared to the box model. Primary sources during the “gates closed” season.

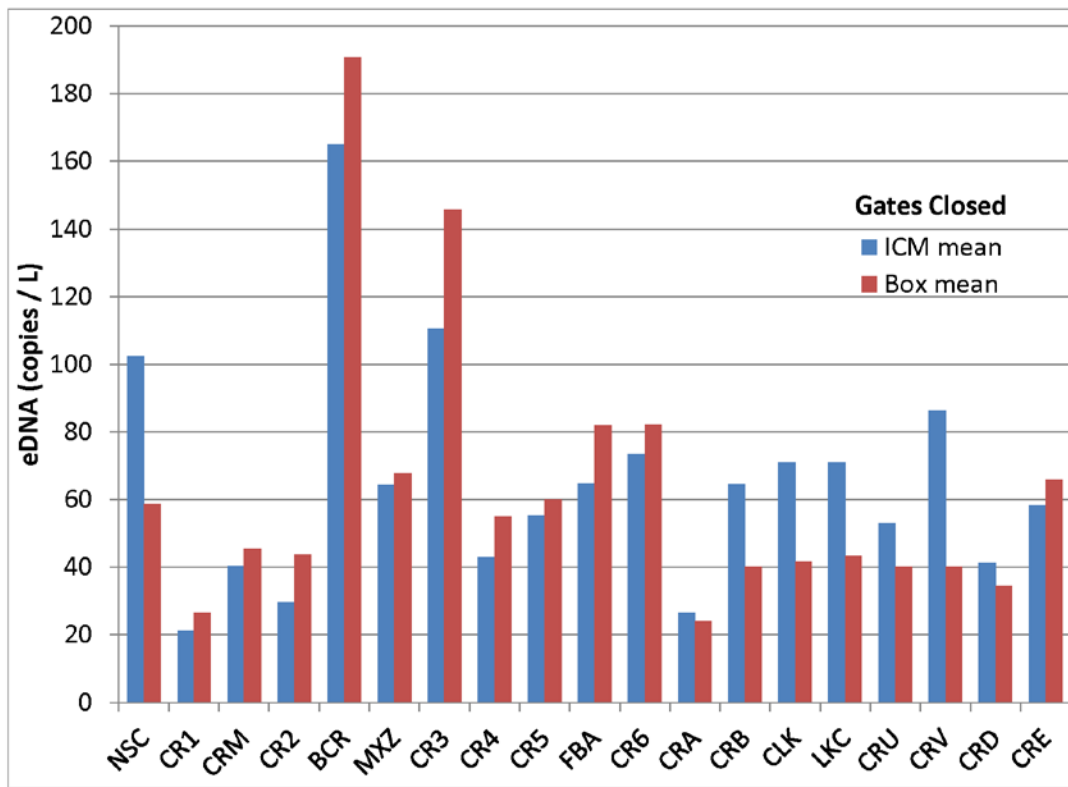


Figure 7.37. Median computed eDNA from the HFFTM compared to the box model. Primary sources during the “gates open” season.

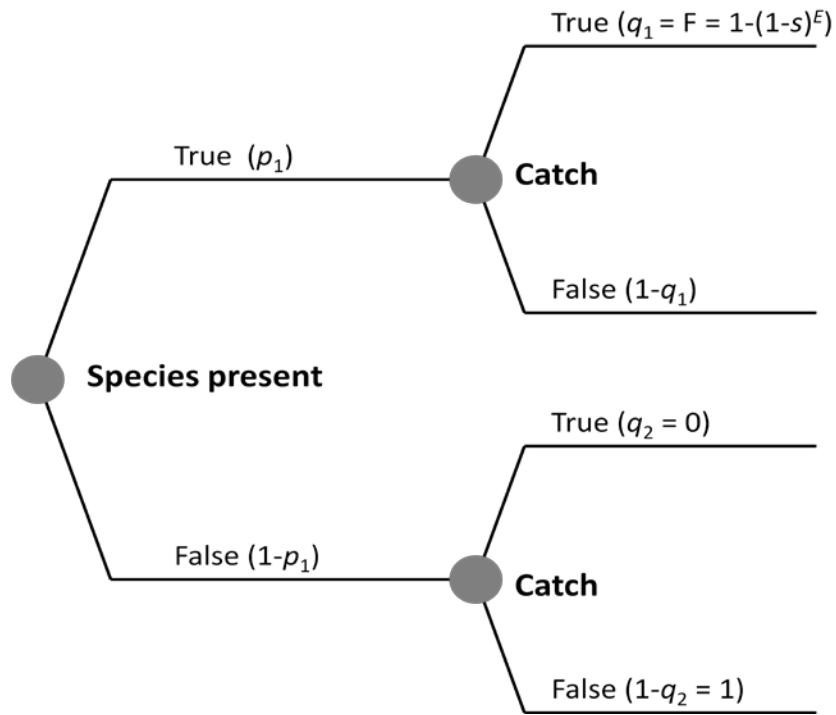


Figure 8.1: Event tree illustrating potential outcomes of a fishing expedition.

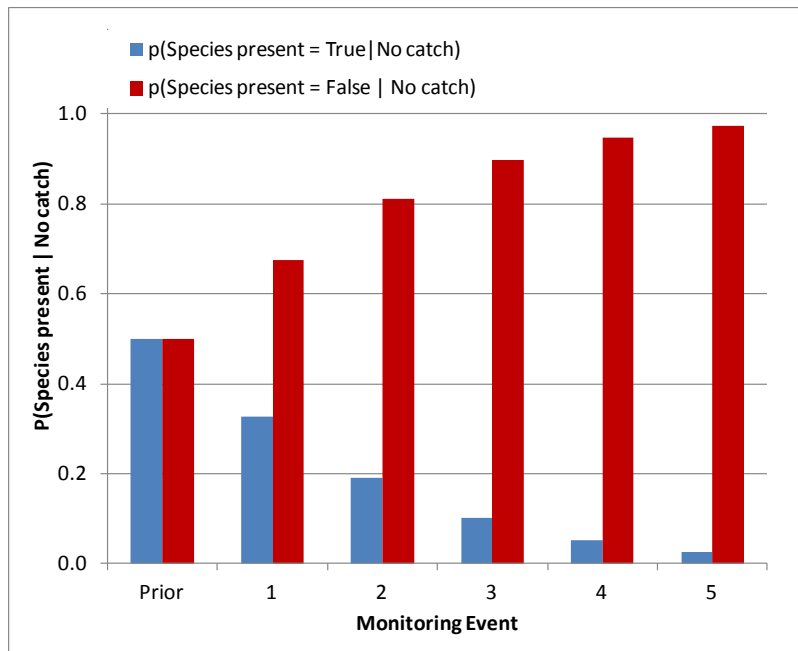


Figure 8.2: Example showing how the posterior probability that a species is present at a search site can be successively updated using as evidence the failure of repeated attempts to capture a specimen.

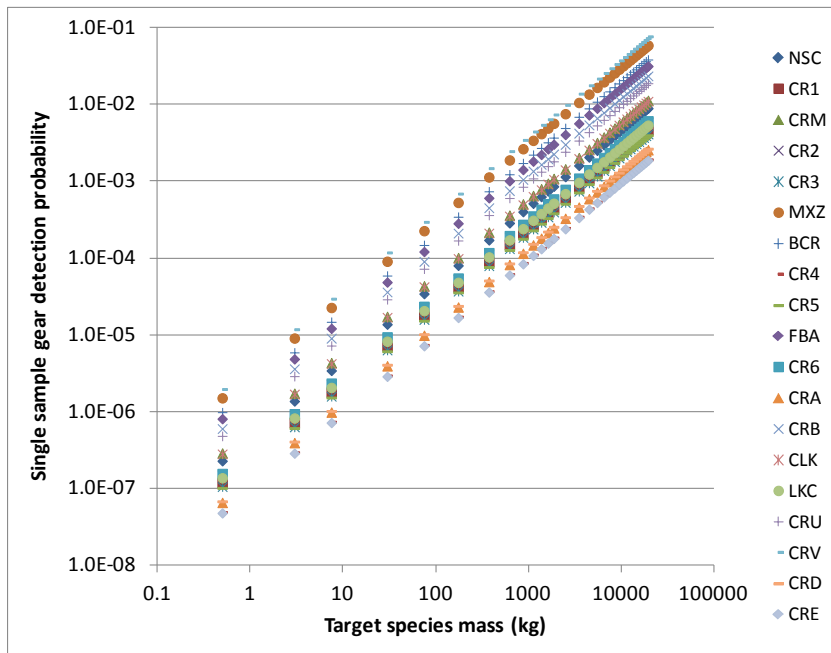


Figure 8.3: Single sample gear detection probabilities by CAWS reach over a range of potential target species mass.

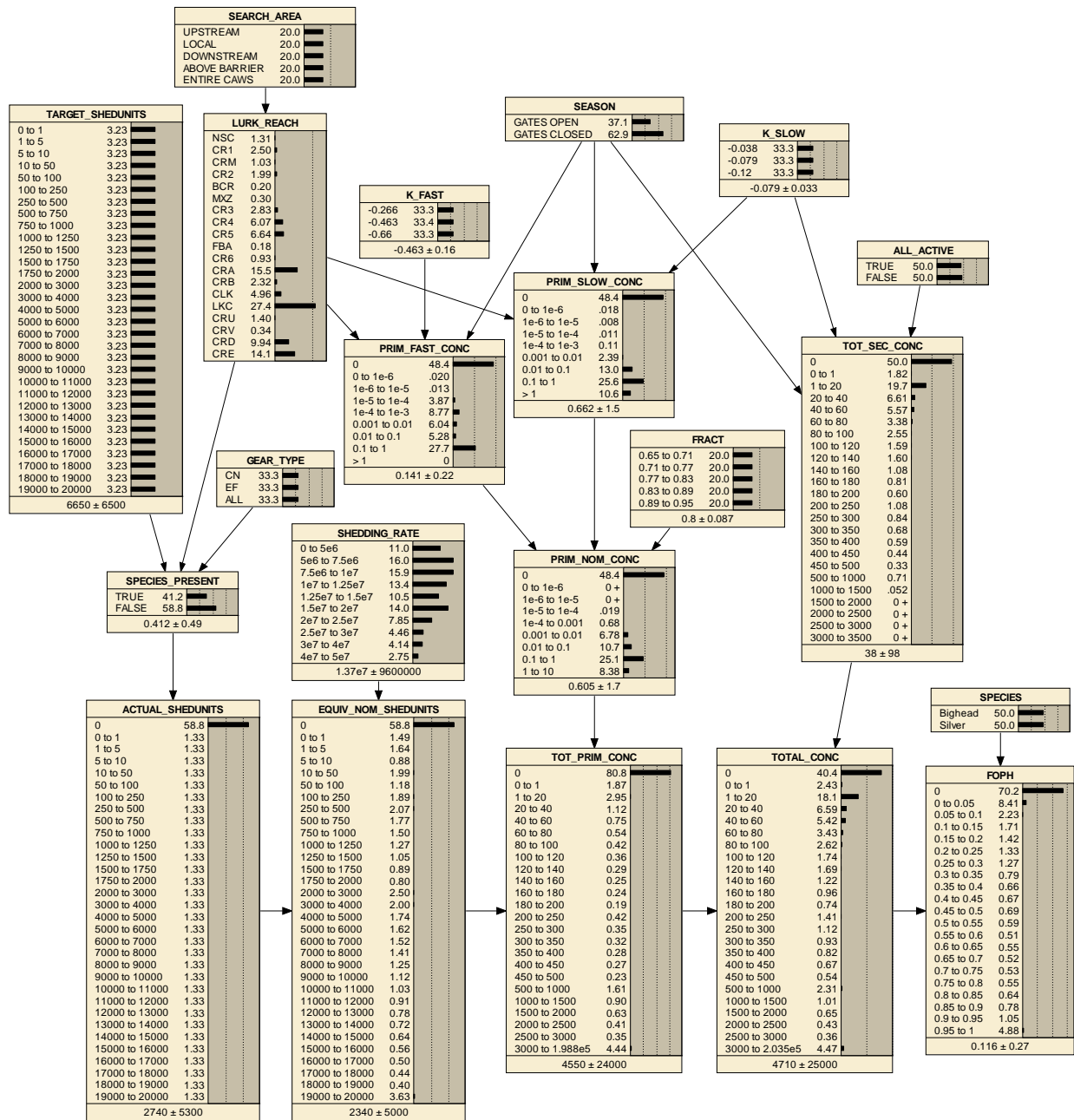


Figure 9.1: Bayesian network graph (4.5)

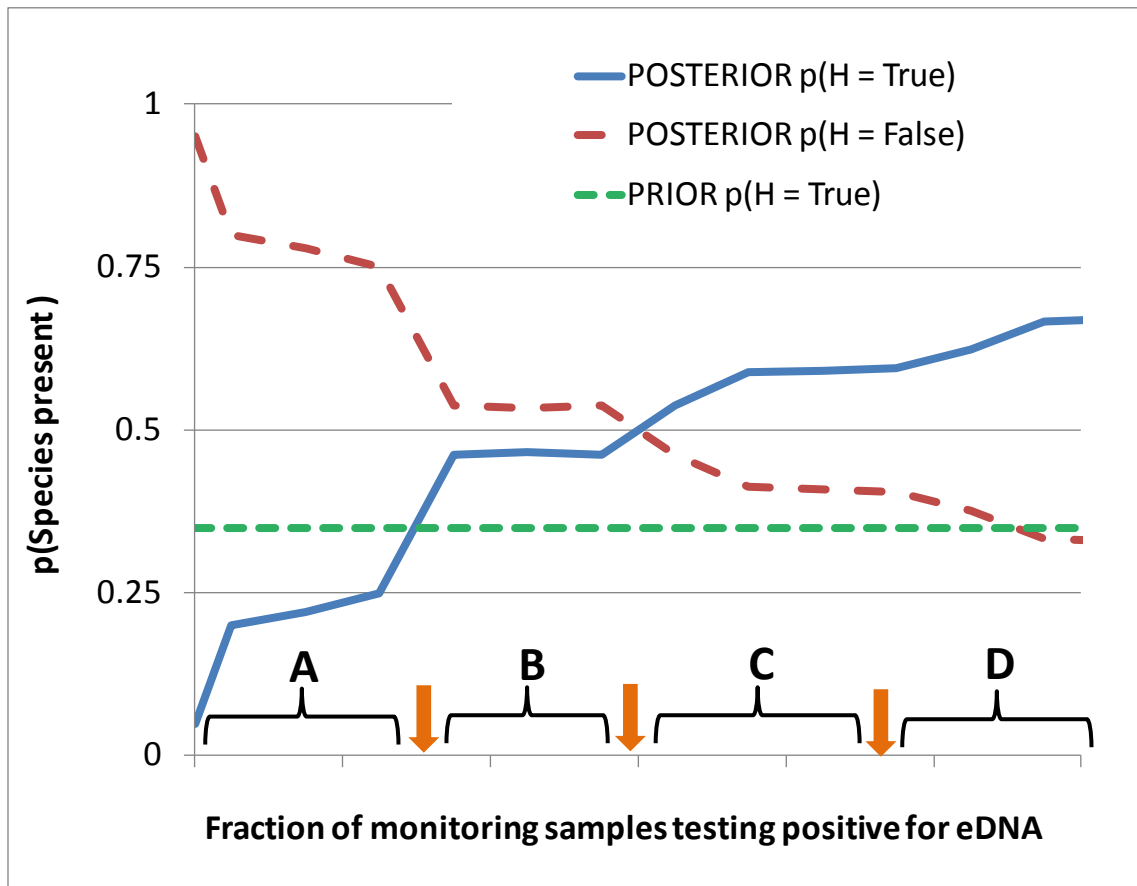


Figure 9.2: Critical regions of probability plots.



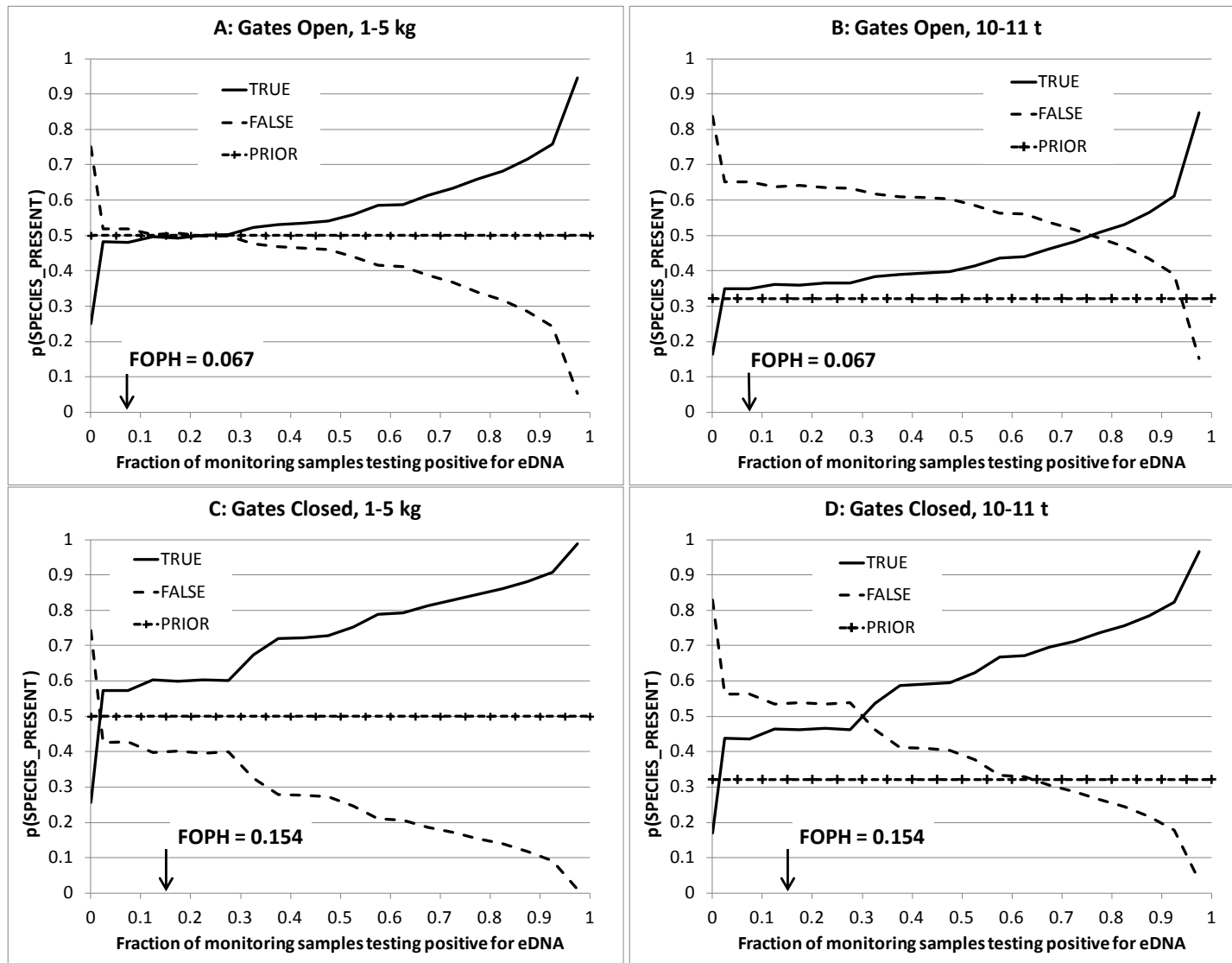
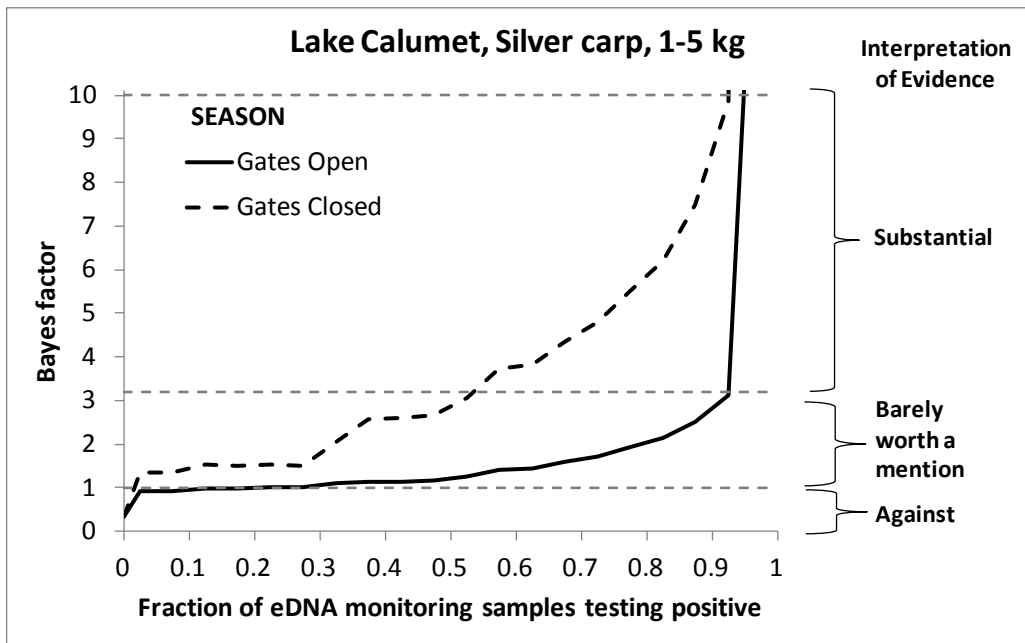
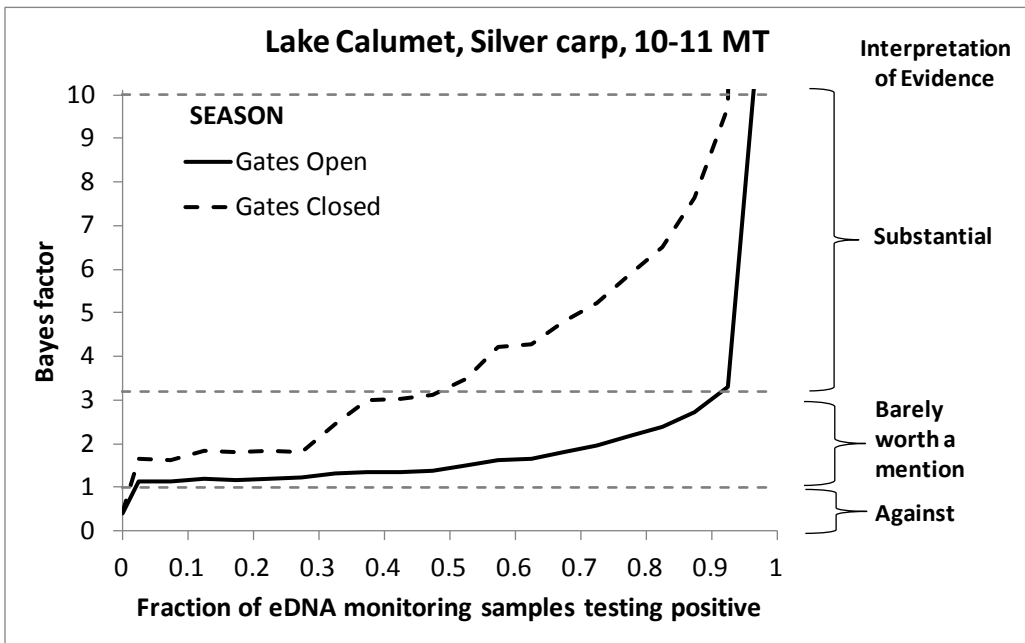


Figure 9.3: Illustration of statistical inference in LKC for silver carp varying SEASON and TARGET\_SHEDUNITS. Plots show the posterior  $p(\text{SPECIES\_PRESENT})$  is *True* and *False* and the prior  $p(\text{SPECIES\_PRESENT} = \textit{True})$ .

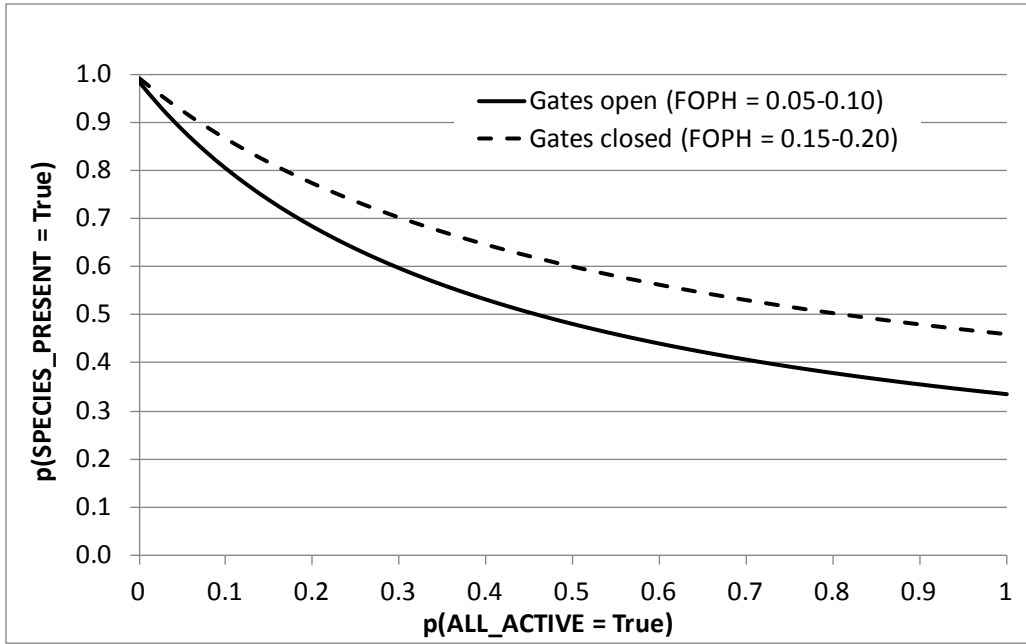


(A)

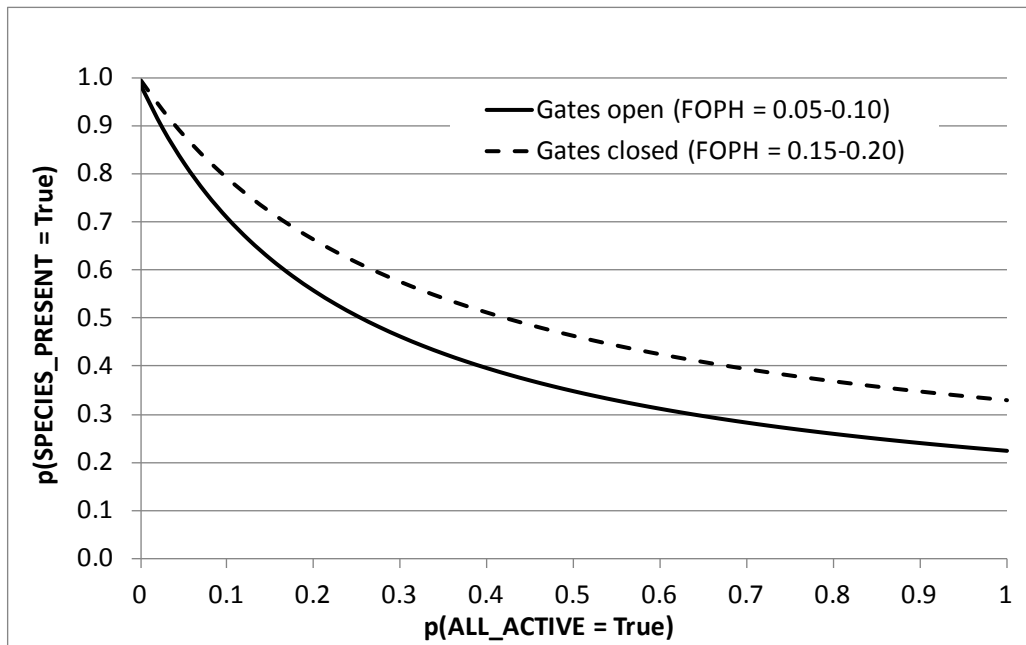


(B)

Figure 9.4: Bayes factor for potential evidence from eDNA monitoring. Results are for silver carp in Lake Calumet by season for two states of TARGET\_SHEDUNITS: (A) 1-5 kg and (B) 10-11 t.

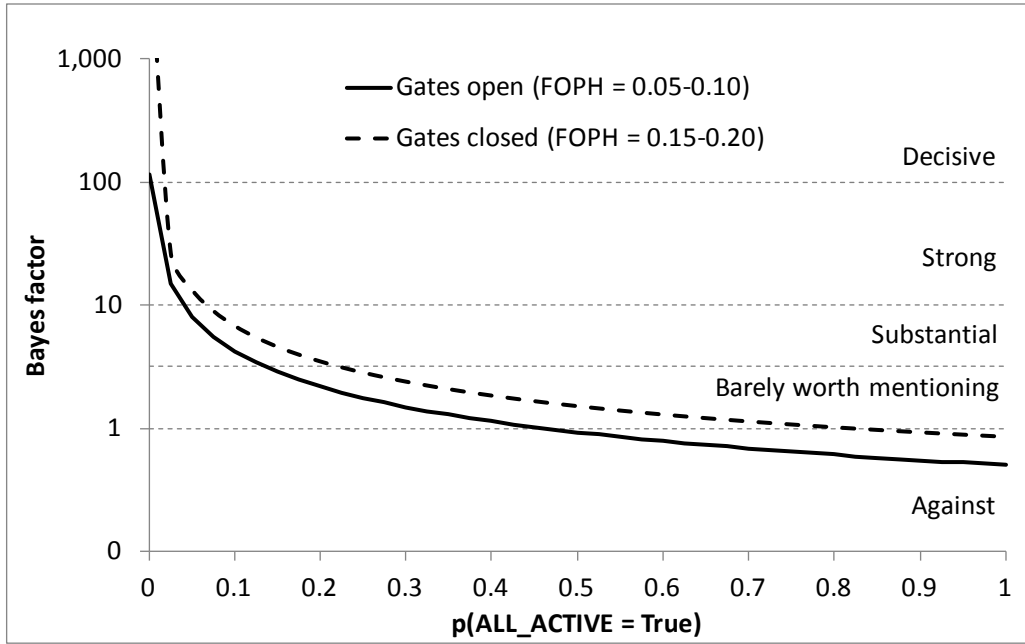


(A)

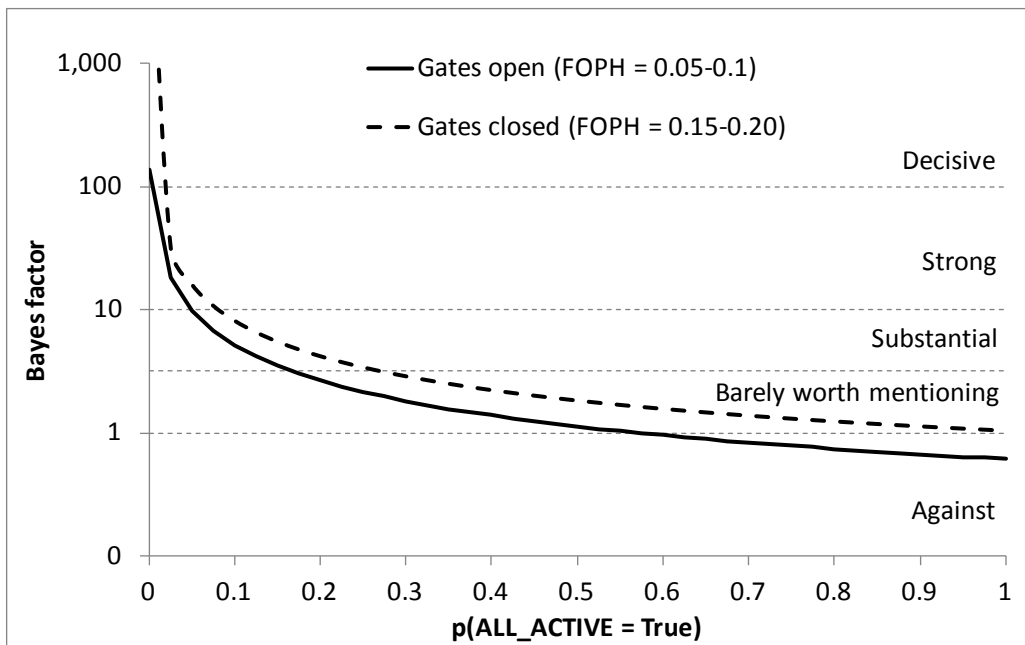


(B)

Figure 9.5: Sensitivity of the posterior probability in LKC given FOPH = 0.05-0.10 varying the ALL\_ACTIVE parameter. Results are for silver carp by season for two states of TARGET\_SHEDUNITS: (A) 1-5 kg and (B) 10-11 t.



(A)



(B)

Figure 9.6: Sensitivity of Bayes factor to parameterization of the ALL\_ACTIVE node for FOPH between 0.05 and 0.10. Results are for silver carp in Lake Calumet by season for two states of TARGET\_SHEDUNITS: (A) 1-5 kg and (B) 10-11 t.

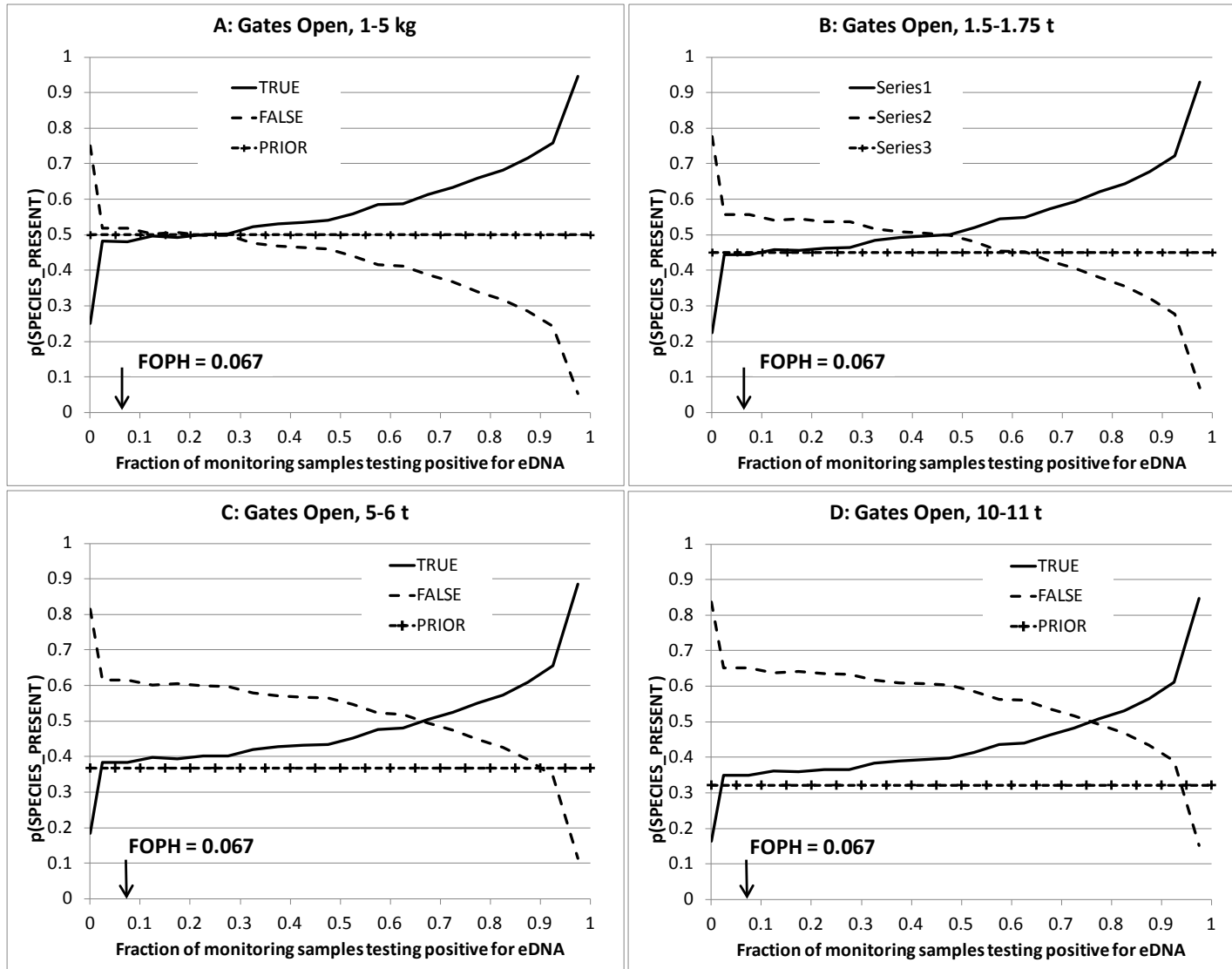


Figure 9.7: Lake Calumet (LKC), Gates Open

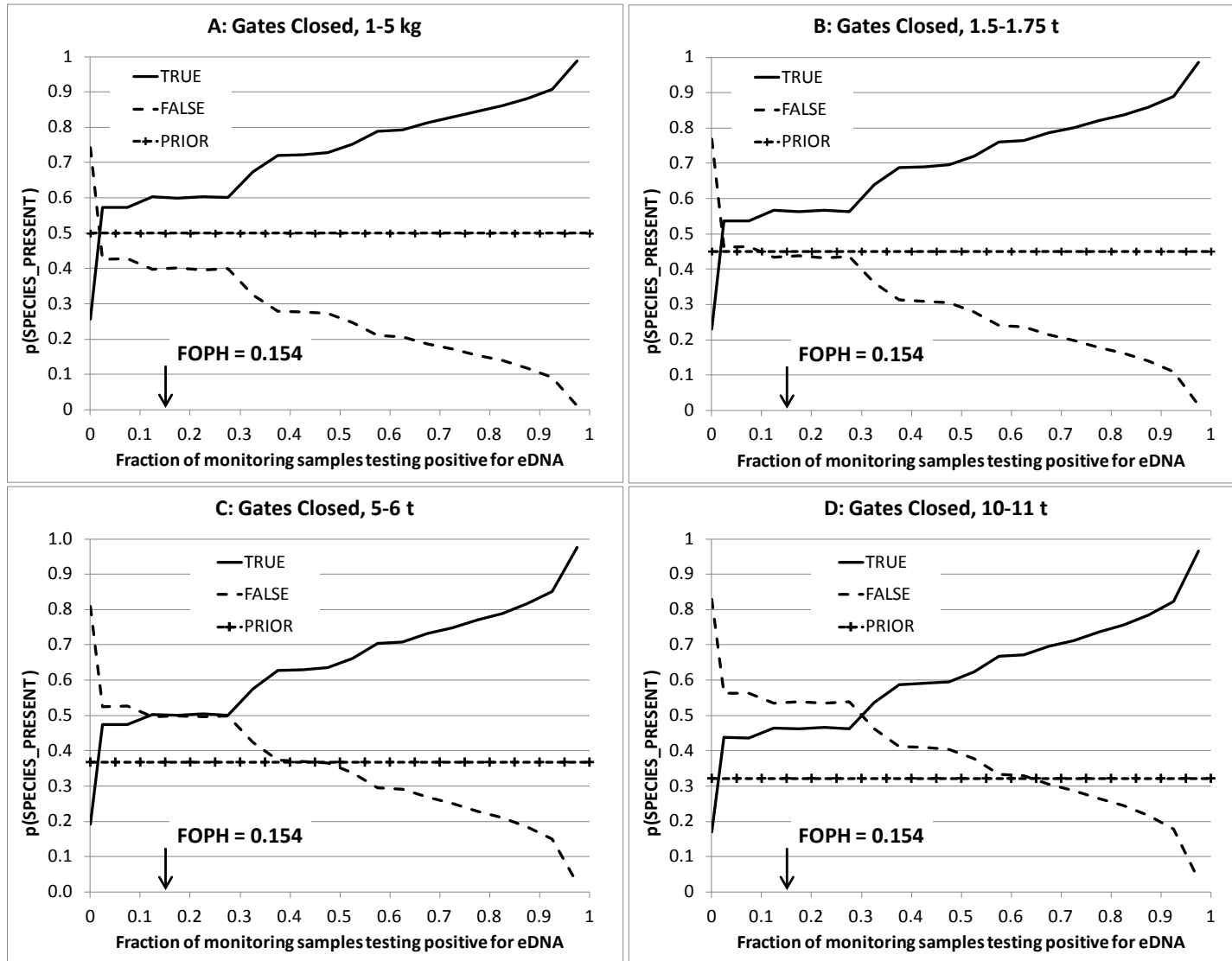


Figure 9.8: Lake Calumet (LKC), Gates Closed

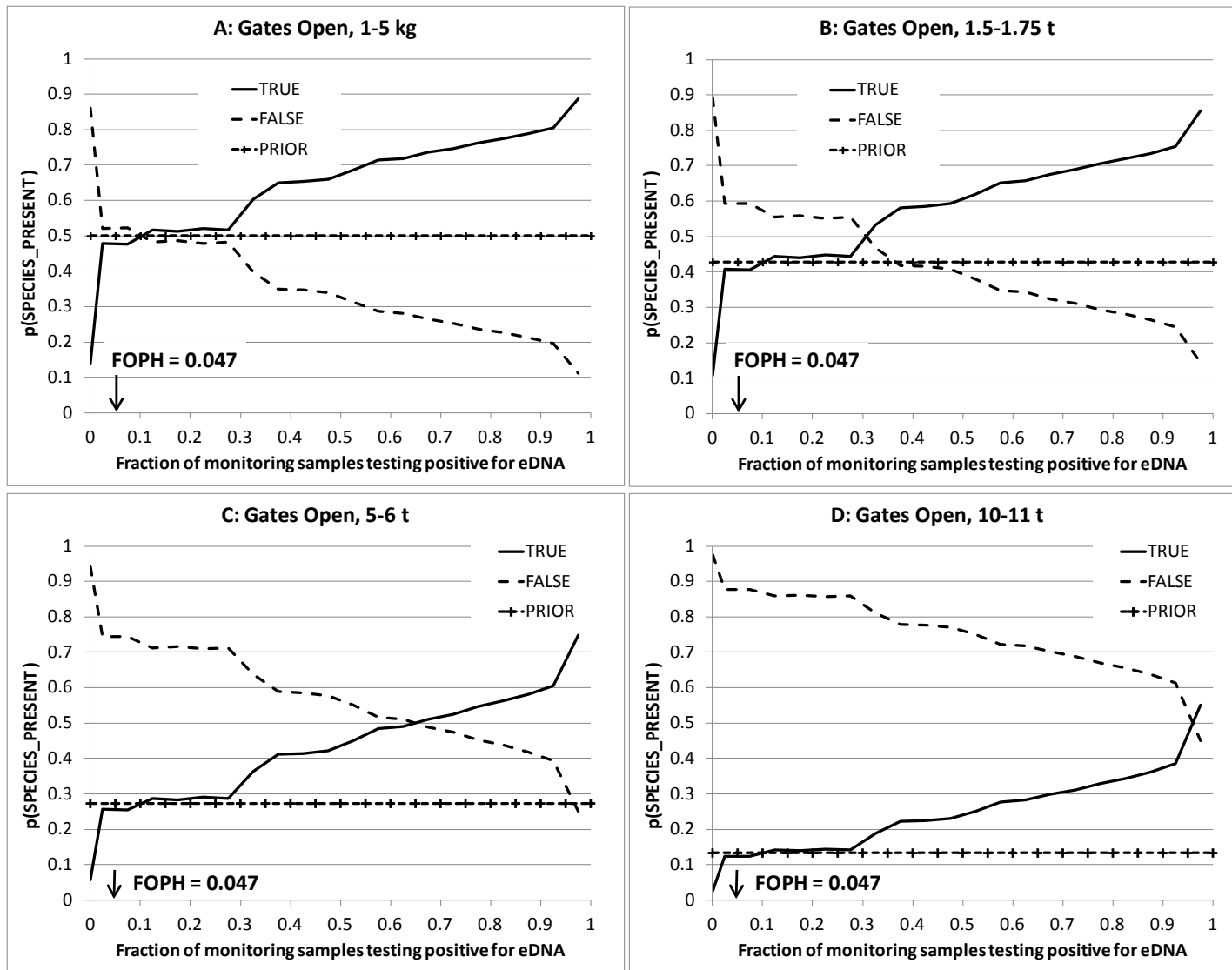


Figure 9.9: North Shore Channel (NSC), Gates Open. F = The NSC has been fished so hard that no amount of eDNA would make you think there were 10-11 t of silver carp in the north shore channel.

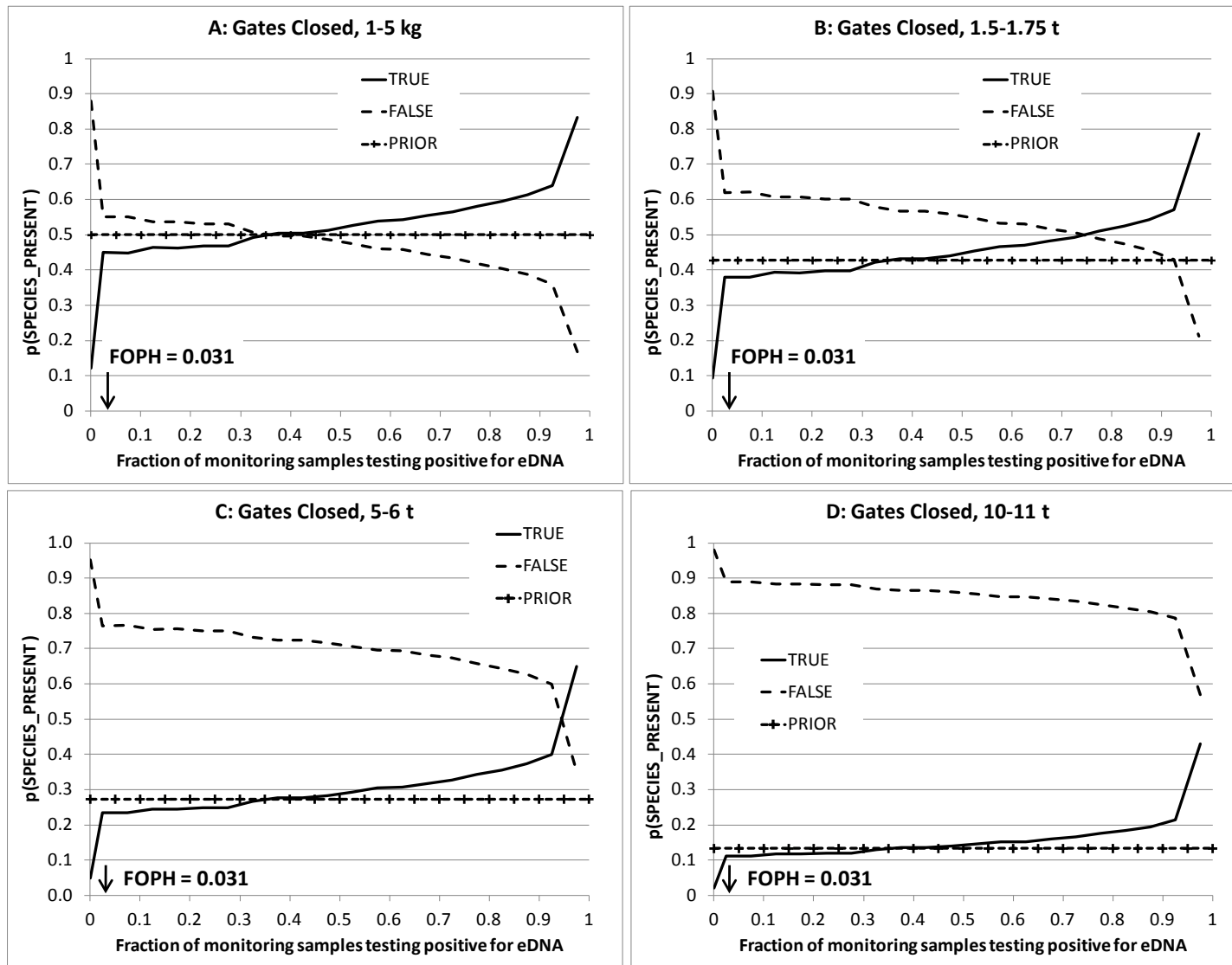


Figure 9.10: North Shore Channel (NSC), Gates Closed. F = The NSC has been fished so hard that no amount of eDNA would make you think there were 10-11 t of silver carp in the north shore channel.



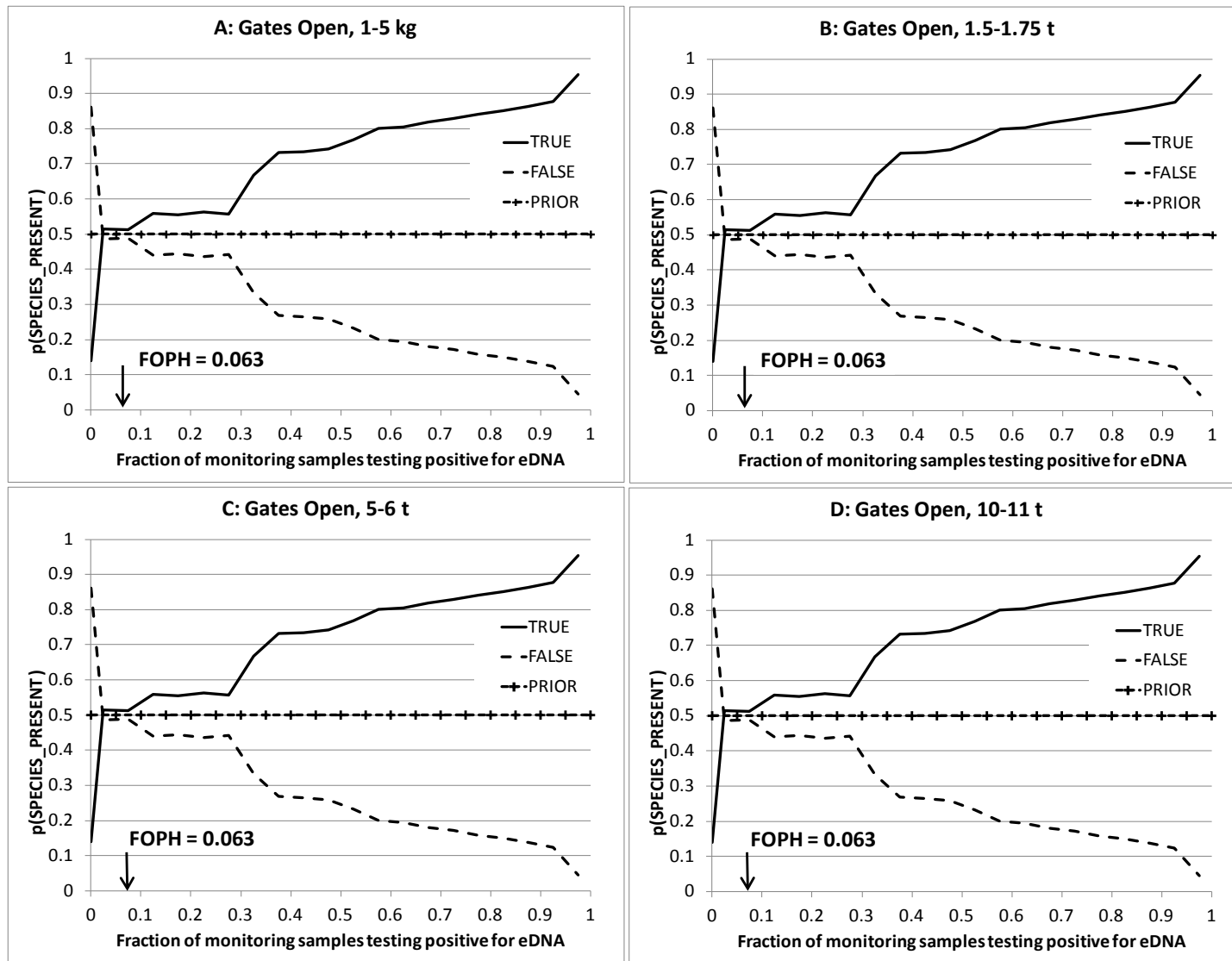


Figure 9.11: Chicago River from Chicago River Controlling Works to its Confluence with the North Branch of the Chicago River (CRM), Gates Open: Prior is 0.5 because no fishing effort there during 2009-2012.

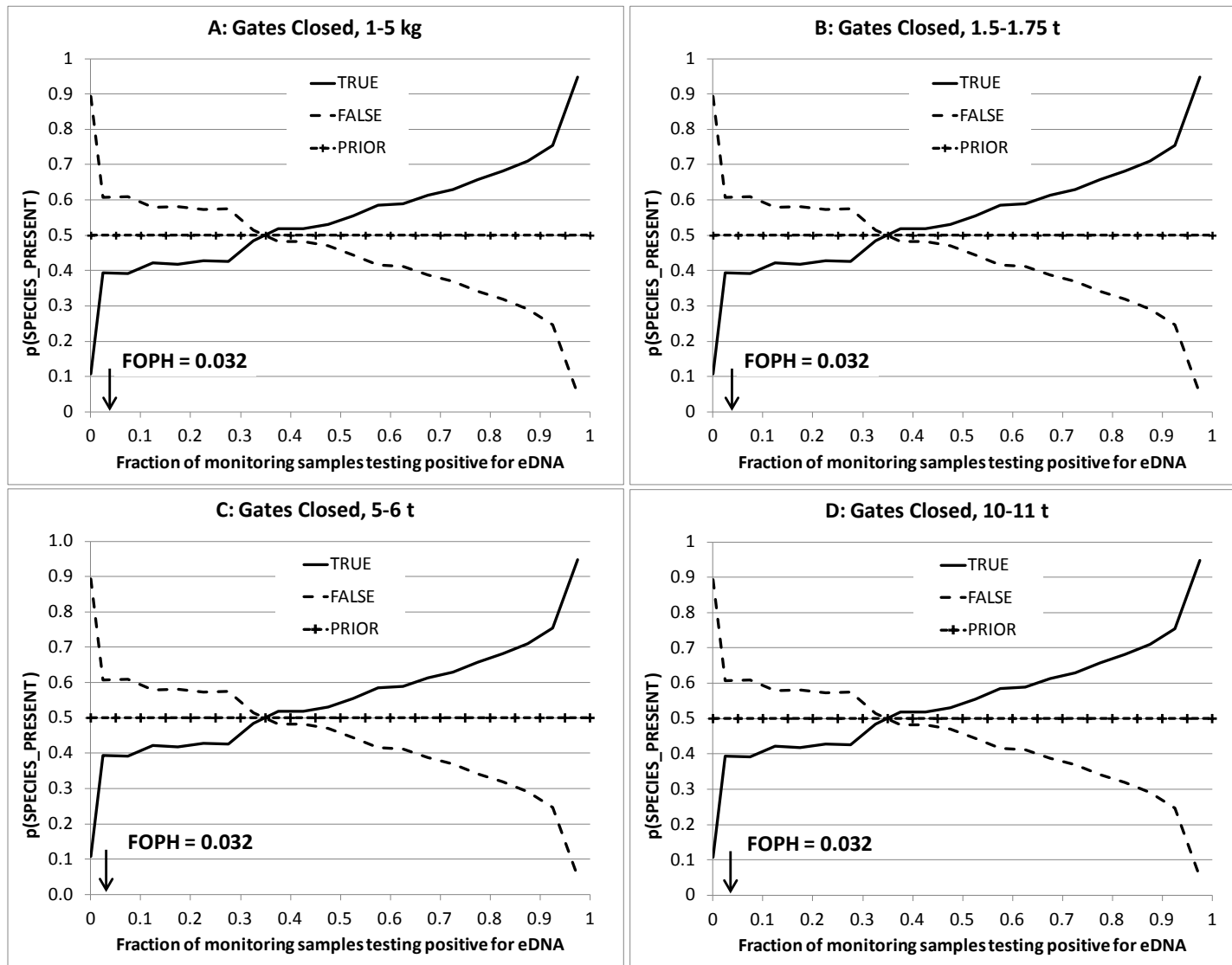


Figure 9.12: Chicago River from Chicago River Controlling Works to its Confluence with the North Branch of the Chicago River (CRM), Gates Closed: Prior is 0.5 because no fishing effort there during 2009-2012.

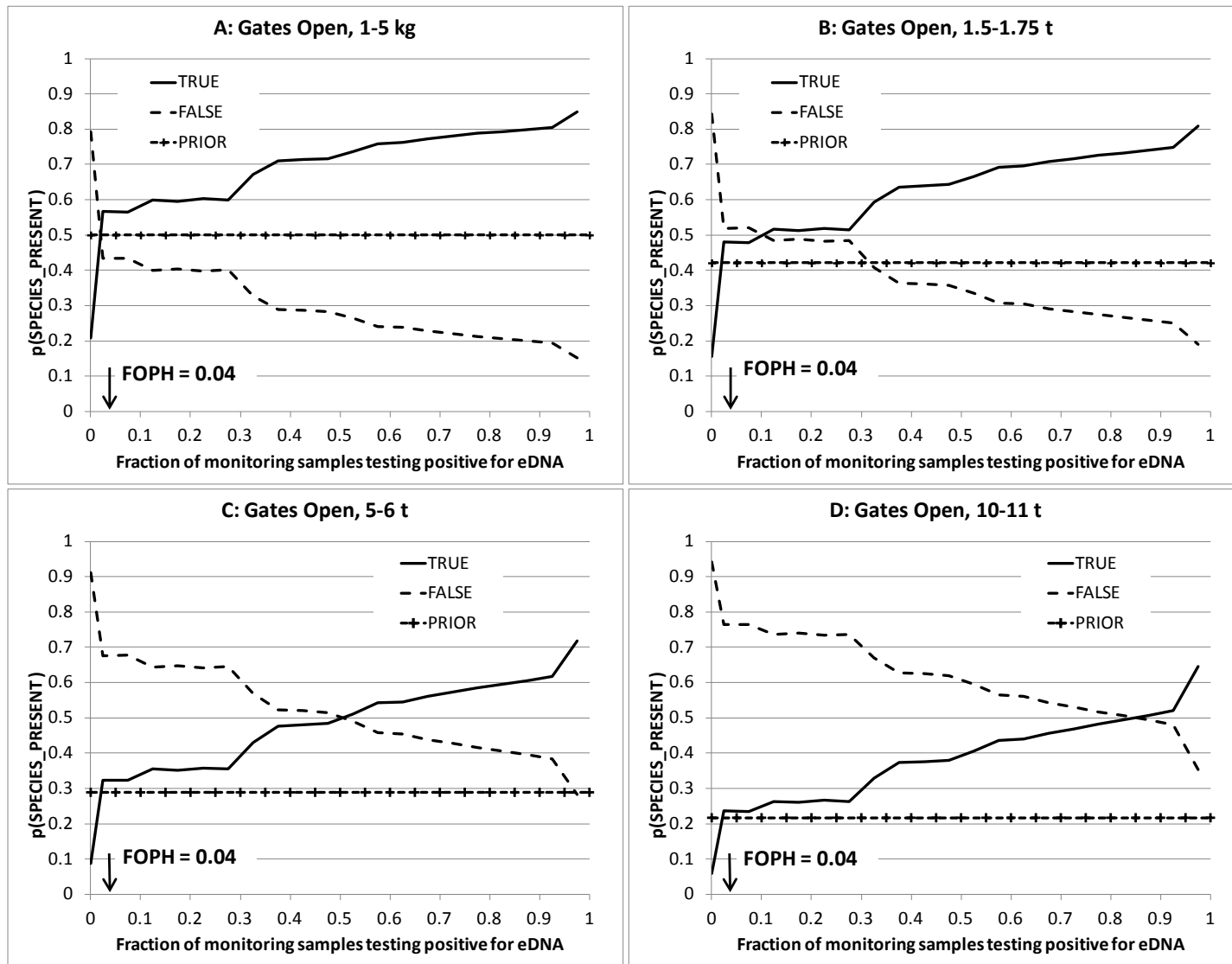


Figure 9.13 Chicago River from its Confluence with North Branch of the Chicago River to Bubbly Creek (CR2), Gates Open

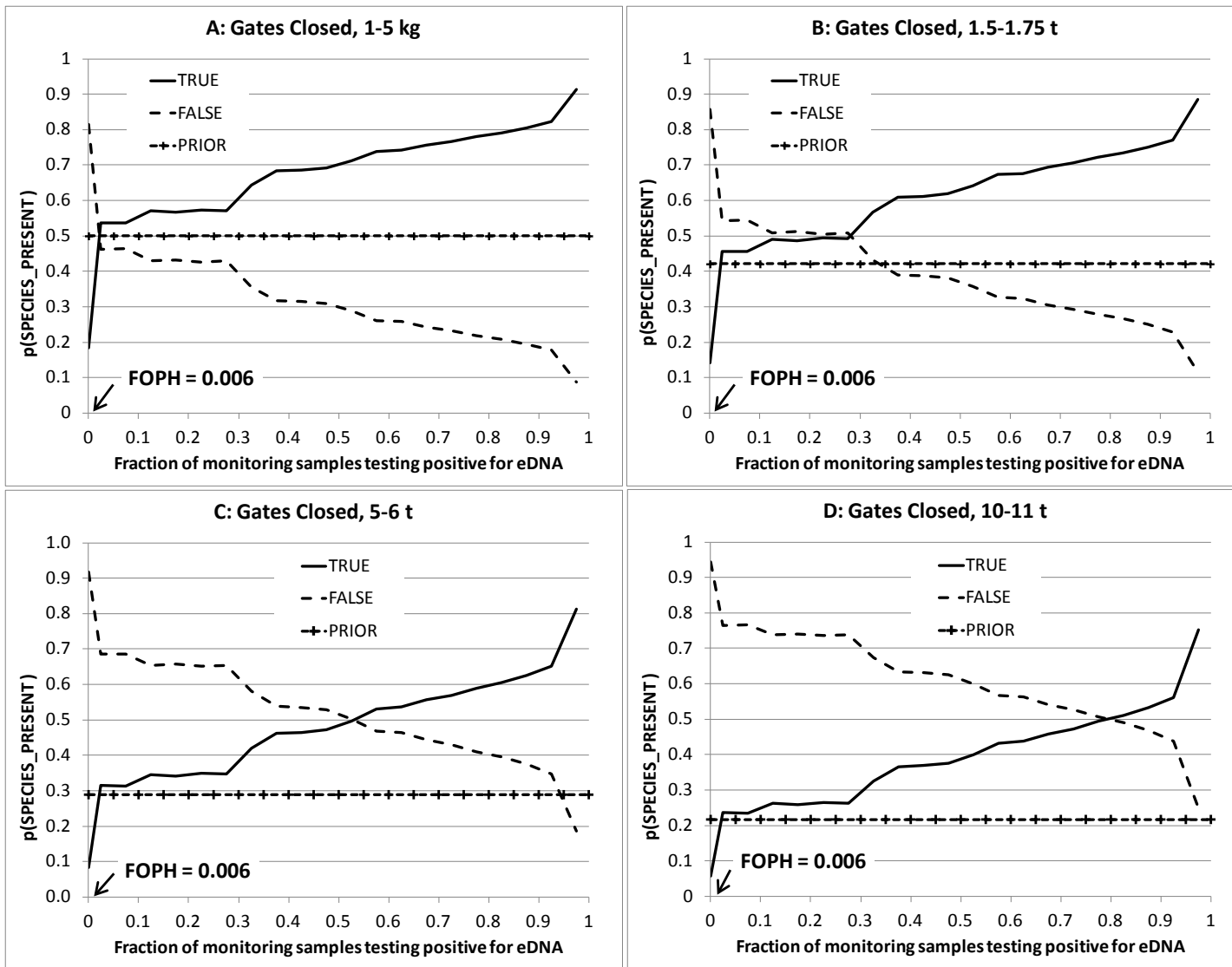


Figure 9.14: Chicago River from its Confluence with North Branch of the Chicago River to Bubbly Creek (CR2), Gates Closed

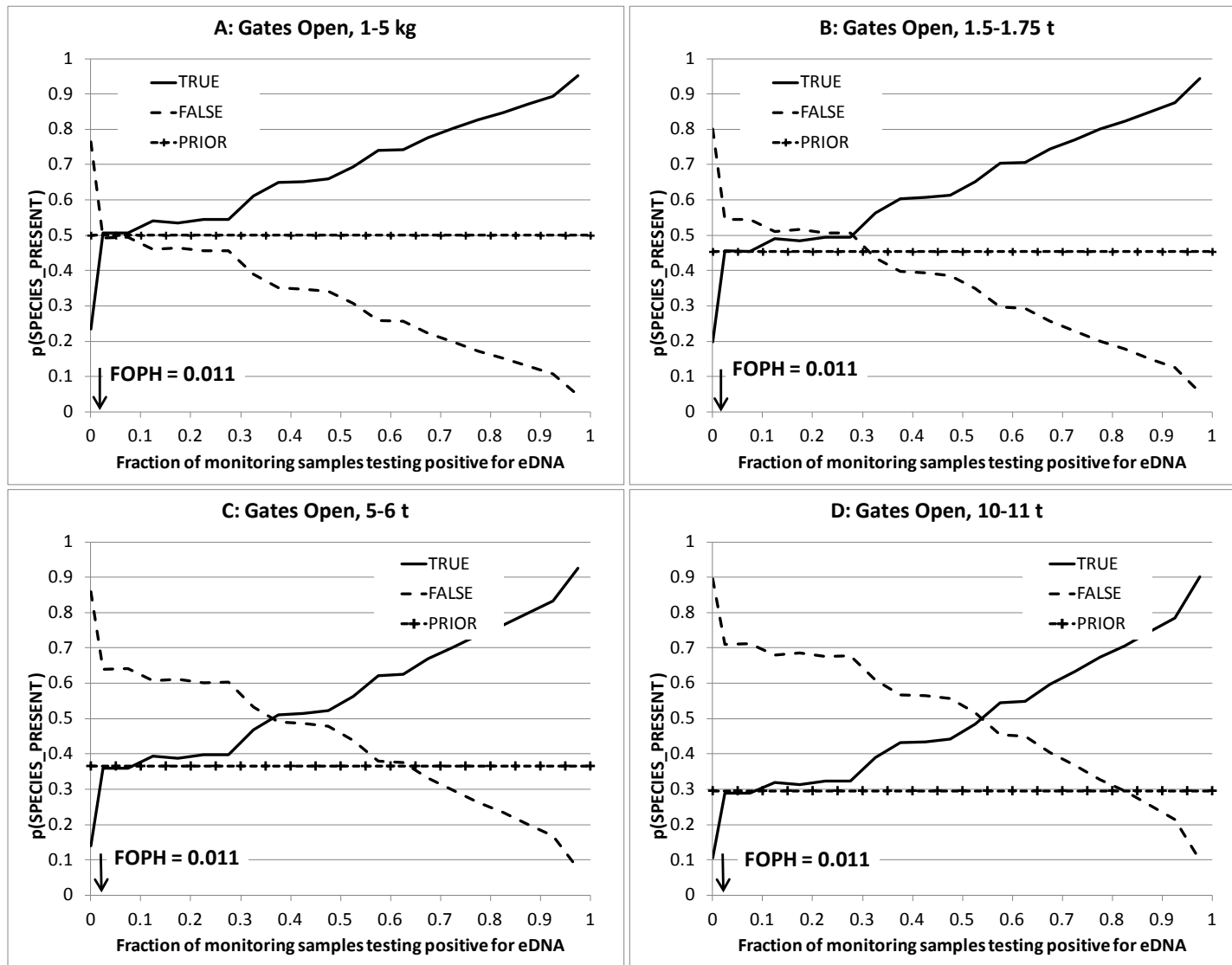


Figure 9.15: Reach CRD, Calumet River from the confluence with the Grand Calumet River to the confluence with the Little Calumet River, Gates Open Season.

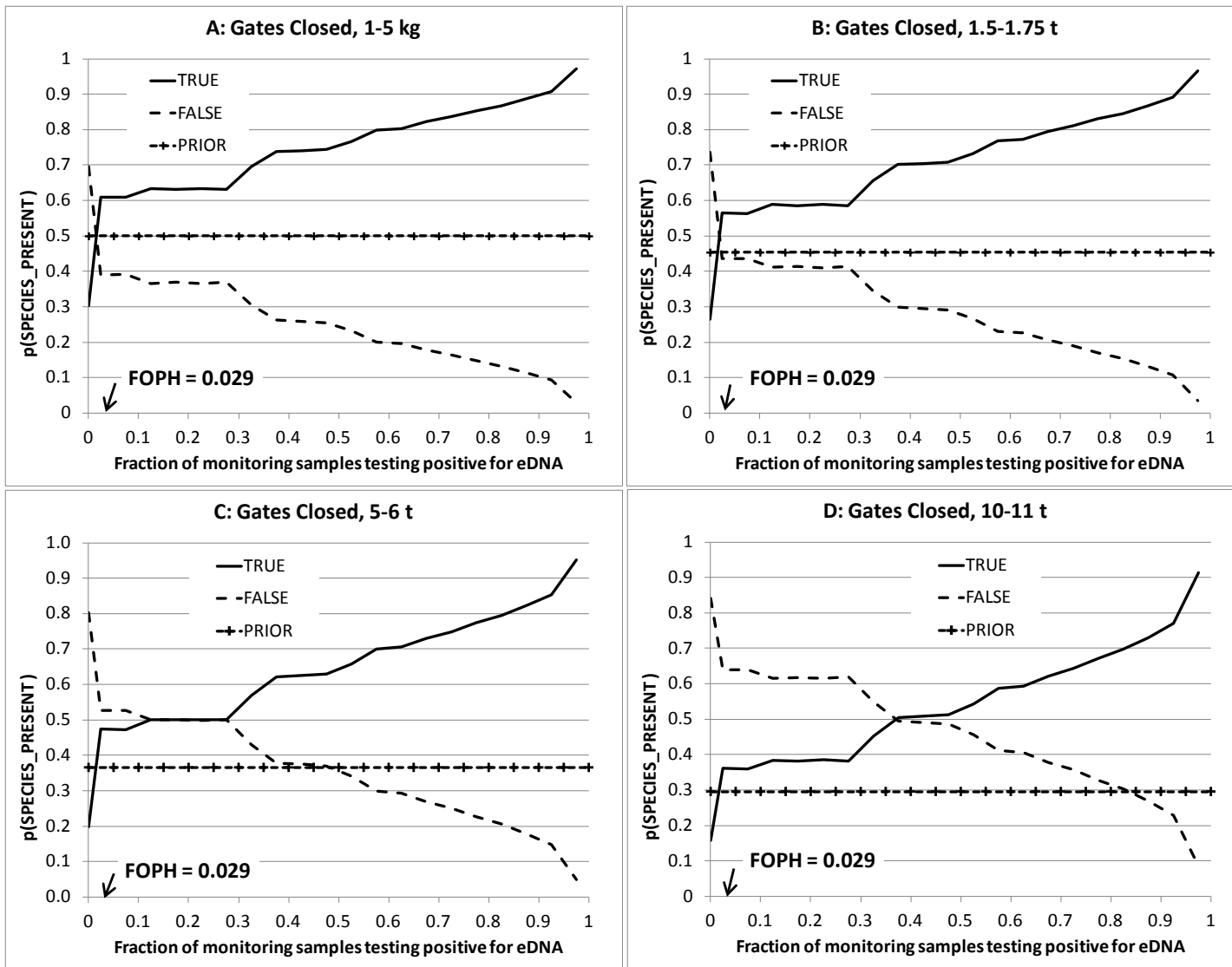


Figure 9.16: Reach CRD, Calumet River from the confluence with the Grand Calumet River to the confluence with the Little Calumet River, Gates Closed Season.

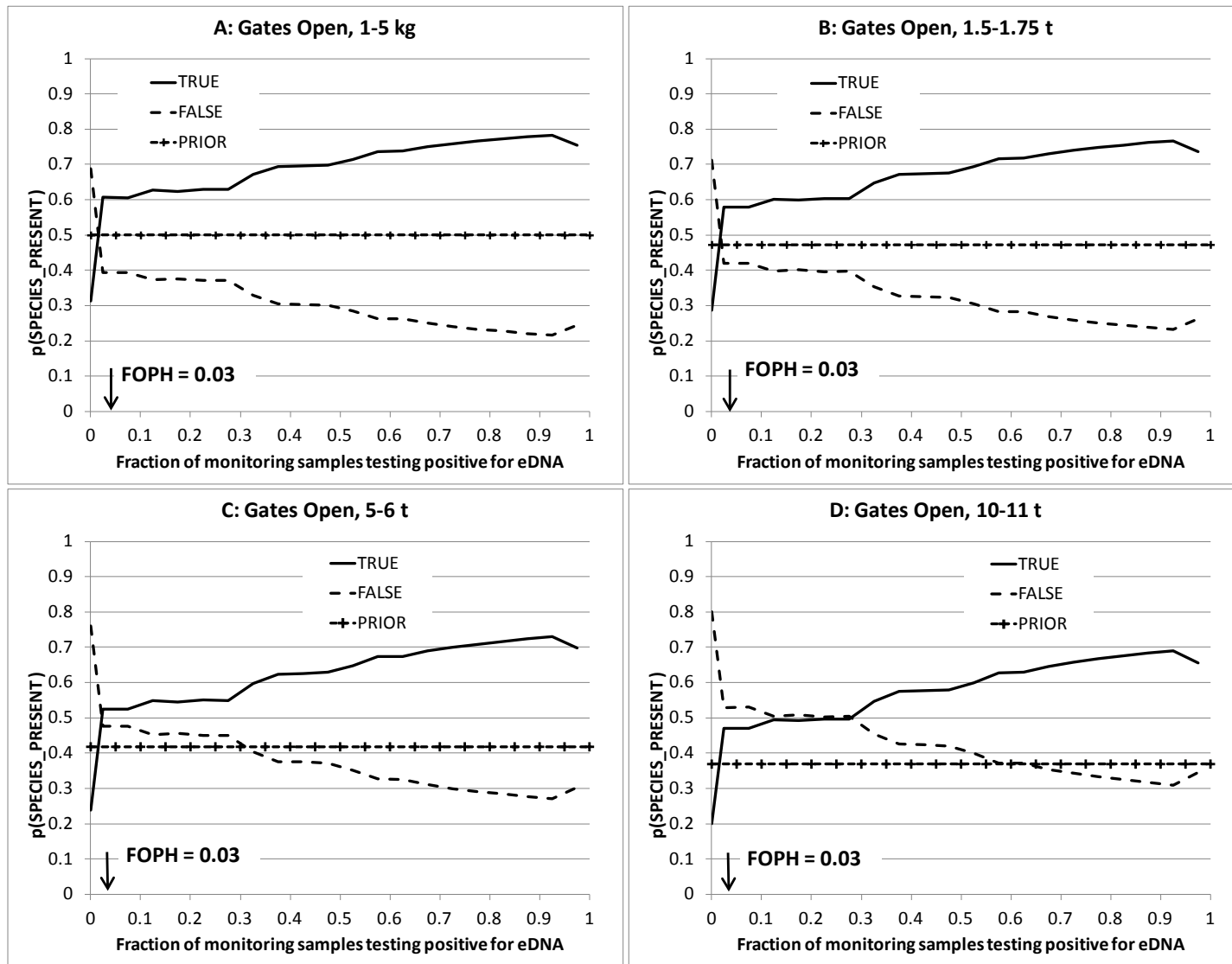


Figure 9.17: Reach CR5, CSSC from its confluence with the Cal-Sag Channel to the electric fish barrier, Gates Open Season.

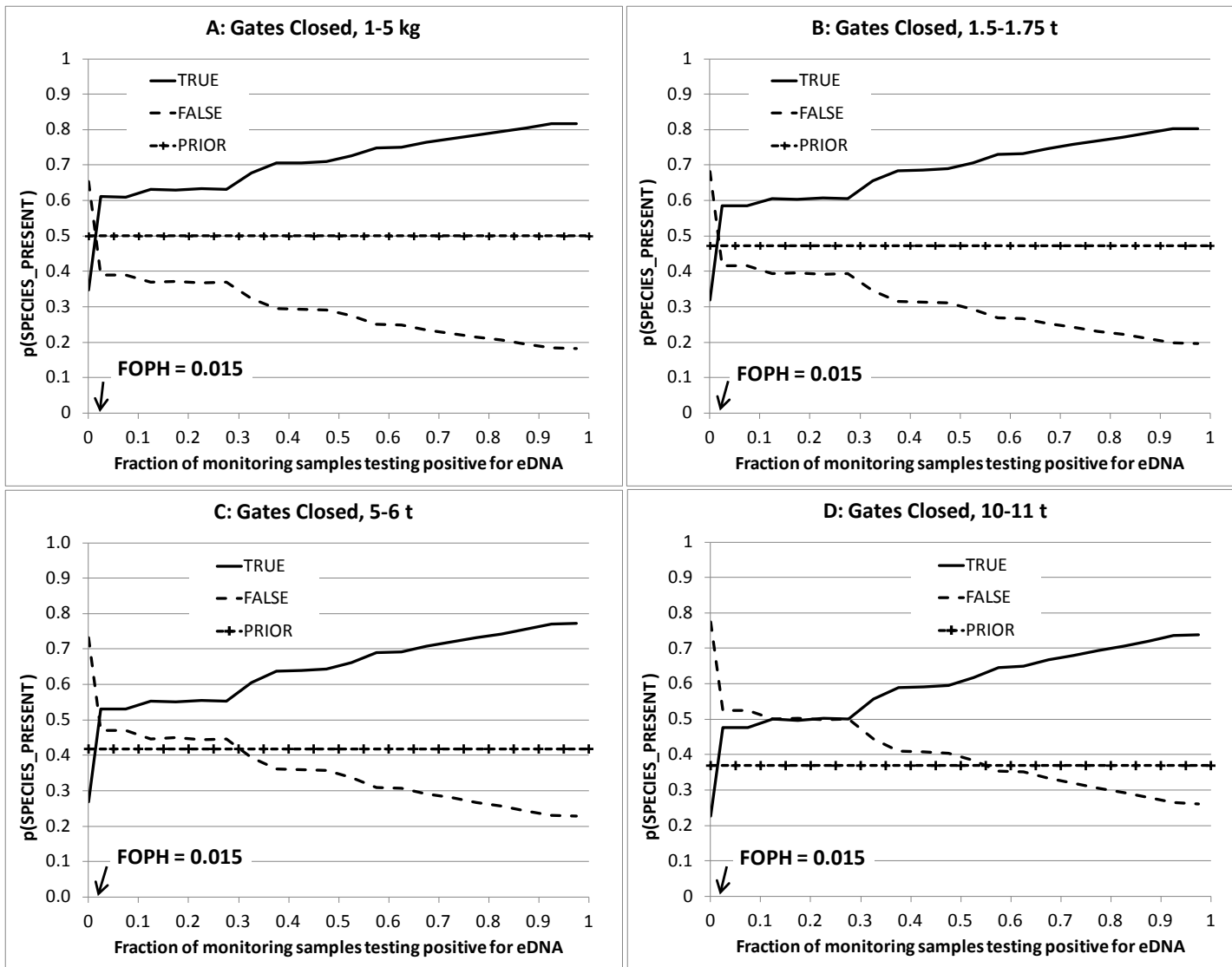


Figure 9.18: Reach CR5, CSSC from its confluence with the Cal-Sag Channel to the electric fish barrier, Gates Closed Season.



*This page left intentionally blank.*

Estimated Copy Number ( $N_A$ )	Bighead Carp			Silver Carp		
	Number of cPCR Replicates	Number of cPCR Reactions Testing Positive	Frequency of Positive Detections	Number of cPCR Replicates	Number of cPCR Reactions Testing Positive	Frequency of Positive Detections
1	60	13	0.217	60	17	0.283
2	30	21	0.700	30	9	0.300
3	30	24	0.800	30	9	0.300
4	30	24	0.800	30	17	0.567
5	60	49	0.817	60	51	0.850
6	30	28	0.933	30	19	0.633
7	30	29	0.967	-	-	-
8	30	29	0.967	30	27	0.900
9	30	30	1.000	30	28	0.933
10	60	60	1.000	60	59	0.983
11	30	30	1.000	30	30	1.000
12	30	30	1.000	30	29	0.967
13	30	30	1.000	30	29	0.967
14	30	30	1.000	30	30	1.000
15	30	30	1.000	30	30	1.000
50	30	30	1.000	30	30	1.000
100	30	30	1.000	30	30	1.000
200	30	30	1.000	30	30	1.000
500	30	30	1.000	30	30	1.000
1000	30	30	1.000	30	30	1.000

Table 2.1: Summary of experimental results used to estimate the probability of detection.

<b>Parameter</b>	<b>Bighead</b>	<b>Silver</b>
$k_D$	1.885	2.092
$\lambda_D$	1.486	2.238

Table 2.2: Parameters of Gamma distributions representing the probability of detection as a function of number of copies of the target marker in the replicate.

Estimated Copy Number ( $N_A$ )	Bighead Carp			Silver Carp		
	Number of Positive cPCR Replicates Sequenced	Number of Sequenced Replicates Matching the Target Species	Fraction of Positive cPCR Replicates Successfully Sequenced	Number of Positive cPCR Replicates Sequenced	Number of Sequenced Replicates Matching the Target Species	Fraction of Positive cPCR Replicates Successfully Sequenced
1	6	0	0.00000	6	6	1.0000
2	21	2	0.09524	9	8	0.8889
3	24	0	0.00000	9	9	1.0000
4	25	6	0.24000	17	16	0.9412
5	28	4	0.14286	21	20	0.9524
6	29	6	0.20690	19	18	0.9474
7	29	13	0.44828	5	5	1.0000
8	30	4	0.13333	27	24	0.8889
9	-	-	-	28	15	0.5357
10	-	-	-	29	29	1.0000
11	-	-	-	30	27	0.9000
12	-	-	-	29	28	0.9655
13	-	-	-	29	28	0.9655
14	-	-	-	30	30	1.0000
15	30	25	0.83333	30	30	1.0000
25	29	13	0.44828	-	-	-
50	30	21	0.70000	-	-	-
100	29	27	0.93103	-	-	-

Table 2.3: Summary of experimental results used to estimate the probability of positive cPCR replicates sequencing positive for the target species.

<b>Parameter</b>	<b>Bighead</b>	<b>Silver</b>
$k_s$	0.877	0.276
$\lambda_s$	41.631	6.963

Table 2.4: Parameters of a gamma distribution representing the probability of successfully sequencing the target marker after it has been detected by cPCR.

Target Marker Concentration ( $C_M$ , Copies/L)	Number of cPCR Replicates Needed to Achieve the stated Probability of Detection			
	$p[\text{ASSAY} = \text{POS}   C_M] = 0.50$		$p[\text{ASSAY} = \text{POS}   C_M] = 0.95$	
	Bighead	Silver	Bighead	Silver
100	> 100	24	> 100	>100
200	> 100	7	> 100	30
300	57	4	> 100	16
400	34	3	> 100	10
500	24	2	> 100	6
600	18	2	76	5
700	14	2	62	5
800	12	1	49	4
900	10	1	42	4
1000	9	1	36	3
2000	4	1	16	2
3000	3	1	11	2
4000	2	1	9	1

Table 2.5: Number of cPCR replicates needed to achieve a detection probability of at least 0.50 and 0.95 at selected source water concentrations,  $C_M$ .

EVENT	YEAR	MONTH	DAY	SEASON
1	2009	6	29	GATES OPEN
2	2009	7	10	GATES OPEN
3	2009	8	3	GATES OPEN
4	2009	8	19	GATES OPEN
5	2009	8	25	GATES OPEN
6	2009	9	4	GATES OPEN
7	2009	9	10	GATES OPEN
8	2009	9	23	GATES OPEN
9	2009	9	24	GATES OPEN
10	2009	10	1	GATES OPEN
11	2009	10	12	GATES OPEN
12	2009	10	15	GATES CLOSED
13	2009	10	22	GATES CLOSED
14	2009	10	29	GATES CLOSED
15	2009	11	24	GATES CLOSED
16	2009	12	1	GATES CLOSED
17	2009	12	2	GATES CLOSED
18	2009	12	8	GATES CLOSED
19	2010	3	30	GATES CLOSED
20	2010	4	15	GATES CLOSED
21	2010	4	20	GATES CLOSED
22	2010	5	6	GATES CLOSED
23	2010	5	12	GATES CLOSED
24	2010	5	20	GATES CLOSED
25	2010	5	27	GATES CLOSED
26	2010	6	29	GATES OPEN
27	2010	7	9	GATES OPEN
28	2010	7	13	GATES OPEN
29	2010	7	20	GATES OPEN
30	2010	7	22	GATES OPEN
31	2010	8	6	GATES OPEN
32	2010	8	11	GATES OPEN
33	2010	8	18	GATES OPEN
34	2010	10	6	GATES OPEN
35	2010	10	13	GATES OPEN
36	2010	11	2	GATES CLOSED
37	2010	11	8	GATES CLOSED
38	2010	11	15	GATES CLOSED
39	2010	11	30	GATES CLOSED
40	2010	12	7	GATES CLOSED
41	2011	5	10	GATES CLOSED
42	2011	5	16	GATES CLOSED
43	2011	6	15	GATES OPEN
44	2011	6	23	GATES OPEN
45	2011	6	27	GATES OPEN
46	2011	7	5	GATES OPEN
47	2011	7	12	GATES OPEN
48	2011	7	19	GATES OPEN
49	2011	8	1	GATES OPEN
50	2011	8	17	GATES OPEN
51	2011	8	22	GATES OPEN
52	2011	8	30	GATES OPEN
53	2011	9	6	GATES OPEN
54	2011	9	13	GATES OPEN
55	2011	9	19	GATES OPEN
56	2011	10	11	GATES OPEN
57	2011	10	18	GATES CLOSED
58	2011	10	25	GATES CLOSED
59	2011	10	26	GATES CLOSED
60	2011	10	27	GATES CLOSED
61	2012	5	22	GATES CLOSED
62	2012	6	11	GATES OPEN
63	2012	6	25	GATES OPEN
64	2012	7	10	GATES OPEN
65	2012	7	11	GATES OPEN
66	2012	7	24	GATES OPEN
67	2012	8	6	GATES OPEN
68	2012	8	20	GATES OPEN
69	2012	9	11	GATES OPEN
70	2012	9	17	GATES OPEN
71	2012	10	2	GATES OPEN
72	2012	10	15	GATES CLOSED
73	2012	10	22	GATES CLOSED
74	2013	6	18	GATES OPEN
75	2013	6	19	GATES OPEN
76	2013	11	5	GATES CLOSED
77	2013	11	6	GATES CLOSED
78	2013	11	7	GATES CLOSED

Table 3.1. Inventory of eDNA monitoring events during the period 2009 – 2013.

Event	Reach																			
	NSC	CR1	CRM	CR2	BCR	MXZ	CR3	CR4	CR5	FBA	CR6	CR7	CR8	CRA	CRB	CRC	CLK	LKC	CRD	CRE
1													0.6875							
2												0.0870	0.4615							
3								0.0000	0.0000	0.0000										
4										0.0435	0.3000									
5									0.0000	0.1053	0.0000									
6																				
7		0.0000	0.0000	0.0000																
8														0.0000		0.0000			0.5909	
9																				
10							0.0000	0.0000	0.0000										0.1429	
11																				
12										0.0909	0.0000									
13	0.0000	0.0000																		
14											0.0000	0.0000								
15									0.0000					0.0000	0.0000	0.0000	0.0000	0.0000	0.0588	0.0250
16			0.0000																	
17										0.0000	0.0000	0.0000								
18														0.0000		0.0000		0.0000	0.0000	
19														0.0000	0.0000	0.0000		0.0000	0.0000	
20																0.0000			0.0000	
21	0.0000	0.0000																		
22																				
23	0.0000																			
24																0.0000			0.0000	
25			0.0000	0.0000	0.0000	0.0000	0.0000													
26												0.0000	0.0000							
27																				
28										0.0000	0.0909	0.0000								
29														0.0000	0.0000	0.0000				
30															0.0000		0.0000	0.0000		
31																				
32																				
33																				
34																				
35									0.0000	0.0476	0.0513									
36			0.0000	0.0123	0.0000	0.0000														
37																0.0000			0.0000	0.0000
38	0.0091	0.0000																		
39									0.0000	0.0000	0.0000									
40								0.0000	0.0426											
41			0.0000	0.0000		0.0000														
42	0.0000	0.0000																		
43															0.0000	0.0000	0.0000	0.0000	0.0000	
44			0.0000	0.0000	0.0000	0.0000														
45	0.0000	0.0000																		
46																				
47															0.0000	0.0000	0.0000	0.0000	0.0000	
48														0.0000	0.0000	0.0000	0.0000	0.0000	0.0000	
49														0.0000	0.0000	0.0000	0.0000	0.0000	0.0000	
50			0.0000	0.0000	0.0000	0.0000	0.0000													
51	0.0000	0.0000																		
52									0.0000	0.0000	0.0000				0.0000	0.0000	0.0000	0.0000	0.0000	
53																				
54			0.0000	0.0000		0.0000														
55	0.0000	0.0000																		
56															0.0000	0.0000	0.0000	0.0000	0.0000	
57			0.0000	0.0000		0.0000														
58	0.0000	0.0000	0.0000	0.0000		0.0000	0.0000													
59								0.0000	0.0000											
60									0.0000						0.0000	0.0000	0.0000	0.0000	0.0000	0.0000
61															0.0000	0.0000	0.0000	0.0000	0.0000	
62	0.0000	0.0000													0.0000	0.0000	0.0000	0.0000	0.0000	
63															0.0000	0.0000	0.0000	0.0000	0.0000	
64	0.0000	0.0000	0.0000	0.0000		0.0000														
65																0.0000	0.0000	0.0000	0.0000	
66															0.0000	0.0000	0.0000	0.0000	0.0000	
67			0.0000	0.0000		0.0000														
68															0.0000	0.0000	0.0000	0.0000	0.0000	
69	0.0000	0.0000	0.0000	0.0000		0.0000														
70															0.0000	0.0000	0.0000	0.0000	0.0000	
71	0.0000	0.0000	0.0000	0.0000		0.0000														
72	0.0000	0.0000																		
73																				
74															0.2500	0.0000	0.0714	0.1667	0.0000	
75	0.0000	0.0000	0.0000	0.0000		0.0000									0.0000	0.0000	0.0000	0.0000	0.0000	
76															0.0000	0.0000	0.0000	0.0000	0.0000	
77			0.0000																	
78	0.0000	0.0000																		

Table 3.2: Fraction of monitoring samples testing positive for bighead carp by monitoring event and CAWS reach.



Event	Reach																			
	NSC	CR1	CRM	CR2	BCR	MXZ	CR3	CR4	CR5	FBA	CR6	CR7	CR8	CRA	CRB	CRC	CLK	LKC	CRD	CRE
1													0.4375							
2												0.3200	0.5833							
3								0.0000	0.0000	0.0000										
4										0.1739	0.1250									
5									0.2500	0.0000	0.1724									
6																				
7		0.0000	0.0000	0.0000																
8														0.0000		0.0000			0.0227	
9																				
10							0.3333	0.0000	0.0357											0.0000
11																				
12										0.0909	0.0000									
13	0.1111	0.0000																		
14											0.0000	0.0000								
15								0.0000						0.0000	0.0000	0.0000	0.0000	0.0000	0.0000	0.0500
16			0.0000																	
17										0.1765	0.3158	0.5000								
18														0.0870		0.0000		0.0000	0.0303	
19														0.0000	0.0000	0.0000		0.0000	0.0233	
20																0.0000			0.0000	
21	0.0149	0.0000																		
22																				
23	0.0000																			
24																0.0000			0.0000	
25			0.0500	0.0222	0.0769	0.3333	0.1176													
26												0.3448	0.6774							
27																				
28										0.1905	0.5909	0.3333								
29														0.0000	0.0000	0.0000				
30															0.0000		0.0000	0.0000		
31																				
32																				
33																				
34																				
35								0.0741	0.0952	0.1538										
36			0.0000	0.0000	0.0000	0.0000														
37																0.0000			0.0104	0.0000
38	0.0091	0.0000																		
39									0.0222	0.0000	0.0000									
40								0.0000	0.0000											
41			0.0000	0.0127		0.0000														
42	0.0000	0.0000																		
43															0.0000	0.0667	0.1667	0.1176	0.0000	
44			0.0000	0.0000	0.0000	0.0000														
45	0.0095	0.0000																		
46																				
47															0.0000	0.0000	0.0000	0.0625	0.0000	
48														0.0000	0.0000	0.0000	0.0000	0.0313	0.0200	
49														0.0000	0.0000	0.0000	0.0000	0.0000		
50			0.0000	0.0137	0.0000	0.0000	0.0000													
51	0.0000	0.0000																		
52															0.0000	0.0000	0.0000	0.0323	0.0000	
53								0.0000	0.0000	0.0000										
54			0.0000	0.0000		0.0000														
55	0.0189	0.0000																		
56														0.0000	0.0000	0.0000	0.0000	0.0000	0.0000	
57			0.0417	0.0000		0.0000														
58	0.0090	0.0000	0.1053	0.0000		0.0000	0.0000													
59								0.0000	0.0192											
60									0.0000						0.0000	0.0000	0.0000	0.0000	0.0196	0.0885
61														0.6667	0.2143	0.2500	0.1667	0.0600		
62	0.0189	0.0000												0.0000	0.0000	0.1429	0.0625			
63														0.0000	0.1538	0.0667	0.1333	0.0000		
64	0.0545	0.0000	0.0000	0.1429		0.1429														
65															0.0000	0.0000	0.0667			
66														0.0000	0.0000	0.0769	0.0645			
67			0.0000	0.0000		0.0000														
68														0.0000	0.1429	0.0000	0.1875	0.0000		
69	0.2075	0.5000	0.8000	0.1429		0.0000														
70														0.0000	0.2308	0.1538	0.2424	0.0588		
71	0.1321	0.2500		0.1290		0.4286														
72	0.1509	0.0000																		
73														0.7500	0.4615	0.6429	0.9167	0.1190		
74														0.0000	0.0000	0.4286	0.0000	0.1613		
75	0.1132	0.0000	0.0667	0.0000		0.0000														
76														0.0000	0.0769	0.0000	0.0000	0.0196		
77			0.0000																	
78	0.0179	0.0000																		

Table 3.3: Fraction of monitoring samples testing positive for silver carp by monitoring event and CAWS reach.

<b>SYMBOL</b>	<b>DESCRIPTION</b>
LMI	Lake Michigan (LMI).
NSC	North Shore Channel (NSC) from the Wilmette Pump Station to the North Branch of the Chicago River (NBC).
NBC	North Branch of the Chicago River (NBC) upstream of its confluence with NSC.
CR1	North Branch of the Chicago River (CR1) below the confluence of NBC and NSC to the South Branch of the Chicago River (CR2).
CRM	Chicago Sanitary and Ship Canal (CSSC) from LMI at the Chicago River Controlling Works (CRCW) to its confluence with CR2.
CR2	CSSC from the confluence of the North Branch of the Chicago River (CR1) and CRM to the upstream boundary of CR3.
BCR	Bubbly Creek (BCR), a canal extending south from the main stem of the CSSC at MXZ to its terminus, 1.3 miles upstream.
MXZ	A turning basin at the base of Bubbly Creek that separates BCR, CR2, and CR3.
CR3	CSSC from MXZ to a point just upstream of Stickney Water Reclamation Plant (WRP).
CR4	CSSC from Stickney WRP to its confluence with the Cal-Sag Channel (CRE).
CR5	CSSC from the confluence of CR4 and CRE to the upstream boundary of the electric fish barrier.
FBA	CSSC between the upstream and downstream boundaries of the electric fish barrier (FBA).
CR6	CSSC from the downstream boundary of FBA to Lockport Lock and Dam.
CR7	Illinois River from Lockport Lock and Dam to Brandon Road Lock and Dam.
CR8	Illinois River from Brandon Road Lock and Dam to Dresden Lock and Dam.
CRA	Calumet River from Lake Michigan to the canal linking the Calumet River to Lake Calumet.
CLK	The canal linking the Calumet River to Lake Calumet.
LKC	Lake Calumet.
CRB	A mixing zone at the confluence of CRA and CLK.
CRU	Little Calumet River from CRB to O'Brien Lock and Dam. This reach was formerly the upstream portion of CRC.
CRV	Little Calumet River from O'Brien Lock and Dam to the confluence with the Grand Calumet River (GCR). This reach was formerly the downstream portion of CRC.
CRD	Little Calumet River from its confluence with GCR to the South Branch of the Little Calumet River (LCR).
CRE	Cal-Sag Canal from the South Branch of the Little Calumet River to CR5
GCR	Grand Calumet River (GCR).
LCR	South Branch of the Little Calumet River (LCR).

Table 3.4: Main stem reaches of the CAWS.

Event	Bighead Carp			Silver Carp		
	5 <sup>th</sup> Percentile	50 <sup>th</sup> Percentile	95 <sup>th</sup> Percentile	5 <sup>th</sup> Percentile	50 <sup>th</sup> Percentile	95 <sup>th</sup> Percentile
1*	145	1500	2855	145	1500	2855
13	0	103	1076	5	214	1315
21	1	42	277	13	110	394
23	1	29	152	12	64	190
38	9	52	164	18	64	156
42	7	42	128	14	48	113
45	6	35	105	18	51	108
51	6	30	89	15	42	89
55	5	26	78	19	45	88
58	4	23	69	22	47	88
62	4	21	62	24	49	87
64	4	19	56	26	50	86
69	4	18	51	28	52	87
71	3	16	47	30	54	89
72	3	15	43	32	56	90
75	3	14	40	33	57	90
78	3	13	38	35	57	89

\* The NSC was not sampled during the first monitoring event; therefore, the prior distribution carries forward until the first monitoring event.

Table 3.5: Median target marker concentrations (copies/L) and 90 percent confidence bounds for bighead carp and silver carp in the NSC.

Degradation Trial	Fast Fraction		Slow Fraction		Fraction Fast
	-k (d <sup>-1</sup> )	R <sup>2</sup>	-k (d <sup>-1</sup> )	R <sup>2</sup>	
1	-0.682	0.492	-0.017	0.026	0.897
2	-0.370	0.514	-0.110	0.325	0.767
3	-0.167	0.869	-0.119	0.573	0.670
4	-0.272	0.467	-0.060	0.071	0.704
5	-0.425	0.567	-	-	-
6	-0.759	0.920	-0.140	0.020	0.915
7	-0.516	0.656	-	-	0.897
Mean	-0.456	-	-0.089	-	0.808
Standard deviation	0.213	-	0.050	-	0.108

Table 4.1: Degradation rates estimated from ECALS degradation rate trials. Data from Lance *et al.* (2013).

Parameter	Fast fraction	Slow fraction
	$-k$ ( $d^{-1}$ )	$-k$ ( $d^{-1}$ )
Mean	-0.463	-0.079
Standard deviation	0.171	0.036

Table 4.2: Mean and standard deviation of the degradation rate from fitted distributions

Secondary source		Loading factor	Loading rate
a	Piscivorous bird feces	Surface area (sq. km)	copies / m <sup>2</sup>
b	Combined sewer overflows	CSO discharge volume (m <sup>3</sup> /day)	copies / m <sup>3</sup>
c	Lake Michigan inflows	Volume (m <sup>3</sup> / day)	copies / m <sup>3</sup>
d	Mud-to-Parks Program sediment	Mass of sediment deposited (tons)	<i>Not estimated directly</i>
e	Commercial navigation	Commercial boat residence time (hrs)	copies / hr
f	Commercial fishing nets	Commercial net length (100 meters)	copies / 100 m
g	Recreational fishing derbies	Recreational boat days (boat-days)	copies / boat-day

Table 4.3: Loading factors and loading rates for confirmed secondary sources of eDNA in the CAWS

#	Reach	Surface Area (Km <sup>2</sup> )													Total Area (Km <sup>2</sup> )	Fraction of Total Area
		Main Stem	Backwaters and Barge Slips													
			A	B	C	D	E	F	G	H	I	J	K	L		
1	NSC	0.348	-	-	-	-	-	-	-	-	-	-	-	-	0.348	0.027
2	CR1	0.667	-	-	-	-	-	-	-	-	-	-	-	-	0.667	0.052
3	CRM	0.200	0.045	0.014	-	-	-	-	-	-	-	-	-	-	0.258	0.020
4	CR2	0.365	0.011	0.001	0.010	0.020	-	-	-	-	-	-	-	-	0.407	0.032
5	CR3	0.657	0.010	0.019	0.017	-	-	-	-	-	-	-	-	-	0.704	0.055
6	MXZ	0.042	0.009	-	-	-	-	-	-	-	-	-	-	-	0.051	0.004
7	BCR	0.091	-	-	-	-	-	-	-	-	-	-	-	-	0.091	0.007
8	CR4	1.617	-	-	-	-	-	-	-	-	-	-	-	-	1.617	0.127
9	CR5	0.566	0.022	0.022	0.022	0.001	0.047	0.046	0.026	0.033	-	-	-	-	0.785	0.062
10	FBA	0.099	-	-	-	-	-	-	-	-	-	-	-	-	0.099	0.008
11	CR6	0.506	0.019	0.007	-	-	-	-	-	-	-	-	-	-	0.532	0.042
12	CRA	1.009	0.022	0.037	0.012	0.009	0.013	0.005	0.014	0.014	0.019	0.015	0.015	0.032	1.215	0.096
13	CRB	0.147	-	-	-	-	-	-	-	-	-	-	-	-	0.147	0.012
14	CLK	0.430	0.074	0.032	-	-	-	-	-	-	-	-	-	-	0.536	0.042
15	LKC	1.723	-	-	-	-	-	-	-	-	-	-	-	-	1.723	0.135
16	CRU	0.204	-	-	-	-	-	-	-	-	-	-	-	-	0.204	0.016
17	CRV	0.048	-	-	-	-	-	-	-	-	-	-	-	-	0.048	0.004
18	CRD	1.306	0.063	0.019	0.008	-	-	-	-	-	-	-	-	-	1.397	0.110
19	CRE	1.884	-	-	-	-	-	-	-	-	-	-	-	-	1.884	0.148
<b>Total Area (Km<sup>2</sup>)</b>															12.721	-

Table 4.4: Surface area of CAWS reaches.

Year	Reach	Seasonal Discharge Volume (1,000 m <sup>3</sup> )	
		Gates Open	Gates Closed
2009	CRD	21	6,027
	CRE	29	8,094
	BCR	5,432	44,056
	NSC	2,689	13,165
	CR1	5,147	25,201
	CR2	1,997	9,779
	CRM	3,150	15,421
	CR3	2,411	4,408
2010	CRD	14,063	2,641
	CRE	18,885	3,547
	BCR	19,867	7,349
	NSC	50,603	6,431
	CR1	96,868	12,310
	CR2	37,591	4,777
	CRM	59,277	7,533
	CR3	69,711	3,980
2011	CRD	6,212	2,912
	CRE	8,342	3,910
	BCR	15,242	21,626
	NSC	9,021	11,409
	CR1	17,269	21,841
	CR2	6,702	8,476
	CRM	10,568	13,365
	CR3	16,773	5,874
2012	CRD	873	328
	CRE	1,172	441
	BCR	5,201	4,022
	NSC	447	1,560
	CR1	856	2,986
	CR2	332	1,159
	CRM	524	1,827
	CR3	4,565	2,611
CR4	10,565	6,044	

Table 4.5: CSO discharge volumes (1000 m<sup>3</sup>) by reach and year.



Diversion Point	Calendar Year	Average Daily Flows from Lake Michigan (m <sup>3</sup> /day)	
		Season: Gates Open	Season: Gates Closed
CRA at Calumet River Entrance	2009	834.6	117.5
	2010	974.6	171.1
	2011	888.2	52.7
	2012	919.2	55.3
CRM at Chicago River Controlling Works (CRCW)	2009	891.6	135.6
	2010	833.8	108.0
	2011	819.1	41.5
	2012	806.5	45.8
NSC at Wilmette Pump Station	2009	319.7	31.1
	2010	188.4	32.8
	2011	348.2	9.5
	2012	204.6	2.6

Table 4.6: Volume of water diversions from Lake Michigan during each season for the period 2009 through 2012.

Year	Sediment Dredged From:	Sediment Transported To:	Tons	Number of Barges
2002	Lower Peoria Lake, East side of Navigation Channel, from the channel to East Port or Spindler Marina	Paxton 1 Landfill near Lake Calumet.	1,000	0.667
2004	Spindler Channel	US Steel South Works. Barges were tied up in the North Slip and deposition was to Park 523 (50 barge loads) on the south side of the slip, and on Park 566 to the north (20 barges).	105,000	70
2007	Spindler Channel	South Works site (Park 566) on the north west side away from the lake.	9,750	6.5
2012	Spindler Channel or East Port Channel	Barges were unloaded to the north side of the North Slip (Park 566), from early Sept until Thanksgiving week.	90,000	60
2013	Spindler Channel	Park 566	30,000	20

Table 4.7: Mud-to-Parks transfers of dredged material from the Illinois River at Peoria, IL to locations near Chicago, IL. Data courtesy of Dr. John Marlin, Prairie Research Institute.

Reach	Calendar Year: 2012				Calendar Year: 2013			
	Season: Gates Closed		Season: Gates Open		Season: Gates Closed		Season: Gates Open	
	D = False	D = True	D = False	D = True	D = False	D = True	D = False	D = True
NSC	0.0	0.0	0.0	0.0	0.0	0.0	0.0	0.0
CR1	413.7	164.4	529.0	55.3	216.8	706.9	52.6	615.8
CRM	2.8	1.7	33.4	0.8	55.4	13.3	49.2	0.8
CR2	1,061.9	454.1	795.8	64.8	603.5	633.8	203.6	1,012.7
CR3	1,042.2	775.9	996.7	245.5	712.5	2,318.6	195.3	957.3
MXZ	45.4	0.2	5,748.5	0.0	40.8	7.3	27.0	15.2
BCR	1.5	0.0	1.2	0.0	2.1	0.0	0.7	0.0
CR4	2,144.2	1353.6	1,030.4	701.4	855.0	2,198.6	2,324.9	1,380.8
CR5	39,556.7	27,637.2	19,290.8	11,039.8	14,737.6	38,369.6	9,188.3	26,274.0
FBA	476.3	587.1	233.3	377.8	260.8	775.0	210.6	557.8
CR6	1,973.3	5,792.2	746.5	1,689.1	1,853.2	5,707.9	2,398.1	2,907.7
CRA	31,001.7	2,930.9	28,175.0	1,985.3	28,403.6	3,041.8	22,734.6	1,859.8
CRB	452.5	97.8	310.5	83.1	274.1	102.6	267.3	51.3
CLK	4,721.0	355.6	1,402.2	175.3	2,488.3	1,291.6	5,697.9	637.9
LKC	24.8	0.0	36.1	1.1	157.5	0.3	150.8	0.7
CRU	831.8	327.7	411.0	465.2	583.2	216.9	455.4	236.6
CRV	195.1	76.9	96.4	109.1	136.8	50.9	106.8	55.5
CRD	982.9	619.9	429.3	624.3	1,300.1	2,571.7	721.2	1,694.4
CRE	2028.8	2,548.4	894.9	1,667.5	1,777.1	3,225.5	2,327.3	923.8

Table 4.8: Commercial vessel residence time (hours) by calendar year, season, reach, and condition D, whether or not vessels had a history of being below Dresden within three months of being detected in a reach.

Year	Month	Commercial vessel sampling rate (% of lock-master counts)		
		Dresden L&D	Lockport L&D	T.J. O'Brien L&D
2012	January	16.11	99.00	46.10
	February	83.71	99.00	47.73
	March	59.91	99.00	54.38
	April	44.14	99.00	77.60
	May	32.38	99.00	89.82
	June	54.67	99.00	86.77
	July	85.53	97.20	89.24
	August	84.75	99.00	88.55
	September	99.00	99.00	87.50
	October	76.82	99.00	84.89
	November	81.90	99.00	91.20
	December	99.00	99.00	93.16
2013	January	93.38	99.00	96.03
	February	52.38	99.00	87.50
	March	86.67	99.00	91.67
	April	87.20	99.00	83.96
	May	93.81	99.00	87.97
	June	98.93	99.00	79.29
	July	89.74	99.00	81.48
	August	97.97	99.00	90.57
	September	99.00	99.00	85.81
	October	100.00	99.00	89.68
	November	92.42	99.00	90.28
	December	97.45	99.00	99.00

Table 4.9: Monthly NAIS commercial vessel sampling rate at three reference points in the CAWS for calendar years 2012 and 2013.

Year	Commercial Vessel Sampling Rate (% of lock-master counts)	
	Lockport L&D (%)	T.J. O'Brien L&D (%)
2009	0.00	0.00
2010	0.00	0.00
2011	32.07	46.09
2012	99.00	78.12
2013	99.00	89.09

Table 4.10: Annual NAIS commercial vessel sampling rate at two reference points in the CAWS for calendar years 2009 - 2013.

Reach	2010	2010	2011	2011	2012	2012	2013
	Gates closed	Gates open	Gates closed	Gates open	Gates closed	Gates open	Gates closed
NSC	6.38	28.44	27.43	51.66	39.15	53.04	32.92
CR1	0.00	21.79	16.46	39.78	43.89	84.12	38.40
CRM	0.00	0.00	0.00	0.00	0.00	0.00	0.00
CR2	0.00	36.93	32.46	64.01	43.70	58.52	16.46
BCR	0.00	1.48	0.00	1.83	0.00	0.00	0.00
MXZ	0.00	8.67	10.52	19.20	23.77	36.58	14.63
CR3	0.00	16.25	17.83	33.83	25.60	38.40	14.63
CR4	0.00	5.91	0.00	7.32	29.26	93.27	36.58
CR5	0.00	0.00	0.00	0.00	0.00	0.00	7.32
FBA	0.00	0.00	0.00	0.00	0.00	0.00	0.00
CR6	0.00	0.00	0.00	0.00	0.00	0.00	0.00
CRA	0.00	0.00	0.00	0.00	9.14	27.43	18.29
CRB	0.00	3.69	1.83	4.57	0.00	7.32	5.49
CLK	0.00	19.21	3.66	27.43	35.66	65.84	20.12
LKC	0.00	160.19	118.87	224.49	89.61	177.42	54.86
CRU	0.00	9.60	3.20	16.46	16.46	27.43	9.14
CRV	0.00	3.69	0.00	4.57	0.00	0.00	0.00
CRD	0.00	107.11	111.10	206.65	91.44	137.16	51.21
CRE	0.00	0.00	34.75	0.00	45.72	71.32	42.06
<b>TOTAL</b>	<b>6.38</b>	<b>422.98</b>	<b>378.10</b>	<b>701.80</b>	<b>493.42</b>	<b>877.85</b>	<b>362.10</b>

Table 4.11: Potentially contaminated commercial gill and trammel net effort in the CAWS from 2010 through 2013 by reach, year and season. Includes imputed FRS fishing effort for 2010 and excludes commercial gill and trammel nets used after May 4, 2013, when the use of such nets was discontinued. Units are 100-meters of net length.

Reach	2010	2010	2011	2011	2012	2012	2013
	Gates closed	Gates open	Gates closed	Gates open	Gates closed	Gates open	Gates closed
NSC	27.36	28.44	27.43	51.66	62.33	53.04	32.92
CR1	0.00	21.79	16.46	39.78	43.89	84.12	38.40
CRM	0.00	0.00	0.00	0.00	0.00	0.00	0.00
CR2	0.00	36.93	32.46	64.01	140.74	58.52	16.46
BCR	0.00	1.48	0.00	1.83	0.00	0.00	0.00
MXZ	0.00	20.26	10.52	19.20	23.77	36.58	14.63
CR3	0.00	16.25	17.83	33.83	25.60	38.40	14.63
CR4	0.00	5.91	0.00	7.32	29.26	93.27	36.58
CR5	0.00	0.00	0.00	0.00	0.00	0.00	7.32
FBA	0.00	0.00	0.00	0.00	0.00	0.00	0.00
CR6	0.00	0.00	0.00	0.00	0.00	0.00	0.00
CRA	43.45	0.00	0.00	0.00	9.14	27.43	18.29
CRB	0.00	3.69	1.83	4.57	0.00	7.32	5.49
CLK	0.00	19.21	3.66	27.43	35.66	65.84	20.12
LKC	0.00	287.28	118.87	419.22	89.61	330.46	54.86
CRU	0.00	9.60	3.20	16.46	16.46	27.43	9.14
CRV	0.00	3.69	0.00	4.57	0.00	0.00	0.00
CRD	0.00	107.11	111.10	206.65	91.44	137.16	51.21
CRE	0.00	0.00	34.75	0.00	45.72	71.32	42.06
TOTAL	70.81	561.65	378.10	896.53	613.64	1030.89	362.10

Table 4.11A: Corrected version of Table 4.11. This is the table that should have been used in calibration. The previous table miscalculated or excluded RR effort.

<b>Tournament Date</b>	<b>Number of Boats</b>	<b>Launch Site</b>	<b>Location</b>
04/21/12	N/A	Waterfront Pub	Cal Sag/Lake Calumet
04/22/12	15	Waterfront Pub	Lake Calumet
05/01/12	15	Waterfront Pub	Cal Sag/Lake Calumet
05/05/12	15	Waterfront Pub	Lake Calumet
05/06/12	15	Waterfront Pub	Lake Calumet
05/06/12	N/A	Waterfront Pub	Cal Sag/Lake Calumet
05/12/12	4-20	N/A	Cal Sag
05/20/12	15-20	Waterfront Pub	Cal Sag/Lake Calumet
05/26/12	15	Waterfront Pub	Lake Calumet
05/27/12	15	Waterfront Pub	Lake Calumet
05/27/12	N/A	Waterfront Pub	Cal Sag/Lake Calumet
06/10/12	15	Waterfront Pub	Lake Calumet
06/16/12	4-15	N/A	Cal Sag
06/17/12	N/A	Waterfront Pub	Cal Sag/Lake Calumet
06/23/12	50	Waterfront Pub	Cal Sag
06/24/12	15-20	Waterfront Pub	Cal Sag/Lake Calumet
07/01/12	N/A	Waterfront Pub	Cal Sag/Lake Calumet
07/14/12	N/A	Waterfront Pub	Cal Sag/Lake Calumet
07/29/12	15	Waterfront Pub	Lake Calumet
08/05/12	15	Waterfront Pub	Cal Sag/Lake Calumet
08/19/12	50	Waterfront Pub	Lake Calumet
09/09/12	N/A	Waterfront Pub	Cal Sag/Lake Calumet
4/14/2013	N/A	Waterfront Pub	Cal Sag/Lake Calumet
4/21/2013	15	Waterfront Pub	Lake Calumet
4/28/2013	20	Waterfront Pub	Cal Sag/Lake Calumet
5/5/2013	N/A	Waterfront Pub	Cal Sag/Lake Calumet
5/11/2013	15	Waterfront Pub	Lake Calumet
5/18/2013	N/A	Waterfront Pub	Cal Sag/Lake Calumet
05/19/13	12-15	Waterfront Pub	Cal Sag
6/1/2013	5-10	Waterfront Pub	Cal Sag
6/2/2013	N/A	Waterfront Pub	Cal Sag/Lake Calumet
6/8/2013	15	Waterfront Pub	Lake Calumet
6/23/2013	N/A	Waterfront Pub	Cal Sag/Lake Calumet
6/29/2013	15	Waterfront Pub	Lake Calumet
6/30/2013	20	Waterfront Pub	Cal Sag/Lake Calumet
07/14/13	12-15	Waterfront Pub	Cal Sag
7/14/2013	N/A	Waterfront Pub	Cal Sag/Lake Calumet
7/21/2013	15	Waterfront Pub	Lake Calumet
8/18/2013	50	Waterfront Pub	Lake Calumet
9/1/2013	N/A	Waterfront Pub	Cal Sag/Lake Calumet
4/13/2014	15	Waterfront Pub	Lake Calumet
5/4/2014	15	Waterfront Pub	Lake Calumet
5/10/2014	13	Waterfront Pub	Cal Sag/Lake Calumet
5/17/2014	15	Waterfront Pub	Cal Sag/Lake Calumet
5/18/2014	15	Waterfront Pub	Lake Calumet
5/24/2014	5-10	Waterfront Pub	Cal Sag/Lake Calumet
6/7/2014	13	Waterfront Pub	Cal Sag/Lake Calumet
6/14/2014	50	Alsip Municipal Ramp	Cal Sag
6/14/2014	50	Alsip Municipal Ramp	Cal Sag
6/22/2014	15	Waterfront Pub	Lake Calumet
7/19/2014	15-20	Waterfront Pub	Cal Sag/Lake Calumet
8/2/2014	50	Waterfront Pub	Cal Sag/Lake Calumet
8/3/2014	15-20	Waterfront Pub	Cal Sag/Lake Calumet
8/10/2014	15	Waterfront Pub	Lake Calumet
10/4/2014	15	Waterfront Pub	Lake Calumet
10/5/2014	50	Alsip Municipal Ramp	Cal Sag
10/5/2014	50	Alsip Municipal Ramp	Cal Sag

Table 4.12: Applications for recreational fishing tournaments, 2012-2014 (Source: ILDNR)



Reach	Calendar Year and Season						Mean Boat Days	
	2012		2013		2014		Gates Closed	Gates Open
	Gates Closed	Gates Open	Gates Closed	Gates Open	Gates Closed	Gates Open		
CLK	140	155	80	155	83	148	101.0	152.7
CRB	140	155	80	155	83	148	101.0	152.7
CRD	85	140	65	85	38	303	62.7	176.0
CRE	85	140	65	85	38	303	62.7	176.0
CRU	140	155	80	155	83	148	101.0	152.7
CRV	140	155	80	155	83	148	101.0	152.7
LKC	140	155	80	155	83	148	101.0	152.7

Table 4.13: Recreational fishing boat days participating in fishing tournaments by reach and year, 2012 - 2014

Reach	2010		2011		2012		2013	
	Gates closed	Gates open	Gates closed	Gates open	Gates closed	Gates open	Gates closed	Gates open
NSC	27.4	0.0	27.4	51.7	62.3	53.0	91.4	75.0
CR1	0.0	0.0	16.5	39.8	43.9	84.1	78.6	85.0
CRM	0.0	0.0	0.0	0.0	0.0	0.0	8.2	8.2
CR2	0.0	0.0	32.5	64.0	140.7	58.5	32.9	33.8
BCR	0.0	0.0	0.0	1.8	0.0	0.0	0.9	0.9
MXZ	0.0	12.9	10.5	19.2	23.8	36.6	32.0	38.4
CR3	0.0	0.0	17.8	33.8	25.6	38.4	28.3	53.0
CR4	0.0	0.0	0.0	7.3	29.3	93.3	78.6	64.0
CR5	0.0	0.0	0.0	0.0	0.0	0.0	7.3	21.9
FBA	0.0	0.0	0.0	0.0	0.0	0.0	0.0	0.0
CR6	0.0	0.0	0.0	0.0	0.0	0.0	0.0	0.0
CRA	43.5	0.0	0.0	0.0	9.1	27.4	27.4	43.9
CRB	0.0	0.0	1.8	4.6	0.0	7.3	5.5	5.5
CLK	0.0	0.0	3.7	27.4	35.7	65.8	40.2	73.2
LKC	0.0	165.8	118.9	419.2	89.6	330.5	95.1	239.6
CRU	0.0	0.0	111.1	206.7	91.4	137.2	89.6	139.0
CRV	0.0	0.0	34.7	0.0	45.7	71.3	69.5	98.8
CRD	0.0	0.0	3.2	16.5	16.5	27.4	16.5	32.9
CRE	0.0	0.0	0.0	4.6	0.0	0.0	0.0	0.0
<b>Total</b>	<b>70.8</b>	<b>178.6</b>	<b>378.1</b>	<b>896.5</b>	<b>613.6</b>	<b>1030.9</b>	<b>702.3</b>	<b>1013.2</b>

Table 4.14: Inventory of commercial net fishing effort (100 meters) from January, 2010 through December, 2013, as reported by ILDNR. Includes gear classified as gill nets, trammel nets, commercial seine, and deep gill nets that were fished less than three hours. Excludes FRS fishing effort from 2010. No fishing effort occurred in 2009.

From: C:\Users\u4eprmts\Desktop\FISHING EFFORT\FINAL\_V4\_ALL Effort\_BY\_REACH\_SEASON.xlsx

<b>Secondary Source</b>	<b>Loading Factor (units)</b>	<b>Loading Rate Function Parameter (units)</b>
Piscivorous bird feces	Surface area (m <sup>2</sup> )	Deposition rate (copies/m <sup>2</sup> /sec)
CSOs	CSO discharge volume (m <sup>3</sup> /sec)	Target marker concentration (copies/m <sup>3</sup> )
Lake Michigan inflows	Inflow volume (m <sup>3</sup> /sec)	Target marker concentration (copies/m <sup>3</sup> )
Commercial navigation	Vessel residence time (vessel hours/sec)	Unit loading rate (copies/vessel hour)
Commercial fishing nets	Commercial net fished (100 m /sec)	Unit loading rate (copies/100 m)
Recreational fishing derbies	Recreational boat days (boat days/sec)	Unit loading rate (copies/boat day)
<b>Primary Source</b>	<b>Loading Factor</b>	<b>Loading Rate Function Parameter</b>
Live Asian carp	Shedding rate (target marker copies/kg/sec)	Mass of live Asian carp (kg)

Table 6.1: Loading factors and their related loading rate function parameters for the secondary and primary sources of eDNA to the CAWS. Note: Loading factors have been converted to units suitable for use in the steady state water quality box model.

Secondary Source	CAWS Reaches	Loading Factor	
		Varies Seasonally	Varies by Year
Piscivorous bird feces	<i>ALL REACHES</i>	X	
CSOs	NSC, CR1, CRM, CR2, BCR, CR3, CR4, CRD, CRE	X	X
Lake Michigan inflows	NSC, CRM, CRA	X	X
Commercial navigation	CR1, CRM, CR2, BCR, MXZ, CR3, CR4, CR5, FBA, CR6, CRA, CRB, CLK, LKC, CRU, CRV, CRD, CRE	X	
Commercial fishing nets	NSC, CR1, CR2, CR2A, CR2B, CR2C, CR2D, BCR, MXZ, MXZA, CR3, CR3A, CR3B, CR4, CRA, CRAC, CRB, CLK, CLKA, CLKB, CRU, CRV, LKC, CRD, CRDA, CRDB, CRE	X	X
Recreational fishing derbies	CRB, CLK, LCK, CRE, CRD, CRU, CRV	X	

Table 6.2: Location of secondary sources in the CAWS by reach and whether or not the loading factor varies by season and year.

Sample Reach	Median Silver Carp Target Marker Concentration by Year and Season (copies/L)							
	2009		2010		2011		2012	
	Open	Closed	Open	Closed	Open	Closed	Open	Closed
NSC	-	64.0	-	47.6	59.4	50.5	66.2	54.6
CR1	-	-	-	5.6	5.6	3.9	27.2	2.8
CRM	-	-	-	24.8	5.6	36.5	55.9	-
CR2	-	-	-	59.4	24.6	31.7	36.6	-
BCR	-	-	-	-	-	-	-	-
MXZ	-	-	-	59.4	8.5	31.9	28.8	-
CR3	-	-	-	-	-	-	-	-
CR4	-	-	-	-	-	-	-	-
CR5	-	-	57.7	34.0	40.3	31.5	-	-
FBA	-	-	68.0	64.6	49.7	-	-	-
CR6	36.4	56.1	87.3	37.0	68.5	-	-	-
CRA	-	34.0	-	-	8.5	-	-	-
CRB	-	-	-	-	1.5	60.9	0.3	108.8
CLK	-	-	-	-	13.4	36.7	24.0	83.8
LKC	-	8.5	-	-	40.8	19.2	53.8	110.7
CRU	-	3.9	-	2.8	11.3	11.7	18.2	21.6
CRV	-	3.9	-	2.8	11.3	11.7	18.2	21.6
CRD	-	30.6	-	36.3	25.1	43.2	22.8	46.6
CRE	-	-	-	-	-	58.6	-	-

Table 6.3: Median silver carp target marker concentrations (copies/L) used in Bayesian MCMC.

Secondary Source	Units	Mean	Standard Deviation	Percentile				
				5th	25th	50th	75th	95th
BRD	Copies/m <sup>2</sup> /day	2524	2434	145	725	1741	3409	7325
CSO1 (CRD)	Copies/L	723	652	39	237	533	1006	1993
CSO2 (CRE)	Copies/L	2055	1436	197	884	1802	2915	4750
CSO3 (BCR)	Copies/L	369	296	30	135	294	519	948
CSO4 (NSC)	Copies/L	955	335	398	723	954	1177	1502
CSO5 (CR1)	Copies/L	123	111	7	38	90	170	343
CSO6 (CR2)	Copies/L	489	401	30	177	385	690	1292
CSO7 (CRM)	Copies/L	139	107	11	55	115	195	346
CSO8 (CR3)	Copies/L	324	279	23	106	250	455	888
CSO9 (CR4)	Copies/L	115	102	8	38	86	162	319
LMI	Copies/L	20	14	2	9	18	29	46
FDB	Copies/boat day	3.82E+09	3.36E+09	1.97E+08	1.28E+09	2.86E+09	5.32E+09	1.03E+10
FIN	Copies/100 meters	8.95E+09	7.25E+09	5.69E+08	3.22E+09	7.20E+09	1.27E+10	2.31E+10
NAV	Copies/vessel Hour	3.85E+08	1.81E+08	8.78E+07	2.52E+08	3.80E+08	5.08E+08	6.91E+08

Table 6.4: Estimates of secondary source loading rate function parameters, from Bayesian MCMC simulation including CSOs. Row headings are: BRD = Piscivorous birds, CSO = Combined sewer overflows, LMI = Lake Michigan inflows, FDB = Recreational fishing derbies, FIN = Fishing nets, and NAV = Commercial navigation. The reach where CSO discharges enter the CAWS is noted in parentheses next to each secondary source abbreviation.

Rank	Secondary Source					
	BRD	CSO	LMI	FDS	FIN	NAV
Largest	0	0.623	0	0	0	0.377
2nd largest	0.003	0.377	0.015	0.02	0.008	0.577
3rd largest	0.128	0	0.282	0.296	0.272	0.023
4th largest	0.204	0	0.287	0.246	0.252	0.01
5th largest	0.292	0	0.232	0.232	0.236	0.007
6th largest	0.373	0	0.185	0.206	0.231	0.005

Table 6.5: Probabilistic ranking of secondary sources in terms of total contribution of eDNA to the CAWS. Column headings are: BRD = Piscivorous birds, CSO = Combined sewer overflows, LMI = Lake Michigan inflows, FDB = Recreational fishing derbies, FIN = Fishing nets, and NAV = Commercial navigation.

Reach	Secondary Source					
	BRD	CSO	LMI	FDB	FIN	NAV
NSC	0.0334	0.7048	0.1761	0.0000	0.0854	0.0002
CR1	0.0604	0.6628	0.1174	0.0000	0.1138	0.0456
CRM	0.0371	0.4148	0.4974	0.0000	0.0267	0.0241
CR2	0.0475	0.5750	0.2298	0.0000	0.0819	0.0658
BCR	0.0217	0.8696	0.0399	0.0000	0.0183	0.0504
MXZ	0.0321	0.5747	0.1505	0.0000	0.0599	0.1828
CR3	0.0390	0.6049	0.1244	0.0000	0.0569	0.1749
CR4	0.0577	0.6084	0.1011	0.0001	0.0591	0.1737
CR5	0.0496	0.4322	0.0708	0.0343	0.0424	0.3707
FBA	0.0500	0.4305	0.0703	0.0341	0.0422	0.3729
CR6	0.0524	0.4238	0.0685	0.0332	0.0411	0.3811
CRA	0.0395	0.0273	0.3354	0.0654	0.0442	0.4882
CRB	0.0656	0.0614	0.2396	0.1492	0.0962	0.3880
CLK	0.0701	0.0592	0.2318	0.1540	0.1045	0.3804
LKC	0.0797	0.0559	0.2207	0.1586	0.1231	0.3620
CRU	0.0660	0.0711	0.2309	0.1559	0.0971	0.3790
CRV	0.0665	0.0834	0.2233	0.1593	0.0981	0.3694
CRD	0.0732	0.1554	0.1869	0.1517	0.1092	0.3236
CRE	0.0788	0.3799	0.1082	0.1171	0.0654	0.2507

Table 6.6: Seasonal probability that eDNA detected in a monitoring sample originated from one of six potential secondary sources for the gates open season. Column headings are: BRD = Piscivorous birds, CSO = Combined sewer overflows, LMI = Lake Michigan inflows, FDB = Recreational fishing derbies, FIN = Fishing nets, and NAV = Commercial navigation.



Reach	Secondary Source					
	BRD	CSO	LMI	FDB	FIN	NAV
NSC	0.0005	0.9283	0.0141	0.0000	0.0569	0.0002
CR1	0.0010	0.8749	0.0099	0.0000	0.0717	0.0425
CRM	0.0012	0.7503	0.1579	0.0000	0.0385	0.0520
CR2	0.0010	0.8093	0.0329	0.0000	0.0643	0.0925
BCR	0.0004	0.9544	0.0064	0.0000	0.0180	0.0207
MXZ	0.0008	0.8449	0.0235	0.0000	0.0590	0.0718
CR3	0.0009	0.8116	0.0190	0.0000	0.0538	0.1146
CR4	0.0015	0.7445	0.0150	0.0001	0.0466	0.1924
CR5	0.0007	0.3397	0.0264	0.0189	0.0186	0.5957
FBA	0.0007	0.3374	0.0262	0.0187	0.0184	0.5985
CR6	0.0008	0.3219	0.0249	0.0178	0.0173	0.6173
CRA	0.0007	0.0225	0.3636	0.0661	0.0205	0.5266
CRB	0.0012	0.0503	0.2783	0.1398	0.0426	0.4879
CLK	0.0013	0.0488	0.2709	0.1442	0.0456	0.4892
LKC	0.0015	0.0479	0.2654	0.1519	0.0540	0.4793
CRU	0.0012	0.0585	0.2700	0.1459	0.0439	0.4805
CRV	0.0012	0.0689	0.2630	0.1492	0.0455	0.4723
CRD	0.0015	0.1489	0.2229	0.1401	0.0603	0.4264
CRE	0.0015	0.4327	0.1017	0.0863	0.0476	0.3302

Table 6.7: Seasonal probability that eDNA detected in a monitoring sample originated from one of six potential secondary sources for the gates open season. Column headings are: BRD = Piscivorous birds, CSO = Combined sewer overflows, LMI = Lake Michigan inflows, FDB = Recreational fishing derbies, FIN = Fishing nets, and NAV = Commercial navigation.

Reach	Secondary Source					
	BRD	CSO	LMI	FDB	FIN	NAV
NSC	0.0170	0.8165	0.0951	0.0000	0.0712	0.0002
CR1	0.0307	0.7689	0.0636	0.0000	0.0927	0.0440
CRM	0.0192	0.5825	0.3277	0.0000	0.0326	0.0381
CR2	0.0242	0.6922	0.1313	0.0000	0.0731	0.0791
BCR	0.0111	0.9120	0.0232	0.0000	0.0182	0.0356
MXZ	0.0164	0.7098	0.0870	0.0000	0.0594	0.1273
CR3	0.0200	0.7082	0.0717	0.0000	0.0554	0.1447
CR4	0.0296	0.6765	0.0581	0.0001	0.0528	0.1830
CR5	0.0252	0.3859	0.0486	0.0266	0.0305	0.4832
FBA	0.0254	0.3839	0.0482	0.0264	0.0303	0.4857
CR6	0.0266	0.3729	0.0467	0.0255	0.0292	0.4992
CRA	0.0201	0.0249	0.3495	0.0657	0.0324	0.5074
CRB	0.0334	0.0559	0.2589	0.1445	0.0694	0.4379
CLK	0.0357	0.0540	0.2513	0.1491	0.0751	0.4348
LKC	0.0406	0.0519	0.2430	0.1553	0.0885	0.4207
CRU	0.0336	0.0648	0.2505	0.1509	0.0705	0.4298
CRV	0.0339	0.0761	0.2431	0.1542	0.0718	0.4208
CRD	0.0373	0.1521	0.2049	0.1459	0.0847	0.3750
CRE	0.0401	0.4063	0.1049	0.1017	0.0565	0.2904

Table 6.8: Fraction of eDNA originating from one of six potential secondary sources over the course of one year by reach. Column headings are: BRD = Piscivorous birds, CSO = Combined sewer overflows, LMI = Lake Michigan inflows, FDB = Recreational fishing derbies, FIN = Commercial fishing nets, and NAV = Commercial navigation.

<b>Moment</b>	<b>Secondary Source</b>					
	<b>BRD</b>	<b>CSO</b>	<b>FDB</b>	<b>FIN</b>	<b>LMI</b>	<b>NAV</b>
Mean	0.03	0.42	0.06	0.06	0.15	0.29
St. dev.	0.01	0.31	0.07	0.02	0.11	0.19

Table 6.9: Mean and standard deviation of the fraction of eDNA originating from one of six potential secondary sources over the course of one year for the entire CAWS. Column headings are: BRD = Piscivorous birds, CSO = Combined sewer overflows, LMI = Lake Michigan inflows, FDB = Recreational fishing derbies, FIN = Commercial fishing nets, and NAV = Commercial navigation.

Rank	Secondary Source					
	BRD	CSO	LMI	FDB	FIN	NAV
Largest	0.004	0	0.005	0.002	0.003	0.986
2nd largest	0.325	0	0.224	0.135	0.308	0.007
3rd largest	0.252	0	0.276	0.222	0.247	0.003
4th largest	0.22	0	0.259	0.291	0.228	0.002
5th largest	0.199	0	0.237	0.349	0.214	0.001
6th largest	0	1	0	0	0	0

Table 6.10: Probabilistic ranking of secondary sources in terms of total contribution of eDNA to the CAWS, excluding CSOs as a potential source. Column headings are: BRD = Piscivorous birds, CSO = Combined sewer overflows, LMI = Lake Michigan inflows, FDB = Recreational fishing derbies, FIN = Commercial fishing nets, and NAV = Commercial navigation.

Reach	Secondary Source					
	BRD	CSO	FDB	FIN	LMI	NAV
NSC	0.2102	0.0000	0.0000	0.2603	0.5283	0.0012
CR1	0.2753	0.0000	0.0000	0.2524	0.2932	0.1791
CRM	0.1261	0.0000	0.0000	0.0527	0.7570	0.0642
CR2	0.1836	0.0000	0.0000	0.1761	0.4397	0.2005
BCR	0.2549	0.0000	0.0000	0.1288	0.2224	0.3938
MXZ	0.1160	0.0000	0.0000	0.1226	0.2743	0.4870
CR3	0.1446	0.0000	0.0000	0.1268	0.2402	0.4884
CR4	0.2035	0.0000	0.0001	0.1233	0.1950	0.4782
CR5	0.1225	0.0000	0.0321	0.0685	0.0965	0.6803
FBA	0.1230	0.0000	0.0318	0.0678	0.0955	0.6819
CR6	0.1265	0.0000	0.0304	0.0651	0.0916	0.6864
CRA	0.0631	0.0000	0.0386	0.0451	0.2836	0.5696
CRB	0.1087	0.0000	0.0929	0.1020	0.2158	0.4806
CLK	0.1153	0.0000	0.0956	0.1100	0.2086	0.4705
LKC	0.1292	0.0000	0.0980	0.1281	0.1981	0.4466
CRU	0.1107	0.0000	0.0983	0.1047	0.2109	0.4755
CRV	0.1131	0.0000	0.1019	0.1078	0.2070	0.4702
CRD	0.1327	0.0000	0.1045	0.1323	0.1870	0.4435
CRE	0.1835	0.0000	0.1069	0.1170	0.1462	0.4464

Table 6.11: Seasonal probability that eDNA detected in a monitoring sample originated from one of six potential secondary sources for the gates open season, from the simulation excluding CSOs. Column headings are: BRD = Piscivorous birds, CSO = Combined sewer overflows, LMI = Lake Michigan inflows, FDB = Recreational fishing derbies, FIN = Fishing nets, and NAV = Commercial navigation.

Reach	Secondary Source					
	BRD	CSO	FDB	FIN	LMI	NAV
NSC	0.0326	0.0000	0.0000	0.5034	0.4540	0.0100
CR1	0.0195	0.0000	0.0000	0.2933	0.1492	0.5380
CRM	0.0106	0.0000	0.0000	0.1233	0.5541	0.3119
CR2	0.0094	0.0000	0.0000	0.1906	0.1932	0.6068
BCR	0.0259	0.0000	0.0000	0.2017	0.1794	0.5930
MXZ	0.0099	0.0000	0.0000	0.2058	0.1849	0.5995
CR3	0.0092	0.0000	0.0000	0.1632	0.1182	0.7094
CR4	0.0099	0.0000	0.0001	0.1090	0.0661	0.8149
CR5	0.0017	0.0000	0.0158	0.0210	0.0352	0.9264
FBA	0.0017	0.0000	0.0156	0.0207	0.0348	0.9272
CR6	0.0017	0.0000	0.0143	0.0190	0.0320	0.9329
CRA	0.0012	0.0000	0.0384	0.0202	0.3170	0.6231
CRB	0.0021	0.0000	0.0866	0.0430	0.2577	0.6106
CLK	0.0022	0.0000	0.0893	0.0460	0.2509	0.6117
LKC	0.0026	0.0000	0.0945	0.0542	0.2469	0.6019
CRU	0.0021	0.0000	0.0916	0.0447	0.2531	0.6084
CRV	0.0022	0.0000	0.0950	0.0468	0.2500	0.6061
CRD	0.0028	0.0000	0.0983	0.0646	0.2334	0.6008
CRE	0.0043	0.0000	0.0924	0.0652	0.1680	0.6699

Table 6.12: Seasonal probability that eDNA detected in a monitoring sample originated from one of six potential secondary sources for the gates closed season, from the simulation excluding CSOs. Column headings are: BRD = Piscivorous birds, CSO = Combined sewer overflows, LMI = Lake Michigan inflows, FDB = Recreational fishing derbies, FIN = Fishing nets, and NAV = Commercial navigation.

Reach	Secondary Source					
	BRD	CSO	FDB	FIN	LMI	NAV
NSC	0.1214	0.0000	0.0000	0.3818	0.4912	0.0056
CR1	0.1474	0.0000	0.0000	0.2728	0.2212	0.3586
CRM	0.0684	0.0000	0.0000	0.0880	0.6556	0.1880
CR2	0.0965	0.0000	0.0000	0.1834	0.3165	0.4037
BCR	0.1404	0.0000	0.0000	0.1653	0.2009	0.4934
MXZ	0.0629	0.0000	0.0000	0.1642	0.2296	0.5433
CR3	0.0769	0.0000	0.0000	0.1450	0.1792	0.5989
CR4	0.1067	0.0000	0.0001	0.1162	0.1305	0.6465
CR5	0.0621	0.0000	0.0239	0.0447	0.0659	0.8033
FBA	0.0624	0.0000	0.0237	0.0443	0.0651	0.8046
CR6	0.0641	0.0000	0.0224	0.0421	0.0618	0.8097
CRA	0.0321	0.0000	0.0385	0.0327	0.3003	0.5964
CRB	0.0554	0.0000	0.0897	0.0725	0.2367	0.5456
CLK	0.0588	0.0000	0.0924	0.0780	0.2297	0.5411
LKC	0.0659	0.0000	0.0963	0.0911	0.2225	0.5242
CRU	0.0564	0.0000	0.0949	0.0747	0.2320	0.5420
CRV	0.0577	0.0000	0.0984	0.0773	0.2285	0.5381
CRD	0.0677	0.0000	0.1014	0.0985	0.2102	0.5222
CRE	0.0939	0.0000	0.0997	0.0911	0.1571	0.5582

Table 6.13: Fraction of eDNA originating from one of six potential secondary sources over the course of one year by reach. Column headings are: BRD = Piscivorous birds, CSO = Combined sewer overflows, LMI = Lake Michigan inflows, FDB = Recreational fishing derbies, FIN = Commercial fishing nets, and NAV = Commercial navigation.

<b>Moment</b>	<b>Secondary Source</b>					
	<b>BRD</b>	<b>CSO</b>	<b>FDB</b>	<b>FIN</b>	<b>LMI</b>	<b>NAV</b>
Mean	0.08	0.00	0.04	0.12	0.23	0.53
St. dev.	0.03	0.00	0.04	0.09	0.14	0.20

Table 6.14: Mean and standard deviation of the fraction of eDNA originating from one of six potential secondary sources over the course of one year for the entire CAWS. Column headings are: BRD = Piscivorous birds, CSO = Combined sewer overflows, LMI = Lake Michigan inflows, FDB = Recreational fishing derbies, FIN = Commercial fishing nets, and NAV = Commercial navigation.



Reach	Mass of Silver Carp (kg)		
	Mean	95% Confidence Interval	
		Lower bound	Upper bound
NSC	271	167	373
CR1	33	1	119
CRM	70	7	155
CR2	170	12	372
BCR	127	4	418
MXZ	58	2	185
CR3	897	34	2662
CR4	546	21	1598
CR5	268	9	870
FBA	345	17	895
CR6	235	8	744
CRA	194	6	613
CRB	91	3	313
CLK	115	4	363
LKC	181	10	447
CRU	48	1	180
CRV	55	2	192
CRD	280	22	634
CRE	683	73	1429
ALL Reaches	4666	3680	5957

Table 6.15: Mass of silver carp (kg) needed to sustain observed target marker concentrations in the CAWS in the absence of secondary sources.

<b>Secondary Source</b>	<b>Loading Rate</b>	<b>Units</b>
Lake Michigan	17,700	copies / m <sup>3</sup>
Birds	0.02	copies / m <sup>2</sup> / s
CSO, Reach CRD	532,000	copies / m <sup>3</sup>
CSO, Reach CRE	1,800,000	copies / m <sup>3</sup>
CSO, Reach BCR	294,000	copies / m <sup>3</sup>
CSO, Reach NSC	950,000	copies / m <sup>3</sup>
CSO, Reach CR1	91,000	copies / m <sup>3</sup>
CSO, Reach CR2	386,000	copies / m <sup>3</sup>
CSO, Reach CRM	114,000	copies / m <sup>3</sup>
CSO, Reach CR3	250,000	copies / m <sup>3</sup>
CSO, Reach CR4	860,000	copies / m <sup>3</sup>
Navigation	3.8 x 10 <sup>8</sup>	copies / vessel hour
Fishing Derbies	2.86 x 10 <sup>9</sup>	copies / boat day
Fishing Nets	7.1 x 10 <sup>9</sup>	copies / 100 m net

Table 7.1: Secondary source loading rates used in HFTTM simulation of silver carp target marker concentrations.

Secondary source	CSSC Grid		Lake Calumet Grid	
	Gates open	Gates closed	Gates open	Gates closed
Lake Michigan inflows	17,893	856	16,042	979
Piscivorous birds	14,612	1,652	6,294	712
CSOs	50,246	24,941	0	0
Commercial navigation	46,257	66,358	6,621	5,942
Recreational fishing derbies	9,148	3,482	13,038	5,471
Commercial fishing nets	24,060	14,018	13,081	6,351

Table 7.2: Average daily eDNA load (million copies d<sup>-1</sup>) from secondary sources calculated from loading rates used in the HFFTM to simulate secondary source concentrations.

Reach	Primary Source (kg)	Primary source density ( $10^{-6}$ kg / m <sup>3</sup> )	Loading rate ( $10^6$ copies / d)
NSC	271	124.0	91,056
CR1	23	5.5	7,728
CRM	66	38.2	22,176
CR2	163	49.0	54,768
BCR	96	189.0	32,256
MXZ	45	135.9	15,120
CR3	720	152.1	241,920
CR4	450	44.4	151,200
CR5	208	42.3	69,888
FBA	307	496.4	103,152
CR6	180	56.3	60,480
CRA	152	20.0	51,072
CRB	68	81.9	22,848
CLK	90	50.7	30,240
LKC	165	45.3	55,440
CRU	33	31.9	11,088
CRV	40	157.5	13,440
CRD	269	36.5	90,384
CRE	663	63.6	222,768
All reaches	4,009	58.3	1,347,024

Table 7.3: Primary source biomass and loading rates used in simulating primary source concentrations.

Reach	2010		2011		2012		2013	
	Gates closed	Gates open	Gates closed	Gates open	Gates closed	Gates open	Gates closed	Gates open
NSC	27.4	0.0	27.4	51.7	62.3	53.0	91.4	75.0
CR1	0.0	0.0	16.5	39.8	43.9	84.1	78.6	85.0
CRM	0.0	0.0	0.0	0.0	0.0	0.0	8.2	8.2
CR2	0.0	0.0	32.5	64.0	140.7	58.5	32.9	33.8
BCR	0.0	0.0	0.0	1.8	0.0	0.0	0.9	0.9
MXZ	0.0	12.9	10.5	19.2	23.8	36.6	32.0	38.4
CR3	0.0	0.0	17.8	33.8	25.6	38.4	28.3	53.0
CR4	0.0	0.0	0.0	7.3	29.3	93.3	78.6	64.0
CR5	0.0	0.0	0.0	0.0	0.0	0.0	7.3	21.9
FBA	0.0	0.0	0.0	0.0	0.0	0.0	0.0	0.0
CR6	0.0	0.0	0.0	0.0	0.0	0.0	0.0	0.0
CRA	43.5	0.0	0.0	0.0	9.1	27.4	27.4	43.9
CRB	0.0	0.0	1.8	4.6	0.0	7.3	5.5	5.5
CLK	0.0	0.0	3.7	27.4	35.7	65.8	40.2	73.2
LKC	0.0	165.8	118.9	419.2	89.6	330.5	95.1	239.6
CRU	0.0	0.0	111.1	206.7	91.4	137.2	89.6	139.0
CRV	0.0	0.0	34.7	0.0	45.7	71.3	69.5	98.8
CRD	0.0	0.0	3.2	16.5	16.5	27.4	16.5	32.9
CRE	0.0	0.0	0.0	4.6	0.0	0.0	0.0	0.0
<b>Total</b>	<b>70.8</b>	<b>178.6</b>	<b>378.1</b>	<b>896.5</b>	<b>613.6</b>	<b>1030.9</b>	<b>702.3</b>	<b>1013.2</b>

Table 8.1: Inventory of commercial net fishing effort (100 meters) from January, 2010 through December, 2013, as reported by ILDNR. Includes gear classified as gill nets, trammel nets, commercial seine, and deep gill nets that were fished less than three hours. The table does not include FRS fishing effort from 2010. No fishing effort occurred in 2009.

From: C:\Users\u4eprmts\Desktop\FISHING EFFORT\FINAL\_V4\_ALL Effort\_BY\_REACH\_SEASON.xlsx

Reach	2010		2011		2012		2013	
	Gates closed	Gates open	Gates closed	Gates open	Gates closed	Gates open	Gates closed	Gates open
NSC	20.0	0.0	15.5	24.8	35.5	19.0	25.8	8.0
CR1	0.0	0.0	5.5	8.3	5.5	10.3	5.6	4.5
CRM	0.0	0.0	0.0	0.0	0.0	0.0	4.4	2.8
CR2	0.0	0.0	15.3	29.0	28.5	15.1	7.8	7.0
BCR	0.0	0.0	0.8	0.3	0.0	0.0	0.5	0.0
MXZ	0.0	4.0	1.8	3.8	1.2	1.3	3.0	1.8
CR3	0.0	0.0	2.8	7.5	4.0	6.9	3.9	3.5
CR4	0.0	0.0	0.0	0.0	4.3	6.3	4.0	2.3
CR5	0.0	0.0	0.0	0.0	0.5	1.3	0.8	1.3
FBA	0.0	0.0	0.0	0.0	0.0	0.0	0.0	0.0
CR6	0.0	0.0	0.0	0.0	0.0	0.0	0.0	0.0
CRA	10.0	0.0	0.0	0.0	4.8	6.8	3.5	4.0
CRB	0.0	0.0	0.0	0.0	1.0	1.0	0.5	1.0
CLK	0.0	0.0	0.0	0.0	1.5	3.3	2.0	3.5
LKC	0.0	54.5	10.5	39.0	8.8	30.0	6.3	15.0
CRU	0.0	0.0	21.0	38.0	16.0	21.3	10.0	8.0
CRV	0.0	0.0	0.3	1.3	6.0	9.3	4.8	4.0
CRD	0.0	0.0	1.0	4.8	1.0	0.8	0.3	1.3
CRE	0.0	0.0	1.3	1.8	0.0	0.0	0.0	0.0
<b>Total</b>	<b>30.0</b>	<b>58.5</b>	<b>75.5</b>	<b>158.3</b>	<b>118.4</b>	<b>132.3</b>	<b>82.9</b>	<b>67.8</b>

Table 8.2: Inventory of electrofishing effort (hours of pedal time) from January, 2010 through December, 2013, as reported by ILDNR. Excludes FRS fishing effort from 2010. No fishing effort occurred in 2009.

From: C:\Users\u4eprmts\Desktop\FISHING EFFORT\FINAL\_V4\_ALL Effort\_BY\_REACH\_SEASON.xlsx

Reach	2010		2011		2012		2013	
	Gates closed	Gates open	Gates closed	Gates open	Gates closed	Gates open	Gates closed	Gates open
NSC	0.0	0.0	0.0	0.0	0.0	0.0	0.0	0.0
CR1	0.0	0.0	0.0	0.0	0.0	0.0	0.0	0.0
CRM	0.0	0.0	0.0	0.0	0.0	0.0	0.0	0.0
CR2	0.0	0.0	0.0	0.0	0.0	0.0	0.0	0.0
BCR	0.0	0.0	0.0	0.0	0.0	0.0	0.0	0.0
MXZ	0.0	0.0	0.0	0.0	0.0	0.0	0.0	0.0
CR3	0.0	0.0	0.0	0.0	0.0	0.0	0.0	0.0
CR4	0.0	0.0	0.0	0.0	0.0	0.0	0.0	0.0
CR5	0.0	0.0	0.0	0.0	0.0	0.0	0.0	0.0
FBA	0.0	0.0	0.0	0.0	0.0	0.0	0.0	0.0
CR6	0.0	0.0	0.0	0.0	0.0	0.0	0.0	0.0
CRA	0.0	0.0	0.0	0.0	0.0	0.0	0.0	3.8
CRB	0.0	0.0	0.0	0.0	0.0	0.0	0.0	0.0
CLK	0.0	0.0	0.0	0.0	0.0	0.0	0.0	5.9
LKC	0.0	0.0	0.0	22.4	0.0	30.3	0.0	16.6
CRU	0.0	0.0	0.0	0.0	0.0	0.0	0.0	0.0
CRV	0.0	0.0	0.0	0.0	0.0	0.0	0.0	0.0
CRD	0.0	0.0	0.0	0.0	0.0	0.0	0.0	0.0
CRE	0.0	0.0	0.0	0.0	0.0	0.0	0.0	0.0
<b>Total</b>	<b>0.0</b>	<b>0.0</b>	<b>0.0</b>	<b>22.4</b>	<b>0.0</b>	<b>30.3</b>	<b>0.0</b>	<b>26.2</b>

Table 8.3: Inventory of trap net effort (net days) from January, 2010 through December, 2013, as reported by ILDNR. Excludes FRS fishing effort from 2010. No fishing effort occurred in 2009.

From: C:\Users\u4eprmts\Desktop\FISHING EFFORT\FINAL\_V4\_ALL Effort\_BY\_REACH\_SEASON.xlsx

Reach	2010		2011		2012		2013	
	Gates closed	Gates open	Gates closed	Gates open	Gates closed	Gates open	Gates closed	Gates open
NSC	0.0	0.0	0.0	0.0	0.0	0.0	0.0	0.0
CR1	0.0	0.0	0.0	0.0	0.0	0.0	0.0	0.0
CRM	0.0	0.0	0.0	0.0	0.0	0.0	0.0	0.0
CR2	0.0	0.0	0.0	0.0	0.0	0.0	0.0	0.0
BCR	0.0	0.0	0.0	0.0	0.0	0.0	0.0	0.0
MXZ	0.0	0.0	0.0	0.0	0.0	0.0	0.0	0.0
CR3	0.0	0.0	0.0	0.0	0.0	0.0	0.0	0.0
CR4	0.0	0.0	0.0	0.0	0.0	0.0	0.0	0.0
CR5	0.0	0.0	0.0	0.0	0.0	0.0	0.0	0.0
FBA	0.0	0.0	0.0	0.0	0.0	0.0	0.0	0.0
CR6	0.0	0.0	0.0	0.0	0.0	0.0	0.0	0.0
CRA	0.0	0.0	0.0	0.0	0.0	0.0	0.0	0.0
CRB	0.0	0.0	0.0	0.0	0.0	0.0	0.0	0.0
CLK	0.0	0.0	0.0	0.0	0.0	0.0	0.0	4.5
LKC	0.0	0.0	0.0	0.0	0.0	0.0	0.0	117.9
CRU	0.0	0.0	0.0	0.0	0.0	0.0	0.0	0.0
CRV	0.0	0.0	0.0	0.0	0.0	0.0	0.0	0.0
CRD	0.0	0.0	0.0	0.0	0.0	0.0	0.0	0.0
CRE	0.0	0.0	0.0	0.0	0.0	0.0	0.0	0.0
Total	0.0	0.0	0.0	0.0	0.0	0.0	0.0	122.4

Table 8.4: Inventory of deep gill net effort (100 meter hours) from January, 2010 through December, 2013, as reported by ILDNR. Excludes FRS fishing effort from 2010. No fishing effort occurred in 2009.

From: C:\Users\u4eprmts\Desktop\FISHING EFFORT\FINAL\_V4\_ALL Effort\_BY\_REACH\_SEASON.xlsx



Reach	2010		2011		2012		2013	
	Gates closed	Gates open	Gates closed	Gates open	Gates closed	Gates open	Gates closed	Gates open
NSC	27.36	28.44	27.43	51.66	62.33	53.04	91.44	74.98
CR1	0.00	21.79	16.46	39.78	43.89	84.12	78.64	85.04
CRM	0.00	0.00	0.00	0.00	0.00	0.00	8.23	8.23
CR2	0.00	36.93	32.46	64.01	140.74	58.52	32.92	33.83
BCR	0.00	1.48	0.00	1.83	0.00	0.00	0.91	0.91
MXZ	0.00	20.26	10.52	19.20	23.77	36.58	32.00	38.40
CR3	0.00	16.25	17.83	33.83	25.60	38.40	28.35	53.04
CR4	0.00	5.91	0.00	7.32	29.26	93.27	78.64	64.01
CR5	0.00	0.00	0.00	0.00	0.00	0.00	7.32	21.95
FBA	0.00	0.00	0.00	0.00	0.00	0.00	0.00	0.00
CR6	0.00	0.00	0.00	0.00	0.00	0.00	0.00	0.00
CRA	43.45	0.00	0.00	0.00	9.14	27.43	27.43	43.89
CRB	0.00	3.69	1.83	4.57	0.00	7.32	5.49	5.49
CLK	0.00	19.21	3.66	27.43	35.66	65.84	40.23	73.15
LKC	0.00	287.28	118.87	419.22	89.61	330.46	95.10	239.57
CRU	0.00	9.60	3.20	16.46	16.46	27.43	16.46	32.92
CRV	0.00	3.69	0.00	4.57	0.00	0.00	0.00	0.00
CRD	0.00	107.11	111.10	206.65	91.44	137.16	89.61	138.99
CRE	0.00	0.00	34.75	0.00	45.72	71.32	69.49	98.76
TOTAL	70.81	561.65	378.10	896.53	613.64	1030.89	702.26	1013.16

Table 8.5: Inventory of commercial net fishing effort (100 meters) from January, 2010 through December, 2013, including imputed effort for 2010. Includes gear classified as gill nets, trammel nets, commercial seine, and deep gill nets that were fished less than three hours. No fishing effort occurred in 2009.

Reach	2010		2011		2012		2013	
	Gates closed	Gates open	Gates closed	Gates open	Gates closed	Gates open	Gates closed	Gates open
NSC	23.70	20.65	15.50	24.82	35.50	19.00	25.78	8.00
CR1	1.85	7.17	5.50	8.25	5.50	10.25	5.55	4.50
CRM	0.00	0.00	0.00	0.00	0.00	0.00	4.37	2.75
CR2	1.62	24.98	15.25	29.00	28.45	15.10	7.83	7.00
BCR	0.00	0.23	0.75	0.25	0.00	0.00	0.53	0.00
MXZ	0.69	6.78	1.75	3.75	1.22	1.25	3.00	1.75
CR3	0.93	6.24	2.75	7.50	4.00	6.92	3.85	3.50
CR4	0.00	0.00	0.00	0.00	4.25	6.25	4.00	2.25
CR5	0.00	0.00	0.00	0.00	0.50	1.25	0.75	1.25
FBA	0.00	0.00	0.00	0.00	0.00	0.00	0.00	0.00
CR6	0.00	0.00	0.00	0.00	0.00	0.00	0.00	0.00
CRA	10.00	0.00	0.00	0.00	4.75	6.75	3.50	4.00
CRB	0.00	0.00	0.00	0.00	1.00	1.00	0.50	1.00
CLK	0.00	0.00	0.00	0.00	1.50	3.25	2.00	3.50
LKC	2.78	68.38	10.50	39.00	8.75	30.02	6.25	15.00
CRU	0.23	4.16	1.00	4.75	1.00	0.75	0.25	1.25
CRV	0.23	1.39	1.25	1.75	0.00	0.00	0.00	0.00
CRD	3.24	31.92	21.00	38.00	16.00	21.25	10.00	8.00
CRE	0.00	1.16	0.25	1.25	6.00	9.25	4.75	4.00
TOATAL	45.26	173.04	75.50	158.32	118.42	132.28	82.92	67.75

Table 8.6: Inventory of electrofishing effort (hours of pedal time) from January, 2010 through December, 2013, including imputed effort for 2010. No fishing effort occurred in 2009.

Fishing Expedition	Prior Probability	Posterior Probability	
		$p(\text{SPECIES PRESENT} = \textit{True} \mid \text{CATCH} = \textit{False})$	$p(\text{SPECIES PRESENT} = \textit{False} \mid \text{CATCH} = \textit{False})$
1	0.500	0.326	0.674
2	0.326	0.190	0.810
3	0.190	0.102	0.898
4	0.102	0.052	0.948
5	0.052	0.026	0.974

Table 8.7: Example showing how the posterior probability that a species is present at a search site can be successively updated using as evidence the failure of repeated attempts to capture a specimen of the target species.

<b>Reach</b>	<b>Gill and Trammel Net (100 Meters)</b>	<b>Electrofishing (Hours)</b>	<b>Deep Gill Nets (100 Meter hours)</b>	<b>Trap Nets (Net days)</b>
NSC	250.26	139.16	0.00	0.00
CR1	206.04	38.52	0.00	0.00
CRM	0.00	0.00	0.00	0.00
CR2	332.67	114.40	0.00	0.00
BCR	3.31	1.23	0.00	0.00
MXZ	110.33	15.44	0.00	0.00
CR3	131.92	28.34	0.00	0.00
CR4	135.75	10.50	0.00	0.00
CR5	0.00	1.75	0.00	0.00
FBA	0.00	0.00	0.00	0.00
CR6	0.00	0.00	0.00	0.00
CRA	80.03	21.50	0.00	0.00
CRB	17.41	2.00	0.00	0.00
CLK	151.79	4.75	0.00	0.00
LKC	1245.44	159.42	0.00	52.70
CRU	73.15	11.89	0.00	0.00
CRV	8.27	4.62	0.00	0.00
CRD	653.47	131.40	0.00	0.00
CRE	151.79	17.91	0.00	0.00
<b>TOTAL</b>	<b>3551.63</b>	<b>702.82</b>	<b>0.00</b>	<b>52.70</b>

Table 8.8: Conventional surveillance fishing effort (2009 – 2012) used in calculating prior probabilities of target species presence. Includes imputed fishing effort from 2010.

TARGET SHEDUNITS (kg)	NSC	CR1	CRM	CR2	CR3	MXZ	BCR	CR4	CR5	FBA	CR6	CRA	CRB	CLK	LKC	CRU	CRV	CRD	CRE
0-1	0.500	0.500	0.500	0.500	0.500	0.500	0.500	0.500	0.500	0.500	0.500	0.500	0.500	0.500	0.500	0.500	0.500	0.500	0.500
1-5	0.500	0.500	0.500	0.500	0.500	0.500	0.500	0.500	0.500	0.500	0.500	0.500	0.500	0.500	0.500	0.500	0.500	0.500	0.500
5-10	0.500	0.500	0.500	0.500	0.500	0.499	0.500	0.500	0.500	0.500	0.500	0.500	0.500	0.500	0.499	0.500	0.500	0.500	0.500
10-50	0.499	0.500	0.500	0.499	0.500	0.498	0.500	0.500	0.500	0.500	0.500	0.500	0.500	0.499	0.497	0.499	0.500	0.499	0.500
50-100	0.498	0.499	0.500	0.498	0.500	0.494	0.499	0.500	0.500	0.500	0.500	0.500	0.500	0.498	0.494	0.499	0.499	0.498	0.500
100-250	0.495	0.498	0.500	0.496	0.500	0.485	0.499	0.499	0.500	0.500	0.500	0.500	0.499	0.496	0.485	0.497	0.499	0.496	0.499
250-500	0.489	0.495	0.500	0.491	0.499	0.469	0.497	0.499	0.500	0.500	0.500	0.499	0.498	0.492	0.468	0.493	0.497	0.492	0.499
500-750	0.482	0.492	0.500	0.484	0.499	0.448	0.496	0.498	0.500	0.500	0.500	0.498	0.497	0.487	0.447	0.489	0.495	0.486	0.498
750-1000	0.475	0.489	0.500	0.478	0.499	0.428	0.494	0.497	0.500	0.500	0.500	0.498	0.495	0.481	0.426	0.485	0.493	0.481	0.497
1000-1250	0.468	0.486	0.500	0.472	0.498	0.407	0.492	0.496	0.500	0.500	0.500	0.497	0.494	0.476	0.405	0.480	0.491	0.475	0.496
1250-1500	0.461	0.483	0.500	0.466	0.498	0.387	0.490	0.495	0.500	0.500	0.500	0.496	0.493	0.471	0.384	0.476	0.489	0.470	0.495
1500-1750	0.454	0.480	0.500	0.459	0.497	0.368	0.489	0.495	0.500	0.500	0.500	0.496	0.491	0.465	0.364	0.471	0.487	0.464	0.494
1750-2000	0.446	0.477	0.500	0.453	0.497	0.348	0.487	0.494	0.500	0.500	0.500	0.495	0.490	0.460	0.345	0.467	0.485	0.458	0.493
2000-3000	0.429	0.469	0.500	0.438	0.496	0.302	0.483	0.492	0.500	0.500	0.500	0.493	0.487	0.447	0.298	0.456	0.480	0.445	0.491
3000-4000	0.401	0.457	0.500	0.413	0.494	0.236	0.476	0.488	0.500	0.500	0.500	0.491	0.482	0.426	0.232	0.438	0.471	0.423	0.487
4000-5000	0.374	0.445	0.500	0.389	0.493	0.181	0.469	0.485	0.500	0.500	0.500	0.488	0.476	0.405	0.176	0.421	0.463	0.401	0.484
5000-6000	0.347	0.433	0.500	0.366	0.491	0.136	0.462	0.482	0.500	0.500	0.500	0.486	0.471	0.384	0.132	0.404	0.455	0.380	0.480
6000-7000	0.322	0.421	0.500	0.343	0.489	0.101	0.455	0.478	0.500	0.500	0.500	0.483	0.466	0.364	0.097	0.387	0.447	0.360	0.476
7000-8000	0.297	0.409	0.500	0.321	0.488	0.074	0.448	0.475	0.500	0.500	0.500	0.480	0.461	0.345	0.071	0.370	0.438	0.339	0.473
8000-9000	0.274	0.397	0.500	0.299	0.486	0.054	0.441	0.472	0.500	0.500	0.500	0.478	0.455	0.326	0.052	0.354	0.430	0.320	0.469
9000-10000	0.252	0.385	0.500	0.279	0.484	0.039	0.434	0.468	0.500	0.500	0.500	0.475	0.450	0.307	0.037	0.338	0.422	0.301	0.465
10000-11000	0.230	0.373	0.500	0.259	0.483	0.028	0.427	0.465	0.500	0.500	0.500	0.472	0.445	0.289	0.027	0.322	0.414	0.282	0.462
11000-12000	0.211	0.362	0.500	0.240	0.481	0.020	0.420	0.462	0.500	0.500	0.500	0.470	0.440	0.272	0.019	0.306	0.405	0.265	0.458
12000-13000	0.192	0.351	0.500	0.222	0.479	0.014	0.414	0.458	0.500	0.500	0.500	0.467	0.434	0.255	0.014	0.291	0.397	0.248	0.455
13000-14000	0.175	0.339	0.500	0.206	0.478	0.010	0.407	0.455	0.500	0.500	0.500	0.465	0.429	0.239	0.010	0.277	0.389	0.232	0.451
14000-15000	0.159	0.328	0.500	0.190	0.476	0.007	0.400	0.452	0.500	0.500	0.500	0.462	0.424	0.224	0.007	0.263	0.381	0.216	0.447
15000-16000	0.144	0.318	0.500	0.175	0.474	0.005	0.393	0.448	0.500	0.500	0.500	0.459	0.419	0.209	0.005	0.249	0.373	0.201	0.444
16000-17000	0.130	0.307	0.500	0.161	0.473	0.004	0.387	0.445	0.500	0.500	0.500	0.457	0.414	0.195	0.003	0.236	0.365	0.188	0.440
17000-18000	0.118	0.297	0.500	0.148	0.471	0.002	0.380	0.442	0.500	0.500	0.500	0.454	0.408	0.182	0.002	0.223	0.357	0.174	0.437
18000-19000	0.106	0.286	0.500	0.135	0.469	0.002	0.374	0.438	0.500	0.500	0.500	0.451	0.403	0.169	0.002	0.211	0.349	0.162	0.433
19000-20000	0.096	0.276	0.500	0.124	0.468	0.001	0.367	0.435	0.500	0.500	0.500	0.449	0.398	0.158	0.001	0.199	0.341	0.150	0.429

Table 8.9: Prior probability the target species is present given fishing effort using commercial fishing nets during the period 2009 - 2012. These prior probabilities are inputs to the probabilistic model.

TARGET SHEDUNITS (kg)	NSC	CR1	CRM	CR2	CR3	MXZ	BCR	CR4	CR5	FBA	CR6	CRA	CRB	CLK	LKC	CRU	CRV	CRD	CRE
0-1	0.500	0.500	0.500	0.500	0.500	0.500	0.500	0.500	0.500	0.500	0.500	0.500	0.500	0.500	0.500	0.500	0.500	0.500	0.500
1-5	0.500	0.500	0.500	0.500	0.500	0.500	0.500	0.500	0.500	0.500	0.500	0.500	0.500	0.500	0.500	0.500	0.500	0.500	0.500
5-10	0.500	0.500	0.500	0.500	0.500	0.500	0.500	0.500	0.500	0.500	0.500	0.500	0.500	0.500	0.500	0.500	0.500	0.500	0.500
10-50	0.500	0.500	0.500	0.500	0.500	0.500	0.500	0.500	0.500	0.500	0.500	0.500	0.500	0.500	0.500	0.500	0.500	0.500	0.500
50-100	0.499	0.500	0.500	0.499	0.500	0.499	0.500	0.500	0.500	0.500	0.500	0.500	0.500	0.500	0.499	0.500	0.500	0.500	0.500
100-250	0.497	0.500	0.500	0.498	0.500	0.498	0.500	0.500	0.500	0.500	0.500	0.500	0.500	0.500	0.498	0.499	0.499	0.499	0.500
250-500	0.494	0.499	0.500	0.497	0.500	0.496	0.499	0.500	0.500	0.500	0.500	0.500	0.500	0.500	0.496	0.499	0.498	0.498	0.500
500-750	0.490	0.499	0.500	0.495	0.500	0.493	0.499	0.500	0.500	0.500	0.500	0.500	0.500	0.500	0.493	0.498	0.497	0.497	0.500
750-1000	0.486	0.498	0.500	0.492	0.499	0.490	0.499	0.500	0.500	0.500	0.500	0.499	0.499	0.499	0.490	0.497	0.496	0.496	0.500
1000-1250	0.482	0.497	0.500	0.490	0.499	0.487	0.498	0.500	0.500	0.500	0.500	0.499	0.499	0.499	0.488	0.497	0.495	0.495	0.500
1250-1500	0.478	0.497	0.500	0.488	0.499	0.484	0.498	0.500	0.500	0.500	0.500	0.499	0.499	0.499	0.485	0.496	0.494	0.494	0.499
1500-1750	0.474	0.496	0.500	0.486	0.499	0.481	0.498	0.500	0.500	0.500	0.500	0.499	0.499	0.499	0.482	0.495	0.493	0.493	0.499
1750-2000	0.470	0.496	0.500	0.484	0.499	0.478	0.497	0.500	0.500	0.500	0.500	0.499	0.499	0.499	0.479	0.495	0.491	0.492	0.499
2000-3000	0.460	0.494	0.500	0.479	0.498	0.471	0.496	0.499	0.500	0.500	0.500	0.498	0.498	0.498	0.473	0.493	0.489	0.489	0.499
3000-4000	0.444	0.492	0.500	0.470	0.498	0.459	0.495	0.499	0.500	0.500	0.500	0.498	0.498	0.498	0.462	0.490	0.484	0.484	0.498
4000-5000	0.429	0.490	0.500	0.461	0.497	0.447	0.493	0.499	0.500	0.500	0.500	0.497	0.497	0.497	0.451	0.487	0.479	0.480	0.498
5000-6000	0.413	0.487	0.500	0.453	0.497	0.436	0.492	0.499	0.500	0.500	0.500	0.496	0.497	0.496	0.440	0.484	0.475	0.475	0.498
6000-7000	0.398	0.485	0.500	0.444	0.496	0.424	0.490	0.498	0.499	0.500	0.500	0.495	0.496	0.496	0.429	0.481	0.470	0.471	0.497
7000-8000	0.383	0.483	0.500	0.436	0.495	0.412	0.489	0.498	0.499	0.500	0.500	0.495	0.495	0.495	0.418	0.478	0.465	0.467	0.497
8000-9000	0.368	0.480	0.500	0.427	0.495	0.401	0.487	0.498	0.499	0.500	0.500	0.494	0.495	0.494	0.408	0.476	0.461	0.462	0.496
9000-10000	0.353	0.478	0.500	0.419	0.494	0.389	0.486	0.498	0.499	0.500	0.500	0.493	0.494	0.494	0.397	0.473	0.456	0.458	0.496
10000-11000	0.338	0.476	0.500	0.411	0.494	0.378	0.484	0.497	0.499	0.500	0.500	0.493	0.494	0.493	0.387	0.470	0.451	0.453	0.495
11000-12000	0.324	0.474	0.500	0.402	0.493	0.367	0.483	0.497	0.499	0.500	0.500	0.492	0.493	0.492	0.376	0.467	0.447	0.449	0.495
12000-13000	0.310	0.471	0.500	0.394	0.492	0.356	0.481	0.497	0.499	0.500	0.500	0.491	0.492	0.492	0.366	0.464	0.442	0.444	0.495
13000-14000	0.297	0.469	0.500	0.386	0.492	0.345	0.480	0.497	0.499	0.500	0.500	0.490	0.492	0.491	0.356	0.461	0.437	0.440	0.494
14000-15000	0.284	0.467	0.500	0.378	0.491	0.334	0.478	0.496	0.499	0.500	0.500	0.490	0.491	0.490	0.346	0.458	0.433	0.436	0.494
15000-16000	0.271	0.464	0.500	0.370	0.490	0.323	0.477	0.496	0.499	0.500	0.500	0.489	0.491	0.490	0.336	0.455	0.428	0.431	0.493
16000-17000	0.258	0.462	0.500	0.362	0.490	0.312	0.475	0.496	0.499	0.500	0.500	0.488	0.490	0.489	0.326	0.452	0.423	0.427	0.493
17000-18000	0.246	0.460	0.500	0.354	0.489	0.302	0.474	0.495	0.498	0.500	0.500	0.488	0.489	0.488	0.317	0.449	0.418	0.422	0.492
18000-19000	0.234	0.457	0.500	0.346	0.489	0.292	0.472	0.495	0.498	0.500	0.500	0.487	0.489	0.488	0.307	0.447	0.414	0.418	0.492
19000-20000	0.223	0.455	0.500	0.338	0.488	0.281	0.471	0.495	0.498	0.500	0.500	0.486	0.488	0.487	0.298	0.444	0.409	0.414	0.492

Table 8.10: Prior probability that the target species is present given fishing effort for electrofishing boats during the period 2009 - 2012. These prior probabilities are inputs to the probabilistic model.

TARGET SHEDUNITS (kg)	NSC	CR1	CRM	CR2	CR3	MXZ	BCR	CR4	CR5	FBA	CR6	CRA	CRB	CLK	LKC	CRU	CRV	CRD	CRE
0-1	0.500	0.500	0.500	0.500	0.500	0.500	0.500	0.500	0.500	0.500	0.500	0.500	0.500	0.500	0.500	0.500	0.500	0.500	0.500
1-5	0.500	0.500	0.500	0.500	0.500	0.500	0.500	0.500	0.500	0.500	0.500	0.500	0.500	0.500	0.500	0.500	0.500	0.500	0.500
5-10	0.500	0.500	0.500	0.500	0.500	0.499	0.500	0.500	0.500	0.500	0.500	0.500	0.500	0.500	0.499	0.500	0.500	0.500	0.500
10-50	0.499	0.500	0.500	0.499	0.500	0.497	0.500	0.500	0.500	0.500	0.500	0.500	0.500	0.499	0.497	0.499	0.500	0.499	0.500
50-100	0.497	0.499	0.500	0.497	0.500	0.493	0.499	0.500	0.500	0.500	0.500	0.500	0.500	0.498	0.492	0.498	0.499	0.498	0.500
100-250	0.492	0.497	0.500	0.494	0.500	0.483	0.499	0.499	0.500	0.500	0.500	0.499	0.499	0.496	0.482	0.496	0.498	0.495	0.499
250-500	0.483	0.495	0.500	0.487	0.499	0.464	0.497	0.499	0.500	0.500	0.500	0.499	0.498	0.492	0.463	0.492	0.495	0.490	0.498
500-750	0.472	0.491	0.500	0.479	0.499	0.441	0.495	0.498	0.500	0.500	0.500	0.498	0.496	0.486	0.438	0.487	0.492	0.483	0.497
750-1000	0.461	0.487	0.500	0.471	0.498	0.418	0.493	0.497	0.500	0.500	0.500	0.497	0.495	0.481	0.413	0.482	0.489	0.477	0.496
1000-1250	0.450	0.484	0.500	0.462	0.497	0.395	0.490	0.496	0.500	0.500	0.500	0.496	0.493	0.475	0.389	0.477	0.486	0.470	0.495
1250-1500	0.439	0.480	0.500	0.454	0.497	0.372	0.488	0.495	0.500	0.500	0.500	0.495	0.492	0.470	0.366	0.472	0.483	0.463	0.494
1500-1750	0.428	0.476	0.500	0.446	0.496	0.350	0.486	0.494	0.500	0.500	0.500	0.495	0.490	0.464	0.343	0.467	0.479	0.457	0.493
1750-2000	0.417	0.473	0.500	0.437	0.496	0.329	0.484	0.493	0.500	0.500	0.500	0.494	0.489	0.459	0.321	0.462	0.476	0.450	0.492
2000-3000	0.390	0.464	0.500	0.417	0.494	0.278	0.479	0.491	0.500	0.500	0.500	0.492	0.485	0.445	0.269	0.449	0.468	0.434	0.490
3000-4000	0.349	0.449	0.500	0.385	0.492	0.208	0.470	0.487	0.500	0.500	0.500	0.488	0.480	0.423	0.197	0.428	0.455	0.408	0.486
4000-5000	0.309	0.435	0.500	0.353	0.490	0.152	0.462	0.484	0.500	0.500	0.500	0.485	0.474	0.402	0.141	0.408	0.443	0.382	0.482
5000-6000	0.273	0.420	0.500	0.323	0.488	0.108	0.454	0.480	0.500	0.500	0.500	0.482	0.468	0.381	0.099	0.389	0.430	0.357	0.478
6000-7000	0.239	0.406	0.500	0.294	0.485	0.076	0.445	0.477	0.499	0.500	0.500	0.478	0.462	0.360	0.069	0.369	0.417	0.333	0.474
7000-8000	0.208	0.392	0.500	0.267	0.483	0.053	0.437	0.473	0.499	0.500	0.500	0.475	0.456	0.340	0.047	0.350	0.405	0.310	0.470
8000-9000	0.180	0.378	0.500	0.242	0.481	0.037	0.428	0.469	0.499	0.500	0.500	0.472	0.450	0.321	0.032	0.332	0.392	0.288	0.465
9000-10000	0.155	0.364	0.500	0.218	0.479	0.025	0.420	0.466	0.499	0.500	0.500	0.468	0.444	0.302	0.022	0.313	0.380	0.266	0.461
10000-11000	0.133	0.351	0.500	0.196	0.476	0.017	0.412	0.462	0.499	0.500	0.500	0.465	0.439	0.283	0.015	0.296	0.367	0.246	0.457
11000-12000	0.114	0.338	0.500	0.175	0.474	0.012	0.404	0.459	0.499	0.500	0.500	0.462	0.433	0.266	0.010	0.279	0.355	0.227	0.453
12000-13000	0.097	0.325	0.500	0.157	0.472	0.008	0.396	0.455	0.499	0.500	0.500	0.458	0.427	0.249	0.007	0.262	0.343	0.209	0.449
13000-14000	0.082	0.312	0.500	0.140	0.469	0.005	0.388	0.451	0.499	0.500	0.500	0.455	0.421	0.232	0.004	0.247	0.331	0.192	0.445
14000-15000	0.070	0.300	0.500	0.124	0.467	0.004	0.379	0.448	0.499	0.500	0.500	0.452	0.415	0.217	0.003	0.232	0.319	0.176	0.441
15000-16000	0.059	0.287	0.500	0.110	0.465	0.002	0.372	0.444	0.499	0.500	0.500	0.448	0.410	0.202	0.002	0.217	0.308	0.161	0.437
16000-17000	0.050	0.276	0.500	0.098	0.463	0.002	0.364	0.441	0.499	0.500	0.500	0.445	0.404	0.188	0.001	0.203	0.296	0.147	0.433
17000-18000	0.042	0.264	0.500	0.087	0.460	0.001	0.356	0.437	0.498	0.500	0.500	0.442	0.398	0.175	0.001	0.190	0.285	0.134	0.429
18000-19000	0.035	0.253	0.500	0.076	0.458	0.001	0.348	0.434	0.498	0.500	0.500	0.439	0.392	0.163	0.001	0.177	0.274	0.122	0.425
19000-20000	0.030	0.242	0.500	0.067	0.456	0.000	0.340	0.430	0.498	0.500	0.500	0.435	0.387	0.151	0.000	0.166	0.263	0.111	0.421

Table 8.11: Prior probability that the target species is present given fishing effort for all gear types during the period 2009 - 2012. These prior probabilities are inputs to the probabilistic model.

<b>SYMBOL</b>	<b>Description</b>
ACTUAL_SHEDUNITS	Number of shedding units targeted in the target reach (kg).
ALL_ACTIVE	Active node controlling all secondary source loading rates ( <i>True, Uncertain, False</i> ).
EQUIV_NOM_SHEDUNITS	Equivalent nominal concentration of shedding units in the source reach (kg)
FOPH	Frequency of positive hits. The fraction of eDNA monitoring samples testing positive for the target marker.
FRACT	Fraction of the target marker shed from a live source that decays at the fast decay rates.
GEAR_TYPE	Fishing effort used in estimating prior p(Fish present = True) ( <i>CN</i> = Commercial net, <i>EF</i> = Electrofishing, <i>ALL</i> )
K_FAST	Fast decay rate ( $d^{-1}$ ).
K_SLOW	Slow decay rate ( $d^{-1}$ ).
LURK_REACH	The CAWS reach where shedding unit(s) are being targeted (NSC, CR1, CRM, ..., CR6).
PRIM_FAST_CONC	Concentration of target marker originating at a primary source that decays by the faster decay rate (copies/L)
PRIM_NOM_CONC	Primary nominal concentration (copies/L). The target marker concentration attributed to a single shedding unit.
PRIM_SLOW_CONC	Concentration of target marker originating at a primary source that decays by the slower decay rate (copies/L).
SEARCH_AREA	Location of the target reach(es) relative to the sample reach ( <i>Upstream, Local, Downstream, Entire CAWS</i> ).
SEASON	Season of the year ( <i>Gates Open, Gates Closed</i> ).
SHED_RATE	Primary source target marker shedding rate (copies/kg/hr).
SPECIES	Target Asian carp species ( <i>Bighead, Silver</i> ).
SPECIES_PRESENT	Whether or not the target species is present in the SEARCH_AREA ( <i>True, False</i> ).
TARGET_SHEDUNITS	The number of shedding units being targeted in the source reach (kg).
TOT_CONC	Total target marker concentration (copies/L).
TOT_PRIM_CONC	Total primary concentration (copies/L). The target marker concentration attributed to primary sources.
TOT_SEC_CONC	Total secondary concentration (copies/L). The target marker concentration attributed to all secondary sources.

Table 9.1: Variables in the Bayesian network (alphabetical list)



Region	Season: Gates open		Season: Gates closed	
	Mass: 1-5 kg	Mass: 10-11 t	Mass: 1-5 kg	Mass: 10-11 t
A	0.00 – 0.20	0.00 – 0.00	0.00 – 0.00	0.00 – 0.00
B	0.20 – 0.20	0.00 – 0.75	0.00 – 0.00	0.00 – 0.00
C	0.20 – 0.90	0.75 – 0.90	0.00 – 0.55	0.00 – 0.50
D	0.90 – 1.00	0.90 – 1.00	0.55 – 1.00	0.50 – 1.00

Table 9.2: Critical regions for interpretation of demonstration results in the LKC

## **APPENDICES TO THE FINAL ECALS MILESTONE REPORT**

**Appendix 1.** Methods Used to Characterize the Probability of Detection for Conventional PCR (cPCR) and Quantitative (qPCR) Assays

**Appendix 2.** Methods Used to Characterize the Probability Distribution Inherent to Sanger Sequencing of PCR Amplicons

**Appendix 3.** Methods to Estimate Percent Sequence Similarity among Silver Carp, Bighead Carp, and Related Species from the Chicago Area Waterways System.

**Appendix 4.** Summary of eDNA Monitoring Data and Concentration Estimates, 2009-2013

**Appendix 5.** Technical results of Bayesian MCMC Supervised Simulation (Available from the lead author by separate request.)

**Appendix 1.** Methods Used to Characterize the Probability of Detection using Conventional PCR (cPCR) and Quantitative (qPCR) Assays

*Conventional PCR (cPCR)*

We assessed the variance in conventional polymerase chain reaction (cPCR) results using markers developed by Jerde et al. (2012) for bighead (*Hypophthalmichthys nobilis*) and silver carp (*H. molitrix*). Whole bighead and silver carp carcasses were obtained from the local area. DNA was extracted from these samples using the DNeasy Blood and Tissue Kit (Qiagen, Germantown, MD, USA) kit. PCR was conducted using primers HN203-F and HN498-R for *H. nobilis* and HMF-2 and HMR-2 for *H. molitrix* from Jerde et al. (2012). PCR protocols were similar to those in Jerde et al. (2012) with PCR reagents and thermal-cycling parameters outlined in Tables 1 and 2.

Table A1.1: PCR reagents, volumes aliquoted into solution, and final concentrations in study PCRs.

Reagent	Solution Volume	Final Concentration
Platinum Taq <sup>®</sup> PCR Buffer (10X) (Thermo Fisher Scientific, Waltham, MA, USA)	2.5 µl	1X
MgCl <sub>2</sub> (50 mM) (Thermo Fisher Scientific)	0.75 µl	1.5 mM
equimolar dNTP mix (10 mM) (New England Biolabs, Ipswich, MA)	0.5 µl	200 µM
Platinum Taq <sup>®</sup> (5 unit/µl) (Thermo Fisher Scientific)	0.25 µl	1.25 units
Forward Primer (10 µM)	0.5 µl	0.2 µM
Reverse Primer (10 µM)	0.5 µl	0.2 µM
Template DNA	1 µl	variable
DNase-free sterile water (Ambion Inc., Austin, TX, USA)	19 µl	--
	<b>25 µl</b>	<b>Total Volume</b>

Table A1.2: PCR thermal-cycling program

Step	Temperature	Time	Cycles
1	94° C	10 min.	1
2	94° C	1 min.	45
	52° C (bighead carp) 50° C (silver carp)	1 min.	
	72° C	1.5 min.	
3	72° C	7 min.	1
4	4° C	until removed	1

PCR amplicons were isolated using Life Technologies™ E-Gel® SizeSelect™ 1.2% agarose gels (Thermo Fisher Scientific). Amplicons were then “sequence verified” as bighead or silver carp DNA on an Applied Biosystems® 3500xL Genetic Analyzer (Thermo Fisher Scientific). We sequenced amplicons in both directions using the same forward and reverse primers as were used for conventional PCR. Sequencing reagents and thermal-cycling parameters are outlined in Tables 3 and 4. Along with each set of cPCR amplicon samples, 2-5 negative control (water blank) cPCR samples, 2 samples with pGEM® positive control template (with 21 M13 control primer), and 2 cPCR positive control samples were sequenced.

Once sequence-confirmed, amplicons from each species were ligated into the double-stranded pCR™4-TOPO vector plasmid and cloned into *E. coli Mach1*™ competent cells using TOPO® TA cloning kit (Thermo Fisher Scientific, Inc.) as per the manufacturer’s instructions. Successfully cloned colonies were cultured and plasmid DNA was extracted using Qiagen Miniprep plasmid extraction kits (Qiagen, Germantown, MD, USA). An estimated plasmid DNA copy number (CN) was “back calculated” by measuring the mass (ng) of DNA in a pure plasmid elution with a NanoDrop™ 1000 (Thermo Fisher Scientific, Inc.) and dividing that mass that by the expected mass of a single plasmid (plus insert). The expected mass of the plasmid was based on a standard conversion of  $1.66 \times 10^{-15}$  ng per Dalton, 650 Daltons per DNA base pair (bp), and 4268 bp and 4147 bp total lengths for the respective bighead and silver carp marker+plasmid constructs. (<http://gc.nci.nih.gov/Sequence%20analysis/Constants%20from%20Eppendorf.html>).

Table A1.3: Sequencing reagents, volumes aliquoted into solution, and final concentrations in sequencing reaction.

Component	Solution Volume	Final Concentration
BigDye Terminator Buffer 5X (Thermo Fisher Scientific)	4 µl	1X
Forward or Reverse Primer (10 µM)	0.8 µl	0.4 µM
BigDye Ready Reaction Premix (Thermo Fisher Scientific)	1 µl	--
Template DNA	4 µl	variable
DNase-free sterile water (Ambion Inc., Austin, TX, USA)	10.2 µl	--
	<b>20 µl</b>	<b>Total Volume</b>

Table A1.4: Sequencing reaction thermal-cycling program

Step	Temperature	Time	Cycles
1	96° C	1 min	1
2	96° C	10 sec.	25
	55° C	5 sec	
	60° C	4 min	
3	4° C	Until removed	1

For both species, different concentrations of plasmid DNA working stock were created by successive dilutions to obtain the full range of 15 CN/  $\mu$ l, 14 CN/  $\mu$ l, . . . 1 CN/  $\mu$ l. Additional working stocks of 100 CN/  $\mu$ l and 50 CN/  $\mu$ l were created for bighead carp. For each concentration class we ran 30 cPCRs, as well as 30 cPCRs with negative control (water blank) templates. PCR protocols were the same as those described in Tables 1 and 2, with the exception of the different concentrations of template DNA. The number of successful cPCRs (produced bands of the appropriate size) within each copy number class that was determined.

*Quantitative PCR (qPCR)*

For quantitative real-time PCR, or qPCR, assays, two markers, BHTM-1 and SCTM, designed by ERDC for hydrolysis probe-based qPCR (i.e. TaqMan<sup>®</sup> qPCR) of bighead and silver carp, respectively, were used to characterize variability surrounding absolute quantitation estimates from qPCR. In order to create concentrated stickes of target DNA for these trials, amplicons from PCR of DNA isolated from Asian carp tissues using the forward and reverse primers, but not hydrolysis probes, from BHTM-1 and SCTM-5, were ligated into the pCR<sup>TM4</sup>-TOPO vector plasmid and cloned into *E. coli Mach1*<sup>TM</sup> competent cells using the TOPO<sup>®</sup> TA cloning kit (Thermo Fisher Scientific, Inc.) following manufacturer’s instructions. Successfully cloned colonies were cultured and plasmid DNAs were extracted using Qiagen Miniprep plasmid extraction kits (Qiagen Inc., Valencia, CA). An estimated plasmid DNA copy number (CN) for each extraction elution was “back calculated” as described above for the cPCR trials. A serial 10-fold dilution of the plasmid DNA stock, in the range of  $2.3 \times 10^0$  to  $2.3 \times 10^7$  copies, was prepared and used to generate a standard curve for calculation of copy number in the qPCR reactions for both BHTM1 and SCTM5, respectively. To assess the variability in quantitation, the following copy number concentration [CN] classes were created by serially diluting a starting stock solution of  $1 \times 10^5$  copies: 1000 CN/  $\mu$ l, 500 CN/  $\mu$ l, 200 CN/  $\mu$ l, 100 CN/  $\mu$ l, 50 CN/  $\mu$ l, 10 CN/  $\mu$ l, 5CN/ul and 1 CN/  $\mu$ l, were tested on both makers. For each qPCR marker and each copy number concentration ten replicate qPCRs were performed.

All qPCR reactions were run 20- $\mu$ l volumes with reagents as listed in Table A1.5 and a thermal-cycling program as detailed in Table A1.6.

Table A1.5: Quantitative real-time PCR (qPCR) reagents, volumes aliquoted into solution, and final concentrations in study qPCRs.

<b>Component</b>	<b>Solution Volume</b>	<b>Final Concentration</b>
Environmental Master Mix 2.0 (2X) (Thermo Fisher Scientific)	10 $\mu$ l	1X
Forward Primer (10 $\mu$ M)	1 $\mu$ l	0.5 $\mu$ M
Reverse Primer (10 $\mu$ M)	1 $\mu$ l	0.5 $\mu$ M
Probe (2.5 $\mu$ M)	1 $\mu$ l	0.125 $\mu$ M
Template DNA	1 $\mu$ l	1-1,000 copies/ $\mu$ l
DNase-free sterile water (Ambion Inc., Austin, TX, USA)	6 $\mu$ l	--
	<b>20 <math>\mu</math>l</b>	<b>Total Volume</b>

Table A1.6: Quantitative real-time PCR (qPCR) thermal-cycling program.

<b>Step</b>	<b>Temperature</b>	<b>Time</b>	<b>Cycles</b>
1	95° C	10 min.	1
2	95° C	15 sec.	40
	60° C	1 min.	

In addition to above experiments, 30 replicate qPCRs were run with copy number concentrations of 0, 1 and 5 copies/ $\mu$ l for both qPCR markers, but with 50 cycles instead of 40 cycles as described for Step 2 in Table A1.6. This test was run in order to determine if additional cycles would result in higher detection rates for low copy number samples.

## **Appendix 2. Methods Used to Characterize Probability Distributions Inherent to Sanger Sequencing of PCR Amplicons**

We assessed the variance in sequencing success of PCR amplicons (cPCR) by attempting to sequence the products of conventional PCR trials described in Appendix 1. In this case, as in other trials described in this report, “sequencing” refers to traditional Sanger sequencing that is based on the incorporation of fluorescently-labeled chain-terminating dideoxynucleotides into growing DNA sequences during PCR amplification. DNA sequences were read using an Applied Biosystems® 3500xL Genetic Analyzer (Thermo Fisher Scientific, Waltham, MA, USA).

In the cPCR variability trials (methods described in Appendix 1) 30 replicate cPCRs were run for each of numerous copy number (CN) concentration classes for both species (CN = 1-15 for both bighead and silver carp, also CN = 25 and 50 for bighead carp). In order to characterize the change in probability of successfully sequencing of PCR amplicons arising from the different copy number concentrations in cPCR, the remaining DNA volumes (~ 15 µl) from each successful cPCR (bands of the appropriate size were observed on gels), for both species and all copy number concentrations, were purified on an E-Gel® SizeSelect™ Gels (Thermo Fisher Scientific, Inc.). These DNA samples (i.e. cPCR amplicons) were then used in separate sequencing reactions with the forward and the reverse PCR primers. Sequencing protocols are described in Table 3 and Table 4 of Appendix 1. Along with each set of cPCR amplicon samples, 2-5 negative control (water blank) cPCR samples, 2 samples with pGEM® positive control template (with 21 M13 control primer), and 2 cPCR positive control samples were sequenced.

The resulting sequences were compared against BHC and SC reference sequences using CodonCode Aligner Version 3.7.1 (CodonCode Corporation, Centerville, MA, USA). Reference sequences were obtained from the National Center for Biotechnology Information’s GenBank and included sequences NC\_010194.1 and EU343733.1 for bighead carp and NC\_010156.1 and EU315941.1 for silver carp. Sequences with matches of 98% or better to reference sequences were considered “sequence-verified.” The number of samples from within each copy number concentration class that could be sequence verified (with either both forward primer and reverse primer sequencing reactions or just one reaction) was then determined.

**Appendix 3.** Methods Used to Estimate Percent Sequence Similarity among Silver Carp, Bighead Carp, and Related Species from the Chicago Area Waterways System

Percent sequence similarities were calculated for the mtDNA regions corresponding to 2 conventional PCR (cPCR) and four quantitative real-time PCR (qPCR) eDNA markers that have either been in use for Asian carp monitoring or that may be used in future monitoring (Table A3.1).

Table A3.1. eDNA markers for which percent sequence similarity estimates were calculated, the species each marker targets, whether the marker is used as a cPCR or qPCR assay, a citation for the scientific manuscript describing the marker, and whether the marker is currently being used for eDNA monitoring for silver and bighead carp or may be used in the future.

Marker	Species	PCR Type	Citation	Use
BH-UND	Bighead carp	cPCR	Jerde et al. 2012	Current
SC-UND	Silver Carp	cPCR	Jerde et al. 2012	Current
BH-TM1	Bighead carp	qPCR	Farrington et al. <i>in revision</i> <sup>1</sup>	Future
BH-TM2	Bighead carp	qPCR	Farrington et al. <i>in revision</i>	Future
SC-TM4	Silver Carp	qPCR	Farrington et al. <i>in revision</i>	Future
SC-TM5	Silver Carp	qPCR	Farrington et al. <i>in revision</i>	Future

In addition to silver carp and bighead carp, ten other fish from within Family Cyprinidae and that are found in the Great Lakes and Chicago Area Waterways System regions were selected for sequence comparisons (Table A3.2). For each species, the National Center for Biotechnology Information’s GenBank® (Benson et al. 2012) was searched for both complete mtDNA genomes and partial sequences that aligned with the different marker regions. Additionally, sequence data for whole mitochondrial haplotypes for six grass carp and one emerald shiner were generated using the Illumina MiSeq system with 150 bp paired-end reads. DNA extractions from fish tissue were enriched for mitochondrial DNA using long PCR to amplify the entire mitochondrial genome either as a single 16.6 kb fragment or as three shorter, overlapping fragments. DNA processing details, including long PCR protocols, are described in Farrington et al.<sup>2</sup> (*in revision*). Sequences obtained from the Illumina Miseq run were assembled with Geneious® software v6.5 (Biomatters Ltd., Auckland, New Zealand). Finally 33 big head carp and 29 silver carp whole mitogenomic sequences that were generated as part of an earlier study (Farrington et al., *in revision*) were incorporated into the sequence similarity data set.

For each marker region, all sequences from all species were aligned in Geneious 6.5, using high quality whole mitogenome sequences from either bighead carp or silver carp as reference sequences for alignment. For each marker region, sequences were globally aligned and a matrix of nucleotide differences among each possible pair of sequences was output. The sequence similarity between each pair of sequences (i.e. both intra- and interspecific pairwise comparisons) was calculated as  $(1 - (N \text{ pairwise nucleotide differences} / \text{length of marker region}))$ . These values were then converted to percent sequence similarity by multiplying by 100. The

<sup>1</sup> <http://dx.doi.org/10.1101/003624>

<sup>2</sup> *see footnote 2.*



mean and standard deviation were then calculated from all individual sequence pairwise percent similarities for each combination of species.

Literature Cited

Benson, D., I. Karsch-Mizrachi, K. Clark, D. Lipman, J. Ostell, and E. Sayers. GenBank. 2012. Nucleic acids research 40:D48-D53.

Table A3.2. Different fish species from within the Cyprinidae that were included in percent sequence similarity estimates for six eDNA marker regions and, for each species, the number of individual sequences utilized in pairwise comparisons for each marker.

<b>Scientific name</b>	<b>Common Name</b>	<b>N BH-UND</b>	<b>N SC-UND</b>	<b>N BH-TM1</b>	<b>N BH-TM2</b>	<b>N SC-TM4</b>	<b>N SC-TM5</b>
<i>Campostoma anomalum</i>	Central stoneroller	93	93	2	2	2	2
<i>Ctenopharyngodon idella</i>	Grass carp	73	73	10	10	68	10
<i>Cyprinella spiloptera</i>	Spotfin shiner	21	22	3	2	2	3
<i>Cyprinus carpio</i>	Common carp	349	349	3	3	3	3
<i>Hypophthalmichthys molitrix</i>	Silver carp	29	29	29	29	29	29
<i>Hypophthalmichthys nobilis</i>	Grass carp	33	33	33	33	33	33
<i>Mylopharyngodon piceus</i>	Black carp	5	5	3	1	1	1
<i>Notemigonus crysoleucas</i>	Golden shiner	2	2	2	2	2	2
<i>Notropis atherinoides</i>	Emerald shiner	1	1	3	1	2	3
<i>Pimephales notatus</i>	Bluntnose minnow	0	0	11	0	0	11
<i>Pimephales promelas</i>	Flathead minnow	0	0	7	0	0	7
<i>Pimephales vigilax</i>	Bullhead minnow	0	0	4	0	0	4

#### **Appendix 4. Summary of eDNA Monitoring Data and Concentration Estimates, 2009-2013**

This appendix summarizes the results of the eDNA monitoring program in the CAWS during the period 2009-2013. Results are summarized in terms of the number of samples analyzed for the target marker of each species and the number of samples testing positive for each target marker. The frequency of positive detections, summarized in Tables 3.2 and 3.3 of the main report are calculated from these summaries. Section 3 of this report describes a Bayesian updating procedure for deriving a probability distribution to characterize uncertainty in target marker concentrations from the frequency of positive detections. This appendix summarizes the estimates of target marker concentration derived using that approach.

As in the text, these tables list CAWS reaches in order of occurrence, from upstream to downstream, beginning with the NSC and continuing through CR8, and then beginning with CRA and continuing through CRE. Tributary reaches, such as CRM and BCR, are listed immediately prior to the downstream reach into which they discharge. For the purpose of estimating concentrations, CRU and CRV have been combined into a single reach, CRC. Some water samples collected between 2009 and 2013 were located outside the hydrologic boundaries of the CAWS as defined for the purpose of this project. In particular, monitoring samples were sometimes collected in the North Branch of the Chicago River, the Little Calumet River, the Grand Calumet River, and Lake Michigan. Results from monitoring samples collected in these reaches are not summarized in these tables.

The first four tables in this appendix show the raw data used to calculate the frequency of positive detections in Tables 3.2 and 3.3. Tables A4.1 and A4.2 list the number of water samples tested for each target marker by reach and monitoring event. Tables A4.3 and A4.4 list the number of water samples testing positive for the target marker of each species. The date and season of each monitoring event have been summarized in Table 3.1 of the main report. Tables A4.5 – A4.7 report 5<sup>th</sup>, 50<sup>th</sup>, and 95<sup>th</sup> percentiles of estimated concentrations for bighead carp. Tables A4.8 – A4.10 report 5<sup>th</sup>, 50<sup>th</sup>, and 95<sup>th</sup> percentiles of estimated concentration for silver carp. The parameters of gamma distributions characterizing uncertainty in the concentrations are summarized in Tables A4.11 – A4.12 for bighead carp and in Tables A4.13 – A4.14 for silver carp. Percentiles and parameters are updated in each reach following each monitoring event. If no sampling occurred during a particular event, percentiles and parameter values are carried forward.

Event	Reach																			
	NSC	CR1	CRM	CR2	BCR	MXZ	CR3	CR4	CR5	FBA	CR6	CR7	CR8	CRA	CRB	CLK	LKC	CRC	CRD	CRE
1													16							
2												23	13							
3								25	9	9										
4										23	10									
5									8	19	16									
6																				
7		13	73	7																
8														14				27	44	
9																				
10							3	38	28											21
11																				
12										11	7									
13	45	7																		
14											2	3								
15									1					11	3	3	3	13	34	40
16			11																	
17										17	19	7								
18														46			14	5	33	
19														39	2		14	7	43	
20																	6	61		
21	67	20																		
22																				
23	58																			
24																		9	35	
25			20	45	13	3	34													
26												29	31							
27																				
28										21	22	3								
29														85	5			8		
30															3	24	68			
31																				
32																				
33																				
34																				
35									54	21	39									
36			27	81	1	5														
37																		13	96	1
38	110	4																		
39									45	6	52									
40								29	47											
41			24	79		11														
42	111	3																		
43															3	12	34	15	51	
44			24	79	2	9														
45	105	9																		
46																				
47															5	11	32	13	41	
48														2	4	11	32	15	50	
49															4	13	32	8		
50			23	73	2	9	7													
51	108	6																		
52															4	14	31	14	51	
53										57	5	52								
54			24	79		8														
55	106	8																		
56															13	14	30	5	51	
57			24	79		11														
58	111	3	19	65		8	3													
59								124	104											
60									1											
61															5	14	31	15	51	113
62	53	4													3	16	30	14	50	
63															5	14	16	7		
64	55	2	15	35		7									4	15	30	13	52	
65																6	30	7		
66															4	13	31	8		
67			15	35		7														
68															3	14	32	14	51	
69	53	4	15	35		7														
70															4	13	33	13	51	
71	53	4	15	35		7														
72	53	4																		
73															4	14	12	13	42	
74															4	14	31	14	31	
75	53	4	15	35		7														
76															5	13	32	13	51	
77			19																	
78	56	1																		

Table A4.1: Number of bighead carp samples by monitoring event and reach.

Event	Reach																			
	NSC	CR1	CRM	CR2	BCR	MXZ	CR3	CR4	CR5	FBA	CR6	CR7	CR8	CRA	CRB	CLK	LKC	CRC	CRD	CRE
1													16							
2												25	12							
3								25	9	40										
4										23	8									
5									8	18	29									
6																				
7		13	73	7																
8													14					27	44	
9																				
10							3	38	28											21
11																				
12									11	7										
13	45	7																		
14											2	3								
15								1					11	3	3	3	13	34	40	
16			11																	
17									17	19	10									
18													46				14	5	33	
19													39	2			14	7	43	
20																		6	61	
21	67	20																		
22																				
23	58																			
24																		9	35	
25			20	45	13	3	34													
26											29	31								
27																				
28									21	22	3									
29													85	5				8		
30														3	24	68				
31																				
32																				
33																				
34																				
35								54	21	39										
36			27	81	1	5														
37																		13	96	1
38	110	4																		
39								45	6	52										
40							29	47												
41			24	79		11														
42	111	3																		
43															3	12	34	15	51	
44			24	79	2	9														
45	105	9																		
46																				
47														5	11	32	13	41		
48													2	4	11	32	15	50		
49														4	13	32	8			
50			23	73	2	9	7													
51	108	6																		
52															4	14	31	14	51	
53								57	5	52										
54			24	79		8														
55	106	8																		
56														13	14	30	5	51		
57			24	79		11														
58	111	3	19	65		8	3													
59								124	104											
60									1											
61														5	14	31	15	51	113	
62	53	4												3	16	30	14	50		
63														5	14	16	7			
64	55	2	15	35		7								4	15	30	13	52		
65															6	30	7			
66														4	13	31	8			
67			15	35		7														
68														3	14	32	14	51		
69	53	4	15	35		7														
70														4	13	33	13	51		
71	53	4		31		7														
72	53	4																		
73														4	14	12	13	42		
74														4	14	31	14	31		
75	53	4	15	35		7														
76														5	13	32	13	51		
77			19																	
78	56	1																		

Table A4.2: Number of silver carp samples by monitoring event and reach.

Event	Reach																			
	NSC	CR1	CRM	CR2	BCR	MXZ	CR3	CR4	CR5	FBA	CR6	CR7	CR8	CRA	CRB	CLK	LKC	CRC	CRD	CRE
1													11							
2												2	6							
3								0	0	0										
4										1	3									
5									0	2	0									
6																				
7		0	0	0																
8														0				0	26	
9																				
10							0	0	0											3
11																				
12										1	0									
13	0	0																		
14											0	0								
15									0					0	0	0	0	0	2	1
16			0																	
17										0	0	0								
18														0			0	0	0	
19														0	0		0	0	0	
20																		0	0	
21	0	0																		
22																				
23	0																			
24																		0	0	
25			0	0	0	0	0													
26												0	0							
27																				
28										0	2	0								
29														0	0			0		
30															0	0	0			
31																				
32																				
33																				
34																				
35									0	1	2									
36			0	1	0	0														
37																		0	0	0
38	1	0																		
39									0	0	0									
40								0	2											
41			0	0		0														
42	0	0																		
43															0	0	0	0	0	
44			0	0	0	0														
45	0	0																		
46																				
47															0	0	0	0	0	
48														0	0	0	0	0	0	
49															0	0	0	0		
50			0	0	0	0	0													
51	0	0																		
52															0	0	0	0	0	
53									0	0	0									
54			0	0		0														
55	0	0																		
56															0	0	0	0	0	
57			0	0		0														
58	0	0	0	0		0	0													
59								0	0											
60									0						0	0	0	0	0	0
61															0	0	0	0	0	
62	0	0													0	0	0	0		
63															0	0	0	0	0	
64	0	0	0	0		0														
65																0	0	0		
66															0	0	0	0		
67			0	0		0														
68															0	0	0	0	0	
69	0	0	0	0		0														
70															0	0	0	0	0	
71	0	0	0	0		0														
72	0	0																		
73																				
74															1	1	2	0	0	
75															0	0	0	0	0	
76	0	0	0	0		0														
77			0																	
78	0	0																		

Table A4.3: Number of eDNA monitoring samples testing positive for bighead carp by monitoring event and reach.

Event	Reach																			
	NSC	CR1	CRM	CR2	BCR	MXZ	CR3	CR4	CR5	FBA	CR6	CR7	CR8	CRA	CRB	CLK	LKC	CRC	CRD	CRE
1													7							
2											8		7							
3								0	0	0										
4										4	1									
5									2	0	5									
6																				
7		0	0	0																
8														0				0	1	
9																				
10							1	0	1											0
11																				
12										1	0									
13	5	0																		
14											0	0								
15								0						0	0	0	0	0	0	2
16			0																	
17										3	6	5								
18														4			0	0	1	
19														0	0		0	0	1	
20																		0	0	
21	1	0																		
22																				
23	0																			
24																		0	0	
25			1	1	1	1	4													
26												10	21							
27																				
28										4	13	1								
29														0	0			0		
30															0	0	0			
31																				
32																				
33																				
34																				
35								4	2	6										
36			0	0	0	0														
37																		0	1	0
38	1	0																		
39									1	0	0									
40							0	0												
41			0	1		0														
42	0	0																		
43															0	2	4	1	0	
44			0	0	0	0														
45	1	0																		
46																				
47															0	0	2	0	0	
48														0	0	0	1	0	1	
49															0	0	0	0		
50			0	1	0	0	0													
51	0	0																		
52															0	0	1	0	0	
53									0	0	0									
54			0	0		0														
55	2	0																		
56															0	0	0	0	0	
57			1	0		0														
58	1	0	2	0		0	0													
59								0	2											
60								0							0	0	0	0	1	10
61															2	4	5	3	3	
62	1	0													0	2	1	0		
63															0	1	4	2	0	
64	3	0	0	5		1														
65																0	2	0		
66															0	1	2	0		
67			0	0		0														
68															0	0	6	2	0	
69	11	2	12	5		0														
70															0	2	8	3	3	
71	7	1		4		3														
72	8	0																		
73																				
74															3	9	11	6	5	
75	6	0	1	0		0									0	6	0	0	5	
76															0	0	0	1	1	
77			0																	
78	1	0																		

Table A4.4: Number of eDNA monitoring samples testing positive for silver carp by monitoring event and reach.

Event	Reach																			
	N5C	CR1	CRM	CR2	BCR	MXZ	CR3	CR4	CR5	FBA	CR6	CR7	CR8	CRA	CRB	CLK	LKC	CRC	CRD	CRE
1	410.7	410.7	410.7	410.7	410.7	410.7	410.7	410.7	410.7	410.7	410.7	410.7	25.8	410.7	410.7	410.7	410.7	410.7	410.7	410.7
2	410.7	410.7	410.7	410.7	410.7	410.7	410.7	410.7	410.7	0.0	0.0	20.4	56.6	410.7	410.7	410.7	410.7	410.7	410.7	410.7
3	410.7	410.7	410.7	410.7	410.7	410.7	410.7	410.7	0.0	0.0	0.0	20.4	56.6	410.7	410.7	410.7	410.7	410.7	410.7	410.7
4	410.7	410.7	410.7	410.7	410.7	410.7	410.7	410.7	0.0	0.0	3.6	26.7	56.6	410.7	410.7	410.7	410.7	410.7	410.7	410.7
5	410.7	410.7	410.7	410.7	410.7	410.7	410.7	410.7	0.0	3.3	4.3	42.1	56.6	410.7	410.7	410.7	410.7	410.7	410.7	410.7
6	410.7	410.7	410.7	410.7	410.7	410.7	410.7	410.7	0.0	3.3	4.3	42.1	56.6	410.7	410.7	410.7	410.7	410.7	410.7	410.7
7	410.7	0.0	0.0	0.0	410.7	410.7	410.7	410.7	0.0	3.3	4.3	42.1	56.6	410.7	410.7	410.7	410.7	410.7	410.7	410.7
8	410.7	0.0	0.0	0.0	410.7	410.7	410.7	410.7	0.0	3.3	4.3	42.1	56.6	0.0	410.7	410.7	410.7	0.0	1.6	410.7
9	410.7	0.0	0.0	0.0	410.7	410.7	410.7	410.7	0.0	3.3	4.3	42.1	56.6	0.0	410.7	410.7	410.7	0.0	1.6	410.7
10	410.7	0.0	0.0	0.0	410.7	410.7	21.0	0.0	2.9	3.3	4.3	42.1	56.6	0.0	410.7	410.7	410.7	0.0	1.6	0.0
11	410.7	0.0	0.0	0.0	410.7	410.7	21.0	0.0	2.9	3.3	4.3	42.1	56.6	0.0	410.7	410.7	410.7	0.0	1.6	0.0
12	410.7	0.0	0.0	0.0	410.7	410.7	21.0	0.0	2.9	12.4	3.7	42.1	56.6	0.0	410.7	410.7	410.7	0.0	1.6	0.0
13	5.5	0.1	0.0	0.0	410.7	410.7	21.0	0.0	2.9	12.4	3.7	42.1	56.6	0.0	410.7	410.7	410.7	0.0	1.6	0.0
14	5.5	0.1	0.0	0.0	410.7	410.7	21.0	0.0	2.9	12.4	3.2	29.5	56.6	0.0	410.7	410.7	410.7	0.0	1.6	0.0
15	5.5	0.1	0.0	0.0	410.7	410.7	21.0	0.0	4.2	12.4	3.2	29.5	56.6	0.1	0.0	0.0	0.0	0.1	3.3	3.3
16	5.5	0.1	0.1	0.0	410.7	410.7	21.0	0.0	4.2	12.4	3.2	29.5	56.6	0.1	0.0	0.0	0.0	0.1	3.3	3.3
17	5.5	0.1	0.1	0.0	410.7	410.7	21.0	0.0	4.2	19.4	9.5	41.2	56.6	0.1	0.0	0.0	0.0	0.1	3.3	3.3
18	5.5	0.1	0.1	0.0	410.7	410.7	21.0	0.0	4.2	19.4	9.5	41.2	56.6	4.4	0.0	0.0	0.1	0.1	12.1	3.3
19	5.5	0.1	0.1	0.0	410.7	410.7	21.0	0.0	4.2	19.4	9.5	41.2	56.6	3.7	0.1	0.0	0.1	0.1	17.9	3.3
20	5.5	0.1	0.1	0.0	410.7	410.7	21.0	0.0	4.2	19.4	9.5	41.2	56.6	3.7	0.1	0.0	0.1	0.0	13.9	3.3
21	13.4	0.1	0.1	0.0	410.7	410.7	21.0	0.0	4.2	19.4	9.5	41.2	56.6	3.7	0.1	0.0	0.1	0.0	13.9	3.3
22	13.4	0.1	0.1	0.0	410.7	410.7	21.0	0.0	4.2	19.4	9.5	41.2	56.6	3.7	0.1	0.0	0.1	0.0	13.9	3.3
23	12.2	0.1	0.1	0.0	410.7	410.7	21.0	0.0	4.2	19.4	9.5	41.2	56.6	3.7	0.1	0.0	0.1	0.0	13.9	3.3
24	12.2	0.1	0.1	0.0	410.7	410.7	21.0	0.0	4.2	19.4	9.5	41.2	56.6	3.7	0.1	0.0	0.1	0.0	11.2	3.3
25	12.2	0.1	4.6	3.3	1.5	21.0	28.0	0.0	4.2	19.4	9.5	41.2	56.6	3.7	0.1	0.0	0.1	0.0	11.2	3.3
26	12.2	0.1	4.6	3.3	1.5	21.0	28.0	0.0	4.2	19.4	9.5	49.7	103.2	3.7	0.1	0.0	0.1	0.0	11.2	3.3
27	12.2	0.1	4.6	3.3	1.5	21.0	28.0	0.0	4.2	19.4	9.5	49.7	103.2	3.7	0.1	0.0	0.1	0.0	11.2	3.3
28	12.2	0.1	4.6	3.3	1.5	21.0	28.0	0.0	4.2	24.6	27.1	57.1	103.2	3.7	0.1	0.0	0.1	0.0	11.2	3.3
29	12.2	0.1	4.6	3.3	1.5	21.0	28.0	0.0	4.2	24.6	27.1	57.1	103.2	3.1	0.1	0.0	0.1	0.0	11.2	3.3
30	12.2	0.1	4.6	3.3	1.5	21.0	28.0	0.0	4.2	24.6	27.1	57.1	103.2	3.1	0.1	0.1	0.1	0.0	11.2	3.3
31	12.2	0.1	4.6	3.3	1.5	21.0	28.0	0.0	4.2	24.6	27.1	57.1	103.2	3.1	0.1	0.1	0.1	0.0	11.2	3.3
32	12.2	0.1	4.6	3.3	1.5	21.0	28.0	0.0	4.2	24.6	27.1	57.1	103.2	3.1	0.1	0.1	0.1	0.0	11.2	3.3
33	12.2	0.1	4.6	3.3	1.5	21.0	28.0	0.0	4.2	24.6	27.1	57.1	103.2	3.1	0.1	0.1	0.1	0.0	11.2	3.3
34	12.2	0.1	4.6	3.3	1.5	21.0	28.0	0.0	4.2	24.6	27.1	57.1	103.2	3.1	0.1	0.1	0.1	0.0	11.2	3.3
35	12.2	0.1	4.6	3.3	1.5	21.0	28.0	0.0	9.1	27.1	30.9	57.1	103.2	3.1	0.1	0.1	0.1	0.0	11.2	3.3
36	12.2	0.1	4.1	4.4	3.2	9.7	28.0	0.0	9.1	27.1	30.9	57.1	103.2	3.1	0.1	0.1	0.1	0.0	11.2	3.3
37	12.2	0.1	4.1	4.4	3.2	9.7	28.0	0.0	9.1	27.1	30.9	57.1	103.2	3.1	0.1	0.1	0.1	0.0	14.8	4.6
38	18.0	0.1	4.1	4.4	3.2	9.7	28.0	0.0	9.1	27.1	30.9	57.1	103.2	3.1	0.1	0.1	0.1	0.0	14.8	4.6
39	18.0	0.1	4.1	4.4	3.2	9.7	28.0	0.0	13.8	22.3	25.7	57.1	103.2	3.1	0.1	0.1	0.1	0.0	14.8	4.6
40	18.0	0.1	4.1	4.4	3.2	9.7	28.0	0.1	11.2	22.3	25.7	57.1	103.2	3.1	0.1	0.1	0.1	0.0	14.8	4.6
41	18.0	0.1	3.7	9.8	3.2	10.4	28.0	0.1	11.2	22.3	25.7	57.1	103.2	3.1	0.1	0.1	0.1	0.0	14.8	4.6
42	14.3	0.0	3.7	9.8	3.2	10.4	28.0	0.1	11.2	22.3	25.7	57.1	103.2	3.1	0.1	0.1	0.1	0.0	14.8	4.6
43	14.3	0.0	3.7	9.8	3.2	10.4	28.0	0.1	11.2	22.3	25.7	57.1	103.2	3.1	0.0	4.3	4.0	2.3	12.5	4.6
44	14.3	0.0	3.3	7.9	3.9	9.3	28.0	0.1	11.2	22.3	25.7	57.1	103.2	3.1	0.0	4.3	4.0	2.3	12.5	4.6
45	18.4	0.0	3.3	7.9	3.9	9.3	28.0	0.1	11.2	22.3	25.7	57.1	103.2	3.1	0.0	4.3	4.0	2.3	12.5	4.6
46	18.4	0.0	3.3	7.9	3.9	9.3	28.0	0.1	11.2	22.3	25.7	57.1	103.2	3.1	0.0	4.3	4.0	2.3	12.5	4.6
47	18.4	0.0	3.3	7.9	3.9	9.3	28.0	0.1	11.2	22.3	25.7	57.1	103.2	3.1	0.0	3.7	7.4	2.3	10.8	4.6
48	18.4	0.0	3.3	7.9	3.9	9.3	28.0	0.1	11.2	22.3	25.7	57.1	103.2	2.7	0.0	3.2	10.0	2.2	13.6	4.6
49	18.4	0.0	3.3	7.9	3.9	9.3	28.0	0.1	11.2	22.3	25.7	57.1	103.2	2.7	0.0	2.9	8.9	2.2	13.6	4.6
50	18.4	0.0	3.0	11.9	3.2	8.1	22.6	0.1	11.2	22.3	25.7	57.1	103.2	2.7	0.0	2.9	8.9	2.2	13.6	4.6
51	15.3	0.0	3.0	11.9	3.2	8.1	22.6	0.1	11.2	22.3	25.7	57.1	103.2	2.7	0.0	2.9	8.9	2.2	13.6	4.6
52	15.3	0.0	3.0	11.9	3.2	8.1	22.6	0.1	11.2	22.3	25.7	57.1	103.2	2.7	0.0	2.7	11.0	2.2	11.9	4.6
53	15.3	0.0	3.0	11.9	3.2	8.1	22.6	0.1	9.5	18.9	20.3	57.1	103.2	2.7	0.0	2.7	11.0	2.2	11.9	4.6
54	15.3	0.0	2.8	9.9	3.2	7.2	22.6	0.1	9.5	18.9	20.3	57.1	103.2	2.7	0.0	2.7	11.0	2.2	11.9	4.6
55	18.7	0.0	2.8	9.9	3.2	7.2	22.6	0.1	9.5	18.9	20.3	57.1	103.2	2.7	0.0	2.7	11.0	2.2	11.9	4.6
56	18.7	0.0	2.8	9.9	3.2	7.2	22.6	0.1	9.5	18.9	20.3	57.1	103.2	2.7	0.0	2.6	10.0	2.2	10.7	4.6
57	18.7	0.0	5.0	8.5	3.2	6.6	22.6	0.1	9.5	18.9	20.3	57.1	103.2	2.7	0.0	2.6	10.0	2.2	10.7	4.6
58	21.6	0.0	7.0	7.4	3.2	6.2	16.8	0.1	9.5	18.9	20.3	57.1	103.2	2.7	0.0	2.6	10.0	2.2	10.7	4.6
59	21.6	0.0	7.0	7.4	3.2	6.2	16.8	0.1	12.7	18.9	20.3	57.1	103.2	2.7	0.0	2.6	10.0	2.2	10.7	4.6
60	21.6	0.0	7.0	7.4	3.2	6.2	16.8	0.1	11.0	18.9	20.3	57.1	103.2	2.7	0.0	2.5	9.2	2.2	12.9	9.7
61	21.6	0.0	7.0	7.4	3.2	6.2	16.8	0.1	11.0	18.9	20.3	57.1	103.2	2.7	10.4	4.2	10.9	2.8	15.2	9.7
62	24.2	0.0	7.0	7.4	3.2	6.2	16.8	0.1	11.0	18.9	20.3	57.1	103.2	2.7	10.3	6.2	13.1	2.7	15.2	9.7
63	24.2	0.0	7.0	7.4	3.2	6.2	16.8	0.1	11.0	18.9	20.3	57.1	103.2	2.7	10.2	8.1	15.2	3.9	13.8	9.7
64	26.1	0.0	6.4	9.9	3.2	8.1	16.8	0.1	11.0	18.9	20.3	57.1	103.2	2.7	10.2	8.1	15.2	3.9	13.8	9.7
65	26.1	0.0	6.4	9.9	3.2	8.1	16.8	0.1	11.0	18.9	20.3	57.1	103.2	2.7	10.2	7.5	16.8	3.7	13.8	9.7
66	26.1	0.0	6.4	9.9	3.2	8.1	16.8	0.1	11.0	18.9	20.3	57.1	103.2	2.7	10.2	8.9	18.7	3.5		







Event	Reach																			
	NSC	CR1	CRM	CR2	BCR	MXZ	CR3	CR4	CR5	FBA	CR6	CR7	CR8	CRA	CRB	CLK	LKC	CRC	CRD	CRE
1	410.7	410.7	410.7	410.7	410.7	410.7	410.7	410.7	410.7	410.7	410.7	410.7	25.8	410.7	410.7	410.7	410.7	410.7	410.7	410.7
2	410.7	410.7	410.7	410.7	410.7	410.7	410.7	410.7	410.7	0.0	0.0	20.4	56.6	410.7	410.7	410.7	410.7	410.7	410.7	410.7
3	410.7	410.7	410.7	410.7	410.7	410.7	410.7	410.7	0.0	0.0	0.0	20.4	56.6	410.7	410.7	410.7	410.7	410.7	410.7	410.7
4	410.7	410.7	410.7	410.7	410.7	410.7	410.7	410.7	0.0	0.0	3.6	26.7	56.6	410.7	410.7	410.7	410.7	410.7	410.7	410.7
5	410.7	410.7	410.7	410.7	410.7	410.7	410.7	410.7	0.0	3.3	4.3	42.1	56.6	410.7	410.7	410.7	410.7	410.7	410.7	410.7
6	410.7	410.7	410.7	410.7	410.7	410.7	410.7	410.7	0.0	3.3	4.3	42.1	56.6	410.7	410.7	410.7	410.7	410.7	410.7	410.7
7	410.7	0.0	0.0	0.0	410.7	410.7	410.7	410.7	0.0	3.3	4.3	42.1	56.6	410.7	410.7	410.7	410.7	410.7	410.7	410.7
8	410.7	0.0	0.0	0.0	410.7	410.7	410.7	410.7	0.0	3.3	4.3	42.1	56.6	0.0	410.7	410.7	410.7	0.0	1.6	410.7
9	410.7	0.0	0.0	0.0	410.7	410.7	410.7	410.7	0.0	3.3	4.3	42.1	56.6	0.0	410.7	410.7	410.7	0.0	1.6	410.7
10	410.7	0.0	0.0	0.0	410.7	410.7	21.0	0.0	2.9	3.3	4.3	42.1	56.6	0.0	410.7	410.7	410.7	0.0	1.6	0.0
11	410.7	0.0	0.0	0.0	410.7	410.7	21.0	0.0	2.9	3.3	4.3	42.1	56.6	0.0	410.7	410.7	410.7	0.0	1.6	0.0
12	410.7	0.0	0.0	0.0	410.7	410.7	21.0	0.0	2.9	12.4	3.7	42.1	56.6	0.0	410.7	410.7	410.7	0.0	1.6	0.0
13	5.5	0.1	0.0	0.0	410.7	410.7	21.0	0.0	2.9	12.4	3.7	42.1	56.6	0.0	410.7	410.7	410.7	0.0	1.6	0.0
14	5.5	0.1	0.0	0.0	410.7	410.7	21.0	0.0	2.9	12.4	3.2	29.5	56.6	0.0	410.7	410.7	410.7	0.0	1.6	0.0
15	5.5	0.1	0.0	0.0	410.7	410.7	21.0	0.0	4.2	12.4	3.2	29.5	56.6	0.1	0.0	0.0	0.0	0.1	3.3	3.3
16	5.5	0.1	0.1	0.0	410.7	410.7	21.0	0.0	4.2	12.4	3.2	29.5	56.6	0.1	0.0	0.0	0.0	0.1	3.3	3.3
17	5.5	0.1	0.1	0.0	410.7	410.7	21.0	0.0	4.2	19.4	9.5	41.2	56.6	0.1	0.0	0.0	0.0	0.1	3.3	3.3
18	5.5	0.1	0.1	0.0	410.7	410.7	21.0	0.0	4.2	19.4	9.5	41.2	56.6	4.4	0.0	0.0	0.1	0.1	12.1	3.3
19	5.5	0.1	0.1	0.0	410.7	410.7	21.0	0.0	4.2	19.4	9.5	41.2	56.6	3.7	0.1	0.0	0.1	0.1	17.9	3.3
20	5.5	0.1	0.1	0.0	410.7	410.7	21.0	0.0	4.2	19.4	9.5	41.2	56.6	3.7	0.1	0.0	0.1	0.0	13.9	3.3
21	13.4	0.1	0.1	0.0	410.7	410.7	21.0	0.0	4.2	19.4	9.5	41.2	56.6	3.7	0.1	0.0	0.1	0.0	13.9	3.3
22	13.4	0.1	0.1	0.0	410.7	410.7	21.0	0.0	4.2	19.4	9.5	41.2	56.6	3.7	0.1	0.0	0.1	0.0	13.9	3.3
23	12.2	0.1	0.1	0.0	410.7	410.7	21.0	0.0	4.2	19.4	9.5	41.2	56.6	3.7	0.1	0.0	0.1	0.0	13.9	3.3
24	12.2	0.1	0.1	0.0	410.7	410.7	21.0	0.0	4.2	19.4	9.5	41.2	56.6	3.7	0.1	0.0	0.1	0.0	11.2	3.3
25	12.2	0.1	4.6	3.3	1.5	21.0	28.0	0.0	4.2	19.4	9.5	41.2	56.6	3.7	0.1	0.0	0.1	0.0	11.2	3.3
26	12.2	0.1	4.6	3.3	1.5	21.0	28.0	0.0	4.2	19.4	9.5	49.7	103.2	3.7	0.1	0.0	0.1	0.0	11.2	3.3
27	12.2	0.1	4.6	3.3	1.5	21.0	28.0	0.0	4.2	19.4	9.5	49.7	103.2	3.7	0.1	0.0	0.1	0.0	11.2	3.3
28	12.2	0.1	4.6	3.3	1.5	21.0	28.0	0.0	4.2	24.6	27.1	57.1	103.2	3.7	0.1	0.0	0.1	0.0	11.2	3.3
29	12.2	0.1	4.6	3.3	1.5	21.0	28.0	0.0	4.2	24.6	27.1	57.1	103.2	3.1	0.1	0.0	0.1	0.0	11.2	3.3
30	12.2	0.1	4.6	3.3	1.5	21.0	28.0	0.0	4.2	24.6	27.1	57.1	103.2	3.1	0.1	0.1	0.1	0.0	11.2	3.3
31	12.2	0.1	4.6	3.3	1.5	21.0	28.0	0.0	4.2	24.6	27.1	57.1	103.2	3.1	0.1	0.1	0.1	0.0	11.2	3.3
32	12.2	0.1	4.6	3.3	1.5	21.0	28.0	0.0	4.2	24.6	27.1	57.1	103.2	3.1	0.1	0.1	0.1	0.0	11.2	3.3
33	12.2	0.1	4.6	3.3	1.5	21.0	28.0	0.0	4.2	24.6	27.1	57.1	103.2	3.1	0.1	0.1	0.1	0.0	11.2	3.3
34	12.2	0.1	4.6	3.3	1.5	21.0	28.0	0.0	4.2	24.6	27.1	57.1	103.2	3.1	0.1	0.1	0.1	0.0	11.2	3.3
35	12.2	0.1	4.6	3.3	1.5	21.0	28.0	0.0	9.1	27.1	30.9	57.1	103.2	3.1	0.1	0.1	0.1	0.0	11.2	3.3
36	12.2	0.1	4.1	4.4	3.2	9.7	28.0	0.0	9.1	27.1	30.9	57.1	103.2	3.1	0.1	0.1	0.1	0.0	11.2	3.3
37	12.2	0.1	4.1	4.4	3.2	9.7	28.0	0.0	9.1	27.1	30.9	57.1	103.2	3.1	0.1	0.1	0.1	0.0	14.8	4.6
38	18.0	0.1	4.1	4.4	3.2	9.7	28.0	0.0	9.1	27.1	30.9	57.1	103.2	3.1	0.1	0.1	0.1	0.0	14.8	4.6
39	18.0	0.1	4.1	4.4	3.2	9.7	28.0	0.0	13.8	22.3	25.7	57.1	103.2	3.1	0.1	0.1	0.1	0.0	14.8	4.6
40	18.0	0.1	4.1	4.4	3.2	9.7	28.0	0.1	11.2	22.3	25.7	57.1	103.2	3.1	0.1	0.1	0.1	0.0	14.8	4.6
41	18.0	0.1	3.7	9.8	3.2	10.4	28.0	0.1	11.2	22.3	25.7	57.1	103.2	3.1	0.1	0.1	0.1	0.0	14.8	4.6
42	14.3	0.0	3.7	9.8	3.2	10.4	28.0	0.1	11.2	22.3	25.7	57.1	103.2	3.1	0.1	0.1	0.1	0.0	14.8	4.6
43	14.3	0.0	3.7	9.8	3.2	10.4	28.0	0.1	11.2	22.3	25.7	57.1	103.2	3.1	0.0	4.3	4.0	2.3	12.5	4.6
44	14.3	0.0	3.3	7.9	3.9	9.3	28.0	0.1	11.2	22.3	25.7	57.1	103.2	3.1	0.0	4.3	4.0	2.3	12.5	4.6
45	18.4	0.0	3.3	7.9	3.9	9.3	28.0	0.1	11.2	22.3	25.7	57.1	103.2	3.1	0.0	4.3	4.0	2.3	12.5	4.6
46	18.4	0.0	3.3	7.9	3.9	9.3	28.0	0.1	11.2	22.3	25.7	57.1	103.2	3.1	0.0	4.3	4.0	2.3	12.5	4.6
47	18.4	0.0	3.3	7.9	3.9	9.3	28.0	0.1	11.2	22.3	25.7	57.1	103.2	3.1	0.0	3.7	7.4	2.3	10.8	4.6
48	18.4	0.0	3.3	7.9	3.9	9.3	28.0	0.1	11.2	22.3	25.7	57.1	103.2	2.7	0.0	3.2	10.0	2.2	13.6	4.6
49	18.4	0.0	3.3	7.9	3.9	9.3	28.0	0.1	11.2	22.3	25.7	57.1	103.2	2.7	0.0	2.9	8.9	2.2	13.6	4.6
50	18.4	0.0	3.0	11.9	3.2	8.1	22.6	0.1	11.2	22.3	25.7	57.1	103.2	2.7	0.0	2.9	8.9	2.2	13.6	4.6
51	15.3	0.0	3.0	11.9	3.2	8.1	22.6	0.1	11.2	22.3	25.7	57.1	103.2	2.7	0.0	2.9	8.9	2.2	13.6	4.6
52	15.3	0.0	3.0	11.9	3.2	8.1	22.6	0.1	11.2	22.3	25.7	57.1	103.2	2.7	0.0	2.7	11.0	2.2	11.9	4.6
53	15.3	0.0	3.0	11.9	3.2	8.1	22.6	0.1	9.5	18.9	20.3	57.1	103.2	2.7	0.0	2.7	11.0	2.2	11.9	4.6
54	15.3	0.0	2.8	9.9	3.2	7.2	22.6	0.1	9.5	18.9	20.3	57.1	103.2	2.7	0.0	2.7	11.0	2.2	11.9	4.6
55	18.7	0.0	2.8	9.9	3.2	7.2	22.6	0.1	9.5	18.9	20.3	57.1	103.2	2.7	0.0	2.7	11.0	2.2	11.9	4.6
56	18.7	0.0	2.8	9.9	3.2	7.2	22.6	0.1	9.5	18.9	20.3	57.1	103.2	2.7	0.0	2.6	10.0	2.2	10.7	4.6
57	18.7	0.0	5.0	8.5	3.2	6.6	22.6	0.1	9.5	18.9	20.3	57.1	103.2	2.7	0.0	2.6	10.0	2.2	10.7	4.6
58	21.6	0.0	7.0	7.4	3.2	6.2	16.8	0.1	9.5	18.9	20.3	57.1	103.2	2.7	0.0	2.6	10.0	2.2	10.7	4.6
59	21.6	0.0	7.0	7.4	3.2	6.2	16.8	0.1	12.7	18.9	20.3	57.1	103.2	2.7	0.0	2.6	10.0	2.2	10.7	4.6
60	21.6	0.0	7.0	7.4	3.2	6.2	16.8	0.1	11.0	18.9	20.3	57.1	103.2	2.7	0.0	2.5	9.2	2.2	12.9	9.7
61	21.6	0.0	7.0	7.4	3.2	6.2	16.8	0.1	11.0	18.9	20.3	57.1	103.2	2.7	10.4	4.2	10.9	2.8	15.2	9.7
62	24.2	0.0	7.0	7.4	3.2	6.2	16.8	0.1	11.0	18.9	20.3	57.1	103.2	2.7	10.3	6.2	13.1	2.7	15.2	9.7
63	24.2	0.0	7.0	7.4	3.2	6.2	16.8	0.1	11.0	18.9	20.3	57.1	103.2	2.7	10.2	8.1	15.2	3.9	13.8	9.7
64	26.1	0.0	6.4	9.9	3.2	8.1	16.8	0.1	11.0	18.9	20.3	57.1	103.2	2.7	10.2	8.1	15.2	3.9	13.8	9.7
65	26.1	0.0	6.4	9.9	3.2	8.1	16.8	0.1	11.0	18.9	20.3	57.1	103.2	2.7	10.2	7.5	16.8	3.7	13.8	9.7
66	26.1	0.0	6.4	9.9	3.2	8.1	16.8	0.1	11.0	18.9	20.3	57.1	103.2	2.7	10.2	8.9	18.7	3.5		

Event	Reach																				
	N5C	CR1	CRM	CR2	BCR	MXZ	CR3	CR4	CR5	FBA	CR6	CR7	CR8	CRA	CRB	CLK	LKC	CRC	CRD	CRE	
1	1339.8	1339.8	1339.8	1339.8	1339.8	1339.8	1339.8	1339.8	1339.8	1339.8	1339.8	1339.8	1339.8	1339.8	1339.8	1339.8	1339.8	1339.8	1339.8	1339.8	
2	1339.8	1339.8	1339.8	1339.8	1339.8	1339.8	1339.8	1339.8	1339.8	1339.8	1339.8	329.4	266.3	1339.8	1339.8	1339.8	1339.8	1339.8	1339.8	1339.8	
3	1339.8	1339.8	1339.8	1339.8	1339.8	1339.8	1339.8	1339.8	1339.8	27.9	27.9	27.9	329.4	266.3	1339.8	1339.8	1339.8	1339.8	1339.8	1339.8	
4	1339.8	1339.8	1339.8	1339.8	1339.8	1339.8	1339.8	1339.8	1339.8	27.9	27.9	62.2	168.9	266.3	1339.8	1339.8	1339.8	1339.8	1339.8	1339.8	
5	1339.8	1339.8	1339.8	1339.8	1339.8	1339.8	1339.8	1339.8	1339.8	27.9	63.2	36.4	139.6	266.3	1339.8	1339.8	1339.8	1339.8	1339.8	1339.8	
6	1339.8	1339.8	1339.8	1339.8	1339.8	1339.8	1339.8	1339.8	1339.8	27.9	63.2	36.4	139.6	266.3	1339.8	1339.8	1339.8	1339.8	1339.8	1339.8	
7	1339.8	27.9	27.9	27.9	1339.8	1339.8	1339.8	1339.8	1339.8	27.9	63.2	36.4	139.6	266.3	1339.8	1339.8	1339.8	1339.8	1339.8	1339.8	
8	1339.8	27.9	27.9	27.9	1339.8	1339.8	1339.8	1339.8	1339.8	27.9	63.2	36.4	139.6	266.3	27.9	1339.8	1339.8	1339.8	27.9	147.5	
9	1339.8	27.9	27.9	27.9	1339.8	1339.8	1339.8	1339.8	1339.8	27.9	63.2	36.4	139.6	266.3	27.9	1339.8	1339.8	1339.8	27.9	147.5	
10	1339.8	27.9	27.9	27.9	1339.8	1339.8	331.1	27.9	51.8	63.2	36.4	139.6	266.3	27.9	1339.8	1339.8	1339.8	27.9	147.5	27.9	
11	1339.8	27.9	27.9	27.9	1339.8	1339.8	331.1	27.9	51.8	63.2	36.4	139.6	266.3	27.9	1339.8	1339.8	1339.8	27.9	147.5	27.9	
12	1339.8	27.9	27.9	27.9	1339.8	1339.8	331.1	27.9	51.8	64.8	25.1	139.6	266.3	27.9	1339.8	1339.8	1339.8	27.9	147.5	27.9	
13	214.1	12.8	27.9	27.9	1339.8	1339.8	331.1	27.9	51.8	64.8	25.1	139.6	266.3	27.9	1339.8	1339.8	1339.8	27.9	147.5	27.9	
14	214.1	12.8	27.9	27.9	1339.8	1339.8	331.1	27.9	51.8	64.8	19.2	93.6	266.3	27.9	1339.8	1339.8	1339.8	27.9	147.5	27.9	
15	214.1	12.8	27.9	27.9	1339.8	1339.8	331.1	27.9	33.1	64.8	19.2	93.6	266.3	12.8	27.9	27.9	27.9	12.8	53.7	53.6	
16	214.1	12.8	12.8	12.8	27.9	1339.8	1339.8	331.1	27.9	33.1	64.8	19.2	93.6	266.3	12.8	27.9	27.9	27.9	12.8	53.7	53.6
17	214.1	12.8	12.8	12.8	27.9	1339.8	1339.8	331.1	27.9	33.1	68.7	34.8	106.3	266.3	12.8	27.9	27.9	27.9	12.8	53.7	53.6
18	214.1	12.8	12.8	12.8	27.9	1339.8	1339.8	331.1	27.9	33.1	68.7	34.8	106.3	266.3	34.0	27.9	27.9	12.8	8.5	59.1	53.6
19	214.1	12.8	12.8	12.8	27.9	1339.8	1339.8	331.1	27.9	33.1	68.7	34.8	106.3	266.3	24.0	12.8	27.9	8.5	5.6	60.6	53.6
20	214.1	12.8	12.8	12.8	27.9	1339.8	1339.8	331.1	27.9	33.1	68.7	34.8	106.3	266.3	24.0	12.8	27.9	8.5	3.9	45.8	53.6
21	109.9	8.5	12.8	12.8	27.9	1339.8	1339.8	331.1	27.9	33.1	68.7	34.8	106.3	266.3	24.0	12.8	27.9	8.5	3.9	45.8	53.6
22	109.9	8.5	12.8	12.8	27.9	1339.8	1339.8	331.1	27.9	33.1	68.7	34.8	106.3	266.3	24.0	12.8	27.9	8.5	3.9	45.8	53.6
23	64.0	8.5	12.8	12.8	27.9	1339.8	1339.8	331.1	27.9	33.1	68.7	34.8	106.3	266.3	24.0	12.8	27.9	8.5	3.9	45.8	53.6
24	64.0	8.5	12.8	12.8	27.9	1339.8	1339.8	331.1	27.9	33.1	68.7	34.8	106.3	266.3	24.0	12.8	27.9	8.5	2.8	36.3	53.6
25	64.0	8.5	34.3	53.7	145.0	331.1	172.6	27.9	33.1	68.7	34.8	106.3	266.3	24.0	12.8	27.9	8.5	2.8	36.3	53.6	
26	64.0	8.5	34.3	53.7	145.0	331.1	172.6	27.9	33.1	68.7	34.8	113.4	268.7	24.0	12.8	27.9	8.5	2.8	36.3	53.6	
27	64.0	8.5	34.3	53.7	145.0	331.1	172.6	27.9	33.1	68.7	34.8	113.4	268.7	24.0	12.8	27.9	8.5	2.8	36.3	53.6	
28	64.0	8.5	34.3	53.7	145.0	331.1	172.6	27.9	33.1	70.8	63.9	119.4	268.7	24.0	12.8	27.9	8.5	2.8	36.3	53.6	
29	64.0	8.5	34.3	53.7	145.0	331.1	172.6	27.9	33.1	70.8	63.9	119.4	268.7	18.6	8.5	27.9	8.5	2.0	36.3	53.6	
30	64.0	8.5	34.3	53.7	145.0	331.1	172.6	27.9	33.1	70.8	63.9	119.4	268.7	18.6	5.6	12.8	5.6	2.0	36.3	53.6	
31	64.0	8.5	34.3	53.7	145.0	331.1	172.6	27.9	33.1	70.8	63.9	119.4	268.7	18.6	5.6	12.8	5.6	2.0	36.3	53.6	
32	64.0	8.5	34.3	53.7	145.0	331.1	172.6	27.9	33.1	70.8	63.9	119.4	268.7	18.6	5.6	12.8	5.6	2.0	36.3	53.6	
33	64.0	8.5	34.3	53.7	145.0	331.1	172.6	27.9	33.1	70.8	63.9	119.4	268.7	18.6	5.6	12.8	5.6	2.0	36.3	53.6	
34	64.0	8.5	34.3	53.7	145.0	331.1	172.6	27.9	33.1	70.8	63.9	119.4	268.7	18.6	5.6	12.8	5.6	2.0	36.3	53.6	
35	64.0	8.5	34.3	53.7	145.0	331.1	172.6	27.9	40.3	68.7	66.9	119.4	268.7	18.6	5.6	12.8	5.6	2.0	36.3	53.6	
36	64.0	8.5	24.8	34.0	52.8	103.1	172.6	27.9	40.3	68.7	66.9	119.4	268.7	18.6	5.6	12.8	5.6	2.0	36.3	53.6	
37	64.0	8.5	24.8	34.0	52.8	103.1	172.6	27.9	40.3	68.7	66.9	119.4	268.7	18.6	5.6	12.8	5.6	1.5	40.5	34.3	
38	63.6	5.6	24.8	34.0	52.8	103.1	172.6	27.9	40.3	68.7	66.9	119.4	268.7	18.6	5.6	12.8	5.6	1.5	40.5	34.3	
39	63.6	5.6	24.8	34.0	52.8	103.1	172.6	27.9	45.1	55.9	56.9	119.4	268.7	18.6	5.6	12.8	5.6	1.5	40.5	34.3	
40	63.6	5.6	24.8	34.0	52.8	103.1	172.6	12.8	36.0	55.9	56.9	119.4	268.7	18.6	5.6	12.8	5.6	1.5	40.5	34.3	
41	63.6	5.6	19.5	41.7	52.8	59.4	172.6	12.8	36.0	55.9	56.9	119.4	268.7	18.6	5.6	12.8	5.6	1.5	40.5	34.3	
42	47.6	3.9	19.5	41.7	52.8	59.4	172.6	12.8	36.0	55.9	56.9	119.4	268.7	18.6	5.6	12.8	5.6	1.5	40.5	34.3	
43	47.6	3.9	19.5	41.7	52.8	59.4	172.6	12.8	36.0	55.9	56.9	119.4	268.7	18.6	3.9	36.4	20.8	10.2	34.2	34.3	
44	47.6	3.9	16.2	31.7	32.8	41.3	172.6	12.8	36.0	55.9	56.9	119.4	268.7	18.6	3.9	36.4	20.8	10.2	34.2	34.3	
45	50.5	2.8	16.2	31.7	32.8	41.3	172.6	12.8	36.0	55.9	56.9	119.4	268.7	18.6	3.9	36.4	20.8	10.2	34.2	34.3	
46	50.5	2.8	16.2	31.7	32.8	41.3	172.6	12.8	36.0	55.9	56.9	119.4	268.7	18.6	3.9	36.4	20.8	10.2	34.2	34.3	
47	50.5	2.8	16.2	31.7	32.8	41.3	172.6	12.8	36.0	55.9	56.9	119.4	268.7	18.6	2.8	25.1	27.2	9.3	29.4	34.3	
48	50.5	2.8	16.2	31.7	32.8	41.3	172.6	12.8	36.0	55.9	56.9	119.4	268.7	15.1	2.0	19.2	31.1	8.7	33.0	34.3	
49	50.5	2.8	16.2	31.7	32.8	41.3	172.6	12.8	36.0	55.9	56.9	119.4	268.7	15.1	1.5	15.7	26.5	8.1	33.0	34.3	
50	50.5	2.8	13.9	37.1	22.8	31.9	98.3	12.8	36.0	55.9	56.9	119.4	268.7	15.1	1.5	15.7	26.5	8.1	33.0	34.3	
51	41.7	2.0	13.9	37.1	22.8	31.9	98.3	12.8	36.0	55.9	56.9	119.4	268.7	15.1	1.5	15.7	26.5	8.1	33.0	34.3	
52	41.7	2.0	13.9	37.1	22.8	31.9	98.3	12.8	36.0	55.9	56.9	119.4	268.7	15.1	1.1	13.4	29.6	7.6	29.2	34.3	
53	41.7	2.0	13.9	37.1	22.8	31.9	98.3	12.8	29.8	46.8	48.1	119.4	268.7	15.1	1.1	13.4	29.6	7.6	29.2	34.3	
54	41.7	2.0	12.2	30.7	22.8	26.1	98.3	12.8	29.8	46.8	48.1	119.4	268.7	15.1	1.1	13.4	29.6	7.6	29.2	34.3	
55	44.8	1.5	12.2	30.7	22.8	26.1	98.3	12.8	29.8	46.8	48.1	119.4	268.7	15.1	1.1	13.4	29.6	7.6	29.2	34.3	
56	44.8	1.5	12.2	30.7	22.8	26.1	98.3	12.8	29.8	46.8	48.1	119.4	268.7	15.1	0.8	11.8	26.2	7.3	26.1	34.3	
57	44.8	1.5	16.6	26.0	22.8	22.2	98.3	12.8	29.8	46.8	48.1	119.4	268.7	15.1	0.8	11.8	26.2	7.3	26.1	34.3	
58	47.2	1.1	20.2	22.6	22.8	19.5	64.5	12.8	29.8	46.8	48.1	119.4	268.7	15.1	0.8	11.8	26.2	7.3	26.1	34.3	
59	47.2	1.1	20.2	22.6	22.8	19.5	64.5	8.5	34.0	46.8	48.1	119.4	268.7	15.1	0.8	11.8	26.2	7.3	26.1	34.3	
60	47.2	1.1	20.2	22.6	22.8	19.5	64.5	8.5	29.4	46.8	48.1	119.4	268.7	15.1	0.6	10.7	23.5	6.9	29.1	41.3	
61	47.2	1.1	20.2	22.6	22.8	19.5	64.5	8.5	29.4	46.8	48.1	119.4	268.7	15.1	21.3						











Event	Reach																			
	N5C	CR1	CRM	CR2	BCR	MXZ	CR3	CR4	CR5	FBA	CR6	CR7	CR8	CRA	CRB	CLK	LKC	CRC	CRD	CRE
1	499.2	499.2	499.2	499.2	499.2	499.2	499.2	499.2	499.2	499.2	499.2	499.2	537.9	499.2	499.2	499.2	499.2	499.2	499.2	499.2
2	499.2	499.2	499.2	499.2	499.2	499.2	499.2	499.2	499.2	499.2	499.2	499.2	532.7	158.1	499.2	499.2	499.2	499.2	499.2	499.2
3	499.2	499.2	499.2	499.2	499.2	499.2	499.2	499.2	499.2	618.8	618.8	618.8	532.7	158.1	499.2	499.2	499.2	499.2	499.2	499.2
4	499.2	499.2	499.2	499.2	499.2	499.2	499.2	499.2	499.2	618.8	618.8	104.9	134.9	158.1	499.2	499.2	499.2	499.2	499.2	499.2
5	499.2	499.2	499.2	499.2	499.2	499.2	499.2	499.2	499.2	618.8	114.5	37.6	53.2	158.1	499.2	499.2	499.2	499.2	499.2	499.2
6	499.2	499.2	499.2	499.2	499.2	499.2	499.2	499.2	499.2	618.8	114.5	37.6	53.2	158.1	499.2	499.2	499.2	499.2	499.2	499.2
7	499.2	618.8	618.8	618.8	499.2	499.2	499.2	499.2	499.2	618.8	114.5	37.6	53.2	158.1	499.2	499.2	499.2	499.2	499.2	499.2
8	499.2	618.8	618.8	618.8	499.2	499.2	499.2	499.2	499.2	618.8	114.5	37.6	53.2	158.1	618.8	499.2	499.2	499.2	618.8	580.5
9	499.2	618.8	618.8	618.8	499.2	499.2	499.2	499.2	499.2	618.8	114.5	37.6	53.2	158.1	618.8	499.2	499.2	499.2	618.8	580.5
10	499.2	618.8	618.8	618.8	499.2	499.2	528.3	618.8	89.0	114.5	37.6	53.2	158.1	618.8	499.2	499.2	499.2	618.8	580.5	618.8
11	499.2	618.8	618.8	618.8	499.2	499.2	528.3	618.8	89.0	114.5	37.6	53.2	158.1	618.8	499.2	499.2	499.2	618.8	580.5	618.8
12	499.2	618.8	618.8	618.8	499.2	499.2	528.3	618.8	89.0	42.8	21.5	53.2	158.1	618.8	499.2	499.2	499.2	618.8	580.5	618.8
13	569.9	72.3	618.8	618.8	499.2	499.2	528.3	618.8	89.0	42.8	21.5	53.2	158.1	618.8	499.2	499.2	499.2	618.8	580.5	618.8
14	569.9	72.3	618.8	618.8	499.2	499.2	528.3	618.8	89.0	42.8	14.6	33.5	158.1	618.8	499.2	499.2	499.2	618.8	580.5	618.8
15	569.9	72.3	618.8	618.8	499.2	499.2	528.3	618.8	32.1	42.8	14.6	33.5	158.1	72.3	618.8	618.8	618.8	72.3	86.4	86.7
16	569.9	72.3	72.3	618.8	499.2	499.2	528.3	618.8	32.1	42.8	14.6	33.5	158.1	72.3	618.8	618.8	618.8	72.3	86.4	86.7
17	569.9	72.3	72.3	618.8	499.2	499.2	528.3	618.8	32.1	28.7	15.3	26.9	158.1	72.3	618.8	618.8	618.8	72.3	86.4	86.7
18	569.9	72.3	72.3	618.8	499.2	499.2	528.3	618.8	32.1	28.7	15.3	26.9	158.1	32.1	618.8	618.8	618.8	72.3	29.4	36.5
19	569.9	72.3	72.3	618.8	499.2	499.2	528.3	618.8	32.1	28.7	15.3	26.9	158.1	19.6	72.3	618.8	29.4	19.5	23.8	86.7
20	569.9	72.3	72.3	618.8	499.2	499.2	528.3	618.8	32.1	28.7	15.3	26.9	158.1	19.6	72.3	618.8	29.4	15.1	17.3	86.7
21	110.2	29.4	72.3	618.8	499.2	499.2	528.3	618.8	32.1	28.7	15.3	26.9	158.1	19.6	72.3	618.8	29.4	15.1	17.3	86.7
22	110.2	29.4	72.3	618.8	499.2	499.2	528.3	618.8	32.1	28.7	15.3	26.9	158.1	19.6	72.3	618.8	29.4	15.1	17.3	86.7
23	42.6	29.4	72.3	618.8	499.2	499.2	528.3	618.8	32.1	28.7	15.3	26.9	158.1	19.6	72.3	618.8	29.4	15.1	17.3	86.7
24	42.6	29.4	72.3	618.8	499.2	499.2	528.3	618.8	32.1	28.7	15.3	26.9	158.1	19.6	72.3	618.8	29.4	12.5	13.5	86.7
25	42.6	29.4	31.9	86.4	595.5	528.3	134.9	618.8	32.1	28.7	15.3	26.9	158.1	19.6	72.3	618.8	29.4	12.5	13.5	86.7
26	42.6	29.4	31.9	86.4	595.5	528.3	134.9	618.8	32.1	28.7	15.3	22.4	69.0	19.6	72.3	618.8	29.4	12.5	13.5	86.7
27	42.6	29.4	31.9	86.4	595.5	528.3	134.9	618.8	32.1	28.7	15.3	22.4	69.0	19.6	72.3	618.8	29.4	12.5	13.5	86.7
28	42.6	29.4	31.9	86.4	595.5	528.3	134.9	618.8	32.1	21.6	13.5	19.3	69.0	19.6	72.3	618.8	29.4	12.5	13.5	86.7
29	42.6	29.4	31.9	86.4	595.5	528.3	134.9	618.8	32.1	21.6	13.5	19.3	69.0	13.9	29.4	618.8	29.4	10.9	13.5	86.7
30	42.6	29.4	31.9	86.4	595.5	528.3	134.9	618.8	32.1	21.6	13.5	19.3	69.0	13.9	19.5	72.3	19.5	10.9	13.5	86.7
31	42.6	29.4	31.9	86.4	595.5	528.3	134.9	618.8	32.1	21.6	13.5	19.3	69.0	13.9	19.5	72.3	19.5	10.9	13.5	86.7
32	42.6	29.4	31.9	86.4	595.5	528.3	134.9	618.8	32.1	21.6	13.5	19.3	69.0	13.9	19.5	72.3	19.5	10.9	13.5	86.7
33	42.6	29.4	31.9	86.4	595.5	528.3	134.9	618.8	32.1	21.6	13.5	19.3	69.0	13.9	19.5	72.3	19.5	10.9	13.5	86.7
34	42.6	29.4	31.9	86.4	595.5	528.3	134.9	618.8	32.1	21.6	13.5	19.3	69.0	13.9	19.5	72.3	19.5	10.9	13.5	86.7
35	42.6	29.4	31.9	86.4	595.5	528.3	134.9	618.8	22.2	16.7	11.7	19.3	69.0	13.9	19.5	72.3	19.5	10.9	13.5	86.7
36	42.6	29.4	18.8	32.4	87.0	126.0	134.9	618.8	22.2	16.7	11.7	19.3	69.0	13.9	19.5	72.3	19.5	10.9	13.5	86.7
37	42.6	29.4	18.8	32.4	87.0	126.0	134.9	618.8	22.2	16.7	11.7	19.3	69.0	13.9	19.5	72.3	19.5	9.8	11.3	31.9
38	26.6	19.5	18.8	32.4	87.0	126.0	134.9	618.8	22.2	16.7	11.7	19.3	69.0	13.9	19.5	72.3	19.5	9.8	11.3	31.9
39	26.6	19.5	18.8	32.4	87.0	126.0	134.9	618.8	16.9	13.4	10.5	19.3	69.0	13.9	19.5	72.3	19.5	9.8	11.3	31.9
40	26.6	19.5	18.8	32.4	87.0	126.0	134.9	72.3	13.1	13.4	10.5	19.3	69.0	13.9	19.5	72.3	19.5	9.8	11.3	31.9
41	26.6	19.5	13.1	22.1	87.0	43.2	134.9	72.3	13.1	13.4	10.5	19.3	69.0	13.9	19.5	72.3	19.5	9.8	11.3	31.9
42	18.3	15.1	13.1	22.1	87.0	43.2	134.9	72.3	13.1	13.4	10.5	19.3	69.0	13.9	19.5	72.3	19.5	9.8	11.3	31.9
43	18.3	15.1	13.1	22.1	87.0	43.2	134.9	72.3	13.1	13.4	10.5	19.3	69.0	13.9	15.1	37.6	13.8	5.6	9.5	31.9
44	18.3	15.1	9.9	15.7	33.2	23.1	134.9	72.3	13.1	13.4	10.5	19.3	69.0	13.9	15.1	37.6	13.8	5.6	9.5	31.9
45	14.3	12.5	9.9	15.7	33.2	23.1	134.9	72.3	13.1	13.4	10.5	19.3	69.0	13.9	15.1	37.6	13.8	5.6	9.5	31.9
46	14.3	12.5	9.9	15.7	33.2	23.1	134.9	72.3	13.1	13.4	10.5	19.3	69.0	13.9	15.1	37.6	13.8	5.6	9.5	31.9
47	14.3	12.5	9.9	15.7	33.2	23.1	134.9	72.3	13.1	13.4	10.5	19.3	69.0	13.9	12.5	21.5	11.8	4.8	8.2	31.9
48	14.3	12.5	9.9	15.7	33.2	23.1	134.9	72.3	13.1	13.4	10.5	19.3	69.0	10.7	10.9	14.6	10.8	4.1	7.4	31.9
49	14.3	12.5	9.9	15.7	33.2	23.1	134.9	72.3	13.1	13.4	10.5	19.3	69.0	10.7	9.8	10.8	8.6	3.6	7.4	31.9
50	14.3	12.5	8.0	12.9	20.3	15.2	53.3	72.3	13.1	13.4	10.5	19.3	69.0	10.7	9.8	10.8	8.6	3.6	7.4	31.9
51	11.6	10.9	8.0	12.9	20.3	15.2	53.3	72.3	13.1	13.4	10.5	19.3	69.0	10.7	9.8	10.8	8.6	3.6	7.4	31.9
52	11.6	10.9	8.0	12.9	20.3	15.2	53.3	72.3	13.1	13.4	10.5	19.3	69.0	10.7	9.0	8.4	8.1	3.2	6.7	31.9
53	11.6	10.9	8.0	12.9	20.3	15.2	53.3	72.3	10.5	10.9	10.2	19.3	69.0	10.7	9.0	8.4	8.1	3.2	6.7	31.9
54	11.6	10.9	6.7	10.6	20.3	11.2	53.3	72.3	10.5	10.9	10.2	19.3	69.0	10.7	9.0	8.4	8.1	3.2	6.7	31.9
55	9.8	9.8	6.7	10.6	20.3	11.2	53.3	72.3	10.5	10.9	10.2	19.3	69.0	10.7	9.0	8.4	8.1	3.2	6.7	31.9
56	9.8	9.8	6.7	10.6	20.3	11.2	53.3	72.3	10.5	10.9	10.2	19.3	69.0	10.7	8.4	6.8	6.8	2.8	6.0	31.9
57	9.8	9.8	6.3	8.9	20.3	8.7	53.3	72.3	10.5	10.9	10.2	19.3	69.0	10.7	8.4	6.8	6.8	2.8	6.0	31.9
58	8.4	9.0	6.2	7.5	20.3	7.0	30.1	72.3	10.5	10.9	10.2	19.3	69.0	10.7	8.4	6.8	6.8	2.8	6.0	31.9
59	8.4	9.0	6.2	7.5	20.3	7.0	30.1	29.4	9.3	10.9	10.2	19.3	69.0	10.7	8.4	6.8	6.8	2.8	6.0	31.9
60	8.4	9.0	6.2	7.5	20.3	7.0	30.1	29.4	8.0	10.9	10.2	19.3	69.0	10.7	7.9	5.6	5.8	2.5	5.6	21.8
61	8.4	9.0	6.2	7.5	20.3	7.0	30.1	29.4	8.0	10.9	10.2	19.3	69.0	10.7	3.2	6.0	6.0	3.0	5.1	21.8
62	7.3	8.4	6.2	7.5	20.3	7.0	30.1	29.4	8.0	10.9	10.2	19.3	69.0	10.7	2.8	6.0	5.5	2.8		

*This page left intentionally blank.*